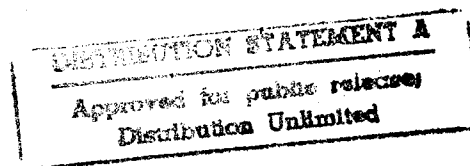NASA Technical Memorandum 80038

COMPOSITES FOR ADVANCED SPACE
TRANSPORTATION SYSTEMS - (CASTS)

TECHNICAL REPORT FOR PERIOD
JULY 1, 1975 - APRIL 1, 1978

COMPILED BY:
JOHN G. DAVIS, JR.

MARCH 1979

NASA
National Aeronautics and
Space Administration

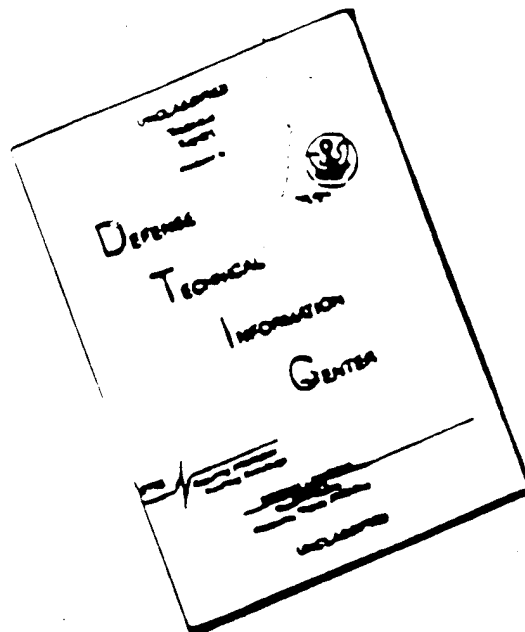**Langley Research Center**
Hampton, Virginia 23665

DEPARTMENT OF DEFENSE
PLASTICS TECHNICAL EVALUATION CENTER
ARRADCOM, DOVER, N. J. 07801

19960223 040

PLASTEC 31119a

DISCLAIMER NOTICE

FOREWORD

This document is the first technical narrative and summarizes the in-house and contract work accomplished under the CASTS Project.
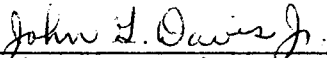
Management structure for the CASTS Project follows:

Project Manager. . . . . Dr. J.G. Davis, Jr.
Deputy Project Manager . . . . H.B. Dexter
Technical Assistant. . . . . L.A. Teichman
Secretary. . . . . J.H. Woodcock
Materials Screening Group Leader . . . . . . Dr. N.J. Johnston
Manufacturing Development Group Leader . . R.M. Baucom
Thermal, Physical and Moisture Properties
  Group Leader. . . . . Dr. D.R. Tenney
Mechanical Properties Group Leader . . . . H.B. Dexter
Structural Integrity Group Leader. . . . . W. Illg
Structural Design, Analysis and Test
  Group Leader. . . . . Dr. S.C. Dixon
Advanced Technology Development Group
  Leader. . . . . H.B. Dexter
Operations Support Group Leader. . . . . . F.F. Eichenbrenner
Fabrication Group Leader . . . . K.C. Hinnant
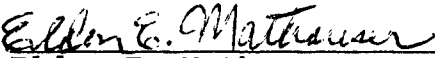Schedules and Analysis Group Leader. . . W.L. Gaster

Researchers that made major contributions to the task reported herein are identified at the beginning of each section.

Identification of commercial products in this report is to adequately describe the materials and does not constitute official endorsement, expressed or implied, of such products or manufacturers by the National Aeronautics and Space Administration.

Approved by:

John G. Davis, Jr.
John G. Davis, Jr.
Project Manager

William A. Brooks, Jr.
William A. Brooks, Jr.
Chief, Materials Division

Eldon E. Mathauser
Eldon E. Mathauser
Head, Materials Application
Branch

Roger A. Anderson
Roger A. Anderson
Chief, Structures and Dynamics
Division

i

1.0 INTRODUCTION

The Composites for Advanced Space Transportation Systems (CASTS) Project was initiated in July 1975 to develop graphite fiber/polyimide matrix (Gr/PI) composite structures with 589K (600°F) operational capability for application to aerospace vehicles. Compared to conventional aluminum structures which must not exceed 450K (350°F), Gr/PI composite structures offer the potential for decreasing structural mass and/or improving the performance of aerospace vehicles. The potential improvements are related to the higher specific strength and stiffness of Gr/PI composites and the higher allowable operating temperature which reduces the amount of insulation required to protect the structure during reentry.

Deficiencies in Gr/PI composites technology identified at the beginning of the CASTS Project included: inadequate materials specifications and fabrication procedures compatible with existing facilities in the aerospace industry, very limited experience on measuring design allowables data at 589K (600°F), insufficient data to assess the effects of exposure to thermal, moisture, chemical and/or mechanical environments predicted for aerospace vehicles, and a need to extend the design and analysis methodology for composite materials to include 589K (600°F) operational structures. Both NASA Langley Research Center in-house and contract efforts were initiated to overcome these technology deficiencies.

Selecting a reduction in mass fraction of approximately twenty five percent for Gr/PI composite structures compared to conventional aluminum aerospace structure as the major goal, the project plan shown in figure 1.0-1 was developed. Major tasks include: screening composites and adhesives for 589K (600°F) service, developing fabrication procedures and specifications, developing design allowables test methods and data, design and test of structural elements and construction of an aft body flap for the Space Shuttle Orbiter Vehicle which will be ground tested. The bubble in figure 1.0-1 entitled advanced technology development includes far term research on new materials, manufacturing procedures and design/analysis methodology.

Significant portions of the information reported herein are from research efforts that are on going and must be considered preliminary. For example, fabrication procedures and material specifications will continue to be modified as more experience is obtained and the data base increases. In addition, definition of the limits on application of Gr/PI structures to aerospace vehicles must await completion of the investigation of the effects of exposure to moisture, thermal and chemical environments.
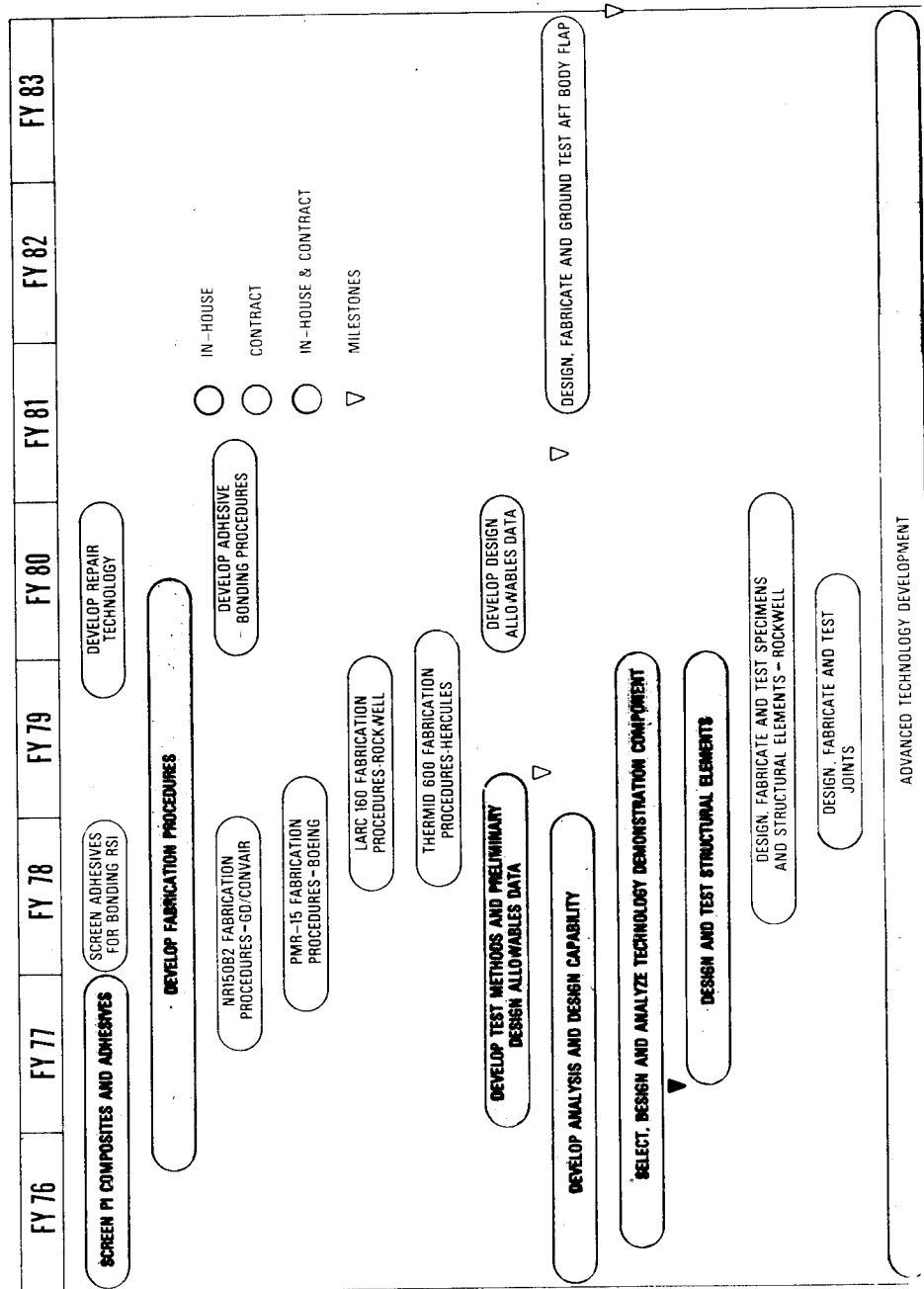
Figure 1.0-1 - Major tasks and schedule for CASTS project.

2.0 SUMMARY

Significant progress has been made toward achieving the CASTS Project goal of developing Gr/PI composite structures that will have 589K (600°F) operational capability and be twenty five percent lighter than conventional metallic structures. Interlaminar shear and flexure data indicates that NR150B2 and THERMID 600 polyimide matrix composites have the potential for 500 hours service at 589K (600°F) and that PMR-15 and LARC 160 polyimide matrix composites have the potential for 125 hours service at 589K (600°F) or 500 hours at 561K (550°F). Screening studies which utilized composite-to-composite and composite-to-metal lap shear specimens and glass/polyimide honeycomb specimens indicate that FM-34, LARC-13 and modified NR150B2G adhesives have the potential to achieve the project goals.

In-house effort has demonstrated the capability to make reproducible graphite fiber/PMR-15 prepreg utilizing a drum winding apparatus. Gr/PMR-15 laminates up to 0.953 cm (0.375 in.) thick and Gr/LARC 160 laminates up to 0.318 cm (0.125 in.) thick have been fabricated. Specifications for characterizing Gr/PMR-15 and Gr/LARC 160 prepreg and procedures for non destructive evaluation of cured laminates have been developed. Status reports on contract efforts to develop fabrication procedures and specifications on NR150B2, PMR-15, LARC 160 and THERMID 600 polyimide matrix composites are summarized herein.

Development of test methods for determining mechanical design allowables including tension, compression, shear, bolt bearing and adhesively bonded scarf joints over the temperature range 117K to 589K (-250°F to 600°F) is underway. The capability to determine strength, strain to failure, Poisson's ratio and modulus for tensile coupons has been demonstrated. ITTRI compression tests have been performed at RT and 589K (600°F) and sandwich beam compression data obtained at 117K (-250°F) and RT are reported herein. Preliminary data from constant amplitude fatigue tests on HTS/PMR-15 indicate a shortening of fatigue life with increasing temperature.

A comprehensive program to assess the effects of moisture, temperature, thermal cycling and shuttle fluids on the thermal, physical and mechanical properties of Gr/PI is underway and preliminary data obtained to date have not uncovered any environmental degradation problems that would preclude the use of Gr/PI in advanced space transportation systems.

A new hybrid, anisotropic quadrilateral finite element which accounts for bending-extensional coupling and recovery of layer stresses has been evaluated and the results indicate the element has broad application to advanced composite structures at elevated temperatures. Work underway to develop a preliminary design of a Gr/PI aft body flap for the Space Shuttle Orbiter indicates that much of the structure will be minimum gage sandwich construction due to the low load levels.

Stiffened and sandwich designs of compression and shear panels are being investigated. Optimum compression crippling specimens have been designed and are currently being fabricated and will be tested at temperatures up to 589K (600°F). Current effort on the shear panels is focussing on definition of the test method and analysis of various structural concepts.

3.0 MATERIALS SCREENING

3.1 Graphite/Polyimide Composite Materials

John G. Davis Jr. and W.T. Hodges

Fourteen resin matrix composite materials have been screened to obtain a preliminary estimate of their maximum continuous service temperature for 500 hours. The initial goal was to identify at least three resin matrix composites with 589K(600°F) service capability for 500 hours. Except for one polyphenylquinoxelene, all matrices were polyimides. Limits of 2.07MPa (300psi) and 5.6K (10°F) per minute were imposed on the maximum allowable pressure and temperature rise rate, respectively, that could be utilized to fabricate laminates. The purpose of this restriction was to insure that cure cycles compatible with most of the aerospace industry's existing capability would be used in laminate fabrication.

Figure 3.1-1 lists the composite materials, the prepregger and fabricator. HR600 and THERMID 600 are the same chemical formulation which was produced first by Hughes and subsequently by Gulf under license with Hughes. Each fabricator had prior experience with the material that was purchased. Laminates obtained from all fabricators were subjected to visual and ultrasonic C-scan inspection to detect cracks, delaminations and porosity. Inspection indicated that four of the composite materials did not warrant testing: HTS/P13N, HTS/PPQ,HTS/SKYBOND703 and HTS/SKYBOND710. The marginal quality of these four sets of laminates was attributed to the fabrication constraints and should not deter consideration of these materials for applications where higher pressures or temperature rise rates are permissible.

Flexure specimens with nominal dimensions of 7.620 X 1.270 X 0.152 cm (3.000 X .500 X .060 in.) and short beam shear specimens with nominal dimensions of 1.613 X 0.635 X 0.318 cm (.635 X .250 X .125 in.) were machined from the remaining sets of laminates and exposed in atmospheric pressure air maintained at 505K(450°F), 533K(500°F), 561K(550°F) or 589K(600°F) for periods up to 500 hours. The flexure specimens were tested in accordance with ASTM standard D790 utilizing a 32-to-1 span-to-depth ratio, whereas the short beam shear specimens were tested in accordance with ASTM standard D2344 utilizing a 4-to-1 span to depth ratio. Specimens tested at elevated temperature were maintained at the test temperature for 15 minutes prior to the initiation of loading.

Figure 3.1-2 lists the test results. Interlaminar shear strength data on undirectional specimens indicate that HTS/HR600, HTS/NR150B2 and HTS/THERMID 600 composites retained approximately

one half of their initial room temperature strength when tested at 589K (600°F) after 500 hours exposure in 589K (600°F) air. Composites with PMR-15 and LARC 160 matrix materials exhibit similiar degradation after 125 hours exposure. Flexure strength data on unidirectional specimens indicate that HTS/NR150B2 and HTS/THERMID 600 composites retain approximately eighty percent of their initial room temperature strength when tested at 589K (600°F) after 500 hours exposure in 589K (600°F) air; whereas, HTS/LARC 160 and HTS/PMR-15 retain approximately two thirds of their initial strength after 125 hours and 500 hours exposure, respectively.

Examination of the data in figure 3.1-2 leads to the conclusion that HTS/NR150B2 and HTS/THERMID 600 are the only materials with 500-hour service capability at 589K (600°F). However, HTS/LARC 160 and HTS/PMR-15 test data indicate 125-hour service capability at 589K (600°F) and 500-hour service capability at 561K (550°F). The other materials listed in figure 3.1-2 did not indicate as much potential for either 561K (550°F) or 589K (600°F) service.

Based on the results reported herein, NR150B2, LARC 160, PMR-15 and THERMID 600 polyimide matrix composites were selected for detailed evaluation including development of fabrication procedures and specifications.

FIBER	MATRIX	PREPREGGER	FABRICATOR
HTS	F178	HEXCEL	ROCKWELL INTERNATIONAL
HTS	HR600	HUGHES	HUGHES
HTS	KERMID 601	FERRO	BOEING AEROSPACE
HTS	LARC 160	NASA LANGLEY	NASA LANGLEY
T300(a)	NR 150A/B	HEXCEL	LOCKHEED
HTS	NR 150B2	WHITTAKER R&D	WHITTAKER R&D
HTS	P13N	TRW SYSTEMS	TRW SYSTEMS
HTS	PMR-15	TRW EQUIPMENT	TRW EQUIPMENT
HTS	PMR-15-II	NASA LEWIS	NASA LEWIS
HTS	PPQ	SRI	SRI
HTS	SKYBOND 703	COMPOSITE HORIZONS	COMPOSITE HORIZONS
HTS	SKYBOND 710	DUPONT	GENERAL DYNAMICS
HTS	THERMID 600	HUGHES	HUGHES
HTS	X5230	NARMCO	ROCKWELL INTERNATIONAL

(a) STYLE 1133 FABRIC

Composite Material	Exposure and Test Temperature									
	294K (70°F)		505K (450°F)		533K (500°F)		561K (550°F)		589K (600°F)	
	Strength									
	MPa	(KSI)	MPa	(KSI)	MPa	(KSI)	MPa	(KSI)	MPa	(KSI)
HTS/F178	90	13.1	48	6.9	14	2.0	11	1.6		
HTS/HR600	82	11.9			61	8.9	53	7.7	40	5.8
HTS/KERMID 600	54	7.9	34	4.9	14	2.1				
HTS/LARC 160	96	13.9					47	6.8	48	6.9a
T300/NR 150A/B	51	7.4	28	4.1	23	3.4	10	1.5		
HTS/NR 150B2	70	10.2			41	5.9	39	5.7	34	5.0
HTS/PMR-15	111	16.1			54	7.8	48	6.9	59	8.5b
HTS/PMR-15-II	93	13.5					36	5.2	28	4.0
HTS/THERMID 600	83	12.1			60	8.7	51	7.4	41	6.0
HTS/X5230	28	4.0	17	2.5	11	1.6				

(a) Exposure limited to 125 hours.　　(b) CELION/PMR-15 exposed for 125 hours.

Figure 3.1-2 - Effect of 500 hours exposure to elevated temperature air

(A) Interlaminar shear strength of unidirectional laminates.

Composite Material	Exposure and Test Temperature									
	294K (70°F)		505K (450°F)		533K (500°F)		561K (550°F)		589K (600°F)	
	Strength									
	MPa	(KSI)	MPa	(KSI)	MPa	(KSI)	MPa	(KSI)	MPa	(KSI)
HTS/F178	1590	231	1260	182	620	90	190	27		
HTS/HR600	1840	267			1150	166	800	116	630	92
HTS/KERMID 600	900	131	700	102	400	58	200	29		
HTS/LARC 160	2130	309					1440	209	1370	199(a)
T300/NR 150A/B	730	106	460	66	420	61	190	27		
HTS/NR150B2	1430	207			1300	189	1210	175	1140	165
HTS/PMR-15	1430	208			1840	267	1240	180	970	140
HTS/THERMID 600	1280	185			1170	169	990	144	1040	151
HTS/X5230	1570	227	1010	146	990	144	130	19		

(a) Exposure limited to 125 hours.

Figure 3.1-2 – Concluded

(B) Flexure strength of unidirectional laminates.

3.2 Structural Adhesives

Donald Progar, Terry St. Clair and Paul Hergenrother[*]

A high temperature structural adhesive is needed in the CASTS Project for joining composite to composite and composite to titanium and for bonding honeycomb sandwich. The bonded structural elements must have operational capability to temperatures as high as 589K (600°F) for a minimum of 125 hours. The ideal adhesive system should exhibit a unique combination of favorable properties which includes autoclave processability, low volatiles content, large-area honeycomb sandwich bonding capability, and high mechanical properties under a variety of environmental conditions.

The primary objective of the initial structural adhesive effort was to screen suitable candidates for 589K performance. The most promising candidates would then undergo more comprehensive evaluation and eventual development into practical structural adhesive systems. The following adhesives were initially selected for screening: American Cyanamid's FM-34, Dupont's modified NR-150B2G, Rhodia's Nolimid A-380, NASA Langley's LARC-13, and polyphenylquinoxalines (PPQ). The Nolimid A-380 has since been taken off the market and has been dropped from the program. Although all the candidate adhesives except LARC-13 have undergone prior evaluation in titanium-to-titanium bonding for 589K use in various laboratories, it was necessary to reevaluate the adhesives with composite adherends. In addition to satisfactorily passing a series of strength and environmental tests the adhesives had also to be capable of being produced in large quantities for commercial use.

No restrictions were placed upon process conditions during the initial part of the screening phase. As work progressed however, PMR-15 composites became the prime adherend and the cure temperature was restricted to 602-616K (625-650°F). Higher temperatures frequently resulted in degradation of PMR-15 composite properties.

The results of the evaluation of each candidate adhesive are discussed in the following sections, except for modified NR150B2G which is discussed in section 12.1. The major portion of adhesive evaluation was confined to lap shear specimen configurations, due primarily to the availability of high quality composite adherends. Variations in the thickness and strength of the composite adherends often resulted in large variations in adhesive performance.

---

[*] Research Associate, Virginia Polytechnic Institute and State University, Blacksburg, VA (NASA Grant NSG-1124).

FM-34 Polyimide

FM-34 adhesive film consists of a polyimide prepolymer filled with aluminum powder and supported on style 112 glass carrier cloth. It is supplied by Bloomingdale Department of the American Cyanamid Company. The adhesive cures by a condensation reaction under moderate time/pressure profiles in a temperature range from 533K (500°F) to 644K (700°F). Volatiles are released during cure. Higher cure temperatures favor maximum strength at the higher operating temperatures. Because excellent metal-to-metal lap shear strengths were reported by the vendor (ref. 3.2-1) and in the literature (ref. 3.2-2), this adhesive was considered a good candidate for the CASTS Project, where high performance composite-to-composite and composite-to-metal bonded systems were required.

The technology developed for bonding metal-to-metal with FM-34 was used as the starting point to develop a process for bonding composite to composite and composite to metal. The vendor's recommended bonding and curing procedures for metal-to-metal bonds covered a broad range; however, a typical bonding cycle involved a 30-minute heat-up to 561K (550°F) and a 90-minute cure at temperature under 280 kPa (40 psi) pressure. For optimum results service temperatures over 561K (550°F) but below 644K (700°F), the cure temperature was recommended to be the same as the service temperature.

The standard lap shear specimen configuration and test procedures for metal-to-metal bonds as given in ASTM D-1002 were used. The specimen consisted of two 2.5 cm (1.0 in.) wide by 6.5 cm (4.0 in.) long adherends bonded with a 1.3 cm (0.5 in.) overlap. Room temperature (RT) and 589K (600°F) tests were conducted on an Instron Universal Testing machine at a cross-head speed of 0.1 cm/min. (0.05 in./min.). A clamshell quartz-lamp furnace was used for elevated temperature tests. Specimens were soaked 10 minutes at temperature prior to testing. Test temperature, lap shear strength and type of failure were recorded for each specimen.

The composite adherends used in this study were fabricated at NASA-Langley from HTS graphite and PMR-15 polyimide (HTS/PMR-15) in unidirectional and pseudoisotropic (0°, +45, 90°, -45°, -45°, 90°, +45°, 0°) layups. The laminates were nominally 0.28 cm (0.11 in.) and 0.15 cm (0.06 in.) thick, respectively. Short beam shear (SBS) strengths were determined for unidirectional composites at RT and 589K using ASTM D-2344. The RT SBS strengths ranged from 78.6 MPa (11,400 psi) to 88.3 MPa (12,080 psi) and at 589K from 27.2 MPa (3,950 psi) to 54.7 MPa (7,940 psi). Ultrasonic inspection was also used to determine the quality of the laminates.

Composite-to-composite lap shear test specimens were fabricated (in-house by bonding two pieces of composite 10.2 cm x 11.9 cm (4.00 in. x 4.68 in.) with a 1.3 cm (0.5 in.) overlap and the 0° fiber direction parallel to the 10.2 cm (4.00 in.) dimension. Specimens similar to those described are shown in figure 3.2-1(a). Individual 2.5 cm (1.0 in.) wide specimens were cut on a diamond wheel saw. Titanium (6Al-4V)-to-titanium (Ti/Ti) specimens were fabricated by bonding two "four-fingered coupons" with a 1.37 cm (0.50 in.) overlap, then shearing the coupons into individual 2.5 cm (1.0 in.) wide specimens (figure 3.2-1(b)).

Variables investigated during this bonding study included use of vacuum and no vacuum, bonding pressures, cure temperatures and times, postcure temperatures, and several primer and adhesive batches.

Procedures for titanium and composite surface preparation, priming, bonding of lap shear specimens, and bonding of flatwise tensile (FWT) specimens are given in Appendix 3.2-A.

Lap shear strengths and process conditions for Ti/Ti bonds are given in figure 3.2-2. The RT strengths for those processed with and without vacuum are within the normal scatter obtained for such tests ad the values agree with those reported by other investigators (ref. 3.2-2). The results of the 589K (600^oF) tests (with and without vacuum) are as good as or better than most of the data reported in the literature, which range from 7.6 MPa (1100 psi) to 13 MPa (1900 psi) (ref. 3.2-2). All failures at 589K were cohesive. Since the strengths obtained for these titanium bonds compared favorably with those reported in the literature, the same process was used for bonding composite adherends.

Lap shear strengths for bonded HTS/PMR-15 unidirectional composite are given in figure 3.2-3. The RT values for composite adherend specimens were 12 percent lower than the Ti specimens [21.08 MPa (3057 psi) versus 18.51 MPa (2685 psi)] with failure occurring in the composite. The test values obtained at 589K for the composite specimens were 11.6 percent less than the Ti values.

Lap shear strengths for titanium-to-HTS/PMR-15 crossply composite specimens are given in figure 3.2-4. Crossply composite (0°, $+45^o$, 90°, -45° -45°, 90°, $+45^o$, 0°) was used instead of unidirectional composite because the latter split during the bonding process due to stresses created by the differences between the coefficients of thermal expansion of the titanium and composite. The RT values were low [average 9.10 MPa (1323 psi)] compared to those obtained for unidirectional composite-to-composite specimens [21.20 MPa (3057 psi), figure 3.2-2], even though all the failures were in the composite. The 589K strengths were almost 17 percent lower [10.5 kPa (1525 psi) versus 12.6 kPa (1828 psi)], although the type of failure was similar, that is, primarily cohesive.

Flatwise tensile (FWT) specimens were fabricated and consisted of 7.6 cm x 7.6 cm x 0.2 cm (3.0 in. x 3.0 x 0.06 in.) HTS/PMR-15 crossply facesheets bonded with FM-34 to 2.5 cm (1 in.) thick glass/polyimide honeycomb core (HRH-327-3/16-6.0). Steel blocks, 7.6 cm x 7.6 cm x 2.5 cm thick, were bonded in a separate process to the sandwich structure with a modified epoxy adhesive (HYSOL EA 9628). Figure 3.2-5 gives the results of RT FWT strengths for several process conditions. From the data presented, the rate of cure did not appear to affect the FWT strengths. Processing with or without vacuum did not affect FWT strengths, as indicated by the insignificant differences in the results. Specimen number 7, which exhibited 100 percent composite failure did not test the full capability of the adhesive. These FWT strengths were very encouraging, especially considering the size of the specimen that was fabricated and tested. Procedures are being developed for testing FWT specimens at 589K (600°F).

Lap shear and FWT specimens will be fabricated for thermal aging and thermal cycling studies. Thermal aging studies will be performed by exposing specimens at 589K for extended periods up to 250 hours and testing at RT and 589°K. Thermal cycling studies will be performed using a thermal cycle yet to be determined; the specimens will be tested at RT and 589K after 10, 50, and 100 cycles.

LARC-13 Polyimide

In order to fabricate structural components from polyimide composites, an adhesive was needed which would be compatible chemically and thermally with polyimide resin matrices. The high temperature [533-539K (500-600°F)] adhesives currently being marketed were developed for bonding either steel or titanium. The LARC-13 (LARC for Langley Research Center) system was designed to be chemically similar to existing high temperature composite matrix materials and to interact with these materials during a bonding cycle to form a continuous bond of very high strength. Also, commercially available high temperature adhesives cannot be used in large area bonding because they give off large amounts of volatiles during the cure process. LARC-13, because of its curing chemistry, evolves relatively few volatiles.

Because of its unique molecular building blocks, LARC-13 adhesive is easily processed at 340 kPa (50 psi) autoclave conditions and has been successfully used to bond a variety of adherends. These include bonding composite to composite, composite to honeycomb, composite to titanium, and titanium to titanium. The 533K (500°F) lap shear strengths of titanium-to-titanium and composite-to-composite bonds made with LARC-13 were essentially the same as room temperature strengths. Also, the shear failures in the composite bonds at room temperature (RT) were within the composite and not at the bond line. This indicated that the LARC-13 adhesive was stronger in shear than the composite itself.

The chemical structure of LARC-13 is shown below:
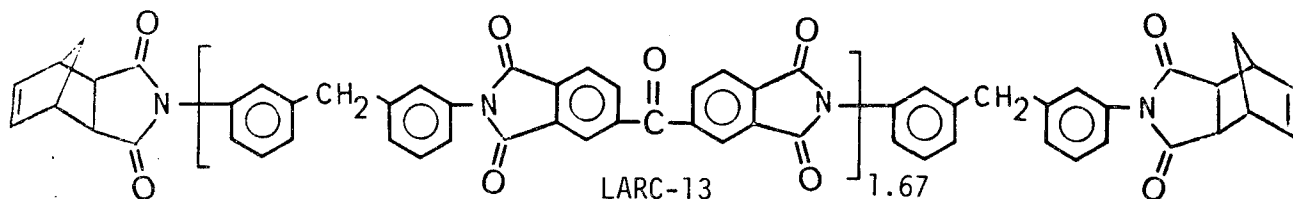
Composite-to-composite lap shear specimens were bonded both with and without a processing vacuum to determine the effect of the vacuum on lap shear strength (LSS) of the bonded joint. The results, given in Figure 3.2-6, show that no significant differences in LSS, either at room temperature (RT) or at 589K (600°F), were observed with specimens processed either with or without vacuum. The failures at RT were primarily in the composite first ply, while the failures at 589K (600°F) were primarily cohesive.

The LSS values at 589K (600°F) shown in figure 3.2-6 were lower than the goal of 14 MPa (2000 psi) set forth in the CASTS Adhesive Screening Task. The low values at 589K (600°F) resulted from the lower glass transition temperature (T_g) of the adhesive when cures were held to 589-602K (600°-625°F). Therefore, the effect of postcuring at 616K (650°F) in order to increase the T_g of the adhesive was studied. The data in Figure 3.2-7 show that the higher postcure temperature increased the LSS at 589K (600°F) by 68 percent [from 8.1 MPa (1174 psi) to 13.6 MPa (1979 psi)]. Thus, the CASTS' goal for LARC-13 adhesive has been achieved. The variation in LSS values at RT was probably due to differences in composite surfaces. While the RT strengths were lower than desired, the LARC-13 bond appeared to be stronger than the strength of the composite adherend itself. Thus, this bonding process seemed to give the best compromise between RT and 589K (600°F) strengths for overall CASTS objectives.

Lab procedures for LARC-13 synthesis, composite surface preparation and priming, tape preparation, bonding and postcuring are given in Appendix 3.2-B.

LARC-13 Ti/Ti bonds will be made and tested at RT and 589K. Composite-to-composite bonded specimens will be fabricated for the thermal aging studies. Flatwise tensile specimens using HTS/PMR-15 facesheets and glass/PI honeycomb core will be fabricated for the thermal aging and thermal cycling studies.

Polyphenylquinoxalines (PPQ)

The purpose of this study was to evaluate PPQ as high temperature structural adhesives for joining titanium-to-titanium (Ti/Ti), titanium-to-composite (Ti/C), composite-to-composite (C/C), and honeycomb sandwich bonding.

Polyphenylquinoxalines were prepared in solution in high molecular weight forms from the reaction of aromatic bis(o-diamines) and aromatic bis(phenyl-α-diketones). These materials have displayed excellent potential for use as high temperature structural adhesives for joining Ti/Ti and honeycomb sandwich structure (refs. 3.2-3 and 3.2-4). Solutions of the PPQ were used to prepare adhesive tapes which were dried to low volatile content levels (<1%). These tapes were processable by virtue of the thermoplastic nature of PPQ. Several PPQ were screened in preliminary adhesive work. One polymer, PPQ 413, from the reaction of 3,3',4,4'-tetraaminobiphenyl and 1,3-bis(phenylglyoxalyl)benzene was selected for more comprehensive adhesive work. The effect of polymer molecular weight, tape volatile content, Ti surface treatment, various composite adherends, and processing parameters on lap shear strength was determined by testing specimens under a variety of conditions. The lap shear data are summarized in Figure 3.2-8. The PPQ 413 used in this work had an inherent viscosity, as measured on a 0.5% solution in m-cresol at 298K (77°F), of 0.61 dl/g and a glass transition temperature (as measured bv differential scanning calorimetry at a heating rate of 20K/minute) of 591K (604°F). A 112, A1100 tape containing ∿4% volatiles was used for Ti/Ti bnding. The composite adherends were brush-coated with the PPQ solution and stage-dried up to 18 hours at 458K (365°F). The Ti surface treatment was phosphate fluoride while the composite adherends were mildly abraded. The bonding conditions were as follows: 1.4 MPa (200 psi) pressure applied at ambient temperature, the temperature increased to 672K (750°F) during 0.5 hr., held at 672K for 20 minutes, and cooled under pressure to 533K (500°F).

Honeycomb sandwich specimens were fabricated using HTS/NR-150B2 face sheets and glass polyimide core under the following conditions: 0.34 MPa (50 psi) pressure applied at ambient temperature, the temperature increased to 644K (700°F) during 0.5 hours, held at 644K (700°F) for 20 minutes, and cooled under pressure to 533K (500°F). The sandwich specimens exhibited good filleting of the adhesive and RT flatwise tensile strength of 3.1 to 3.4 MPa (455 to 500 psi) with the failure occurring at the interface of the PPQ and the composite.

After significant PPQ adhesive work was performed with no restriction placed on processing temperature, HTS/PMR-15 was selected as the composite adherend for future adhesive work. The use of this adherend restricted the adhesive bonding temperatures to 602K (625°F) to 616K (650°F) because higher temperatures frequently resulted in degradation of composite properties. The PPQ used to obtain the adhesive data in figure 3.2-8 was modified through solvent enhancement to accommodate the new processing temperature limit. In addition, a new acetylene-terminated PPQ was screened in adhesive work. Preliminary adhesive results are reported in figure 3.2-9.

In summary, polyphenylquinoxalines with low volatile contents provided excellent adhesive performance when processed at 672K (750°F) under 1.4 MPa. However, the commercial unavailability and the high processing temperature of PPQ has discouraged further evaluation in this program. The acetylene-terminated PPQ at this stage of development is expensive and in limited supply. Therefore, no further work is planned with it on the CASTS program.

The excellent performance of PPQ 413 for joining Ti/Ti, Ti/C, C/C, and honeycomb sandwich bonding is presented in ref. 3.2-5.

Appendix 3.2-A

Surface preparation

A. Titanium (6 Al-4V)

1. Remove markings by washing with wipers soaked in acetone.

2. **Abrade the surface with a light grit blast using 120 aluminum oxide and 600-7.** **kPa (80-100 psi) air pressure. Hold panel 20 - 25 cm (8-10 in.)** **from the nozzle.**

3. Wash grit blasted surface with alcohol and air dry.

4. Phosphate-fluoride preparation

    a. Alkaline clean: Immerse parts in alkaline cleaner (Sprex AN-9, 30.1 g/ℓ) for 15 minutes at 355K (180°F).

    b. Rinse: Use hot water from faucet.

    c. Pickle: Immerse for 2 minutes at RT in solution containing 31 ml/ℓ of 48% hydrofluoric acid; 352 ml/ℓ of 70% nitric acid.

    d. Rinse: Use water at RT.

    e. Phosphate fluoride treatment: Soak parts for 2 min. at RT in solution containing:

        50.5 g/ℓ trisodium phosphate

        20.6 g/ℓ potassium fluoride

        29.3 g/ℓ of 48% hydrofluoric acid

    f. Rinse: Use water at RT

    g. Hot water soak: Use deionized water at 339K (150°F) for 15 minutes.

    h. Final rinse: Use deionized water at RT for 1 minute.

    i. Dry: Place in forced air oven at 339K (150°F) for 30 minutes.

    j. Prime within 8 hours.

B. Composite

    1. Abrade the surface with a light grit blast using 120 aluminum oxide and approximately 600-700 kPa (80-100 psi) air pressure. Hold panel 20-25 cm (8-10 in.) from the nozzle. Remove enough material to just dull the surface (2 to 3 sweeps across the bond area.)

    2. Wash the grit blasted area in alcohol using a light brushing with an acid or similar brush.

    3. Dry panel overnight (approx. 16 hours) in a forced air oven at 473K (392°F).

    4. Store in desiccator until primed.

C. Polyimide/glass honeycomb core

    1. Wash in alcohol.

Priming

    1. Dilute 3 parts (by weight) of BR-34 (81% solids) with one part (by weight) of BR-34 thinner.

    2. For titanium and composite bond areas: Apply a very thin coat of primer (approx. 2.5×10^{-3} cm (0.001 in.)) with acid brush or appropriate method such that blisters do not form during staging. For honeycomb 8 cm x 8 cm (3 in. x 3 in.): Dip honeycomb into primer to a depth of 0.16 cm (1/16 in.) on both sides to be bonded.

    3. Air dry 30 minutes.

    4. Place coated panel in forced air oven at RT, heat to 373K (212°F), hold for 30 minutes, heat to 483K (410°F), hold 45 minutes.

    5. Remove parts and store in sealed plastic bag in a desiccator.

Bonding of Lap Shear Specimens

    1. Cut sufficient FM-34 adhesive tape to cover area to be bonded.

    2. Place adherends with adhesive in fixture and maintain 1.27 cm (0.5 in.) overlap, locate thermocouples close to bond area.

3. Process with or without vacuum (fig. 3.2-10). If vacuum bag is used, apply full vacuum throughout bonding procedure.

4. Apply 1.38 MPa (200 psi) pressure either by press or autoclave.

5. Heat from RT to 616K (650°F) at a heating rate of 5K/min. (9°F/min.), hold 90 minutes.

6. Cool to 423K (300°F) @ 3K/min. (5°F/min).

7. Release pressure and vacuum, if used, and remove assembly.

8. Place unrestrained bonded panels in a forced air oven for postcure. Heat from RT to 616K (650°F) and hold for 2 hours.

9. Cool oven to RT at 1.5K/min. (3°F/min) and remove.

10. Cut panels into individual 2.3 cm (1 in.) wide specimens.

Bonding FWT Specimens for RT Testing

1. Arrange adhesive, primed honeycomb core, primed facesheets as shown in figure 3.2-11. Place thermocouples in close proximity to bond areas.

2. Process with or without vacuum. If vacuum is used, apply full vacuum throughout bonding procedure.

3. Apply 300 kPa (50 psi) pressure either by press or autoclave.

4. Heat from RT to 616K (650°F) at a heating rate of 5 K/min. (9°F/min.) and hold 90 minutes.

5. Cool to 423K (300°F) at 3K/min (5°F/min).

6. Release pressure and vacuum, if used, and remove.

7. Place unrestrained sandwich structure in forced air oven for postcure. Heat from RT to 616K (650°F) and hold for 2 hours.

8. Cool oven to RT at 1.5 K/min. (3°F/min.) and remove.

9. Grit blast surfaces of 7.6 cm x 7.6 cm x 2.54 cm thick (3 in. x 3 in. x 1 in.) steel blocks and wash with alcohol.

10. Cut modified epoxy adhesive film (HYSOL EA9628) into two 7.6 cm (3 in.) squares and place between facesheets and grit blasted metal blocks.

11. Place in press and apply 172 kPa (25 psi).

12. Heat from RT to 394 K (250°F) in 30 minutes, hold 15 minutes.

13. Cool to RT and remove.

Appendix 3.2-B

I. <u>Surface preparation of composite adherend</u>

1. Abrade the surface with a light grit blast using 120 aluminum oxide and 600-700 kPa (80-100 psi) air pressure. Hold panel 20-25 cm (8-10 in.) from the nozzle. Remove sufficient material to dull the surface (usually, several sweeps across the bond area).

2. Wash the grit blasted area with alcohol using a light sweeping action of an acid or similar brush.

3. Dry panel overnight (approx. 16 hrs.) in a forced air oven at 473K (392°F).

4. Store in desiccator until priming is initiated.

II. <u>Procedure for Synthesis of LARC-13 Adhesive</u>

<u>Materials</u>

Flake benzophenone tetracarobxylic dianhydride (BTDA) was used as-received from Gulf Chemicals, m.p. 488-493K (419° - 428°F). The use of powdered BTDA is not recommended. It has a tendency to form lumps in solution which are hard to break up and dissolve. The flake BTDA dissolves more slowly but doesn't lump and is easier to handle.

Burdick and Jackson glass-distilled dimethylformamide (DMF) was used as received.

Nadic anydride was used as received from Eastman or Fallek, m.p. 435-437K (324 - 327°F).

3, 3'-methylenedianiline (3, 3'-MDA) was used as received from Ash-Stevens (Detroit), m.p. 348-351K (167 - 172°F).

Alcan MD 105 aluminum powder of 325 mesh was used as received.

<u>Procedure</u>

A wide-mouth resin kettle was used for convenience so that viscous liquid could easily be removed after the aluminum powder had been added. No heat or cooling was required since the reaction exotherm was slight. Ambient conditions were employed throughout and a nitrogen atmosphere was not necessary. Proportions can be varied as needed. MDA, 118.8 grams, was dissolved in 445 grams of DMF in a one-liter resin kettle using mechanical stirring. 73.8 grams of nadic anhydride and 120.75 grams of

flake BTDA were added, each in ten equal portions over a period of 5-6 hours as follows. A tenth-portion of nadic anhydride and a tenth-portion of BTDA were added in succession. After these were partially dissolved so the next addition would not cause undissolved material to lump, a second portion of each was added. The time between additions increased since material in later additions dissolved more slowly in the more concentrated media. Stirring was continued until complete solution was obtained, usually 24-36 hours. Then, 134 grams of aluminum powder was added in 10 equal portions. The solution can be stored in a refrigerator at approximately 277K (40°F).

III. Priming with LARC-13 Adhesive

1. Brush on a thin coat 2.5×10^{-3} cm (0.001 in.) of LARC-13/30% aluminum powder with an acid or similar brush.

2. Air dry 30 min.

3. Place in forced air oven and heat to 348K (167°F), hold 30 min.

4. Heat to 373K (212°F), hold 30 min.

5. Heat to 408K (275°F), hold 2 hrs.

6. Cool in oven to RT and store in desiccator for indefinite period.

IV. Preparation of LARC-13 Adhesive Tape

1. Stretch 112, A1100 E glass cloth on frame.

2. Brush LARC-13/30% aluminum mixture onto cloth.

   a. Dry overnight under fume hood.

   b. Place in oven, heat from RT to 408K (275°F), hold 2 hrs.

   c. Cool slowly to RT.

3. Coat both front and back surface of cloth with LARC-13 mixture.

   a. Air dry 1 hr.

   b. Place in oven, heat from RT to 348K (167°F), hold 15 min.

   c. Heat to 373K (212°F), hold 30 min.

   d. Heat to 408K (275°F), hold 2 hrs.

   e. Cool slowly to RT.

4. Repeat 3.

5. Repeat 3 again except continue step d. heating to 430K (315°F), hold 30 min.

   a. Heat to 452K (352°F), hold 30 min.

   b. Cool slowly to RT.

6. Adhesive tape thickness should be 0.025-0.030 cm (0.010-0.012 in.).

V. Bonding of Lap Shear Specimens with LARC-13

   A. Bonding procedure

      1. Cut adhesive tape to cover area to be bonded.

      2. Place adherends and adhesive tape in fixture to maintain 1.3 cm (0.5 in.) overlap. Locate thermocouple as close to bond area as possible.

      3. If vacuum bag is used, pull full vacuum throughout bonding process.

      4. Heat at 5K/min. from RT to 477K (400°F), hold 1 hour; heat to 580K (585°F), hold 1 hour; apply 344 kPa (50 psi); heat to 602K (625°F), hold 1 hour.

      5. Cool slowly to 423K (300°F), release vacuum and pressure. Remove for postcure.

   B. Postcure

      1. Place unrestrained bonded panels in forced air oven, heat from RT to 616K (650°F), hold approximately 16 hours (overnight).

      2. Cool in oven to RT, remove and cut into 2.54 cm (1 in.) wide specimens.

References

3.2-1. American Cyanamid Co. Inc., Technical Bulletin "FM-34 Adhesive Film," Jan. 25, 1968.

3.2-2. Pike, R. A., Novak, R. C.; and DeCrescente, M. A.: An Evaluation of FM-34 Polyimide Adhesive, 30th Anniversary Technical Conference, Reinforced Plastics/Composite Institute, The Society of Plastics Industry Inc., Section 18-G, pages 1-10, 1975.

3.2-3. Hergenrother, P. M.: High Temperature Organic Adhesives. SAMPE Quarterly, vol. 3, no. 1, 1971, pp. 1-16.

3.2-4. Hergenrother, P. M.: Polyphenylquinoxalines - High Temperature Thermoplastics. Polymer Eng. and Sci. vol. 16, no. 5, 1976, pp. 303-308.

3.2-5. Hergenrother, P. M.; and Progar, D. J.: High Temperature Composite Bonding with PPQ Sci. Adv. Mat'r and Process Eng. Series (SAMPE), vol. 22, 1977, pp. 211-226. Adhesives Age, vol. 20, no. 12, 1977, pp. 38-43.
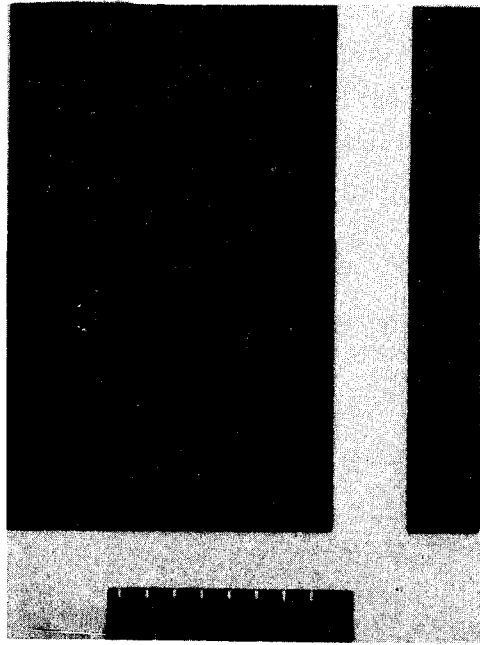
(a) Composite to composite.

(b) Titanium to titanium.

Figure 3.2-1 - (a) Composite configuration.
(b) Titanium four-fingered coupon configuration.

Process Conditions		Test Temp.	Lap Shear Strength		Type failure[a]
Cure	Postcure		MPa	psi	
5K/min., 1.38 MPa (200 psi); RT → 616K (650°F), hold 90 min.	Unrestrained RT → 616K (650°F), hold 2 hr	RT	18.3 17.9 24.1 23.7 20.8 21.6 AV. 21.1	2650 2650 3500 3440 3025 3130 AV.3057	50% Coh 50% Coh 100% Coh 100% Coh 100% Coh 100% Coh
		589K (600°F)	11.9 13.1 12.8 12.6 AV. 12.6	1730 1900 1855 1825 AV.1828	100% Coh 100% Coh 100% Coh 100% Coh
Full vacuum; 5K/min.; 1.38 MPa (200 psi), RT → 616K (650°F), hold 90 min.	Unrestrained RT → 616K (650°F), hold 2 hr	RT	19.8 19.9 20.5 19.0 AV. 19.8	2880 2890 2980 2760 AV.2878	100% Coh 90% Coh 100% Coh 100% Coh
		589K (600°F)	11.4 11.1 11.3 11.9 AV. 11.4	1660 1610 1640 1725 AV.1659	100% Coh 100% Coh 100% Coh 100% Coh

a. Coh: cohesive failure

b. Phosphate-fluoride surface preparation

Figure 3.2-2 – Lap shear strengths and process conditions for FM-34 bonded Titanium (6Al-4V)[b].

Test temperature	Lap shear strength		Type failure[a]
	MPa	psi	
RT	16.7	2430	100% Comp. 1st layer
	19.2	2780	100% Comp. 1st layer
	17.6	2560	100% Comp. 1st layer
	16.9	2460	100% Comp. 1st layer
	18.1	2620	100% Comp. 1st layer
	20.5	2975	95% Comp. 1st layer, 5% Coh
	20.6	2990	100% Comp. 1st layer
	AV. 18.5	AV. 2685	
589K (600°F)	13.4	1650	100% Coh
	11.0	1600	100% Coh
	11.2	1625	100% Coh
	10.7	1550	100% Coh
	11.2	1620	100% Coh
	11.7	1700	100% Coh
	11.0	1600	100% Coh
	10.8	1570	100% Coh
	AV. 11.1	AV. 1615	

a. Comp. 1st layer: failure in the first ply of the composite;
   Coh: cohesive failure

b. Process conditions: 5K/min., 1.38 MPa (200 psi), RT → 616K (650°F), hold 90 min.; postcure: unrestrained, RT → 616K (650°F), hold 2 hours.

Figure 3.2-3 - Lap shear strength for FM-34 bonded HTS/PMR-15 unidirectional composite.[b]

Test temperature	Lap shear strength		Type failure[a]
	MPa	psi	
RT	9.8	1430	100% Comp. 1st layer
	8.4	1220	100% Comp. 1st layer
	9.1	1320	100% Comp. 1st layer
	AV. 9.1	AV. 1323	
589K (600°F)	10.6	1545	90% Coh, 10% Comp. 1st layer
	9.6	1400	70% Coh, 30% Comp. 1st layer
	10.9	1580	80% Coh, 20% Comp. 1st layer
	10.9	1585	60% Coh, 40% Comp. 1st layer
	AV. 10.5	AV. 1527	

a. Comp. 1st layer: failure in the first ply of the composite;
    Coh: cohesive failure

b. Process conditions: 5K/min., 1.38 MPa (200 psi), RT → 616K (650°F),
    hold 90 min.; postcure: unrestrained,
    RT → 616K (650°F), hold 2 hours

Figure 3.2-4 – Lap shear strength for FM-34 bonded titanium (6Al-4V)-to-
HTS/PMR-15 crossply composite.

Spec. No.	Process conditions	FWT strength		Type failure
		MPa	psi	
1	344 kPa (50 psi), RT → 616K (650°F) in 40 min., hold 90 min.	4.0	590	85% Comp. failure, 15% core to adhesive
2	344 kPa (50 psi), RT → 616K (650°F) in 55 min., hold 90 min.	4.3	622	60% Comp. failure, 40% core to adhesive
3	344 kPa (50 psi), RT → 616K (650°F) in 60 min., hold 90 min.	4.2	604	70% Comp. failure, 30% core to adhesive
4	344 kPa (50 psi), RT → 616K (650°F) in 60 min., hold 90 min.	4.3	624	40% Comp. failure, 60% core to adhesive
5	Full vacuum and 344 kPa (50 psi), RT → 616K (650°F) in 35 min., hold 90 min.	4.3	620	50% Comp. failure, 50% core to adhesive
6	Full vacuum and 344 kPa (50 psi), RT → 616K (650°F) in 40 min., hold 90 min.	4.2	613	50% Comp. failure, 50% core to adhesive
7	Full vacuum and 344 kPa (50 psi), RT → 616K (650°F) in 50 min., hold 90 min.	3.6	524	100% Comp. failure

a. Flatwise Tensile specimens: 7.6 cm x 7.6 cm (3 in. x 3 in.)

b. Honeycomb: HRH-327-3/16-6.0, polyimide/glass

c. Crossply layup: $0°$, $+45°$, $90°$, $-45°$, $-45°$, $90°$, $+45°$, $0°$.

Figure 3.2-5 – Room temperature flatwise tensile strength[a] of PI/glass honeycomb[b] bonded to HTS (crossply)/PMR-15 facesheets[c] with FM-34.

Vacuum[a]	Test temp. K(°F)	Lap shear strength MPa (psi)		Type failure[b]
No	RT	20.6	(2995)	50% Comp. 1st surface, 50% Coh
	589 (600)	9.8	(1425)	10% Comp. 1st surface, 90% Coh
Yes	RT	21.6	(3130)	100% Comp. 1st surface
		21.8	(3160)	100% Comp. 1st surface
		AV. 21.7	(3145)	
	589 (600)	8.1	(1175)	100% Coh
		9.1	(1320)	100% Coh
		AV. 8.6	(1248)	

a. Processing conditions: 5K/min. (9°F/min.), RT to 477K (400°F), hold 1 hr; heat to 580K (585°F), hold 1 hr; apply 344 kPa (50 psi); heat to 602K (625°F), hold 1 hr; postcure: no vacuum, unrestrained, RT to 589K (600°F), hold approx. 16 hrs

b. Comp. 1st surface: failed by removing matrix polymer and graphite fibers; Coh: cohesive

c. HTS/PMR-15 unidirectional composite, nominal 0.28 cm (0.110 in.) thick; LARC-13, 30% aluminum on 112,A1100 E glass cloth.

Figure 3.2-6 – Effect of vacuum processing on the lap shear strength of LARC-13 bonded composite specimens[c].

Postcure[a]	Test temp. K (°F)	LSS MPa (psi)		Type failure[b]
Unrestrained, RT to 589K (600°F), hold ≈ 16 hrs	RT	18.7	(2625)	100% Comp. 1st ply
		17.3	(2510)	100% Comp. 1st ply
		21.6	(3130)	100% Comp. 1st ply
		21.8	(3160)	100% Comp. 1st ply
		AV. 19.7	(2856)	
	589 (600)	7.9	(1150)	100% Coh
		7.2	(1050)	100% Coh
		8.1	(1175)	100% Coh
		9.1	(1320)	100% Coh
		AV. 8.1	(1174)	
Unrestrained, RT to 616K (650°F), hold ≈ 16 hrs	RT	16.0	(2320)	100% Comp. 1st ply
		16.0	(2320)	100% Comp. 1st ply
		16.1	(2330)	100% Comp. 1st ply
		15.5	(2250)	100% Comp. 1st ply
		20.5	(2980)	100% Comp. 1st ply
		20.0	(2900)	100% Comp. 1st ply
		18.4	(2670)	100% Comp. 1st ply
		13.5	(1960)	100% Comp. 1st ply
		AV. 17.0	(2466)	
	589 (600)	12.2	(1775)	50% Comp. 1st ply, 50% Coh
		13.7	(1990)	50% Comp. 1st ply, 50% Coh
		13.1	(1900)	50% Comp. 1st ply, 50% Coh
		14.8	(2150)	70% Comp. 1st ply, 30% Coh
		15.2	(2200)	50% Comp. 1st ply, 50% Coh
		14.5	(2100)	50% Comp. 1st ply, 50% Coh
		11.3	(1645)	50% Comp. 1st ply, 50% Coh
		14.3	(2075)	75% Comp. 1st ply, 25% Coh
		AV. 13.6	(1979)	

a. Processing conditions: full vacuum, 5K/min. (9°F/min.), RT to 477K (400°F), hold 1 hr; heat to 580K (585°F), hold 1 hr; apply 344 kPa (50 psi), heat to 602K (625°F), hold 1 hr Postcure as above.

b. Comp. 1st ply: failed by removing matrix polymer and graphite fibers. Coh: cohesive failure

c. LARC-13, 30% aluminum on 112,A1100 E glass cloth; HTS/PMR-15 unidirectional composite, nominal 0.28 cm (0.110 in.) thick

Figure 3.2-7 - Effect of postcure on lap shear strength of LARC-13 bonded composite specimens[c].

Adherend	RT	Avg. lap shear strength, MPa (psi)			
		561K(550°F) no exposure	561K(550°F) after 300 hr @ 561K(550°F), air	589K(600°F) no exposure	589K(600°F) after 300 hr @ 589K(600°F), air
Ti/Ti	30.3(4400)	17.2 (2500)	16.5 (2400)	2.1 (300)*	3.4 (500)*
Ti/C(710 HTS)**	13.8(2000)	21.4 (3100)	19.3 (2800)	11.1 (1600)	13.1 (1900)
C/C(710 HTS)**	20.7(3000)	29.0 (4200)	17.9 (2600)	20.7 (3000)	14.5 (2100)
C/C(NR- 150B2 HTS)**	41.4(6000)	25.5 (.3700)	22.7 (3300)	19.3 (2800)	17.2 (2500)

* Thermoplastic failure

** All composite adherends exhibited predominantly shear-type failure in the composite.

Figure 3.2-8 - Preliminary PPQ lap shear data.

Resin	112-A1100 Tape	Bonding Conditions	Avg. Lap Shear Strength, MPa (psi)		Failure
			RT	589K(600°F)	
PPQ 413	Wet, 30 phr Al	RT→602K (625°F) under 2.1 MPa (300 psi), hold 2 hr.	28.4 (4120)	11.4 (1650)	RT, 70% composite; 589K(600°F), 50% Composite
Acetylene-Terminated PPQ	Dry, 30 phr Al	RT→602K (625°F) under 0.34 MPa (50 psi), hold 2 hr.	22.2 (3220)	12.1 (1750)	RT, 100% composite; 589K (600°F), 50% Composite

Table 3.2-9.- Preliminary PPQ composite-to-composite (HTS/PMR-15) Lap Shear Data.
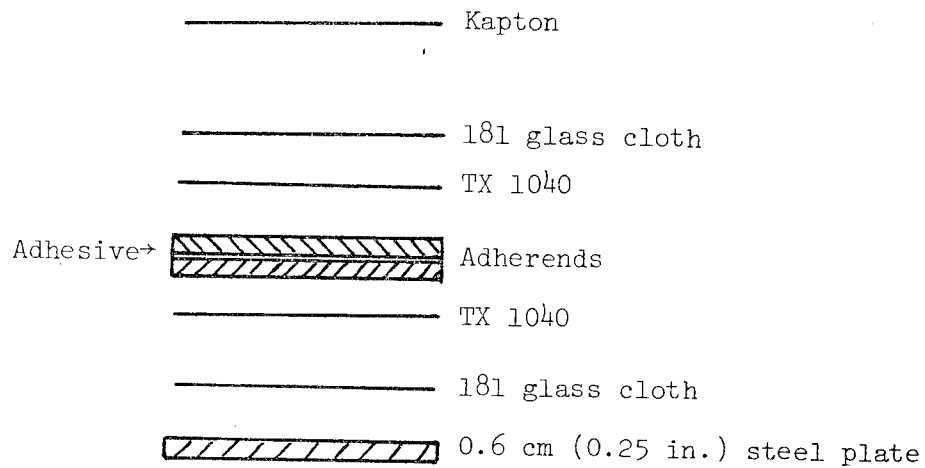
Figure 3.2-10 — Vacuum bag layup used for bonding studies.

← HTS/PMR-15 crossply facesheet
← BR-34 primer

← FM-34 adhesive

← BR-34 primed, HRH-327-3/16-6.0 glass/PI honeycomb core

← FM-34 adhesive

← BR-34 primer
← HTS/PMR-15 crossply facesheet
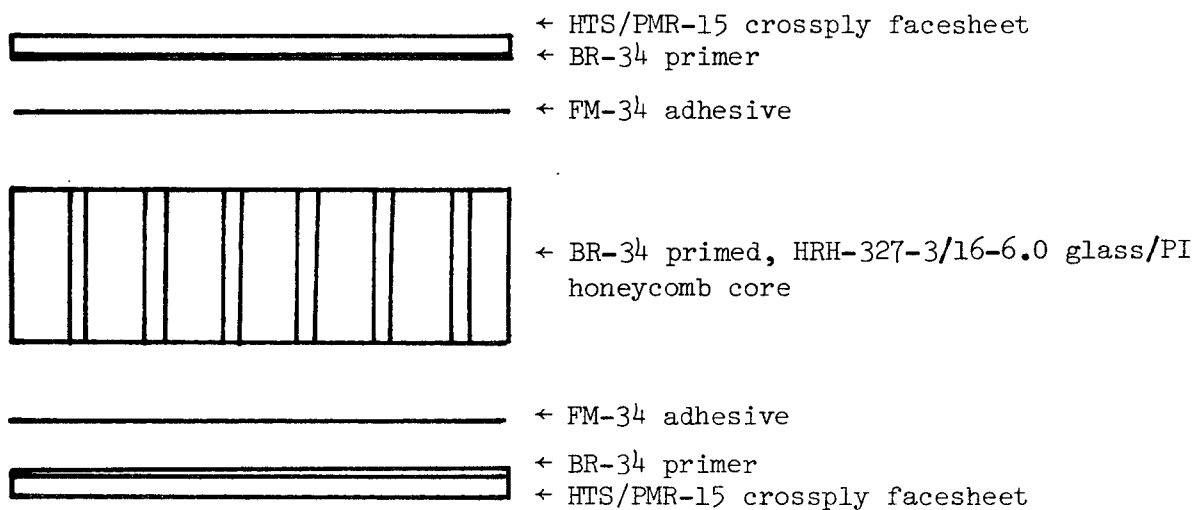
Figure 3.2-11 - Arrangement for bonding FWT specimen.

3.3   Adhesives for Bonding RSI

Russell Hopko

Effective utilization of Gr/PI composite materials in aerospace structures is dependent upon identification or development of an adhesive for bonding reusable surface insulation (RSI) to the exterior surface of the structure. The adhesive must be capable of operating between 117K and 644K (-250°F and 700°F) and must be compatible with manufacturing, inspection and repair criteria imposed on aerospace vehicles such as the Space Shuttle Orbiter.

A contract (NAS1-15152) has been awarded to Rockwell International to perform the required research and development effort. The master schedule and tasks to be performed are shown in figure 3.3-1. The contract is scheduled to be completed in December 1978.

Screening of materials effort has identified a modified RTV elastomeric adhesive which will be evaluated in more detail. The adhesive is essentially a low volatile content RTV which, contains a glass resin as part of its formulation.

TASK DESCRIPTION	MONTHS AFTER GO-AHEAD

The Gantt chart "MONTHS AFTER GO-AHEAD" spans columns 1 through 12.

TASK I   CRITERIA
- 1.1 CRITERIA DEVELOPMENT — CRITERIA DEFINED
- 1.2 CANDIDATE MATERIALS
- 1.3 QUALITY ASSURANCE

TASK II   BONDING EVALUATION METHODS
- 2.1 MATERIALS
- 2.2 BONDING

TASK III   SCREENING AND SELECTION
- 3.1 SCREENING
- 3.2 SELECTION — 1ST PROJECT REVIEW (SELECTION)

TASK IV   SYSTEM DEVELOPMENT AND CHARACTERIZATION
- 4.1 MATERIALS PROPERTIES
- 4.2 BOND PROPERTIES
- 4.3 REFURBISHMENT

TASK V   SPECIFICATIONS
- 5.1 PROCUREMENT
- 5.2 PROCESS

TASK VI   PROGRAM MANAGEMENT
- 6.1 MANAGEMENT

  2ND PROJECT REVIEW
- 6.2 REPORTING
- FINAL REPORT — DRAFT — FINAL

Figure 3.3-1   Master program schedule

4.0 IN-HOUSE MANUFACTURING DEVELOPMENT

4.1 PMR-15 Prepreg Development
Robert M. Baucom

The purpose of this task was to develop an in-house capability for the manufacture of consistent high quality graphite fiber-reinforced polyimide prepreg. Research was performed to evaluate prepregging parameters, develop quality control methods, establish specifications for vendor supplied prepreg, and manufacture prepreg for in-house cure cycle development and laminate fabrication.

The custom-made drum winding equipment shown in Figure 4.1-1 with a 58 cm (23 in) diameter by 147 cm (58 in) length drum has been adapted to manufacture prepreg sheets up to 185 cm (73 in) long by 145 cm (57 in) wide. Hercules HTS, Celion 3000, and Celion 6000 graphite fibers have been prepregged with PMR-15, LARC 160, and NR150B2 polyimide resin matrix systems. The majority of in-house prepreg research has been concentrated on the Hercules HTS/PMR-15 system.

Exceptional prepreg quality has been obtained with the PMR-15 system by formulating resin in-house to assure maximum prepreg shelf life and by metering the resin onto the fiber with a solvent pump. This provides excellent resin content control, distribution, and reproducibility. Resin delivery to the drum is accomplished by pumping the resin through a hollow handled brush which spreads a uniform film of resin that improves fiber wetting while minimizing non-uniform fiber wicking. The resin solution has approximately 50 percent solvent and 50 percent PMR-15 solids by weight in the as-prepregged state. The excess solvent is driven off by heating the prepreg on the drum to a temperature of 311K (100°F) with a bank of infrared heat lamps (shown in Figure 4.1-1). Prepreg reproducibility with this system has been excellent, as shown in Figure 4.1-2. The prepreg had an average resin content of 29.5±2% and fiber areal weight of 276±11 gm/m^2 (34±1 gm/ft^2). A photograph of a typical section of a sheet of HTS/PMR-15 prepreg made in-house is shown in Figure 4.1-3.

In addition to the continuation of the fabrication of HTS/PMR-15 prepreg for in-house requirements for the CASTS project, development work is planned for the manufacture of prepreg utilizing various graphite fibers as a reinforcement for LARC-160, NR150B2, and other selected resin systems.
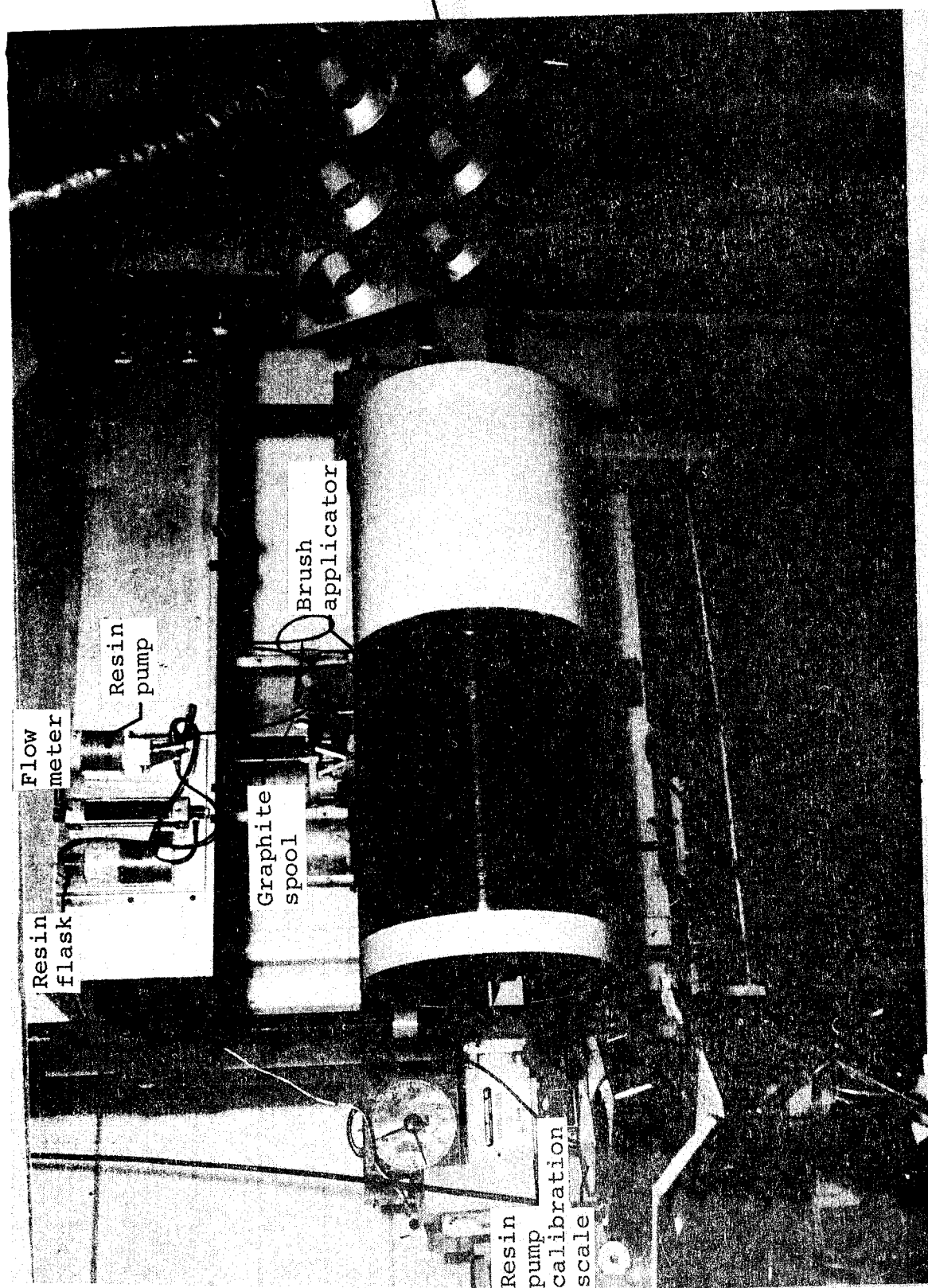
Figure 4.1-1 – Prepreg manufacturing equipment.

Applied resin wt, grams R_w	Applied fiber wt, grams F_w	Fiber wt, % F w/o	Resin wt, % R w/o	Total wt after drum cure, grams	Prepreg width, cm	Prepreg area wt, gm/cm^2
433	277	56.13	29.64	556	82.80	0.03543
430	282	56.74	29.03	553	81.28	0.03590
438	278	55.94	29.83	546	82.40	0.03496
431	285	56.94	28.83	568	83.82	0.03576
428	285	57.11	28.66	569	83.32	0.03582
448	283	55.82	29.95	575	82.85	0.03662
431	279	56.42	29.35	563	81.36	0.03651
426	280	56.80	28.97	554	81.58	0.03583
445	277	55.46	30.31	572	81.58	0.03700

NOTE: The length of each sheet was 189.5 cm (74.61 inches).

The number of tows/cm was approximately 2.20.

Area Weight = Weight of Prepreg Sheet ÷ Area of Prepreg Sheet

Figure 4.1-2 – In-house prepreg data.
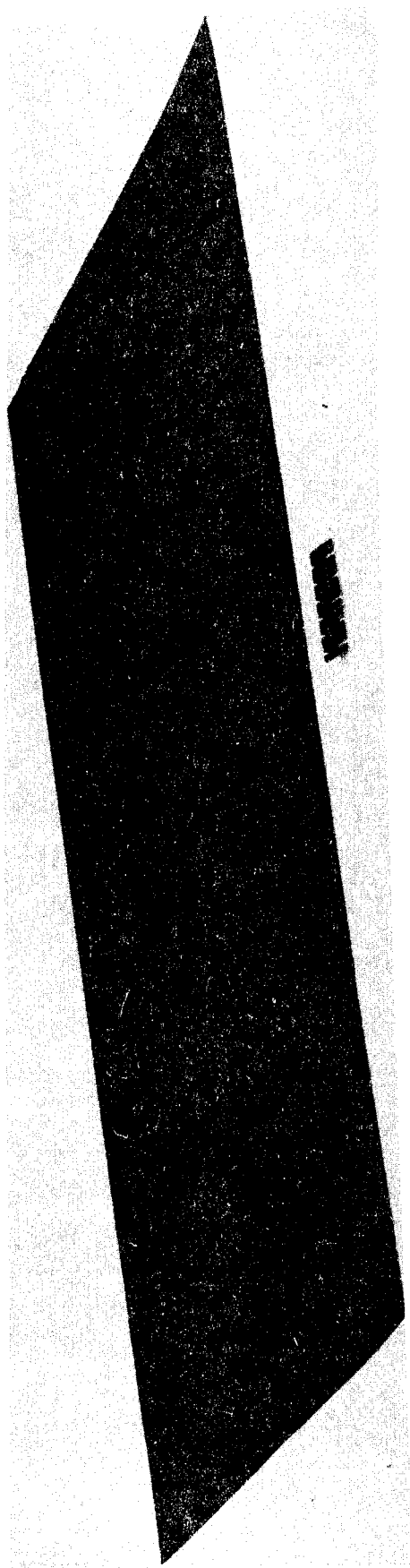
Figure 4.1-3 - Typical in-house fabricated prepreg sample.

4.2 Graphite/Polyimide Fabrication Methods
Robert Baucom, Robert Jewell, and Terry St. Clair

The purpose of this task is to establish optimum laminate processing parameters for graphite fiber reinforced PMR-15 and LARC-160 polyimide resin. This study was initiated by conducting a comprehensive literature survey on the subject materials followed by procurement of prepreg from commercial vendors and monomers, solvent, etc. from chemical suppliers. Preliminary attempts to cure vendor-supplied and in-house manufactured prepreg resulted in laminates of marginal quality. More detailed materials procurement and prepreg process control specifications were needed in order to provide consistent quality prepreg for determination of properties.

PMR-15

The Polymeric Monomeric Reactant (PMR) resin system was originally formulated by NASA-Lewis Research Center (ref. 4.2-1). These studies revealed general processing trends for fiber reinforced PMR-15. During a typical cure cycle for this material, solvent removal takes place in the 366 - 423 K (200-300°F) range followed by imidization in the 423 - 477 K (300-400°F) range. Melt flow of the resin then takes place between 519 and 533K (475-500°F) and finally, extended crosslinking completes the cure in the 589-602 K (600 - 625°F) range. Initial difficulties in curing commercially supplied HTS graphite/PMR-15 material was traced to the substitution of mixed solvents in the prepreg by the vendor. Standardization of methanol as the prepregging solvent provided a solution to this problem. Subsequent problems with specifications were solved by rigidly defining prepreg requirements in materials specification documents (Appendices 4.2-A and 4.2-B).

The initial vacuum bagging sequence and baseline cure cycle for HTS/ PMR-15 laminate fabrication are shown in Figure 4.2-1 and 4.2-2, respectively. The heat-up rate to 522°K (480°F) proved not to be critical; only a light vacuum, 17 kPa (5 in Hg), was needed to preclude the removal of low molecular weight species in tandem with the low boiling methanol. This was followed by a hold at 522°F (480°F) to allow partial resin gelation prior to application of pressure. This hold time depends on several factors: chemical purity of the monomers, temperature exposure during resin formulation, molecular weight distribution of the prepregged resin, and residual solvent. In general, use of higher purity monomers result in a higher molecular weight level during resin mixing, which requires the application of pressure and full vacuum early at the 522°K (480°F) hold level. Residual solvents require the application of pressure and full vacuum later in the 522°K hold period. It was critically important that the pressure be applied during this period at the correct hold time to reduce the vapor pressure of cyclopentadiene below the point where it becomes a gas and blisters the laminate. After pressure and full vacuum are applied the temperature was increased to 602°K (625°F) and held for a minimum of 2 hours in order to allow sufficient crosslinking of the polymer for the glass transition temperature, T_g, to exceed 589°K (600°F). The laminate was then cooled down at a rate not exceeding 2.5K/min

until a temperature of 355°K (180°F) was reached. The pressure and temperature were then reduced and the laminate was removed.

This cure cycle has been routinely applied to the fabrication of high quality HTS/PMR-15 unidirectional laminates not exceeding a thickness of 0.2 cm (0.06 in). Unidirectional HTS-PMR-15 laminates up to 0.5 cm (0.2 in) in thickness are also easily produced. Mixed results have been obtained in the fabrication of multidirectional laminates that exceed 0.2 cm (0.06 in) in thickness. Ultrasonic C-scans and photomicrographs for typical HTS/PMR-15 unidirectional and isotropic laminates are shown in Figure 4.2-3. The unidirectional laminate C-scan results are substantially better than the isotropic laminates at the same ultrasonic gain level, probably due to the presence of extensive microcracking in the isotropic laminates. Attempts to reduce the level of microcracking by using very slow cool down rates continue. Also, a determination is being made to establish the impact of microcracking on applicable mechanical properties before and after exposure to elevated temperatures.

There may be an effect of the fiber itself on the processability of graphite reinforced PMR-15. This preliminary conclusion is based on similar cure cycles on HTS I, HTS II, and Celion 6000 sized with NR150B2 resin graphite fiber reinforced PMR-15. Early results obtained with HTS I/PMR-15 were generally satisfactory when the baseline cure cycle was used. The long term stability of this fiber at elevated temperatures was quite variable, so it was replaced with the more stable HTS II fiber. Laminates produced from HTS II/PMR-15 prepreg have exhibited mixed results under ultrasonic C-scan inspection. The sound transmission in thick panels [> 0.15 cm (0.06 in)] made from this prepreg appears to be somewhat more attenuated than in similar HTS I/PMR-15 panels. Further, several Celion 6000/PMR-15 laminates have been produced with excellent C-scan results in thick (> 0.2 cm (0.06 in)) multidirectional laminates. The effect of the graphite fiber type on laminate quality will be investigated further.

LARC-160

LARC-160, developed at NASA-Langley, is a modification of the well-known PMR-15 polyimide resin. Since the resin is a liquid in the neat form, the LARC-160 system makes possible the fabrication of solventless prepreg with good tack and drape at room temperature. These properties are important considerations when selecting a resin to be used in the fabrication of large graphite reinforced polyimide parts such as those proposed for CASTS.

Commercialization of LARC-160 has begun and prepreg can currently be obtained from several companies. (The LARC-160 neat resin can be formulated by most prepreg vendors and is also available from some resin manufacturers.) The commercially available graphite/LARC-160 prepreg is primarily made using hot-melt techniques, but it can also be made with solvent casting techniques. Unidirectional tape as well as woven goods are available.

The cure cycle that has been developed for LARC-160 is similar to those for other addition-type polyimides. During a typical cure the graphite/ LARC-160 lay-up is "B-staged" under partial vacuum [7-14 kPa (2-4 in Hg)] for one hour at 436°K (325°F) in order to allow the monomeric reactants to form oligomeric imide chains. During this imidization step, condensation by-products, water, and ethanol are lost, resulting in a well-consolidated laminate. Care must be exercised during this step by limiting the number of plies of bleeder material to prevent excessive flow of the resin. The temperature of the laminate is then increased to 602 K (625°F) at a rate of 2.6 (5°F) per minute. During this heat-up, autoclave pressure of 1.4 MPa (200 psi) is applied at 547 K (525°F). The final cure temperature of 602 K (625°F) is held for two hours, after which the laminate is cooled down at a rate of 2.6 K (5°) per minute to ambient temperature and removed from the autoclave or press. The cure profile for HTSI/LARC-160 is shown in Figure 4.2-4.

The mechanical properties obtained from in-house fabricated and test specimens are given in figure 4.2-5. The ultrasonic C-scans of these laminates indicate that they are well consolidated and essentially void free. These results have been verified by taking photomicrographs of cross sections of typical unidirectional and isotropic laminates.

Thick section laminates have been successfully fabricated from HTSI/ LARC-160, both in-house and under contract. Flat laminates 0.64 cm (0.25 in) thick with a unidirectional lay-up pattern have been fabricated in-house and hat sections with a net section thickness of 0.95 cm (0.38 in) have been fabricated under contract. The quality of both of these laminates has been verified by ultrasonic C-scan inspection.

REFERENCES

4.2-1   Cavano, P. J., "Resin/Graphite Fiber Composites", NASA CR 121275,
        March 15, 1974.

APPENDIX 4.2-A

SPECIFICATION LARC P-01

GRAPHITE/POLYIMIDE PREPREG

1.   SCOPE AND CLASSIFICATION

1.1   Scope. This specification establishes the requirement for graphite reinforced polyimide prepreg sheets.

1.2   Classification. The material covered by this specification shall be of one type and shall be identified as LARC-P-01.

2.   APPLICABLE DOCUMENTS

2.1   The following documents form a part of this specification to the extent specified on the date of the request for quotation to the National Aeronautics and Space Administration, Langley Research Center, Hampton, Virginia 23665.

SPECIFICATIONS

    NASA

        LARC-R-02 Polyimide, Impregnating

STANDARDS

    Federal

        FED-STD-406 Plastics, Methods of Testing

    Hercules

        HD-SG-2-6001B Test Methods for Determining Physical Properties of Carbon and Graphite Tows

        HG-SG-2-6006C Test Methods for Determining Properties of Carbon and Graphite Prepregs

LARC-P-01

PUBLICATIONS

NFPA SPD-1-C. Fire Protection Guide on Hazardous Materials.
National Fire Protection Association, 1975.

3. REQUIREMENTS

3.1 Material. The material shall consist of collimated graphite
fibers impregnated with polyimide resin.

3.1.1 Graphite. The continuous filament graphite fiber twist-
free tow shall be in the as-produced, residue-free state without a coating
or resin sizing. The graphite fiber tow shall have a 2757 MN/m^2 (400 ksi)
minimum tensile strength and a 234 MN/m^2 (34×10^6 psi) minimum modulus of
elasticity. The tow tensile strength and modulus of elasticity shall be
determined in accordance with procedures 5.3.6 and 5.3.7 in Hercules
document HD-SG-2-6001B.

3.1.2 Resin. The resin shall meet the requirements set forth
in LARC-R-02 and shall be fully suitable for use in the manufacture of
structural laminates.

3.1.3 Prepreg. The graphite reinforced polyimide prepreg shall
be in the form of sheets with a nominal width of 30 cm. (12 in.) and a
nominal cured thickness (per ply) of .18 mm (.007 in.)
determined from a laminate processed at no greater than 1.7 kN/m^2
(250 psi) with a 60 percent fiber volume.

3.2 Properties of uncured prepreg.

49

3.2.1 <u>Physical properties</u>. The prepreg material shall meet the physical requirements outlined in Table I.

TABLE I

Property	Tolerance	Procedure
Volatile Content	12 ± 3% by wt.	4.6.2
Resin Solids Content	40 ± 4% by wt.	4.6.3
Resin Flow (LARC-R-02)	10 ± 5% by wt.	4.6.4
Tack	> 30 minutes	4.6.5
Gel Time (LARC-R-02)	1 minute minimum @ 450K (350°F)	4.6.6

3.2.2 <u>Shelf life</u>. The shelf life of the prepreg (computed from the date of manufacture) shall be such that the requirements set forth in 3.2.1 shall be met as follows: 120 days at 256K (0°F) or 90 days at 278K (40°F) or 7 days at 294K (70°F).

3.2.3 <u>Uniformity</u>. The graphite fiber tows shall be completely wetted and the areal density of the prepreg shall be 172^{+5}_{-10} gram/m2 ($16^{+5}_{-1.0}$ gram/ft^2). Misalignment of tows shall not be more than 1 tow per 10.2 cm (4 in.) of width of an individual sheet or tape or prepreg and the angle of misalignment shall not exceed 2 degrees.

3.2.6 <u>Hazardous materials</u>. If hazardous materials are included in the prepreg, all containers of such materials shall be labeled as outlined in the Fire Protection Guide on Hazardous Materials, NFPA SPP-1-C, 1975.

3.2.7 <u>Storage of material</u>. Immediately upon receipt, the material in its original sealed bag shall be placed in storage at a maintained temperature of 256K (0°F) or below. Material in the sheet form shall be stored horizontally. Material in the tape form shall be stored with the axis of the core or spool in a vertical position. When material is removed from the freezer it is brought to within 5K (10°F) of room temperature prior to opening the sealed bag. The amount required for use during the remainder of that work shift shall be cut from the sheet and the unused portion shall be replaced in its original bag, the bag resealed by heat application, and the material returned to storage without delay. Bags shall not remain open longer than 1 hour at any one time, and total elapsed open time shall not be more than 20 hours. Total elapsed time out of storage for any one sealed unit shall never exceed 14 days. At no time shall the material which is to be returned to storage be subjected to environmental temperatures greater than 303K (85°F).

3.2.8 <u>Storage history</u>. A log of the storage history shall be kept on each unit of material. Material that has exceeded the 14-day out-of-storage time or exceeded the 120-day in-storage time shall be retested for conformance to the flow, volatile content, and the flexural requirements of Tables I and II before being used for fabrication of structural parts. Allowable open time shall be considered as in-storage time.

3.2.9 <u>Product markings</u>. Product markings shall be in accordance with the preparation for delivery section of this specification. See 5.3.

3.3 <u>Properties of cured laminates</u>.

3.3.1 <u>Mechanical and physical properties</u>. The cured laminates shall meet the mechanical and physical property requirements of Table II.

TABLE II

Mechanical and Physical Properties of Cured Laminates

Property	Press or Vacuum Augmented Autoclave Cure Cycle		Test Procedure
	<u>RT</u>	<u>589K (600°F)</u>	
Long. Flexural Str., MN/m^2 (ksi), min. (LARC-R-02)	1447.9 (210.0)	1241.0 (180.0)	4.6.9
Short Beam Shear Str., MN/m^2 (ksi), min. (LARC-R-02)	96.5 (14.0)	41.4 (6.0)	4.6.10
Specific Gravity, minimum	(LARC-R-02)1.60	–	4.6.11
Resin Content, % by wt., minimum (LARC-R-02)	33	–	4.6.12
Fiber Volume, %, minimum	60 ± 3	–	4.6.12
T_g, K (°F) (LARC-R-02)	603 (625)	–	4.6.7
Void Content, % maximum	5	–	4.6.13

4.   QUALITY ASSURANCE PROVISIONS

4.1   <u>Responsibility for inspection</u>. Unless otherwise specified in the contract or order, the supplier is responsible for the performance

of all inspections and test requirements as specified herein. Except as otherwise specified, the supplier may use his own facilities or any commercial laboratory acceptable to Langley Research Center. Langley reserves the right to perform any or all of the inspections set forth herein where such inspections are deemed necessary to assure that the material to be furnished conforms to the prescribed requirements.

4.2   Inspection records. Inspection records of examinations and tests shall be kept complete and available to Langley. These records shall contain all data necessary to determine compliance with the requirements of this specification.

4.3   Classification of examinations and tests. The examination and tests of the material shall be classified as follows:

        a.   Qualification verification

        b.   Acceptance verification

        c.   Receiving inspection.

4.3.1   Qualification verification. Qualification verification shall consist of all the examinations and tests specified herein.

4.3.2   Acceptance verification. Acceptance verification shall be performed on representative samples of each unit of prepreg, and shall consist of the following:

        a.   Examination of product

        b.   Resin solids content

        c.   Volatile content

    d. Flow

    e. Tack

    f. Longitudinal flexural strength at room temperature

    g. Short beam shear strength at room temperature

    h. Glass transition temperature

4.3.3 <u>Receiving inspection</u>. Receiving inspection shall consist of an examination of the material and such sampling and verification of test data as deemed necessary.

4.4 <u>Sampling plan</u>. The material, as offered for acceptance by Langley, shall meet the requirements specified herein by random selection of one sealed unit of material per batch.

4.4.1 <u>Batch</u>. A batch shall consist of all material of the same type manufactured in one continuous, unchanged production run.

4.4.2 <u>Unit of product</u>. A unit of product shall consist of one sealed unit of material, and shall contain no more than 20 sheets.

4.5 <u>Test conditions</u>.

4.5.1 <u>Room temperature</u>. Unless otherwise specified, all tests shall be conducted at a temperature of $298K \pm 3$ ($77°F \pm 5$), and 50 percent ± 10 relative humidity.

4.5.2 <u>Exposure at 589K (600°F)</u>. Test panels shall be heated to $589K \pm 5$ ($600°F \pm 10$) within 15 minutes in a test chamber previously heated to temperature, held at temperature for $10 \, ^{+1}_{-0}$ minutes, and tested immediately.

4.5.3 Work and test area. The relative humidity of the layup and test area shall not exceed 60 percent.

4.6 Test methods.

4.6.1 Examination of product. The material shall be examined to verify that its markings, packaging, and all visual physical characteristics conform to the requirements of this specification.

4.6.2 Volatile content. The volatile content of the prepreg shall be determined as outlined below.

4.6.2.1 Test specimens. Test specimens shall be as follows:

a. Two 5.1 cm. (2-in.) square specimens (1.0 ± 0.2 grams) of prepreg are to be analyzed.

b. Release paper must be removed prior to analyzing. Any resin adhering to the release paper will be lost to the test.

4.6.2.2 Test procedure. The test procedure shall be as follows:

a. Condition new Gooch filtering crucibles in beaker containing concentrated HNO_3 for a minimum of 1 hour at $373 \pm 5^\circ K$ ($212 \pm 5^\circ F$). Wash with water, dry in oven at $367 \pm 3^\circ K$ ($200 \pm 3^\circ F$) and desiccate.

b. Weigh conditioned filtering crucible to the nearest 0.1 milligram (mg).

c. Carefully remove release paper from prepreg specimen and place specimen in tared crucible.

d. Weigh crucible containing specimen to the nearest 0.1 mg.

e. Condition cruicble and specimen in an oven at $367 \pm 3^{\circ}K$ $(392 \pm 3^{\circ}F)$ for 60 minutes followed by 30 minutes at $644 \pm 3^{\circ}K$ $(700 \pm 3^{\circ}F)$.

f. Remove crucible from oven, cool to room temperature in a desiccator, and reweigh.

g. Calculate volatiles content of prepreg as follows:

$$\text{Weight \% Volatiles} = \frac{W_2 - W_3}{W_2 - W_1} \times 100$$

where: W_1 = weight of empty conditioned filtering crucible, grams (g)

W_2 = original weight of crucible and specimen before heating, g

W_3 = final weight of crucible and specimen after heating, g

4.6.3 _Resin solids content._ The resin solids content of the prepreg shall be determined as outlined below.

4.6.3.1 _Test specimens._

a. Two 2.5 cm. (1 in.) by 5.1 cm. (2 in.) samples shall be taken from each end of a 2.5 cm (1 in.) by 30.5 cm. (12 in.) strip of prepreg.

b. Carefully remove release paper from the prepreg samples.

4.6.3.2 _Test procedure._

a. Weigh clean filtering crucible to the nearest 0.1 mg.

b. Place the prepreg specimens as prepared in 4.6.3.1 in tared crucible.

c. Weigh crucible containing specimen to the nearest 0.1 mg.

d. Add 150 ml NMP to a 250 ml beaker, place beaker on a steam bath and bring to a boil. (Beaker should be covered with a watch glass to minimize evaporation.)

e. Add prepreg sample to the hot MEK, being careful not to splash the hot NMP. Stir occasionally and let heat for ten minutes.

f. Transfer the NMP and fiber into the original tared filtering crucible positioned in a filtering flask with vacuum trap and vacuum pump.

g. Wash the fiber three times with methanol (absolute).

h. Remove the crucible containing fibers and dry in an oven maintained at $436 \pm 3°K$ ($325 \pm 3°F$) for 15 to 20 minutes.

i. Remove crucible from oven, cool in a desiccator, and weigh to the nearest 0.1 mg.

j. Calculate resin content as follows:

$$\text{Weight \% Resin} = \left[\frac{W_2 - W_3}{W_2 - W_1} \times 100 \right] - V$$

where: W_1 = weight of empty crucible, g

W_2 = original weight of crucible and specimen, g

W_3 = final weight of crucible and fibers, g

V = weight percent volatiles from 4.6.2, %.

4.6.4 <u>Flow</u>. Flow shall be determined as outlined below.

4.6.4.1 <u>Test specimens</u>.

a. Cut eight 10 cm. (4 in.) by 10 cm. (4 in.) plies of sample prepreg.

b. Cut six 10 cm. (4 in.) by 10 cm. (4 in.) plies of style 181 glass fabric.

c. Lay up the prepreg plies in a (0°/90°) laminate.

4.6.4.2 <u>Test procedure</u>.

a. Weigh the laminate fabricated in 4.6.4.1 to the nearest 0.1g.

b. Cut two 10 cm. (4 in.) by 10 cm. (4 in.) plies of porous Teflon coated glass release fabric. Place one ply on the top and one on the bottom of the laminate.

c. Place three plies each of style 181 glass cloth on the top laminate in 4.6.4.2.b.

d. Place the layup between 0.64 cm. (0.25 in.) thick aluminum caul plates which have been coated with Frekote 33 release agent.

e. Place entire assembly in a preheated 450K (350°F) press under pressure and hold for 1 hour.

f. Remove from oven, strip away bleeder and release fabric, clean excess resin from panel edges and weigh the panel to the nearest 0.1 g.

g. Calculate the resin flow as follows:

$$\text{Resin flow, percent} = \frac{W_1 - W_2}{W_1} \times 100$$

where: W_1 = original weight of prepreg layup, g.

W_2 = final weight of panel, g.

4.6.5   Tack.   Tack shall be determined as follows:

4.6.5.1 Test specimens.   The test specimen shall consist of two 5.1 cm. (2.0 in.) by 5.1 cm. (2.0 in.) prepreg squares.

4.6.5.2 Test procedure.

   a.   A stainless steel sheet, alloy 302 or equivalent with a commercial 2D finish, any thickness by 10.2 cm. (4.0 in.) by 20.3 cm. (8.0 in.), shall be cleaned to a water-break-free condition with chlorine-free powder and distilled water, then air dried at a temperature below 339K (150°F).

   b.   Mark a horizontal line across the plate width 4 inches from the end.

   c.   Mount the plate vertically.

   d.   Remove the release paper from one of the prepreg squares and then apply the side of the square from which the release paper was removed to the plate with the line at the bottom of the square. The unidirectional filament direction of the square shall be vertical and perpendicular to the line on the plate. A second square of prepreg shall be applied to the first square with the same fiber orientation.

   e.   Smooth out all creases and wrinkles with light up and down motion with the fingers and start a timing device to monitor the test.

   f.   An absence of movement of the squares on the steel plate after 30 minutes qualifies the prepreg for sufficient tack.

g. Repeat steps d through f for a duplicate tack test.

Success of both tests qualifies the prepreg for accepta-

ble tack.

4.6.6 Gel time. Gel time shall be determined as follows.

4.6.6.1 Test specimens. The test specimen shall consist of a small
piece of newly thawed material, approximately 0.64 x 0.64 cm. (0.25 x 0.25 in.),
between two glass slides.

4.6.6.2 Test procedure.

a. Preheat and stabilize a Fisher-Johns Melting Point

Apparatus at 450K (350°F).

b. Place the test specimen on the melting point block and

start a timing device.

c. Periodically apply light pressure to the top glass slide

with a small, blunt-end wooden stick.

d. The time at which no fiber or resin movement is detected

is the gel time.

4.6.7 Glass transition temperature. The glass transition tempera-
ture, Tg, shall be determined as follows.

4.6.7.1 Test specimen. A 0.64 x 0.64 cm. (0.25 x 0.25 in.) sample shall
be taken from a laminate fabricated as outlined in the following section, 4.6.8.

4.6.7.7 Test procedure.

a. The test specimen shall be placed on the stage of a Dupont 990

Thermomechanical Analyzer.

b. The Analyzer probe is weighted with approximately 5 gms of weight and placed in contact with the sample. Heat is then gradually applied to the system.

c. Probe displacement is monitored as the sample expands upon the application of heat.

d. The temperature at which the expansion curve for the sample changes slope is recorded as the glass transition temperature.

4.6.8 <u>Preparation of test panels</u>. Flat laminate test panels, as required, shall be fabricated using the processes and procedures described below. Total number of plies shall be dictated by the test specimen thicknesses specified in the following test methods.

4.6.8.1 <u>Panel layup</u>. Flat laminate test panels of appropriate size, but no smaller than 15 x 15 cm. (6 x 6 in.), shall be prepared by a parallel layup of unidirectionally oriented plies of the material. Dams shall be used around the perimeter of the panels to prevent fiber "wash-out". A release agent shall be used on the caul plate to prevent panel sticking. Bleeder shall consist of one ply of Mauchberg paper CW-1850 or style 181 fiberglass per every three plies of material, and the bleeder shall be divided evenly beneath and above the layup. The bleeder shall be separated both top and bottom from the material layup by a ply of perforated Teflon-coated fiberglass fabric and a ply of Celgard venting film. The Teflon-coated fiberglass fabric shall be in contact with the laminate on both top and bottom. A pressure plate of the same size as the basic laminate shall be used to minimize upper surface waviness. This plate shall be separated from the laminate by a thin film of Teflon or Mylar. A vacuum bag capable of withstanding long term exposure at 700K (800°F) shall be placed over the assembly and sealed on the edges with A-800 silicone sealant.

Figure 4.2-A-1 shows typical layup. Cure by either press cycle or vacuum augmented autoclave cycle.

4.6.8.2 Press cure. The layup as described in 4.6.8.1 shall be placed in heated platen press and cured using the following B-stage and cure cycle and a maximum pressure of 1724 kN/m^2 (250 psi) on the layup at all times during the cure cycle.

    -Apply 5 inches Hg vacuum

    -Heat laminate to 522K (480°F) at 6K (10°F)/min and hold for 30 minutes

    -Apply full vacuum and pressurize autoclave to 1724 kN/m^2 (250 psi).

    -Heat to 603K (625°F) min. under full vacuum and 1724 kN/m^2

    (250 psi) and hold for 3 hours

    -Cool to 356K (180°F) at 3K (5°F)/min. and remove vacuum and pressure

    -Cool to 311K (100°F) at .6K (1°F)/min. and remove laminate

4.6.8.3 Vacuum augmented autoclave cure. The layup as described in 4.6.8.1 shall be vacuum bagged and the entire assembly of caul plate, layup, vacuum bag, etc., shall be placed in an autoclave and cured using the cure cycle outlined in 4.6.8.2.

4.6.9 Longitudinal flexural strength.

4.6.9.1 Laminate preparation. Laminates shall be in accordance with 4.6.8.

4.6.9.2 Test specimens. Fibers are aligned parallel to the longitudinal axis. Specimen configuration is shown in Figure 4.2-A-2.

KAPTON BAG

PRESSURE PLATE

DAM

DAM

CAUL PLATE

A-800
SEALANT

GRAPHITE/POLYIMIDE

TEFLON COATED GLASS

181 GLASS CLOTH

TEFLON OR MYLAR
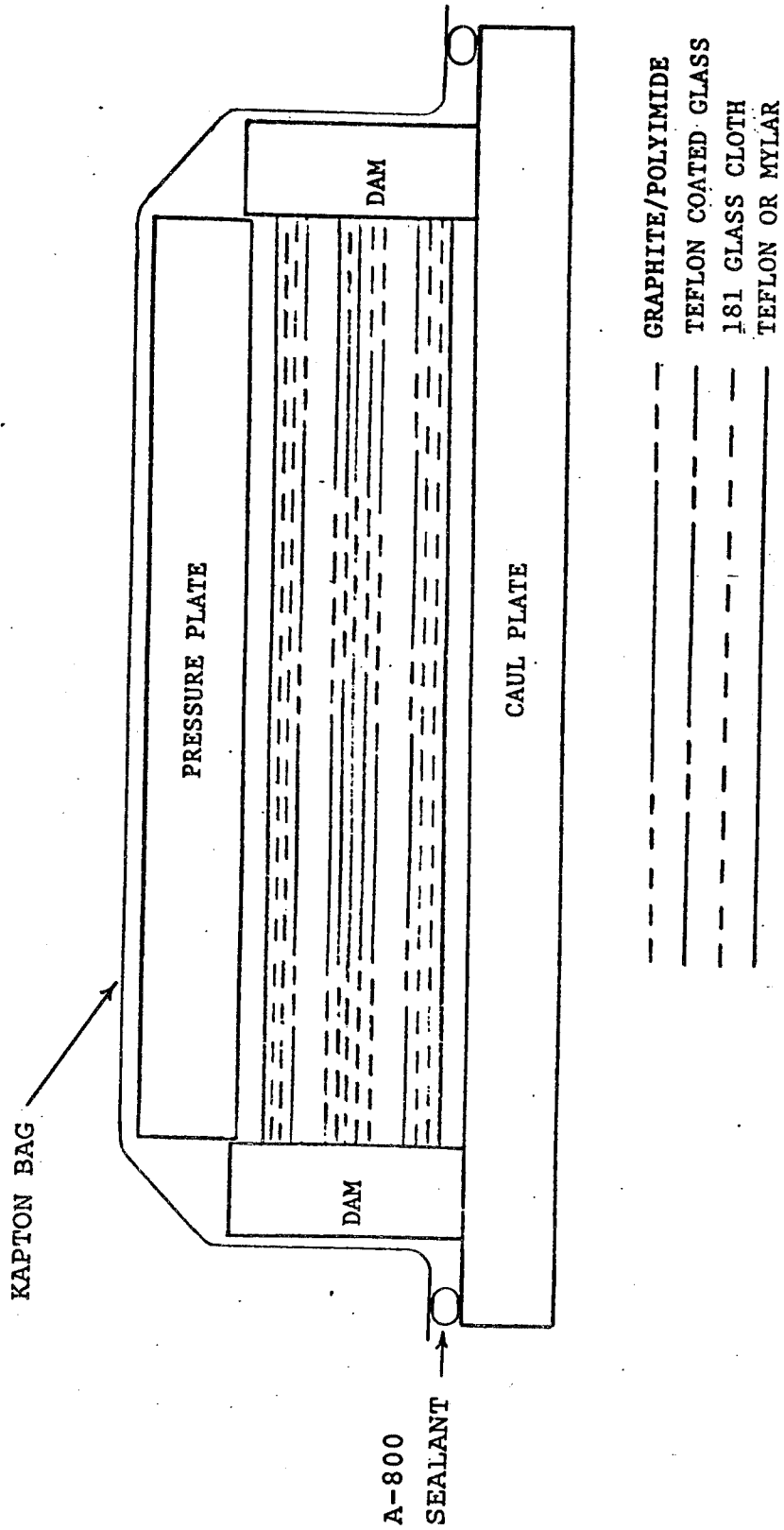
Figure 4.2-A-1. Layup of Unidirectional Graphite/Polyimide Panel.
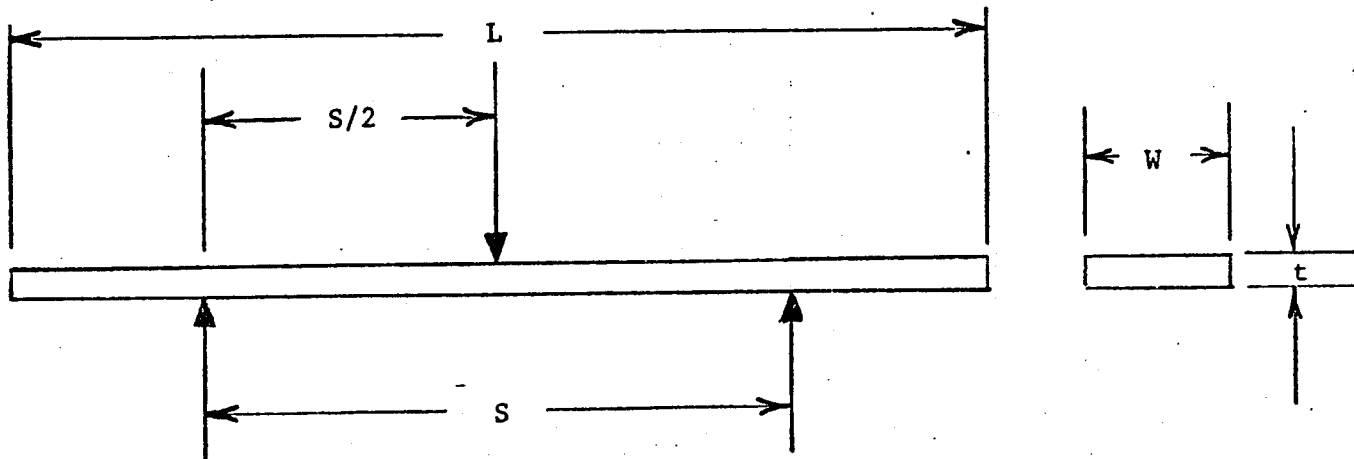
SPECIMEN DIMENSIONS

LENGTH (L)   = 10.2cm.(4.0 in.)

WIDTH (W)   = 1.27 cm.(0.500 in.)

THICKNESS (t) = 0.152 - 0.299 cm.
                        (0.060 - 0.090 in.)

SPAN(S)   = 4 x t

ALL FILAMENTS 0° TO L DIMENSION

LOAD & REACTION SUPPORTS

0.32 cm. (0.12 in.) RADIUS STEEL ROD.

SPAN DIMENSIONS

FOR t = 0.152 - 0.178 cm., S = 5.08 cm.
               (0.060 - 0.070 in.,S = 2.00 in.)

      t = 0.180 - 0.203 cm., S = 5.72 cm.
               (0.071 - 0.080 in.,S = 2.25 in.)

      t = 0.206 - 0.229 cm., S = 6.35 cm.
               (0.081 - 0.090 in.,S = 2.50 in.)

Figure 4.2-A-2. Longitudinal Flexure Test Specimen.

4.6.9.3 <u>Test procedure</u>. Unless otherwise specified, conditions of the test shall be in accordance with Federal Test Method Standard No. 406, Method 1031. The specimen shall be loaded to failure at a 0.127 cm ± 0.013 (0.050 in. ± 0.005) per minute crosshead speed in a testing machine. Testing shall be performed at ambient temperature and 589K ± 5 (600°F ± 10) after a 10 $^{+1}_{-0}$ minute exposure at temperature (see 4.5). The specimen shall be loaded as shown in Figure 4.2-A-2.

4.6.9.4 <u>Calculation</u>. A mean value based on a minimum of three determinations shall be reported for longitudinal flexural strength using the formula below:

$$F_L = \frac{3PS}{2Wt^2}$$

where: F_L = Ultimate longitudinal flexural strength, kN/m^2 (psi)

   P = Maximum load carried by the specimen, N (pounds)

   S = Span, cm. (in.)

   W = Specimen width, cm. (in.)

   t = Specimen thickness, cm. (in.)

4.6.10 <u>Short beam shear</u>.

4.6.10.1 <u>Laminate preparation</u>. Laminate shall be in accordance with 4.6.8.

4.6.10.2 <u>Test specimens</u>. Fibers are aligned parallel to the longitudinal axis. Specimen configuration is shown in Figure 4.2-A-3.
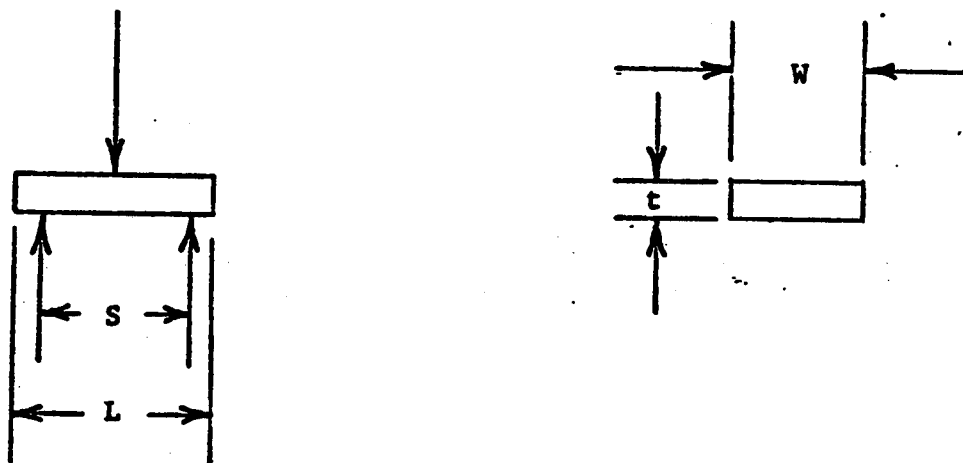
SPECIMEN DIMENSIONS

LENGTH (L) = 0.15 cm.
(0.06 in.)

WIDTH (W) = 0.64 cm.
(0.25 in.)

THICKNESS (t) = 0.152 - 0.229 cm.
(0.060 - 0.090 in.)

SPAN (S) = 4 x t
ALL FILAMENTS 0° TO L DIMENSION

LOAD & REACTION SUPPORTS

0.32 cm. (0.12 in.) RADIUS STEEL ROD.

Figure 4.2-A-3. Short Beam Shear Test Specimen

4.6.10.3 <u>Test procedure</u>. The specimen shall be loaded to failure at a 0.127 cm. ± 0.013 (0.050 in. ± 0.005) per minute crosshead speed in a testing machine. Test temperatures shall be at room temperature and at 589K ± 5 (600°F ± 10) after a 10 $^{+1}_{-0}$ minute exposure at temperature (see 4.5). The specimen shall be loaded as shown in Figure 4.2-A-3 with the smooth side up.

4.6.10.4 <u>Calculation</u>. A mean value based on a minimum of three determinations shall be reported for short beam shear strength using the formula below:

$$F_s = \frac{3P}{4 \, Wt}$$

where:

F_s = Ultimate short beam shear strength, psi

P = Maximum load carried by specimen, pounds

W = Specimen width, inch

t = Specimen thickness, inch

4.6.11 <u>Specific gravity</u>.

4.6.11.1 <u>Laminate preparation</u>. Laminate shall be in accordance with 4.6.8.

4.6.11.2 <u>Test method</u>. Specimen configuration and test procedure shall be in accordance with Federal Test Method Std. No. 406, Method 5011.

4.6.11.3 <u>Calculation</u>. Specific gravity calculations shall be per Federal Test Method Std. No. 406, Method 5011. A mean value based on a minimum of three determinations shall be reported.

4.6.12 <u>Cured resin content and fiber volume</u>.

4.6.12.1 <u>Laminate preparation</u>. Laminate shall be in accordance with 4.6.8.

4.6.12.2 <u>Specimen</u>. Test specimens shall be approximately 1.3 x 1.3 cm. (0.5 x 0.5 in.) by laminate thickness.

4.6.12.3 <u>Procedure</u>. The cured resin content and fiber volume shall be determined by acid/peroxide digestion as follows:

a. Weigh the test specimen to the nearest 0.1 mg (W_1), place in a 300 ml tall-form beaker, and add 20 ml of concentrated sulfuric acid. Place the beaker on a hot plate and heat the acid until fumes occur.

b. When the composite is visibly disintegrated and resin particles and fibers are dispersed throughout the sulfuric solution, carefully add the hydrogen peroxide (50% strength) dropwise down the side of the beaker. Rubber gloves and a fume hood with appropriate safety glass shield shall be used throughout the addition and precautions shall be taken as recommended by the applicable safety regulations and procedures for handling hydrogen peroxide.

c. The reaction is considered complete when the hot sulfuric acid solution below the fibers becomes clear and colorless. At this point add two more ml of hydrogen peroxide to the solution, and heat the

solution to fumes for another 10 minutes to ensure

complete decomposition of the polymer. Remove the

beaker from the hot plate, and allow to cool to 294 to

300K (70 to 80°F), and then place in an ice bath.

d. Collect fibers by vacuum filtration through a medium-

porosity, sintered-glass crucible that has been

weighed to nearest mg (W_2). After the sulfuric acid

has been filtered off, wash the fibers in the crucible

thoroughly with 600 ml of distilled water, added a

few milliliters at a time. Verify removal of sulfuric

acid traces by checking pH of the filtrate.

e. Remove the crucible from the filtering system and

place in an open beaker in an oven at 422K (300°F)

for 45 minutes. After drying, cool the crucible in

a desiccator and weigh (W_3).

4.6.12.4 <u>Resin and fiber content calculation.</u> Calculate the
resin and fiber content according to the following equation:

$$\text{Resin content, percent by weight } (W_4) = \frac{W_1 - (W_3 - W_2)}{W_1} \times 100$$

$$\text{Fiber content, percent by weight } (W_5) = \frac{W_3 - W_2}{W_1} \times 100$$

4.6.12.5 <u>Fiber volume calculation.</u> Calculate the fiber volume
using the data generated from the resin and fiber content determinations
and the following formula:

$$\text{Fiber volume, percent} = (1 - W_4) \frac{D_C}{D_F} \times 100$$

where: W_4 = Weight percent of resin

D_C = Composite density, g/cc

D_F = Fiber density. g/cc

A mean value based on three determinations shall be reported.

4.6.13   Void content.   The void content is calculated from the resin fiber content determinations.

4.6.13.1   Calculation.   A mean value based on three determinations shall be reported.

$$V_C = 100 - \frac{W_4 D_C}{D_E} + \frac{W_5 D_C}{D_R}$$

where: V_c = Void content, volume percent

W_4 = Weight percent of resin

W_5 = Weight percent of fiber

D_C = Composite density, g/cc

D_R = Resin density, g/cc

D_F = Fiber density, g/cc

5.   PREPARATION FOR DELIVERY

5.1   Preservation and packaging.   The material shall be packaged with a non-adherent separator applied to both sheet faces. The material within one package shall be of the same length and width

to preclude damage to the material during shipment. Packaged material
shall be sealed within a moisture-proof plastic bag.

5.2   Packing. The packaged material shall be packed in
shipping containers of a type which will ensure acceptance by common
carrier at lowest rates and will ensure protection of the material
during handling, transit, and storage.

5.3   Marking of interior package. Each interior package
shall be legibly marked with a label or tab which includes the following
minimum information:

      a. LARC-P-01

      b. Manufacturer's material designation

      c. Manufacturer's name and address

      d. Batch number and sheet number

      e. Date of manufacture

      f. Weight

      g. Recommended storage conditions and temperature
         range for maximum shelf life.

      h. Estimated maximum shelf life based on recommended
         storage conditions and temperature range

      i. Hazardous warnings as applicable.

5.4   Marking of exterior shipping container. Each exterior
shipping container shall be legibly and permanently marked with the
following information:

a. LARC-P-01

b. Purchase order number

c. Manufacturer's material designation

d. Manufacturer's name and address

e. Batch number

f. Quantity contained (sheet size and number of sheets)

g. Date of manufacture

h. Date of shipping

i. Manufacturer's recommended storage conditions and temperature range

j. Precautionary and handling markings

In addition, the shipping container shall be identified with a strip of one-inch wide green plastic tape (Scotchlite 3277 or equivalent) completely around the container from top to bottom and approximately one inch from the side.

6.   NOTES

6.1   Intended use. The material covered by this specification is intended for use in the manufacture of spacecraft structural components subject to temperatures from 117K (-250°F) to 589K (600°F). Use is not restricted to these applications.

6.2   Ordering information. The following information should be included on the purchase order, together with the conditions of 6.2.1 and 6.2.2.

a. Number, title, and date of specification

b. Material name and quantity.

6.2.1   Rejection and retest. In the event of failure of a sample to meet any of the requirements of this specification, a second sample of uncured material taken adjacent to the first, or a second laminate panel prepared in accordance with 4.6.8 may be submitted for retest. If the retest sample fails to meet the requirements of the specification, the batch represented by the sample shall be rejected.

6.2.2   Reports. Unless otherwise specified, the supplier shall furnish with each lot three copies of the reports showing the results of tests made on each batch in the shipment to determine conformance of the material to the specification requirements. The report shall include volatile content, resin solids, resin flow, tack, T_G, specific gravity, and mechanical properties, as applicable. The report shall also include the purchase order number, the material specification number, supplier designation, quantity, batch number, and date of manufacture. The report shall also include fiber properties as reported by the fiber manufacturer, and the batch numbers of fiber used in making each of the sheets of material.

APPENDIX 4.2-B

SPECIFICATION LARC-R-02

POLYIMIDE IMPREGNATING RESIN

1. SCOPE AND CLASSIFICATION

1.1 <u>Scope</u>. This specification establishes the requirements for a heat reactive resin system which can be thermally cured to a linear polyimide.

1.2 <u>Classification</u>. The material covered by this specification shall be of one type and shall be identified as LARC-R-02.

2. APPLICABLE DOCUMENTS

2.1 The following documents form a part of this specification to the extent specified on the date of the request for quotation to the National Aeronautics and Space Administration, Langley Research Center, Hampton, VA 23665.

PUBLICATIONS

NFPA SPP-1-C. Fire Protection Guide on Hazardous Materials. National Fire Protection Association, 1975.

3. REQUIREMENTS

3.1 <u>Chemical Structure of Polymer</u>

3.1.1 <u>Varnish</u>. The monomer solvent for PMR-15 varnish (see 6.3.1.) shall be ACS reagent grade, acetone-free, absolute methanol with a maximum water content of 0.05%. The monomers shall be those shown in the following sketch:
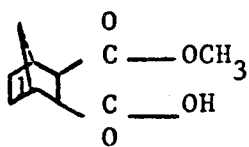
Monomethylesteracid of
nadic anhydricle (NE)
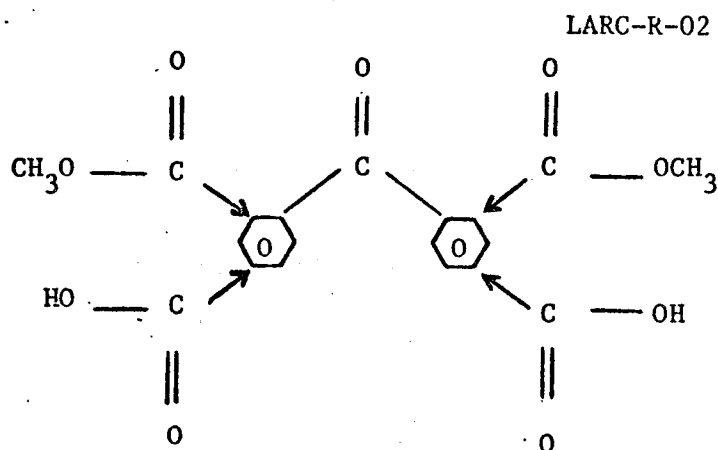
Sym-dimethylesterdiacid of benzophenone-
tetracarboxylic acid dianhydtide (BTDE)
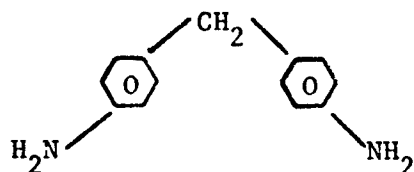
4,4'-Methylenedianiline (MDA)

The molar ratio of NE/BTDE/MDA shall be 2.000/2.087/3.087

3.1.2 <u>Cured Resin.</u> The cured resin shall have the general structure

shown below:
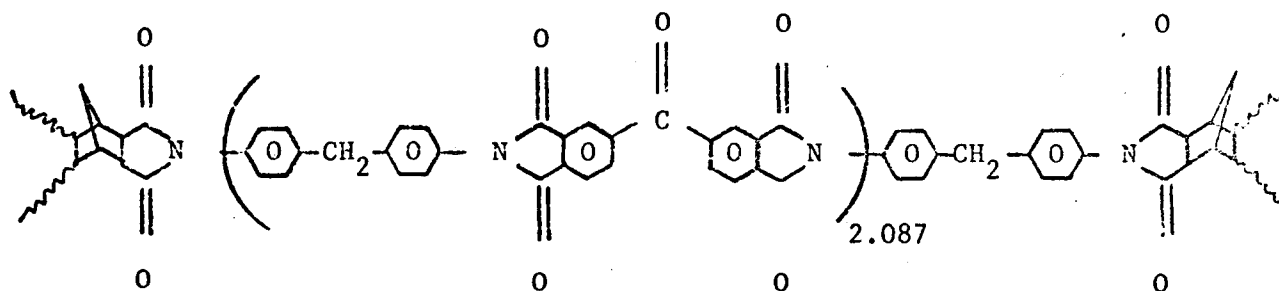
where the repeat unit averages 2.087. The method of crosslinking is

generalized as that shown above since the actual structure has not been

fully elucidated.

3.2 <u>Resin Fillers and Diluents</u>. There shall be no fillers, extenders or diluents in the varnish.

3.3 <u>Physical Properties</u>.

TABLE I

Property	Requirement	Test Paragraph
Resin solids, percent	54 minimum	4.6.2
Viscosity (Brookfield), cps	75 ± 10 @ 296-297K ($72-75°F$)	4.6.3
Specific gravity	1.0 ± 0.2	4.6.5

3.4 <u>Reaction products</u>. As a result of the cure reaction, water is released. In addition, the initial solvent, methanol, is released.

3.5 <u>Shelf life</u>. The varnish shall meet the requirements of 3.3 when stored for a minimum of 90 days at 256K ($0°F$).

3.6 <u>Workmanship</u>. The material shall be free of contaminants or debris which could be detrimental to a fully processed product.

3.7 <u>Hazardous materials</u>. If hazardous materials are included in the resin, all containers of such materials shall be labeled as outlined in the Fire Protection Guide on Hazardous Materials, NFPA SPP-1-C, 1975.

3.8 <u>Product markings</u>. Product markings shall be in accordance with the preparation for delivery section of this specification, 5.3.

4. QUALITY ASSURANCE PROVISIONS

4.1 <u>Responsibility for inspection</u>. Unless otherwise specified in the contract or order, the varnish supplier is responsible for the

performance of all inspections and test requirements as specified herein. Except as otherwise specified, the varnish supplier may use his own facilities or any commercial laboratory acceptable to Langley Research Center. Langley, through its preimpregnated-material suppliers, reserves the right to perform any or all of the inspections set forth herein where such inspections are deemed necessary to assure that the material furnished or to be furnished conforms to the prescribed requirements.

4.2 <u>Inspection records</u>. Inspection records of examinations and tests shall be kept complete and available to Langley. These records shall contain all data necessary to determine compliance with the requirements of this specification.

4.3 <u>Classification of examinations and tests</u>. The examinations and tests of the material shall be classified as follows:

        a. Qualification verification

        b. Acceptance verification

        c. Receiving inspection

4.3.1 <u>Qualification verification</u>. Qualification verification shall consist of all the examinations and tests specified herein.

4.3.2 <u>Acceptance verification</u>. Acceptance verification shall be performed on representative samples of each batch of material, and shall consist of the following:

    a.   Examination of product

    b.   Resin solids content

    c.   Viscosity

    d.   Gel time

    e.   Specific gravity

4.3.3 <u>Receiving inspection (for Langley or Langley's preimpregnated material suppliers use only)</u>. Receiving inspection shall consist of an examination of the material and such sampling and verification of test data as deemed necessary.

4.4 <u>Sampling plan</u>. The material, as offered for acceptance by Langley or Langley's preimpregnated-material suppliers, shall be sampled according to the following procedures.

4.4.1 <u>Batch</u>. A batch shall consist of all material of the same type manufactured in one continuous, unchanged production run.

4.5 <u>Test conditions</u>

4.5.1 <u>Room temperature</u>. Unless otherwise specified, all tests shall be conducted at a temperature of 298K ± 3 (77°F ± 5), and 50 percent ± 10 relative humidity.

4.6 <u>Test methods</u>

4.6.1 <u>Examination of product</u>. The material shall be examined to verify that its markings, packaging, and visual physical characteristics conform to the requirements of this specification.

4.6.2 Solids content

4.6.2.1 Preparation of specimens. Preheat three marked drying dishes in an oven at 408K $\pm$ 2 (275°F $\pm$ 5) for a minimum of 3 hours. Cool the dishes in a desiccator to room temperature and weigh to the nearest 0.1 mg (W_1). Weigh 3 gram $\pm$ 0.1 samples to the nearest 0.1 mg. (W_2) and place into each of the tared, dried dishes. Place the samples on a grid tray in a gravity convection type drying oven preheated to 408K $\pm$ 2 (275°F $\pm$ 5) so that the samples are at the same level as the thermometer bulb and grouped around the bulb. Heat for 3 hours $\pm$ 3 minutes at 408K $\pm$ 2 (275°F $\pm$ 5), and then transfer the samples to a desiccator and cool to room temperature. Reweigh the samples to the nearest 0.1 mg (W_3).

4.6.2.2 Calculation. The mean value of three resin content determinations calculated as follows shall be reported.

$$\text{Resin Content, weight percent} = \frac{W_3 - W_1}{W_2} \times 100$$

where W_1 = Weight of drying dish

W_2 = Initial weight of varnish

W_3 = Weight of drying dish plus specimen after volatile removal

4.6.3 Viscosity. Determine the viscosity of the varnish using a Brookfield Synchro-Lectric Viscometer, Model LVF. Testing shall be conducted at 296 - 297K (72 - 75°F). Place solution to be tested in a jar at least 7.00 cm (2.75 in.) in diameter, cover, and place in a constant temperature bath

accurate to ±0.2K (± 0.4°F). Allow material to reach the proper tempera-
ture before making viscosity measurement. Check with an accurate thermo-
meter. Select the speed and spindle that will most closely give a reading
on the upper end of the dial. The mean value of three viscosity determi-
nations, each made on a separate sample, shall be reported.

4.6.4 <u>Gel time</u>. Gel time of the varnish shall be conducted by use
of a General Electric gel meter. Sample weight shall be 5.0 ± 0.1 gm,
and it shall be held in a clean 18 by 150 mm test tube. The bath tempera-
ture shall be 408K ± 1 (275°F ± 2). The mean value of three gel time
readings, each made on a separate sample, shall be reported.

4.6.5 <u>Specific gravity</u>. The specific gravity of the varnish shall
be determined at 298K ± 0.1 (77°F ± 0.2) using a Westphal Balance. The
mean value of three specific gravity readings, each made on a separate
sample, shall be reported.

4.6.6 <u>Resin flow and softening points</u>. Resin flow and softening
points shall be determined on the vacuum stripped polyimide varnish at
three different heating rates: 1, 3, and 5K per minute (1.8, 5.4, and
9°F per minute) using a Fisher-Johns melting point apparatus. The
polyamic acid type residue shall be virtually free of all solvent prior
to flow and softening point determinations. Vacuum stripping of solvents
shall be conducted at 298K ± 2 (77°F ± 5), and < 50 mm Hg pressure for
a minimum of 15 hours. Five different characteristics of the residue
shall be determined: (1) melting point, (2) initial flow, (3) good flow,
(4) start of gellation, and (5) gellation. Points (2) and (3) are more
subjective and shall be more dependent on interpretation by the instru-
ment operator.

5. PREPARATION FOR DELIVERY

5.1 <u>Preservation and packaging.</u> All material furnished under this specification shall be in suitable containers in quantities as specified on the purchase order. The material shall be packaged to ensure protection from physical damage during handling, shipping, and storage.

5.2 <u>Packing.</u> The material shall be packed in shipping containers of a type which will ensure acceptance by common carrier at lowest rates, and will ensure protection of the unit containers during shipment.

5.3 <u>Marking for shipment.</u> Each unit and shipping container shall be legibly identified with label, tag, or markings which include the following data.

  a. LARC-R-02.

  b. Purchase order number.

  c. Manufacturer's material description and identifying designation.

  d. Manufacturer's name and address

  e. Quantity (shipping container only) and unit size

  f. Batch number and date of manufacture

  g. Date of shipping

  h. Manufacturer's recommended storage conditions and temperature

  i. Hazardous warnings and handling markings as applicable

6. NOTES

6.1 Intended use. The material covered by this specification is intended for impregnating graphite fiber used in the manufacture of spacecraft laminated structural parts subject to temperatures from 117K (-250°F) to 589K (600°F). Use is not limited to these applications.

6.2 Ordering information. The following information together with the requirements of 6.2.1 and 6.2.2 should be included on the purchase order.

      a. Number, title, and date of this specification

      b. Material name and quantity

6.2.1 Rejection and retest. In the event of failure of a sample to meet any requirements of this specification, a second sample of varnish may be submitted for retest. If the retest sample fails to meet the requirements of the specification, the batch represented by the sample shall be rejected.

6.2.2 Reports. Unless otherwise specified, the supplier shall furnish with each batch three copies of the reports showing the results of tests made on each batch in the shipment to determine conformance of the material to the specification. The report shall include resin solids content, viscosity, gel time, and specific gravity. The reports shall also include the purchase order number, the material specification number, supplier's material designation, quantity, batch number(s), and date(s) of manufacture.

6.3 Definitions

6.3.1 <u>Varnish</u>. For the purposes of this specification, varnish is defined as a composition of resin and liquid carrier.

Vacuum inlet
Kapton bag
2 plies 1044 FG
Top caul
Kapton
3 plies 181 FG
3 plies 120 FG
TX1040 release
Laminate
TX1040 release
Kapton
Bottom caul
2 layers 1044 FG
Clamp bar
A-800 sealant
Support plate

Temp.,
$^{\circ}F$

700 — 600 — 500 — 400 — 300 — 200 — 100

400

Hold 3 hr

6 K (10 $^{\circ}F$)/min

Apply 1.72 MPa (250 psi)
+ Full vacuum

3 K (5 $^{\circ}F$)/min

Hold
1/2 hr

6 K (10 $^{\circ}F$)/min

Reduce pressure 16.9 kPa (5 in Hg)

Time, min

100   200   300

600 — 500 — 400 — 300

Temp.,
K

Figure 4.2-2 – NASA autoclave cure cycle for HTS2/PMR-15.
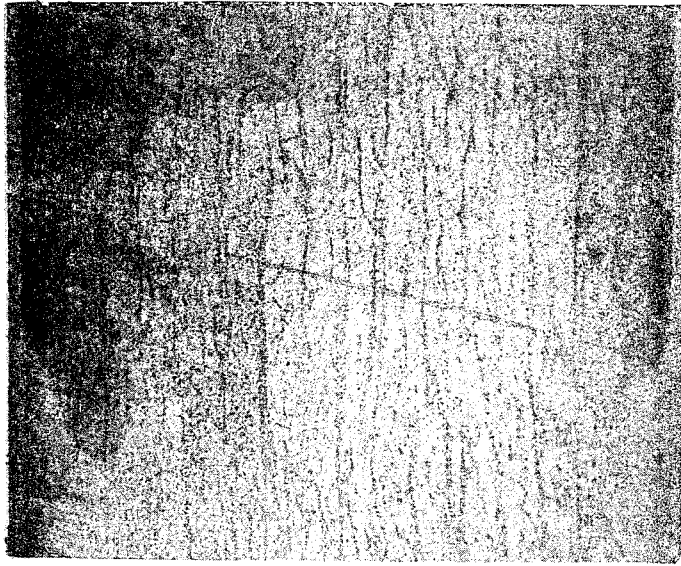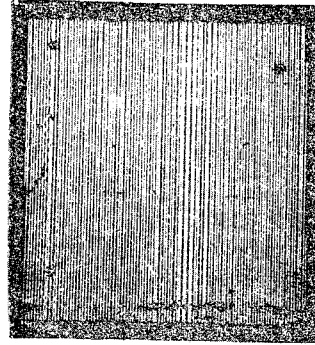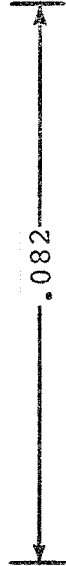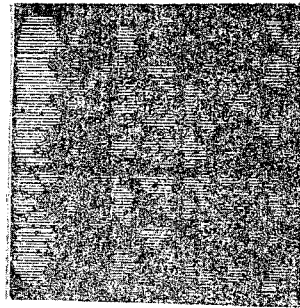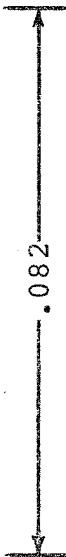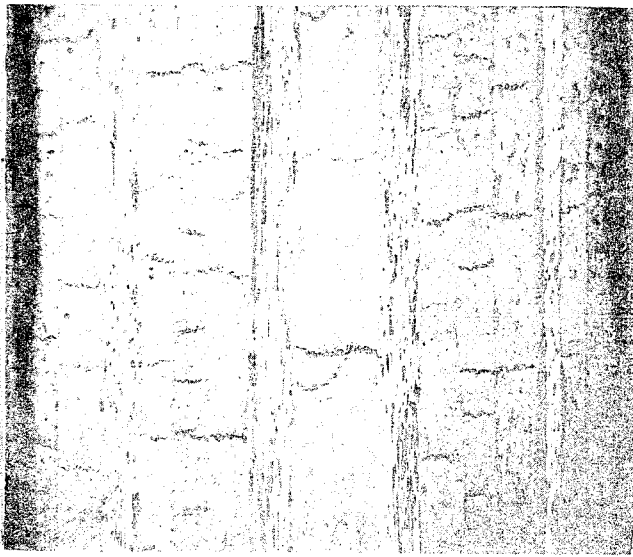
Figure 4.2-3 - Typical C-scans and photomicrographs of HTS-II/PMR-15 laminates.
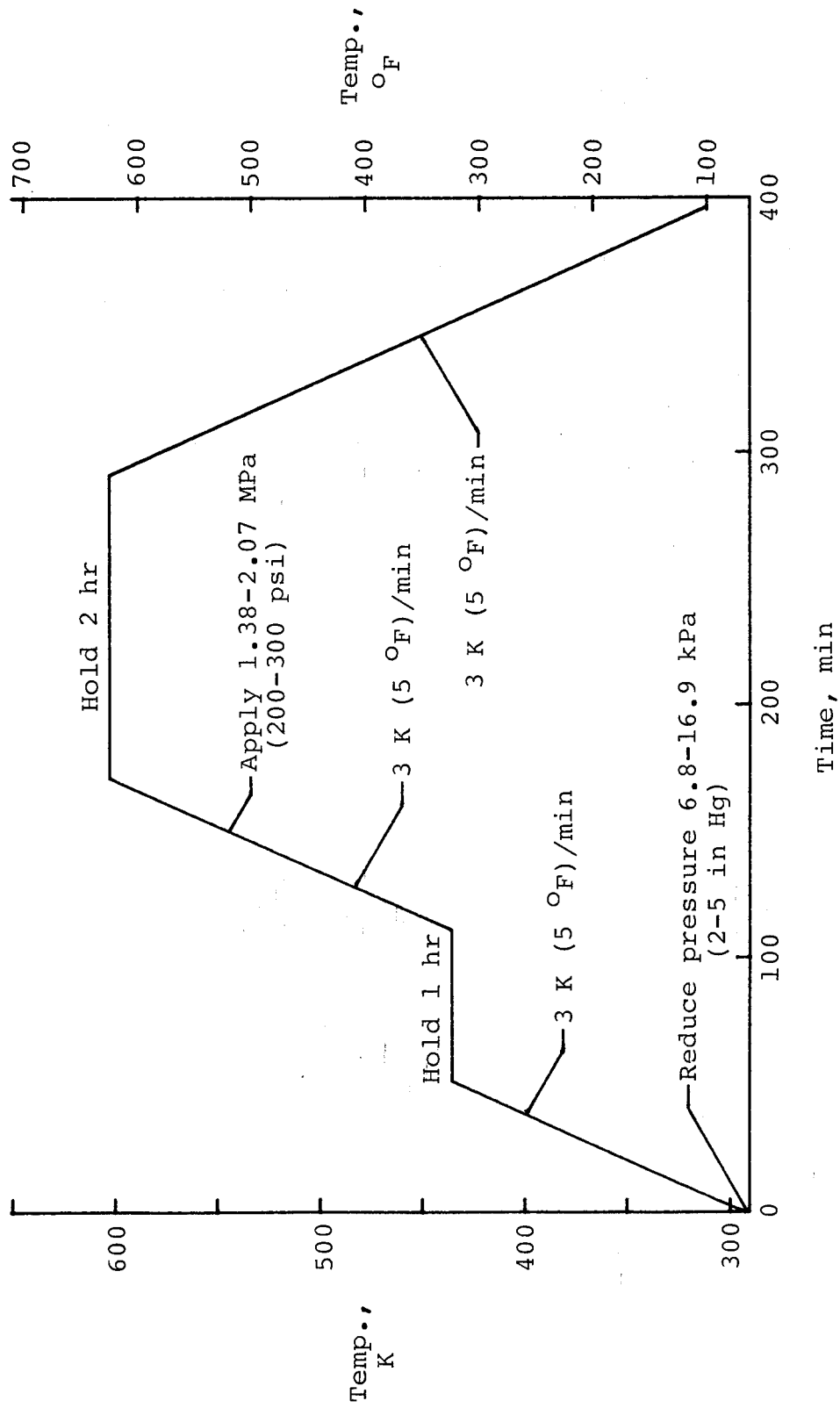
Figure 4.2-4 – NASA autoclave cure cycle for HTS1/LARC-160.

Fiber/resin type	Exposure at 589°K(600°F)hr.	Flexure strength, MPa (ksi)		Interlaminar shear strength, MPa (ksi)	
		RT	589°K(600°F)	RT	589°K (600°F)
HTSI/LARC-160	0	2068(300)	1234 (179)	95.8 (13.9)	44.8 (6.5)
	125		1372. (199.)		47.6 (6.9)
Celion 6000/ LARC-160	0	1875(272)		103.4 (15.0)	44.1 (6.4)

Figure 4.2-5 – Graphite/LARC-160 mechanical properties.

4.3 Quality Control and NDE
Robert Baucom and Philip R. Young

Quality control of vendor and in-house produced prepreg is required in order to insure that established processing envelopes will apply to the manufacture of high quality graphite reinforced NR150-B2, LARC-160, and PMR-15 laminates on a repeatable basis. A determination of the areal weight and the weight percent of resin, graphite fiber, and solvent in each separate lot of prepreg is first made according to the procedures outlined in Appendix A. Laminates subsequently fabricated from these prepreg lots require the removal of free solvent, reaction by-products and the bleed-out of excess resin during cure. After curing, the percent of fiber, resin, and voids can be determined by the procedures outlined in Appendix 4.2-A.

In addition to the above mentioned quality control procedures, high pressure liquid chromatography inspection of a sample of each lot of incoming material is made. This inspection is performed in order to provide a fingerprint of the soluble components in the prepreg. In arriving at the best phase separation technique to be applied to analysis of NR150-B2, PMR-15, and LARC-160, several normal phase, reverse phase, and size separation procedures were initially considered. One particular separation, which provides an analysis of all three resin systems, was selected as being the most informative. This separation uses a CN-μ-Bondapak column and n-propanol as the mobile phase. This procedure requires a sample of approximately 5 mg of resin (10 mg of prepreg). This sample is transferred to a 3 ml vial and 1 ml of n-propanol is added. After sufficient agitation to produce resin solution, the mixture is filtered through a 0.45 μm filter and run under the following chromatographic conditions:

SAMPLE: NR150-B2, PMR-15, or LARC-160

COLUMN: CN-μ-Bondapak

SOLVENT: n-propanol

FLOW RATE: 0.5 ml/min (6.2 MPa (900 psi))

SIZE: 1-2 μℓ

DETECTOR: UV (254 nm)

Figure 4.3-1 gives a summary of the results obtained on NR150-B2 prepreg received from five different sources. Retention time data and preparative chromatography followed by mass spectral analysis were used to identify most of the major peaks. Some variability in relative peak heights of the major components was observed. Figure 4.3-2 gives similar information on seven different lot numbers of PMR-15 prepreg obtained from the same source. Again, some variability was noted. Figure 4.3-3 shows the effect of aging on the same batch of LARC-160 resin. The amine peak practically disappears with time. The results given in these figures are typical of the chromatographic

behavior observed for the three CASTS materials. Reference files containing chromatograms of various NR-150-B2, PMR-15, and LARC-160 samples are being maintained.

In summary, differences were observed in CASTS resins and prepregs obtained from different sources, different batches from the same source, and the same batch subjected to different aging conditions. The effect of this variability on processing or ultimate composite properties will be determined.

A study to determine the effect of aging on LARC-160 resin and prepreg is being planned. The desired result of this study is to correlate changes in resin chemistry with processing and composite properties. The aged samples will be analyzed by high pressure liquid chromatography, torsional braid analysis, C^{13} NMR, and perhaps rotary rheometry prior to fabrication and testing.

Nondestructive evaluation (NDE) of laminates and structures produced from graphite fiber reinforced polyimide prepreg is required to insure structural integrity. The purpose of NDE is to detect defects which could cause static or fatigue degradation. Evaluation studies are underway to develop techniques to detect defects in graphite/polyimide laminates and structural elements.

Preliminary defect types and applicable methods of detection have been defined. Defect types include interply delaminations, interlaminar delaminations, surface and subsurface cracks, voids, inclusions, ply misalignments, improper resin mix and improper resin cure. Detection techniques being studied include ultrasonic immersion C-scan, x-radiography, infrared transmission, neutron radiography, liquid penetrant, eddy current, optical holography, and acoustic holography. Other applicable techniques will also be evaluated when shown to be applicable.

The primary testing technique developed to date has been pulse-echo ultrasonic immersion C-scan. In this technique a high frequency (15 MHz) sound beam is transmitted through the laminate or structure, reflected off a glass plate, and returned to the transducer through the laminate or structure. The reflected sound energy is measured and the energy above a specified level or receiver gain is displayed on a cathode ray tube and recorded on polaroid film. The result is a plan view of the tested part with areas that do not transmit sound above the given level indicated as dark areas, thus outlining flawed areas (see figure 4.3-4). The technique was calibrated by defect-free reference standards for varied thicknesses and ply orientations. Limited studies have shown good correlation between C-scan results and interlaminar shear strength for good and poor quality laminates. More correlation studies are needed to define acceptance levels.

X-radiography techniques have been developed for the detection of certain defects in laminates and structural elements. Soft x-rays (20-50 Kev) can detect inclusions, ply misalignment, and gross resin mix variations. The

technique can detect crushed and filled cells in honeycomb structures and can detect absences of adhesive in bonds. Limited studies with neutron radiography indicate a much greater sensitivity to resin mix variations and organic inclusions. This higher level of sensitivity is due to the higher specific attenuation of neutrons by hydrogenous material when compared to the sensitivity experienced with x-radiography. Further neutron radiography studies are planned.

The remaining detection techniques will be studied further and the use of optical and acoustic holography will be investigated. Standards for each applicable technique will be developed for laminates, honeycomb panels, stiffeners, and skin-stiffened panels.

Sample: NR-150-B2
Column: CN-μ-BONDAPAK
Solvent: n-ProH
Rate: 0.5 ml/min (6.2 MPA (900 psi))
Concd: 10 mg prepreg/ml
Detector: UV (254 nm)

Fiberite prepreg

Dupont-saugus prepreg

Reliable prepreg

In-house prepreg

Ferro prepreg (not completely soluble)

Dupont resin

Amine

Ester

Tetra-acid

Retention time, min
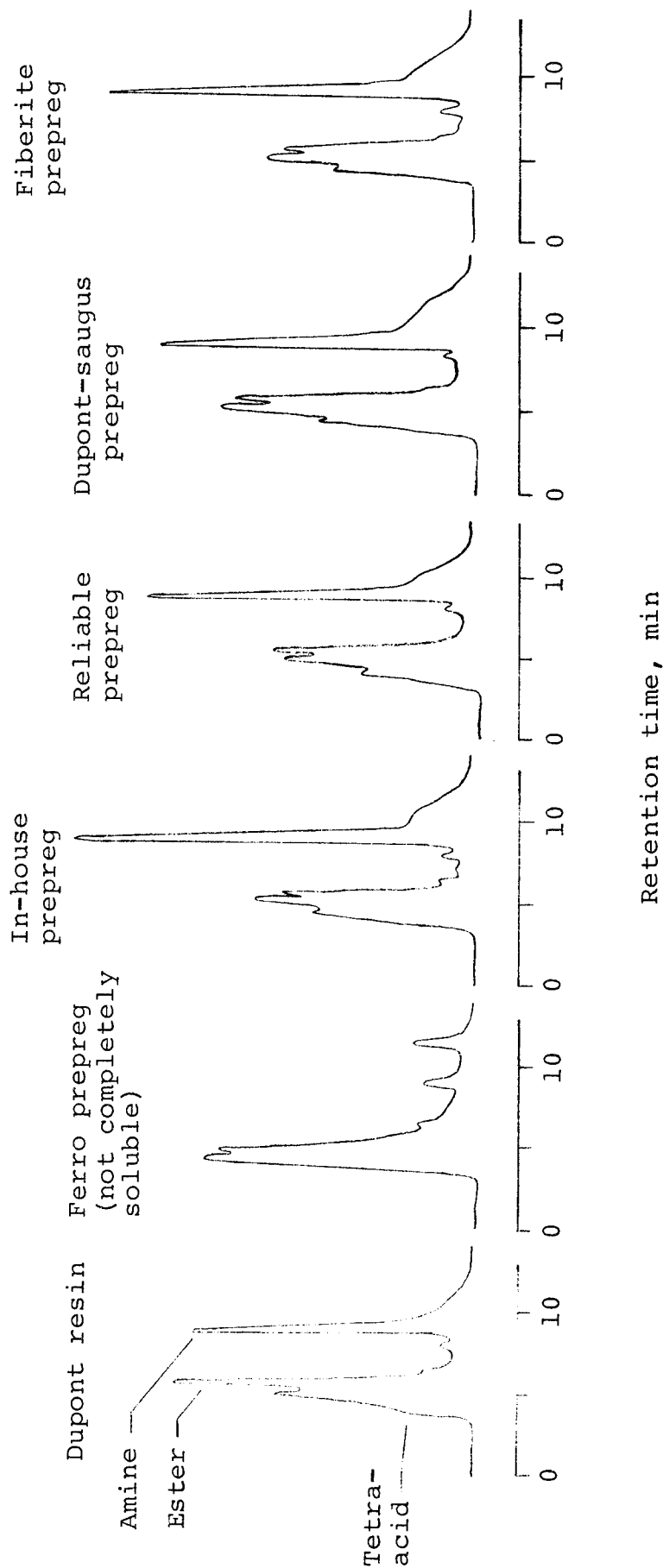
Figure 4.3-1 - Liquid chromatograms of NR-150-B2 resin and prepreg obtained from five sources.

Sample: PMR-15
(FERRO PREPREG)

Column: CN-µ-BONDAPAK
Solvent: n-PrOH
Rate: 0.5 ml/min (6.2 MPa (900 psi))
Concd: 10 mg prepreg/ml
Detector: UV (254 nm)

Retention time, min
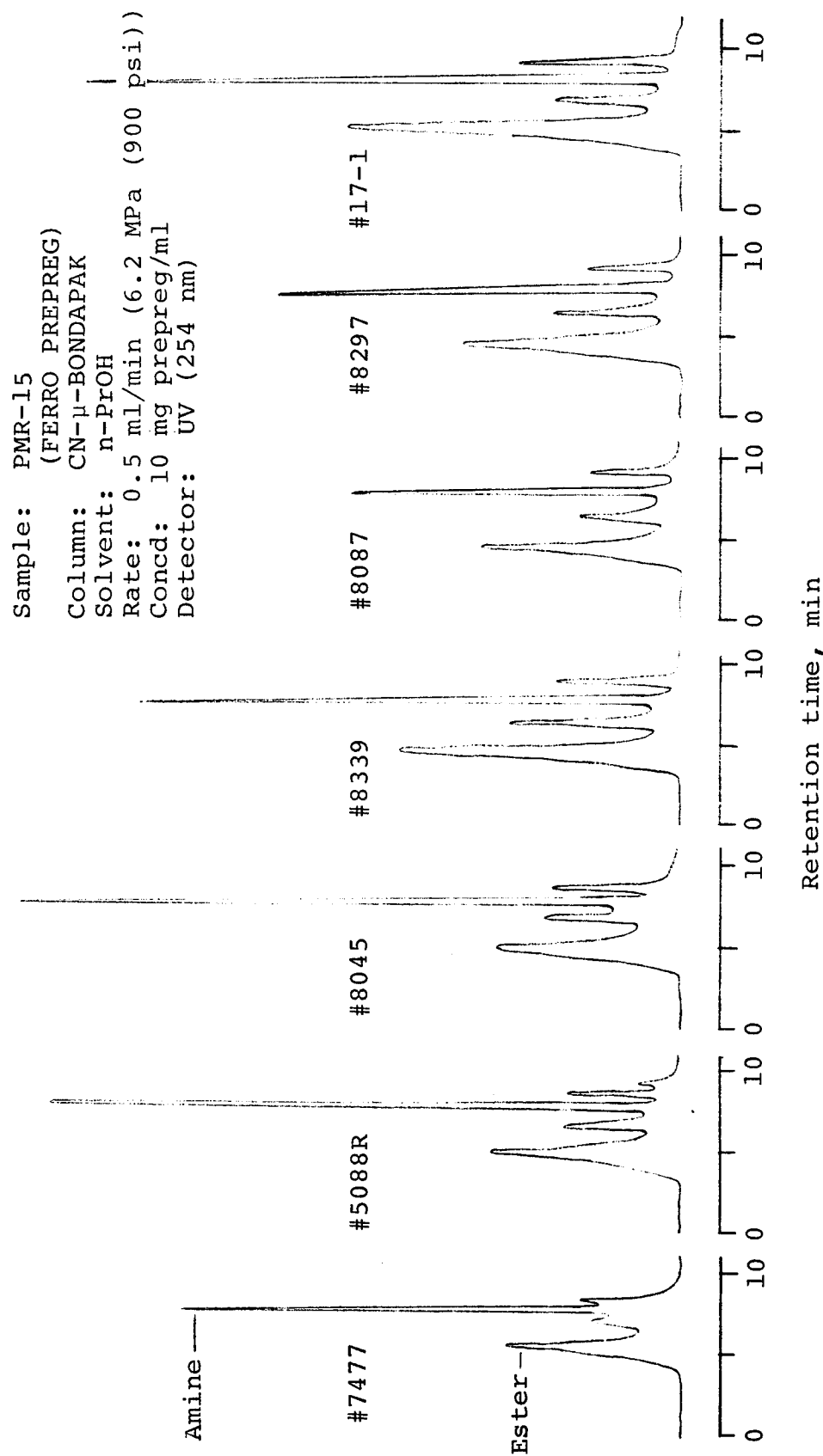
Figure 4.3-2 — Liquid chromatograms of seven lot numbers of PMR-15
obtained from one source.

8 months at 40 °F

18 days at RT

4 days at RT

Amine ——

Ester ——
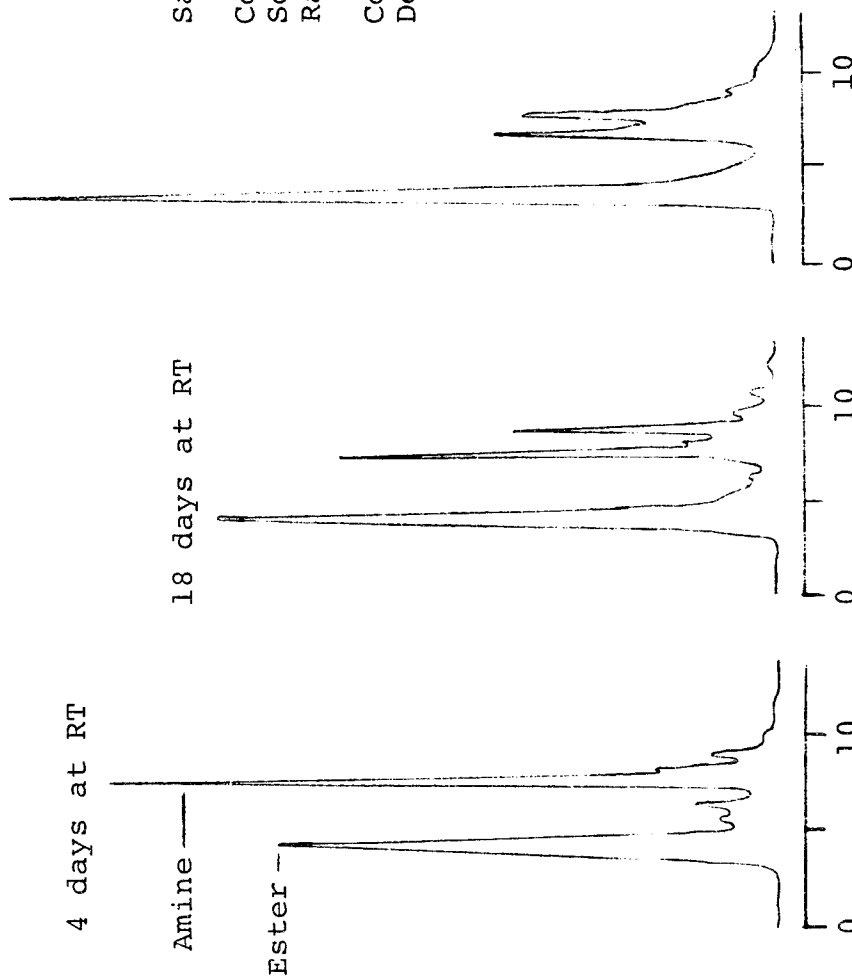
Sample: LARC-160 resin
          (Riggs No. 3)
Column: CN-μ-BONDAPAK
Solvent: $Pr_r OH$
Rate: 0.5 ml/min
          (6.2 MPa (900 psi))
Concd: 10 mg/ml
Detector: UV (254 nm)

Retention time, min

0   10

0   10

0   10

(b) C-scan, gain 30.

(a) Flaw locations
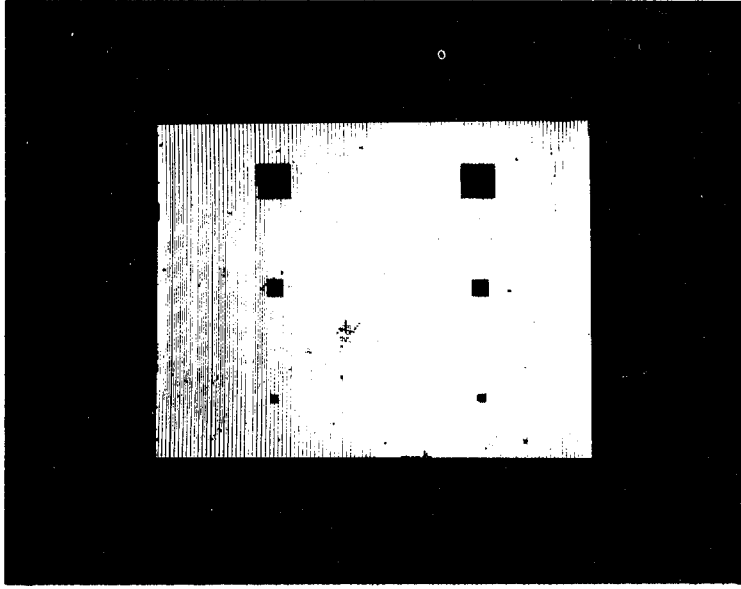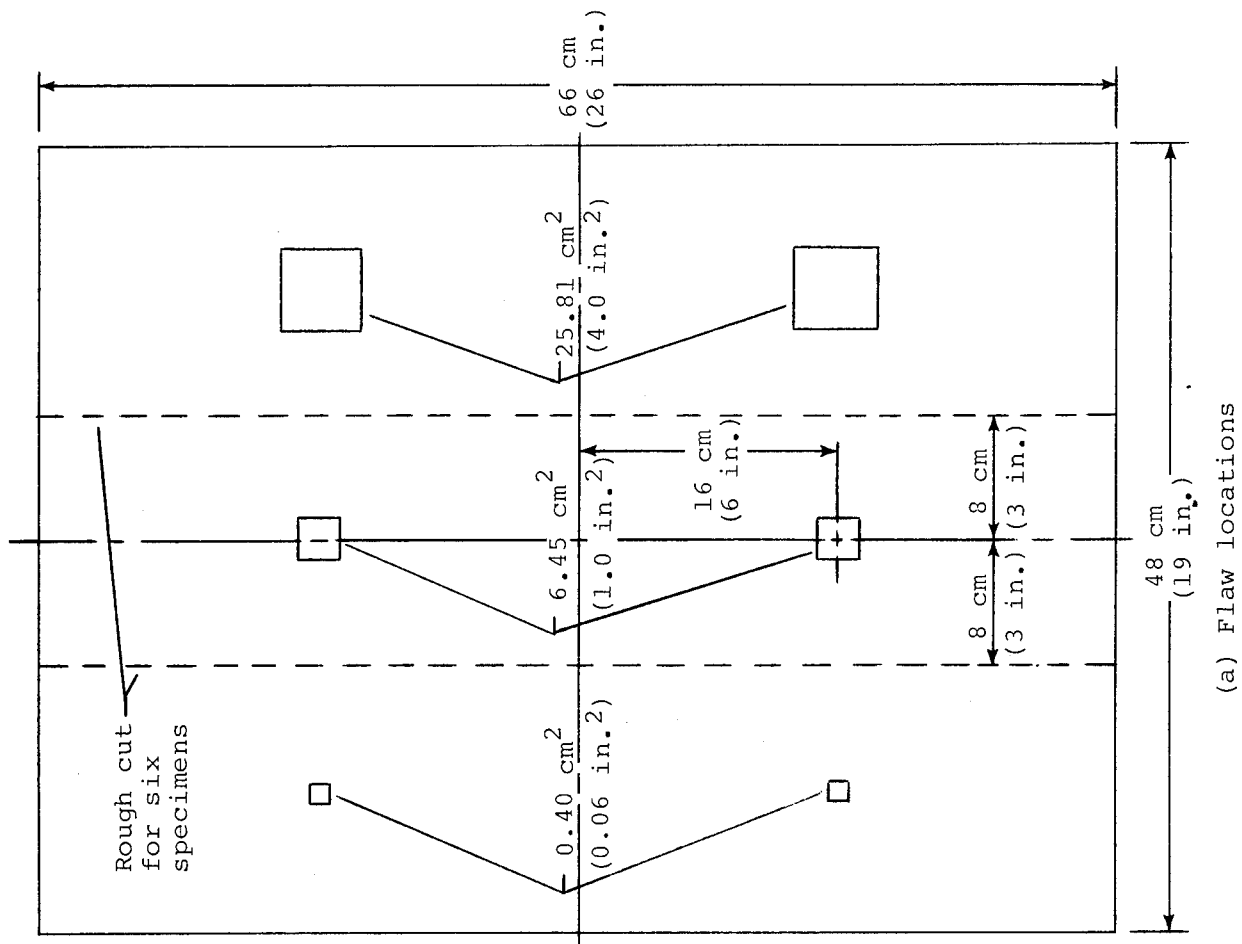
Figure 4.3-4 - Typical repair technology laminate showing location of simulated unbonds and NDE record.

4.4 Repair Technology
Jerry W. Deaton

The preceding section describes the nondestructive evaluation procedures being developed for the CASTS project. An important consideration that arises from the NDE work is whether a detected flaw is critical to safe use of the structure and whether a repair can be made. The Repair Technology task will address this problem through in-house testing of thin laminates, stiffened elements, and honeycomb panels. In addition to the in-house experimental work, a contractual effort will investigate technology deficiencies identified by the in-house program.

In the repair program, both manufacturing (M) and service (S) damage type flaw are being considered. Eight ply (0 + 45 90-45) and sixteen ply (0 + 45 90-45)$_s$ laminates are being used to determine the effect on compressive strength of the following types of flaws: (1) interlayer delaminations (M, S); (2) surface cracks (M, S); (3) foreign object inclusions (M); (4) delaminations between graphite/polyimide and metal inserts (M, S); and (5) impact damage (S). These five flaw types will also be used in the study to determine their effect on performance of stiffened elements representative of structural elements in the aft body flap. Honeycomb-core panels will be used to determine the effects on panel performance due to (1) crushed cell areas (M, S), (2) filled cell areas (M, S), and (3) skin to core bond defects (M, S).

Accomplishments in the repair program include the fabrication of all the eight ply laminates having simulated unbonds that are either 0.4, 6.4, or 25.8 cm^2 (0.06, 1.0, or 4.0 in^2) in area. These unbonds were made by placing one piece of heat treated 0.3 mil (0.8 mm) Kapton film on top of another during the laminate fabrication process. Unbonds were placed 2 plies, 3 plies, and 4 plies from the surface of the laminates. The laminates were fabricated to nominal dimensions of 48 cm by 66 cm (19 in. by 26 in.) and had six unbonds located such that each laminate could be cut into six compression test specimens 15 cm by 30 cm (6 x 12 in) (see Figure 4.3-4). The laminates have been cut and machined to these dimensions and are ready to be strain gaged prior to testing. These specimens will be used to determine the effect on compressive strength due to interlayer delaminations as well as foreign object inclusion and impact damage.

Attempts to fabricate the sixteen ply laminates with similar unbonds have not been successful and this effort will continue in the next reporting period.

During the next reporting period, 30 eight-ply compression specimens will be strain gaged and tested to determine the effect of the three different size unbonds on the compressive behavior of the laminates. The experimental data will also be compared with analytical predictions as given in reference 4.4-1. When the problems associated with the fabrication of the sixteen ply laminates is solved five laminates, 48 cm by 66 cm (19 x 26 in) will be fabricated. Each of these laminates will also have six unbonds located such that six compression specimens will be machined from each laminate and tested.

REFERENCES

4.4-1   Howard, S. A., and Daugherty, R. L., "Effects of Debonds on the Strength of Composite Plates", Proceedings of the Second International Conference on Composite Materials, April 16-20, 1978, Toronto Canada.

5.0 MANUFACTURING DEVELOPMENT CONTRACTS
Edward L. Hoffman, John G. Davis, Jr., and Robert M. Baucom

The primary objective of the manufacturing development contracts is to develop processes for fabricating graphite polyimide structural elements which could be applied to components of advanced space transportation systems. A contract is being or has been awarded to investigate the processing of graphite reinforced prepreg for each of the polyimide materials: NR150B2, PMR-15, LARC-160, and Thermid 600. The period of performance of the contracts varies from 18 to 24 months. Each contract contains the following tasks:

Process Development

Develop quality assurance program

Develop fabrication processes

Fabricate specimens and conduct tests

Demonstration Components

Fabricate laminates

Fabricate skin-stringer panels

Fabricate honeycomb-core panels

Fabricate chopped fiber moldings

Fabricate aft body flap representative component

NR150B2 polyimide is a proprietary polymer available from the E. I. Dupont de Nemours Company. It is the most thermally stable of the polyimides being investigated but is also the most difficult to process. The as-received NR150B2 resin and prepreg are being received in 100 percent N-methylpyrrolidone (NMP) solvent rather than the more common NMP-ethanol solvent mixture. The most difficult task for the NR150B2 contract is the development of the fabrication processes. Since contract award on March 8, 1977, the contractor has essentially completed development of a quality assurance program and is approaching completion of fabrication process development. Dielectric monitoring has been used to develop the cure and postcure processes depicted in figures 5.0-1 and 5.0-2.

The PMR-15 and LARC-160 polyimides are not proprietary*and are each prepared by mixing three monomers. Norbornene-2, 3-dicarboxyl acid monomethyl ester (NE), methylene dianiline (MDA), and benzophenonetetracarboxylic dimethylester diacid (BTDE) are mixed in a methanol solvent to produce PMR 15.

The NE, Jeffamine AP-22, and BTDE are mixed essentially solvent free to produce LARC-160. Both polyimides are easier to process than NR150B2, but require considerably more effort for quality assurance. The PMR-15 contract was awarded July 27, 1977. Development and documentation of the quality assurance program has essentially been completed and used to evaluate prepreg from two suppliers. Development of the fabrication processes has also essentially been completed. See figure 5.0-3 for the cure cycle.

The contracts for Thermid 600 polyimide and LARC-160 polyimide should be awarded in May and June 1978 respectively. Thermid 600 was developed by Hughes Aircraft Company which has licensed Gulf Oil Chemicals Company for production of the polyimide.

* PMR-15 and LARC-160 were developed by NASA and non-exclusive licenses for production thereof have been granted by NASA.

Figure 5.0-2 - General Dynamics autoclave posture cycle for Celion 3000/NR150B2.
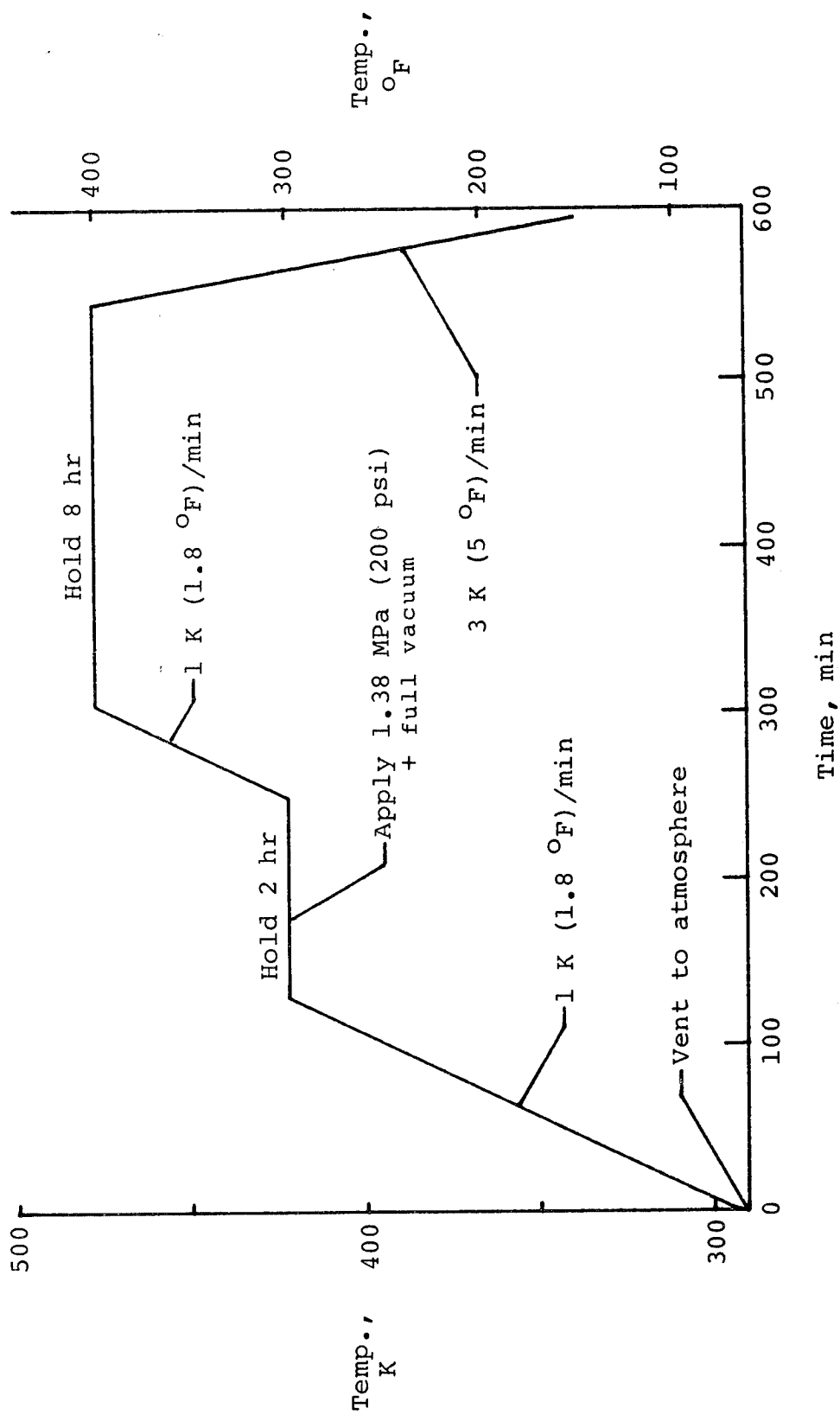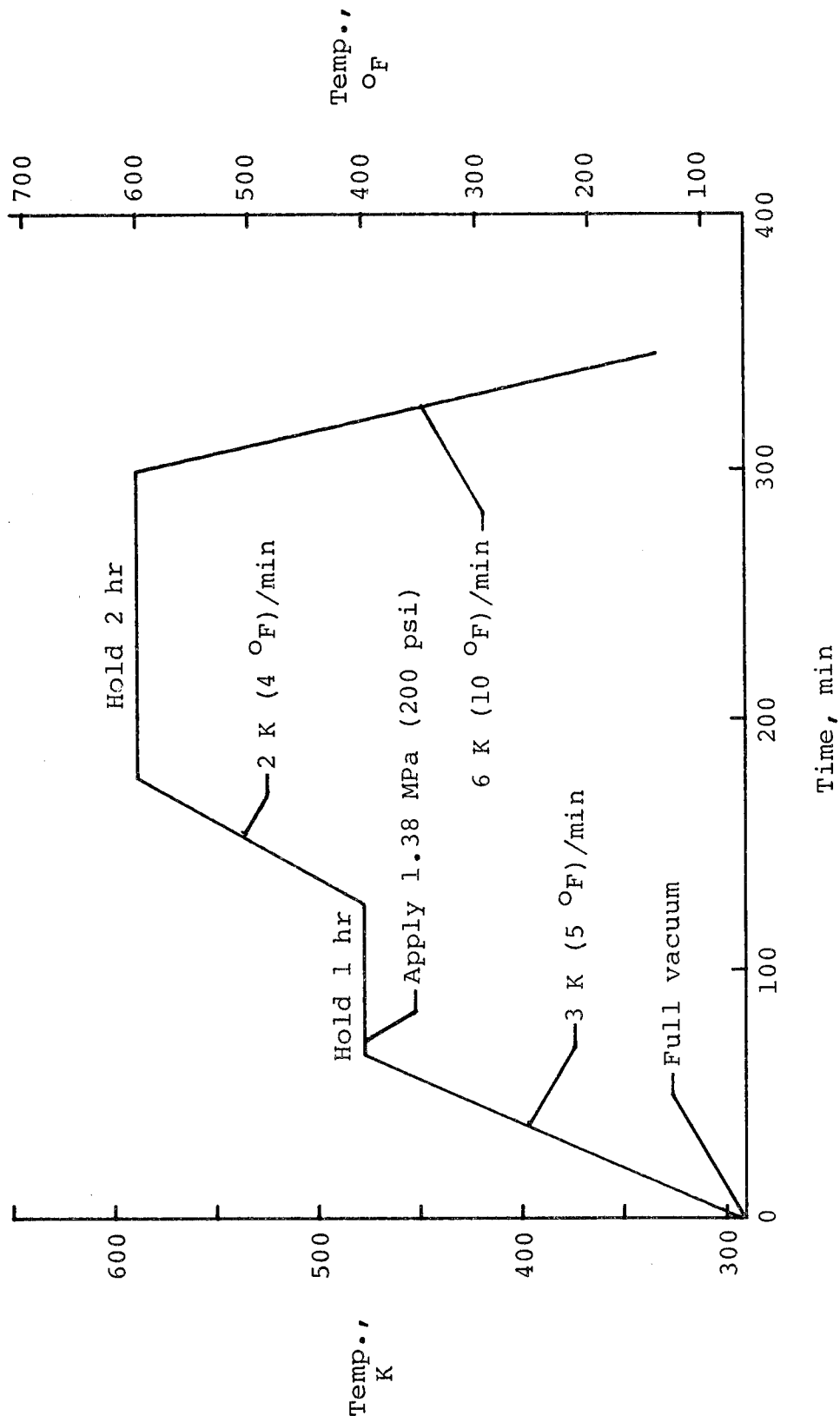
Figure 5.0-3 – Boeing autoclave cure cycle for HTS2/PMR-15.

6.0 IN-HOUSE MECHANICAL DESIGN ALLOWABLES AND TEST METHODS

6.1 Tension Test Method
Andrew J. Chapman

Introduction

Before structures can be designed using graphite/polyimide materials, their mechanical properties must be characterized at the temperatures of intended use. Special considerations include controlling the test temperature, load transfer to the test specimen, durability of adhesive bonds, and accurate response and reliability of strain measuring techniques. This task is being performed to establish the test methodology for measuring tension properties of the graphite/polyimide laminates at temperatures from 117 K (-250°F) to 589 K (600°F).

In order to characterize mechanical properties such as modulus and Poisson's ratio, strains must be accurately measured on a test specimen in several directions at all loading and temperature conditions. Several strain measuring techniques, including high temperature resistance strain gages, a capacitive strain gage, and an extensometer are being evaluated. Resistance strain gages bonded to the specimen surface appear to be the most practical and convenient method for measuring strains in several directions over limited surface areas, and a primary activity of this task is to evaluate their accuracy and reliability at temperatures up to 589 K (600°F).

Tension properties of several developmental graphite/polyimide materials have been measured over the desired temperature range while developing the test methodology. The established test methods will be used to characterize design allowable properties of improved graphite/polyimide systems currently being developed in the CASTS Project.

Materials and Specimens

The graphite/polyimide materials tested include HTS/PMR-15 and HTS/NR-150B2 in $[0]_8$ and $[0,\pm45,90]_s$ laminates. These laminates were made early in the CASTS Project and quality and mechanical properties are not fully representative of laminates which could be produced with the better materials and processing techniques presently being developed. However, laminates used in the present investigation were adequate for test methodology and instrumentation development.

Test specimens are listed in figure 6.1-1 and specimen configuration is shown in figure 6.1-2. Tabs for gripping specimens in the test machine were made from graphite/polyimide laminates similar to the test specimens and were bonded to the specimens using FM-34 polyimide adhesive. Correct processing is critical for obtaining a satisfactory bond with this adhesive.

Instrumentation

Resistance Strain Gages. - Resistance strain gages were Micro-Measurement's Series WK which are fully described in the manufacturer's literature. The advertised use temperature range for these gages is 4K (-452°F) to 672K (750°F). Strain gages evaluated in the present tests were single element gages having a gage length of 3.2 mm (0.125 in). In some tests, gages were mounted along the transverse as well as the longitudinal axis of the specimen to measure Poisson's ratio. Gages were bonded to the specimen surface using the manufacturer's recommended BLH PLD-700 polyimide adhesive. Gage application is process and technique critical and manufacturer's specifications should be observed to obtain consistently satisfactory results. A tension specimen instrumented with a resistance strain gage is shown in Figure 6.1-3.

Capacitive Strain Gage. - The capacitive strain gage used in this investigation is described in reference 6.1-1, where linear response, small sensitivity change, and high resolution are reported for temperatures as high as 1089 K (1500°F) and strain as great as 0.02. Details of the capacitive gage are shown in figure 6.1-4 and gage installation on a graphite/polyimide specimen is shown in figure 6.1-5a, with further gage details shown in figure 6.1-5b. The gage attachment strips are bonded to the specimen using a polyimide adhesive; the distance between the attachment strips defines the gage length. Stress induced specimen dimension changes displace the concentric capacitive rings in the gage, and the resulting change in capacitance modulates a carrier voltage, producing an analog voltage proportional to strain. Three lead-wires shown in the figures carry excitation voltage and modulated sensing voltage. The capacitance sensor is assembled around a longitudinal rod which compensates for thermally induced strains if the rod and specimen have closely matched coefficients of expansion.

Extensometer. - A rod-in-tube extensometer, attached to the specimen gage section adjacent to the resistance strain gage, transmitted specimen longitudinal displacement to a transducer (Hewlett-Packard model 7 DCDT) which produced a voltage signal proportional to displacement. The extensometer was attached to the specimen through knife-edge clamps spaced at 1-inch gage length so that recorded displacement measurements were equivalent to strain. Figure 6.1-6a shows the extensometer attached to a tension specimen mounted in a hydraulically actuated test machine. Figure 6.1-6b shows a cylindrical resistance heater enclosing the specimen gage section; the transducer is well away from the heated area.

Thermocouples. - Specimens were instrumented with chromel-alumel thermocouples which were bonded to the specimen surface near the strain gage using PLD-200 polyimide adhesive. Thermocouple installations are shown in figures 6.1-3 and 6.1-5. Thermocouple output provided signals for control of heating and cooling. Specimen temperatures were also recorded digitally along with load and strain data.

Test Apparatus

Specimens are tested in a load-rate controlled hydraulically actuated test machine (figure 6.1-6), or in a strain-rate controlled mechanically actuated machine. An environmental chamber used with the mechanically actuated machine (figure 6.1-7) produces test temperatures from 117K (-250°F) to 589 K (600°F). Cryogenic temperatures are produced by controlled liquid nitrogen flow into an open ended heat exchanger where the nitrogen is evaporated and circulated through the chamber by a blower. Elevated temperatures are produced by electrical resistance heating elements shielded to protect specimens from radiation. Test temperatures in the chamber are controlled to within $\pm$ 3 K.

A cylindrical resistance heater which enclosed the specimen gage area is shown in figure 6.1-6b. Specimen temperatures were controlled within $\pm$ 5 K in this chamber. This heater does not enclose the specimen grips and imposes minimum interference on specimen and load train installation. During high temperature tests, heater openings are covered by sections of insulation which surround, but do not interfere with, the extensometer.

Bolted specimen grips, shown in figure 6.1-6, were found to be much more satisfactory than wedge action grips such as those shown in figure 6.1-7, because of the positive locking action which essentially eliminated specimen slipping, and because of the more compact size.

Tests and Results

In preparation for testing, specimen tabs were securely locked in the grips, and the specimen assembly was suspended from the upper pull rod while enclosed in the environmental chamber. Grips were connected prior to heating because the chamber door could not be opened at temperatures above 422 K (300°F). During heating or cooling to test temperatures, the lower pull rod was not connected to the test machine to avoid thermally induced loads. When the test temperature had stabilized, as indicated by the specimen thermocouple, the lower pull rod was connected to the machine and load and strain indications were zeroed. Specimens were loaded at strain rates no greater than 0.005/min.

Two specimens instrumented with capacitive and resistance strain gages (figure 6.1-1) were tested at room temperature, 422 K (300°F), 478 K (400°F), 533 K (500°F), 561 K (550°F), and 589 K (600°F) to evaluate performance of the resistance gages while the capacitive gage served as a standard. During tests at each temperature, specimens were loaded to a strain level of approximately 0.004, and unloaded before testing again at a different temperature following the procedure described in the paragraph above. These specimens were tested repeatedly rather than testing to failure because of the high cost of the capacitive gages, and so that the resistance gages could be evaluated after repeated loading.

Load-strain curves for the $[0,\pm45,90]_s$ laminate of HTS/PMR-15 (specimen A-1) are shown in figure 6.1-8. Resistance gages were mounted on opposite sides of the specimen and the capacitive gage was mounted adjacent to one resistance gage. Strains indicated by the resistance and capacitive gages agreed closely at each temperature. The load-strain curves showed a slight increase in stiffness with load at test temperatures below 480 K, but were nearly linear at higher temperatures.

Load-strain curves for the $[0]_8$ laminates of HTS/PMR-15 (specimen A-2) are shown in figure 6.1-9. Strains indicated by the adjacent resistance and capacitive gages differed no-more-than five-percent at the highest strain levels. At all test temperatures, the curves displayed a pronounced increase in laminate stiffness with load.

Tension modulus values for each test of specimen A-1 and A-2 are shown in figure 6.1-10 as a function of test temperature. Modulus was calculated from each strain gage indication using a least square fit to the initial linear portion of the load-strain curves. Resistance gage indications were corrected for gage factor variation with temperature. For the $[0,\pm45,90]_s$ laminate (specimen A-1), modulus values from the resistance gages and the capacitive gage agreed closely for each test, and modulus from test-to-test was essentially constant with temperature. For the $[0]_8$ laminate (specimen A-2), modulus values indicated by the resistance and capacitive gages differed by no more than eleven-percent during any test. The variation of modulus with temperature, for any one gage, was no more than ten-percent.

The close agreement between resistance and capacitive strain gage indications during repeated tests throughout the temperature range has demonstrated accurate and repeatable performance for the resistance gages at temperatures as-high-as 589 K (600°F).

An HTS/NR-150B2 $[0,\pm45,90]_s$ laminate (specimen B-1), instrumented with resistance strain gages and a rod-in-tube extensometer, was tested at room temperature and 589 K (600°F). The load-strain curves in figure 6.1-11(a) show fair agreement between the strain-gage and the extensometer at room-temperature, although the extensometer indication is somewhat erratic. The load-strain curves in figure 6.1-11(b) for 589 K (600°F) show an expected linear response for the resistance gage, but erratic response for the extensometer. Performance of the rod-in-tube extensometer has not proven to be reliable and this device has not been considered for further use.

The test methods described in this section are being used to characterize tension properties of graphite/polyimide laminates which are being developed and produced under the CASTS Project. Some typical test results are shown in figure 6.1-12 where tension modulus for HTS/NR-150B2 laminates in $[0]_8$, $[0,\pm45,90]_s$, and $[\pm45]_4$ ply orientations is shown for tests at temperatures of 117 K (-250°F), 297 K (75°F), and 589 K (600°F). Each data point represents a test of one specimen which was tested to failure. These specimens are not listed elsewhere in this report. Modulus values of fiber dominated $[0]_8$ and $[0,\pm45,90]_s$ laminates varied only slightly throughout the test temperature range, whereas modulus of the resin dominated $[\pm45]_4$ laminate decreased somewhat with increasing temperature.

Improved graphite/polyimide laminates, presently being developed in the CASTS Project, will be tested through an expanded matrix of conditions which include test temperatures of 117K (-250°F), room temperature, and 589K (600°F). Pre-test conditioning of 125-hours at 589K, 100 cycles from 117K to 589K, and "as received" will be employed. Laminate orientations will include [0], [+45], and [0,+45,90]. Improved fiber/resin systems such as Celion 6000/PMR-15 and Celion 6000/LARC-160 will be characterized.

Concluding Remarks

Tension properties of graphite/polyimide laminates have been obtained at temperatures from 117 K (-250°F) to 589 K (600°F).Throughout this temperature range, resistance strain gages provided accurate and repeatable results suitable for characterizing mechanical properties of the graphite/polyimide laminates. Strain values indicated by the resistance gages at temperatures as-high-as 589 K agreed closely with values measured with a capacitive gage calibrated for temperatures as-high-as 1089 K (1500°F).

References

6.1-1. Harting, Darrell R.; Evaluation of a Capacitive Strain Measuring
System for use to 1500°F. 21st International Instrumentation
Symposium, Philadelphia, Penn. May 19-21, 1975. Instrument
Society of America Paper.

Specimen	Material Graphite Fiber/ Polyimide Resin	Laminate	Number of plies	Resistance strain gages[1]		Displacement gages
				Number Longitudinal	Number Transverses	
A-1	HTS/PMR-15	$[0,\pm45,90]_s$	8	2	-	Capacitive strain gage
A-2		$[0]_8$	8	1	-	
B-1	HTS/ NR-150B2	$[0,\pm45,90]_s$	8	1	1	Extensometer

Figure 6.1-1 - Test specimens and instrumentation for measuring strain.

[1]Micro-Measurments Series WK-06-125AD-350

2.54 cm
(1.00 in.)

Tab thickness
2.5 mm (0.10 in)

(Tab adhesive:
FM-34)

6.35 cm
(2.50 in.)

15.25 cm
(6.0 in.)

Specimen
thickness
1.5 to 1.7 mm
(.06 to .07 in.)

Thermocouple (C-A)

Longitudinal
strain gage

Transverse
strain gage

(Strain gage
adhesive:
PLD-700)

30.5 cm
(12.0 in.)

20°-30°
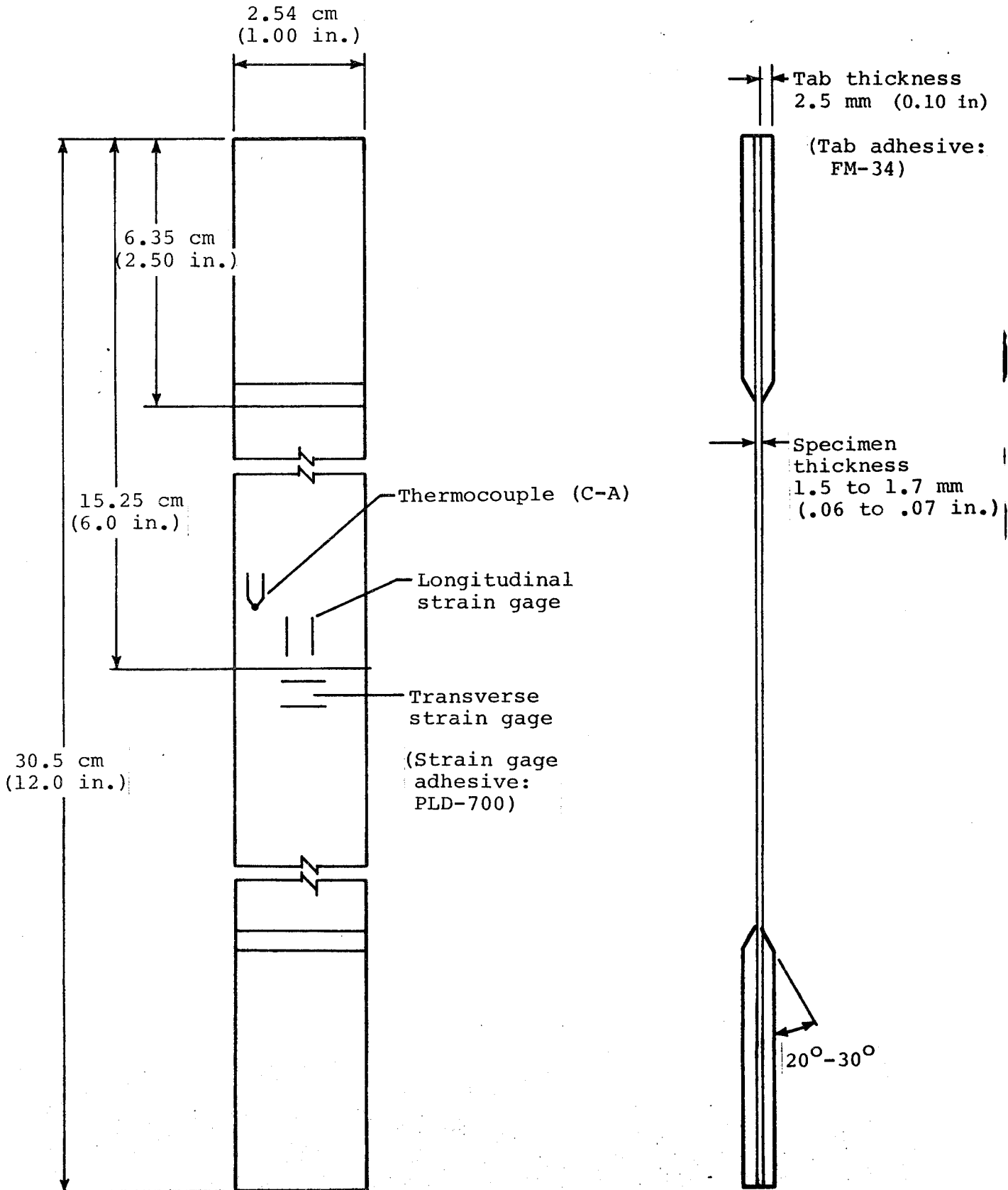
Figure 6.1-2 -   Graphite/polymide tension specimen configuration.
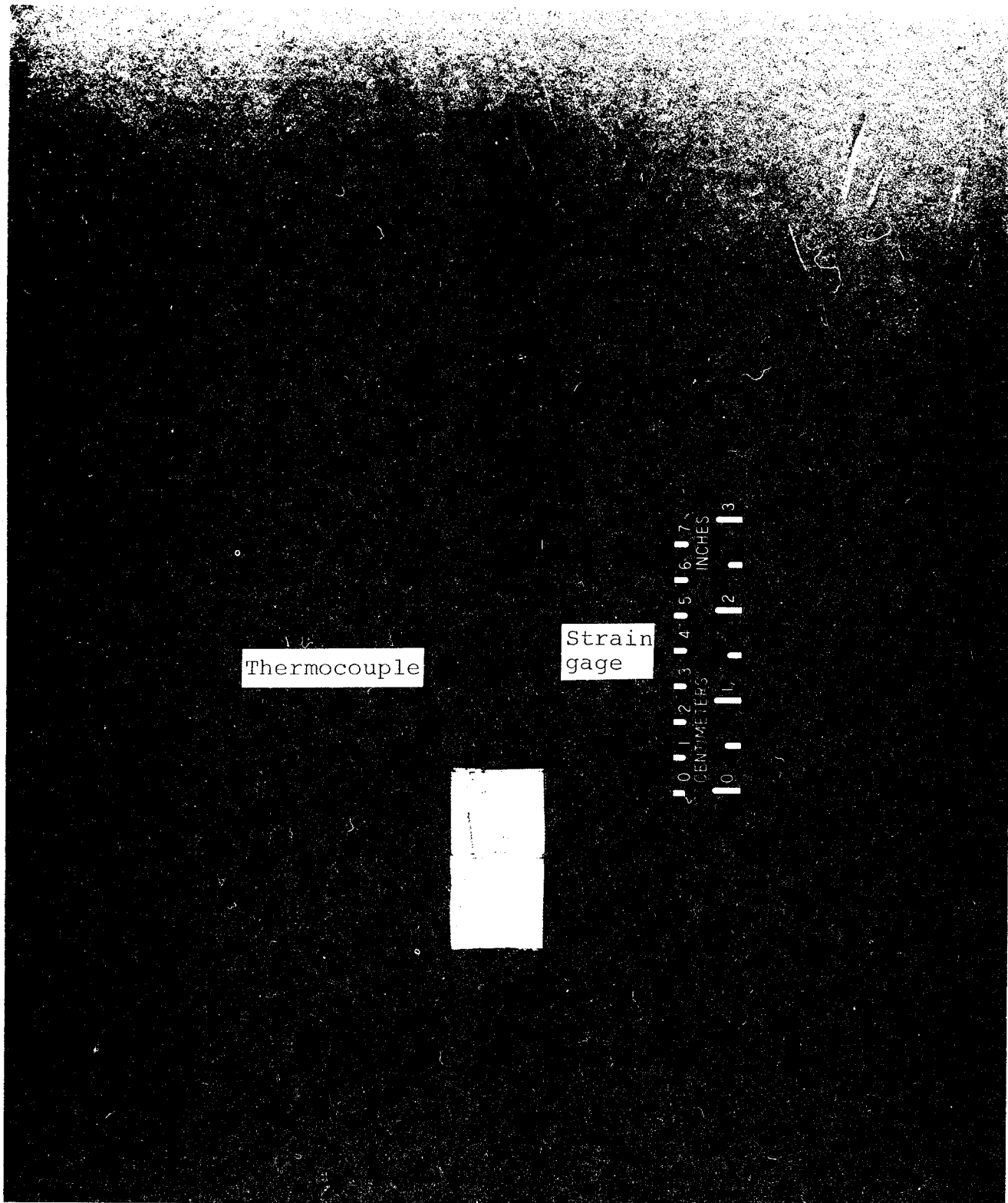
Figure 6.1-3 - Tension specimen with resistance strain gage.
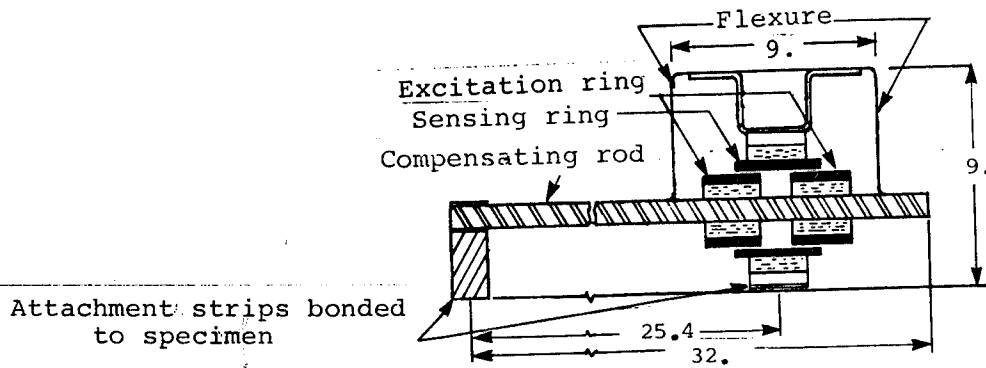
(a) Capacitive strain gage - cross section view.
(dimensions in millimeters)
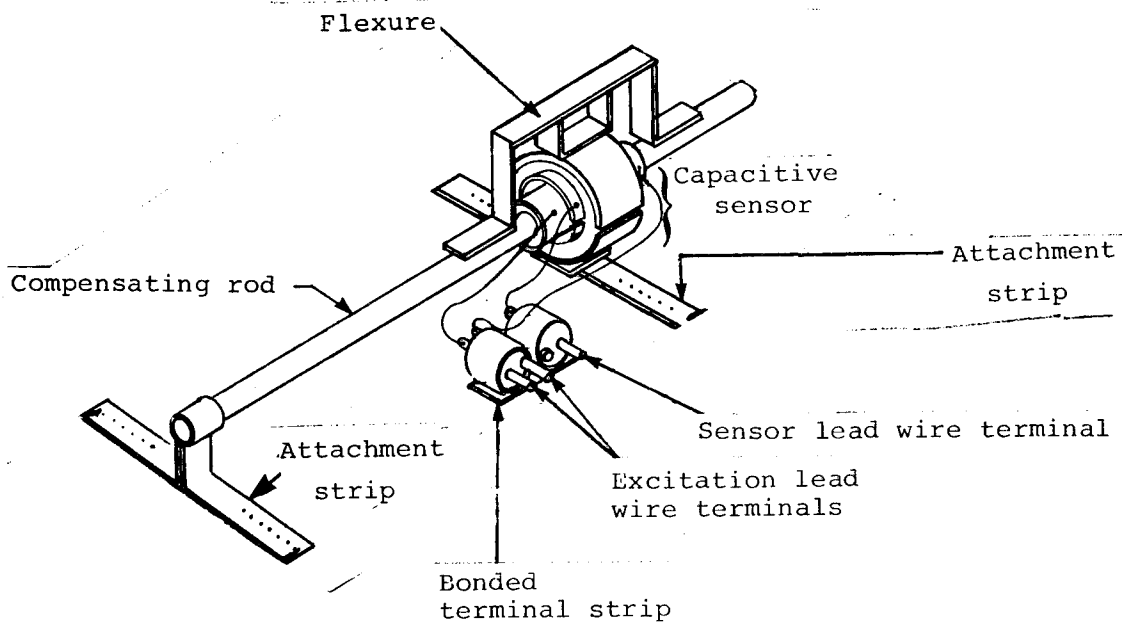
(b) Capacitive strain gage-perspective view.

Figure 6.1-4 Capacitive strain gage installation and details.

Capacitive
strain gage

Thermocouple

Resistance
strain gage

HTC
DC-100-06
S/N 118
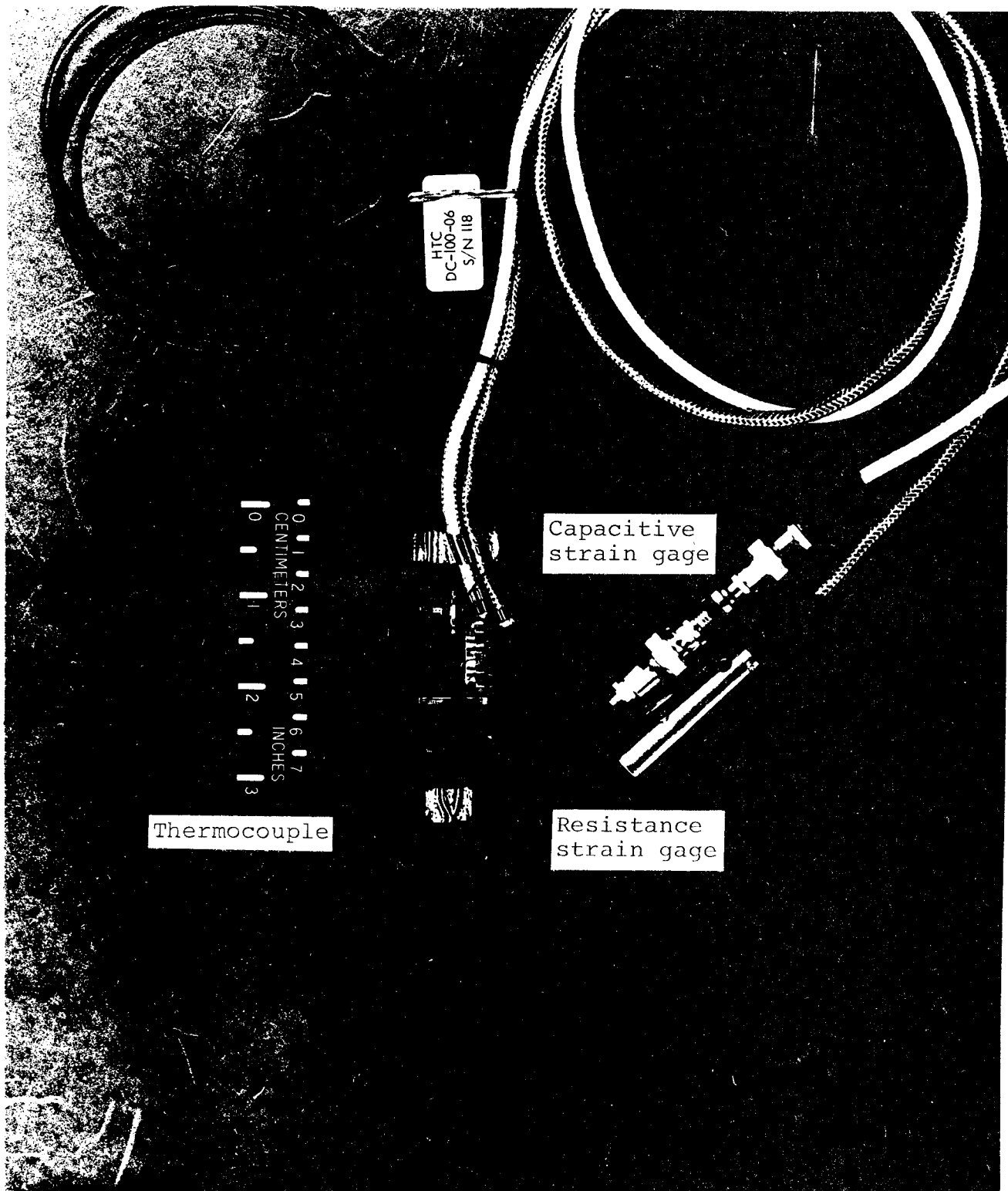
(a) Overall view

Figure 6.1-5a - Capacitive strain gage installed on tension specimen.

Capacitive strain gage

Concentric capacitive
plate

Leads

Attachment
strip

Thermocouple

Terminal strip

Compensating rod

Attachment strip

Resistance
strain gage

(b) Detail view.

Figure 6.1-5b - Concluded.
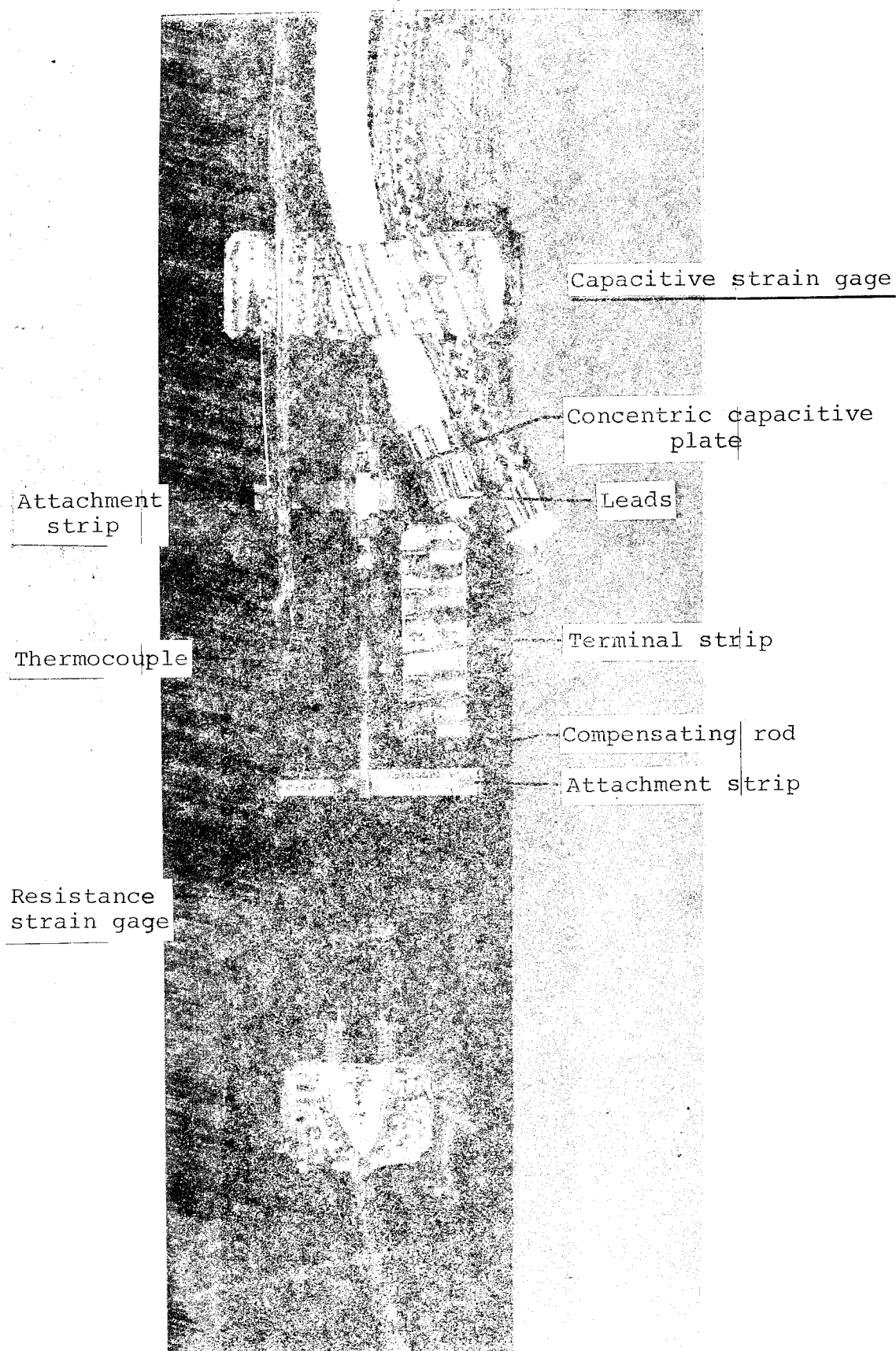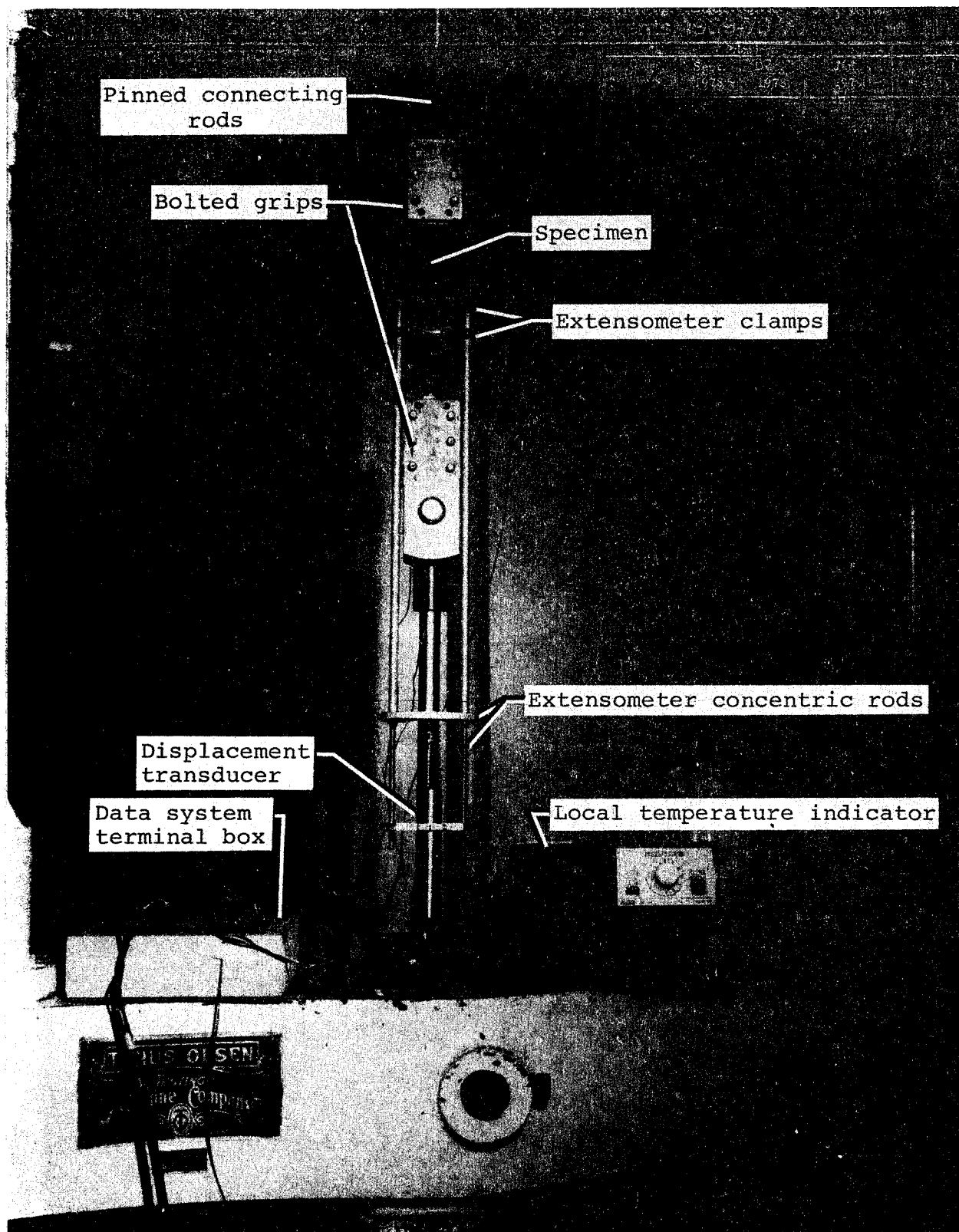
(a) Heating chamber removed.

Figure 6.1-6 - Tension specimen with extensometer mounted in hydraulically actuated test machine.
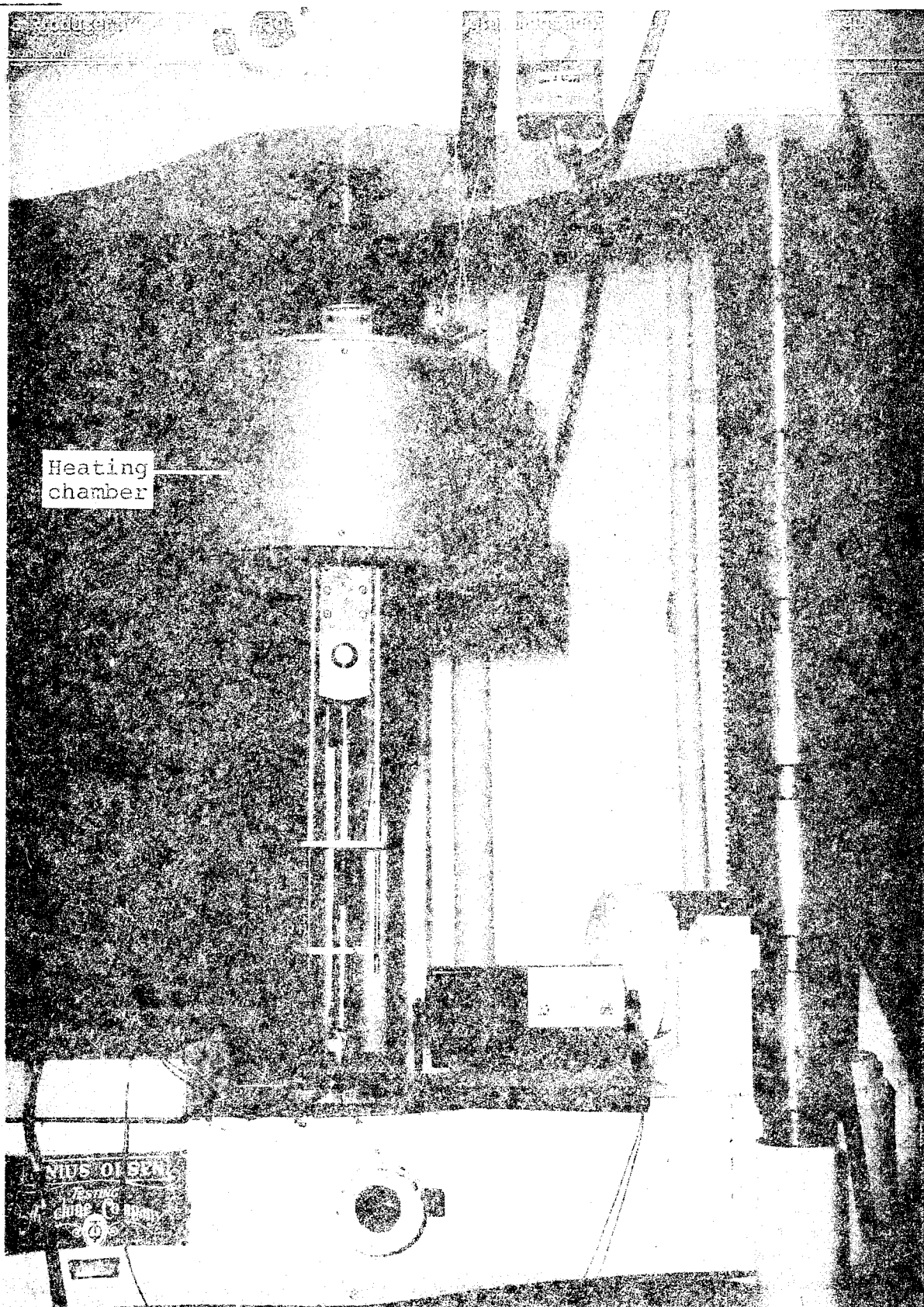
Heating
chamber

(b) Heating chamber in position.

Figure 6.1-6 - Concluded.
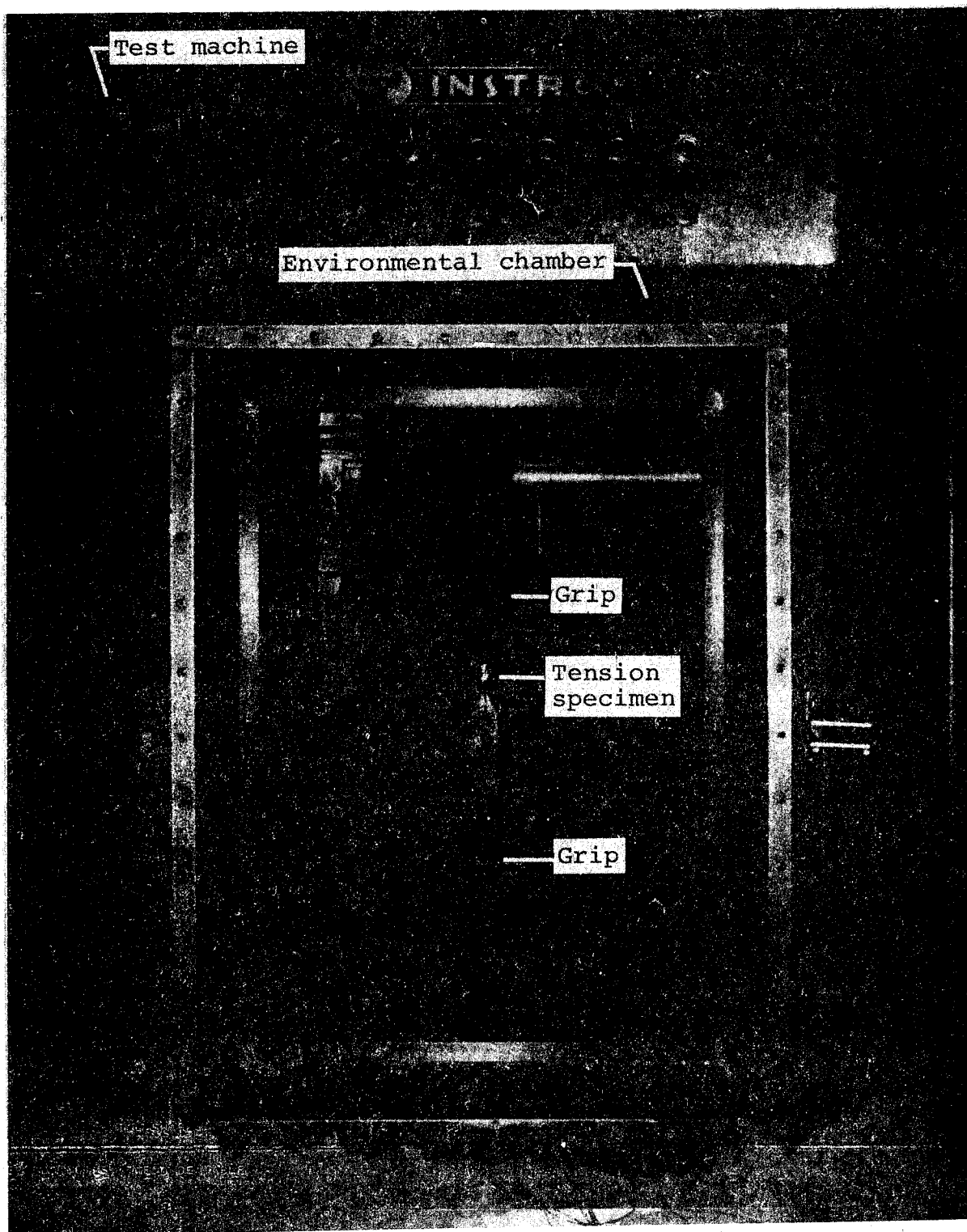
Figure 6.1-7 – Environmental chamber with tension specimen mounted in
mechanically driven test machine.
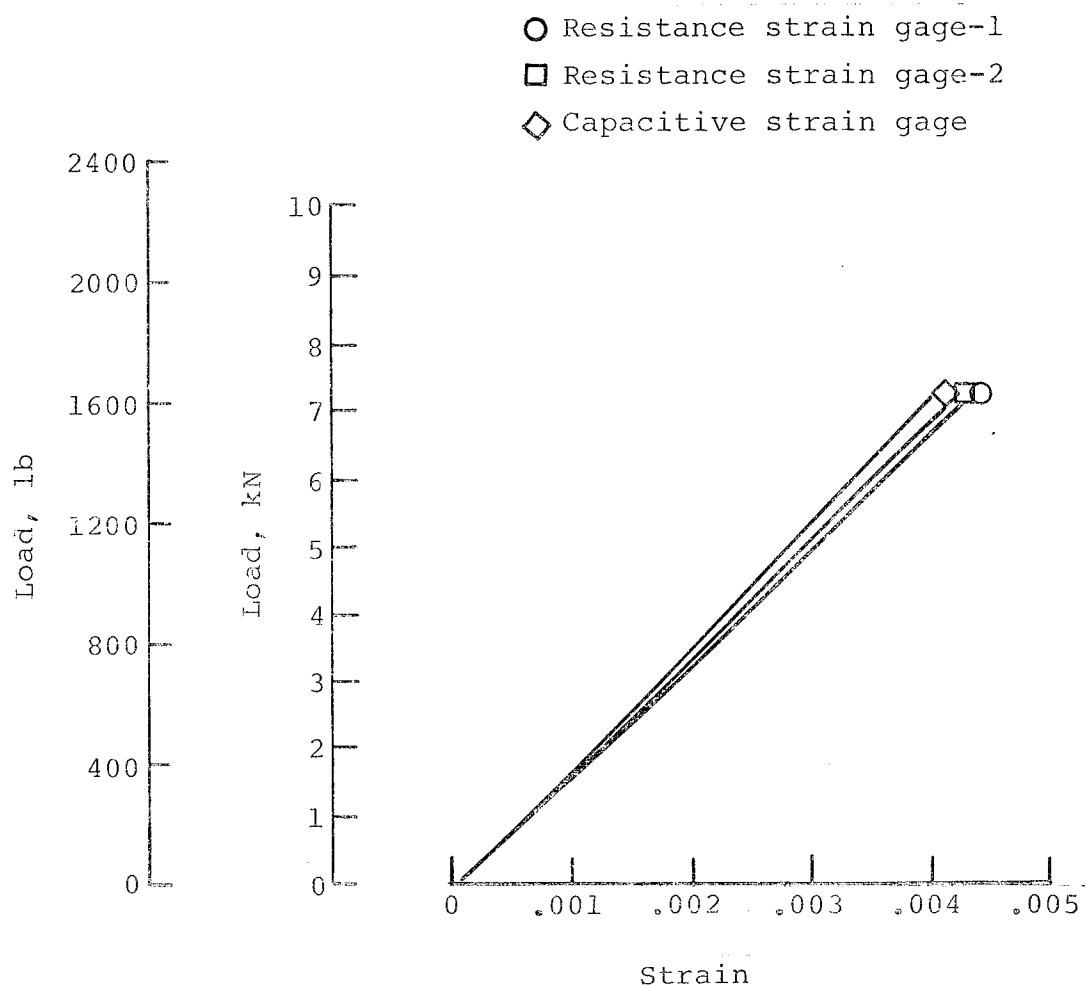
(a) Room temperature.

Figure 6.1-8 — Tension load-strain curves for $[0, \pm 45, 90]_s$ laminates of HTS/PMR-15. Resistance and capacitive strain gage indications are identified by symbols listed above figure.

O Resistance strain gage-1
□ Resistance strain gage-2
◇ Capacitive strain gage
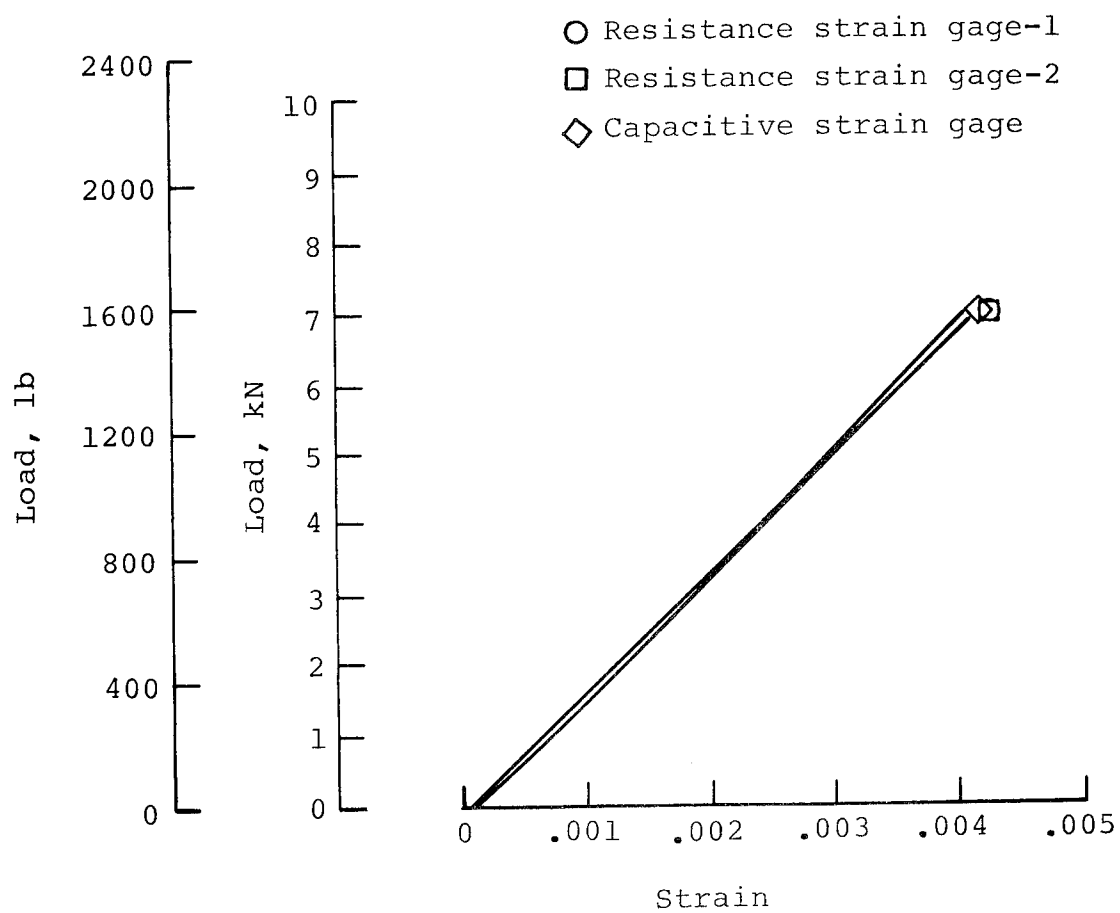
(b) 422 K (300 °F) .

Figure 6.1-8 - Continued.

120
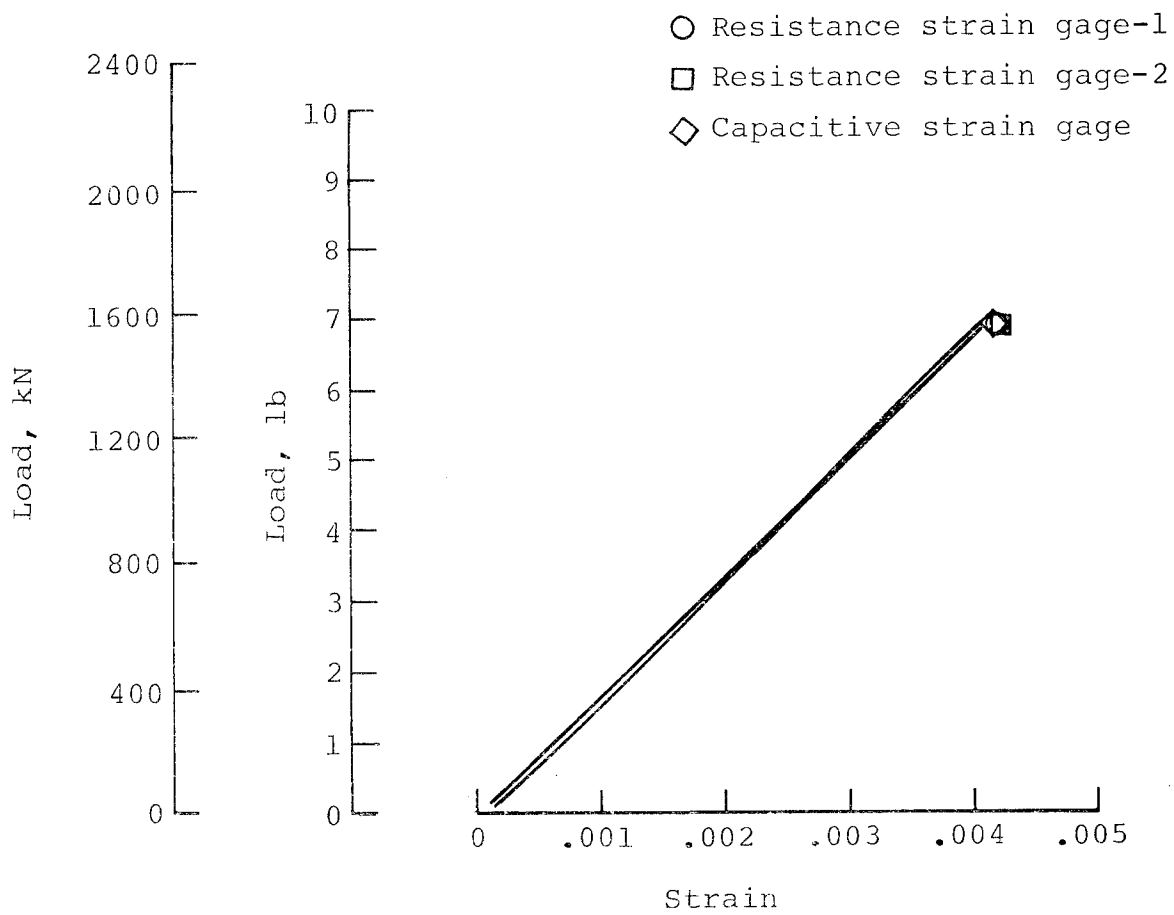
(c) 478 K (400 °F) .

Figure 6.1-8 - Continued.
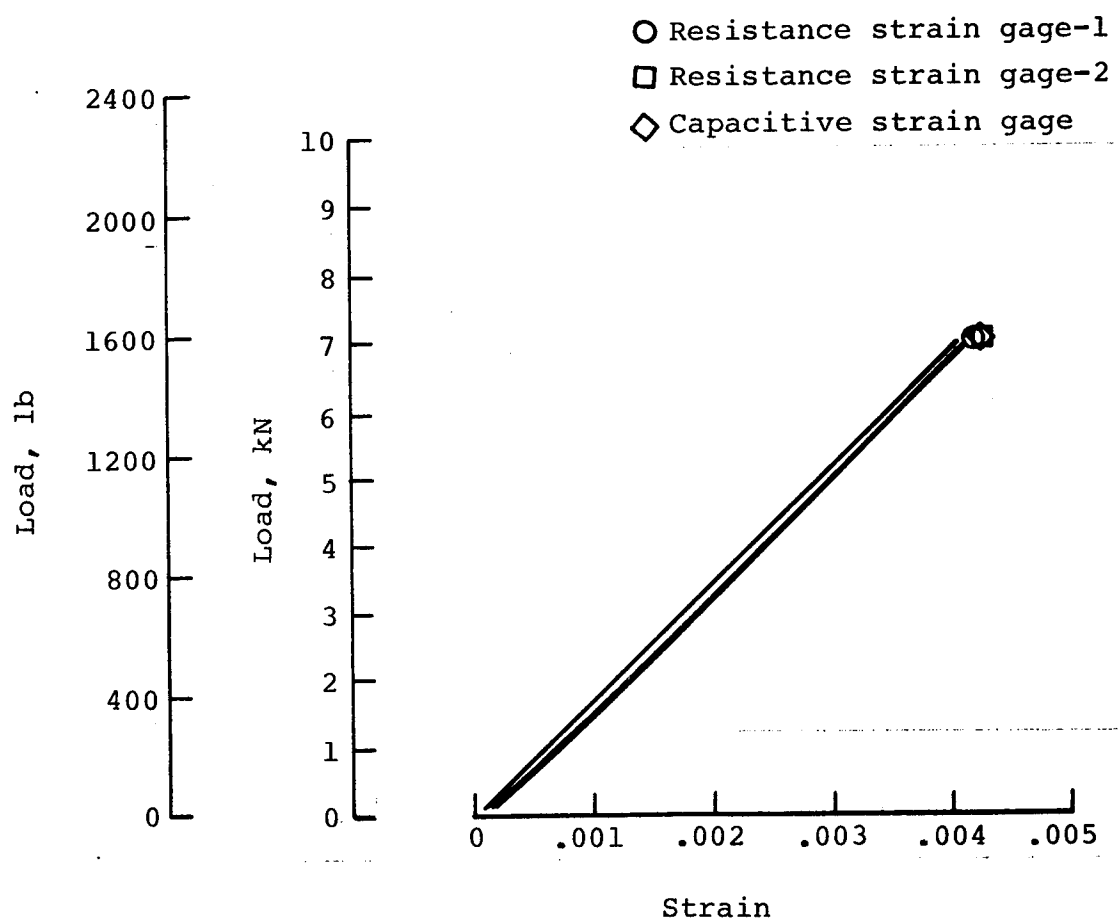
(d) 533 K (500 °F) .

Figure 6.1-8 - Continued.
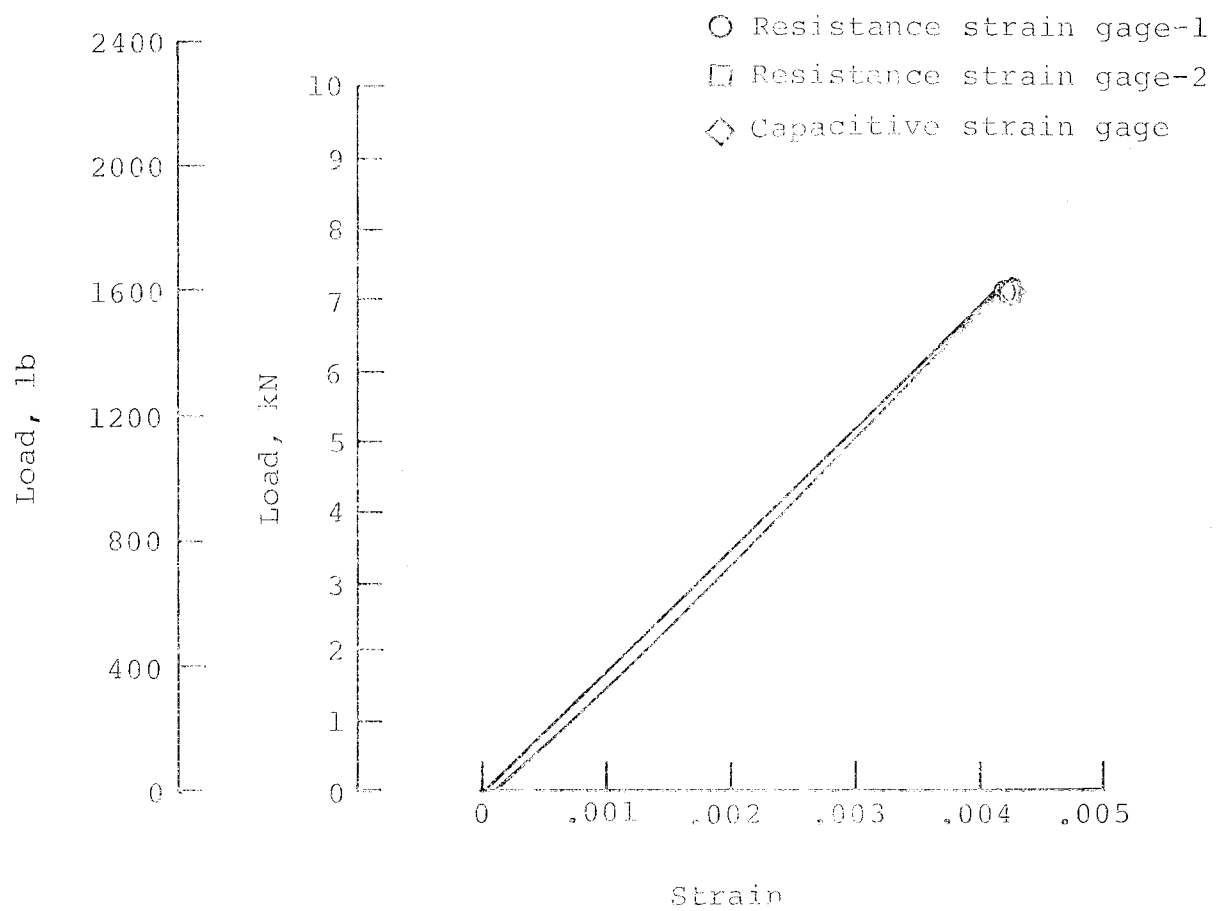
(e) 561 K (550 °F) .

Figure 6.1-8 – Continued.
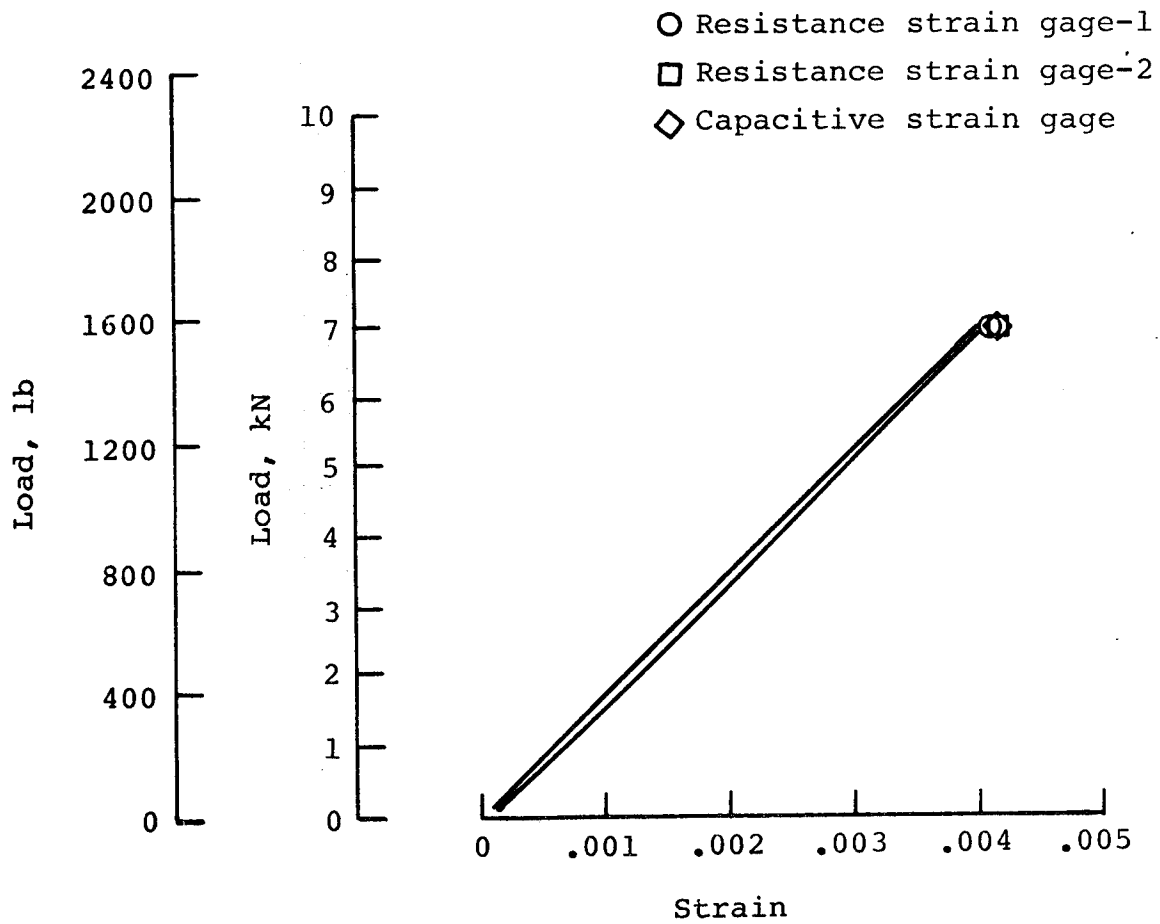
(f) 589 K (600 °F) .

Figure 6.1-8 - Concluded.
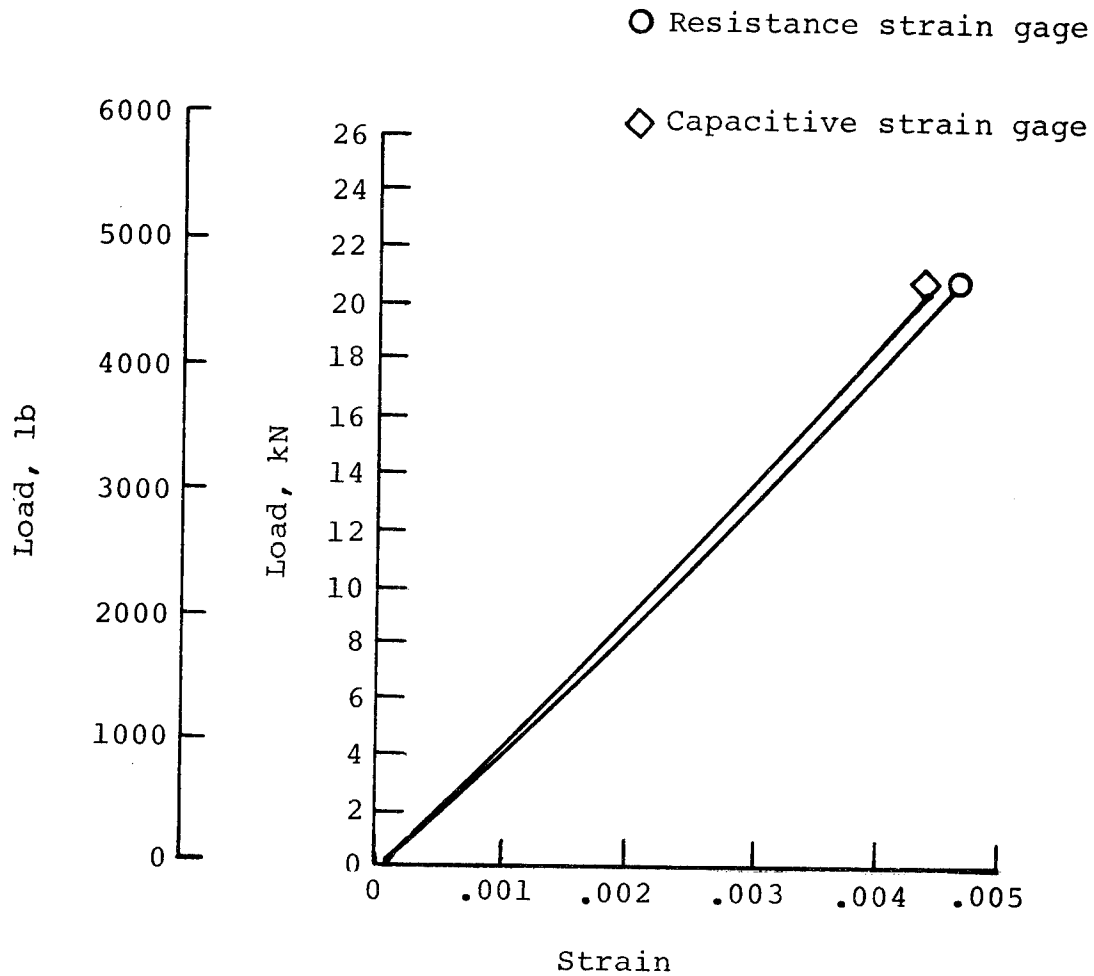
(a) Room temperature .

Figure 6.1-9 – Tension load-strain curves for [0]$_8$ laminates of
             HTS/PMR-15.   Resistance and capacitive strain gage
             indications are identified by symbols listed above
             figure.
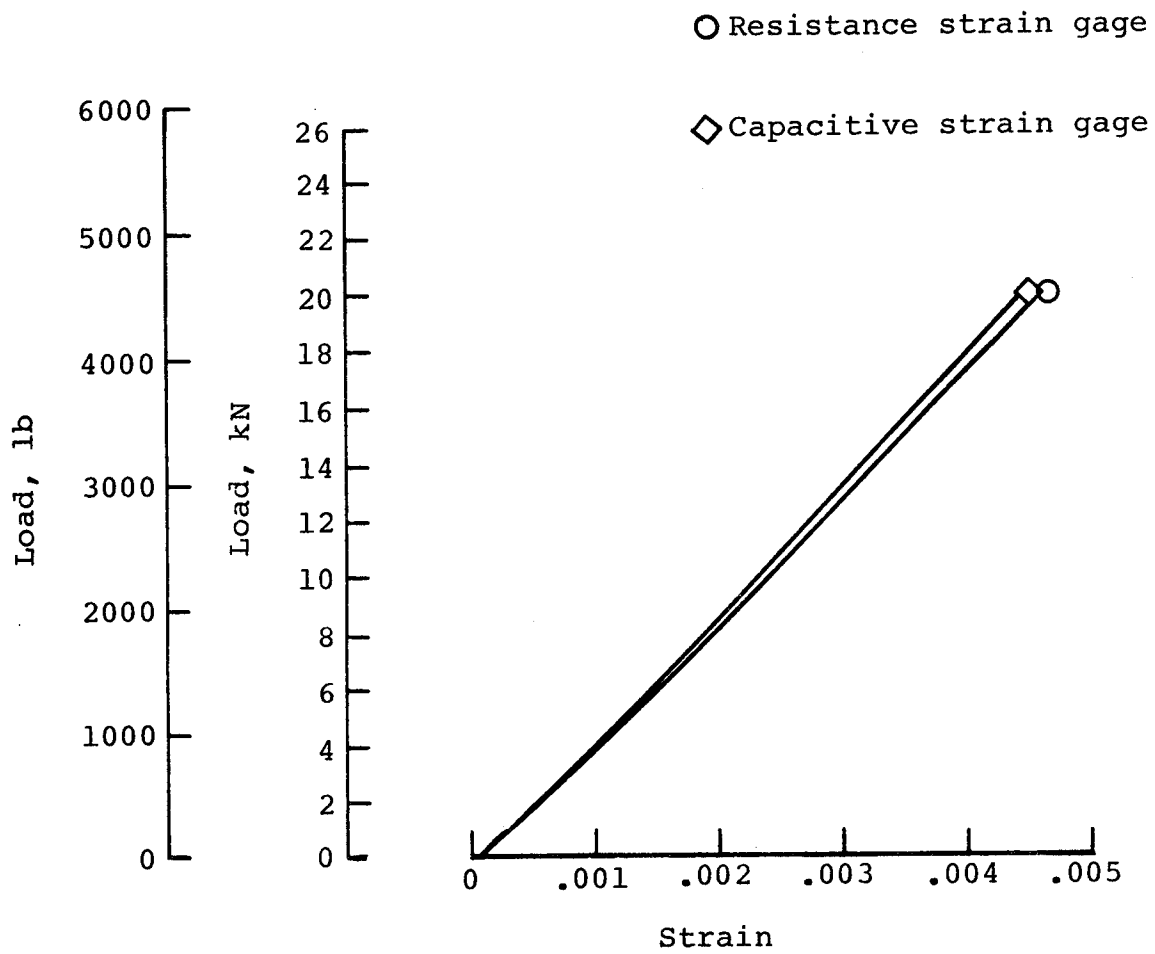
(b) 422 K (300 ^{O}F) .

Figure 6.1-9 - Continued.
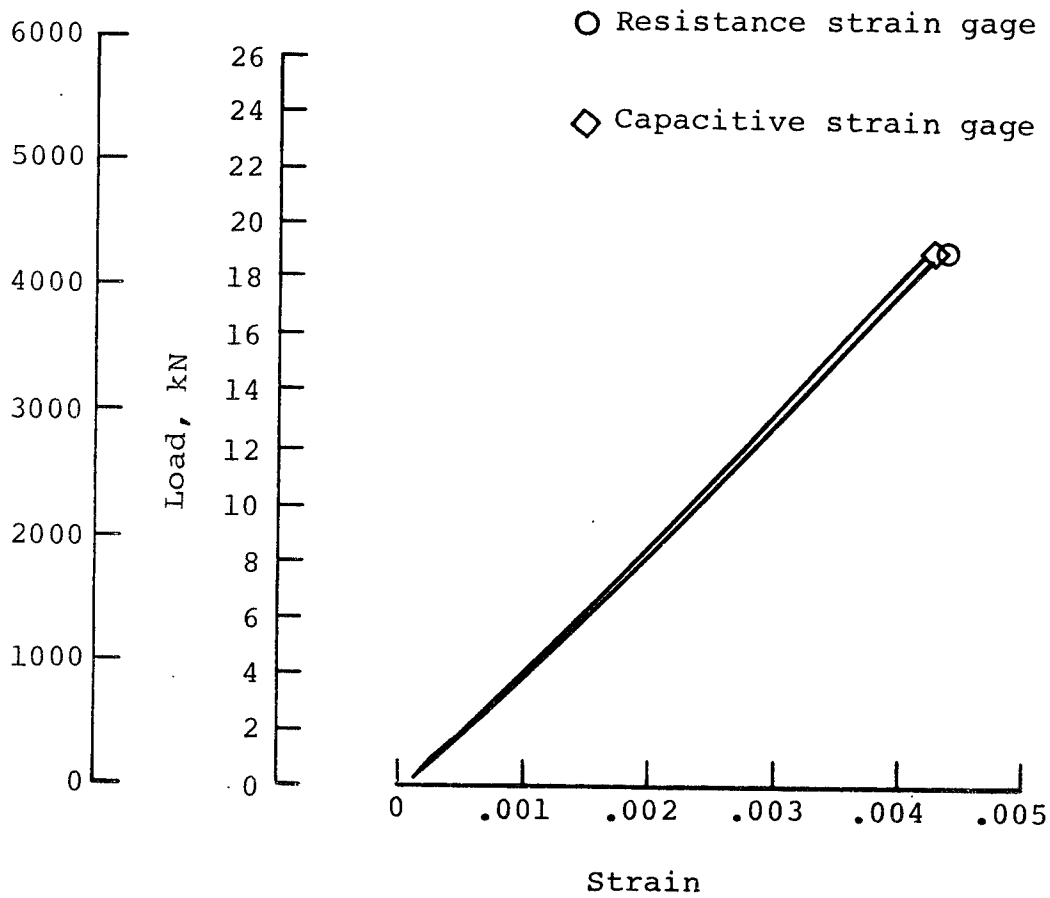
(c) 478 K (400 °F) .

Figure 6.1-9 - Continued.
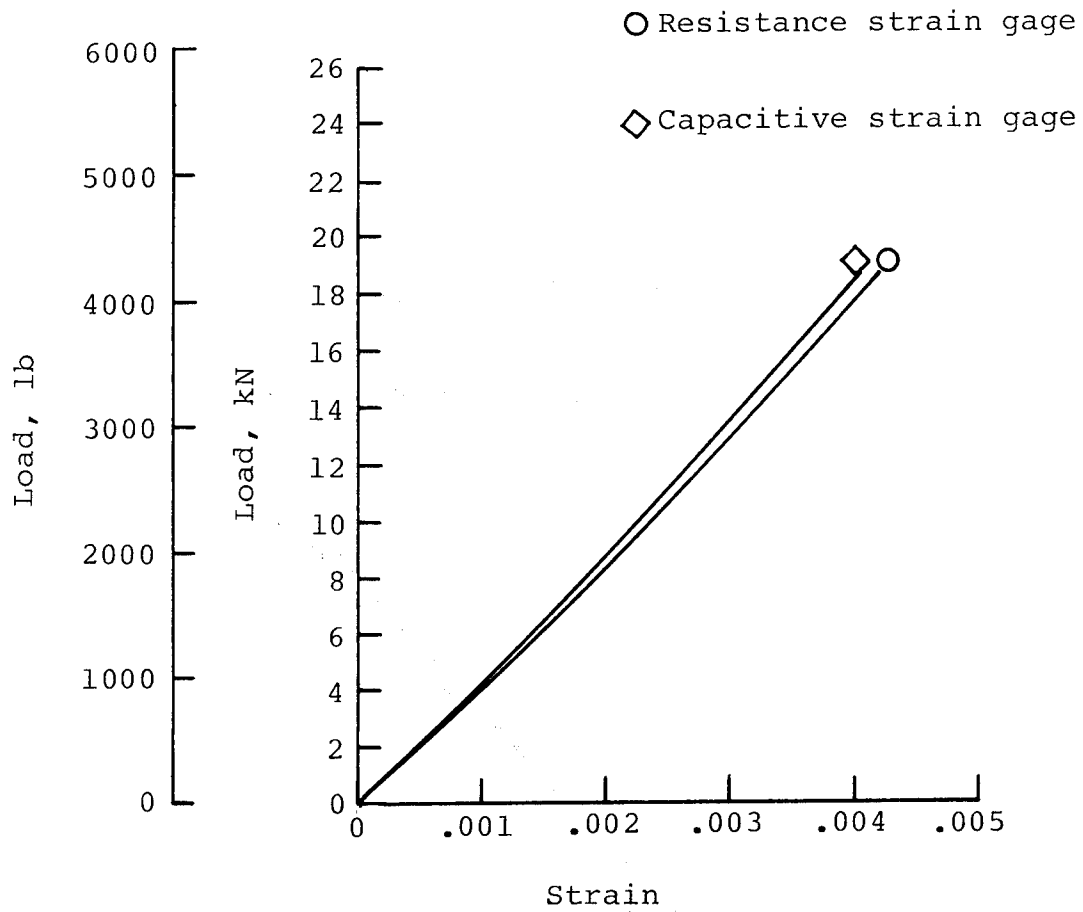
(d) 533 K (500 °F) .

Figure 6.1-9 - Continued.
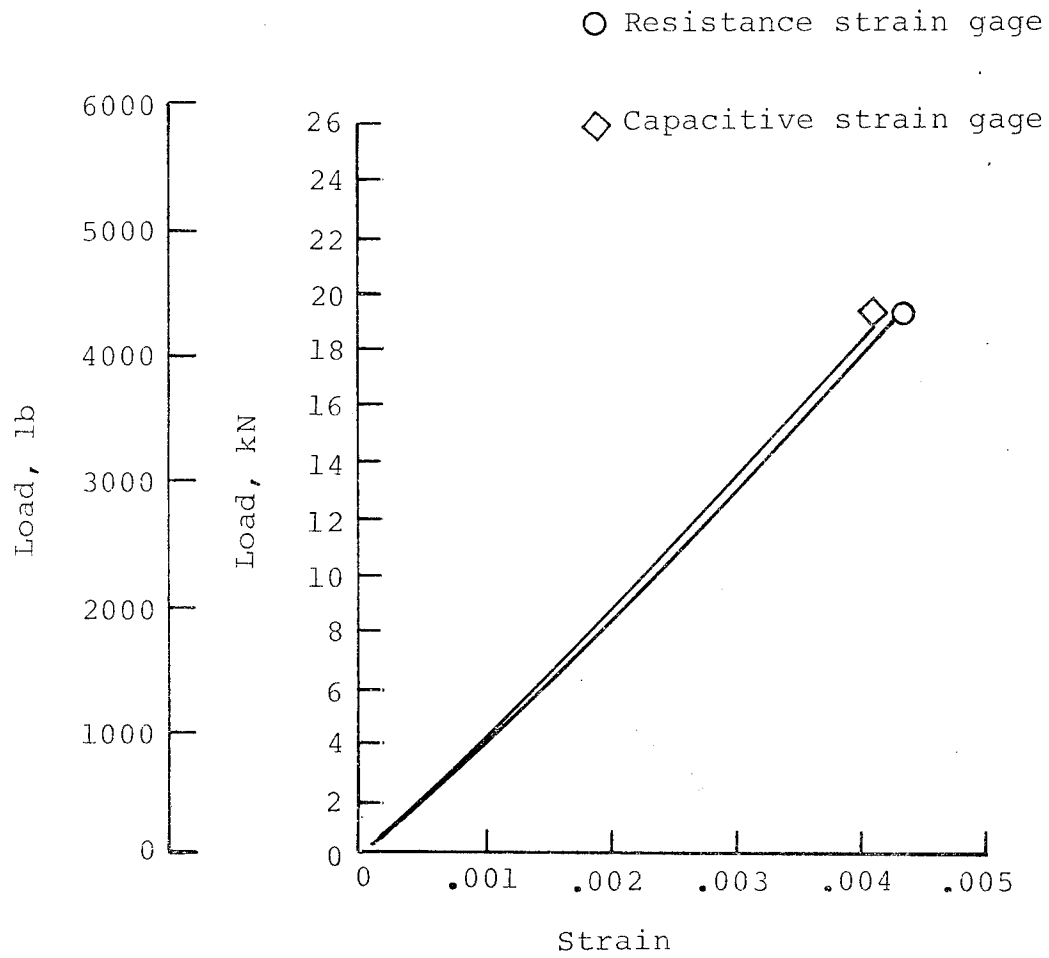
(e) 561 K (550 °F) .

Figure 6.1-9 - Continued.
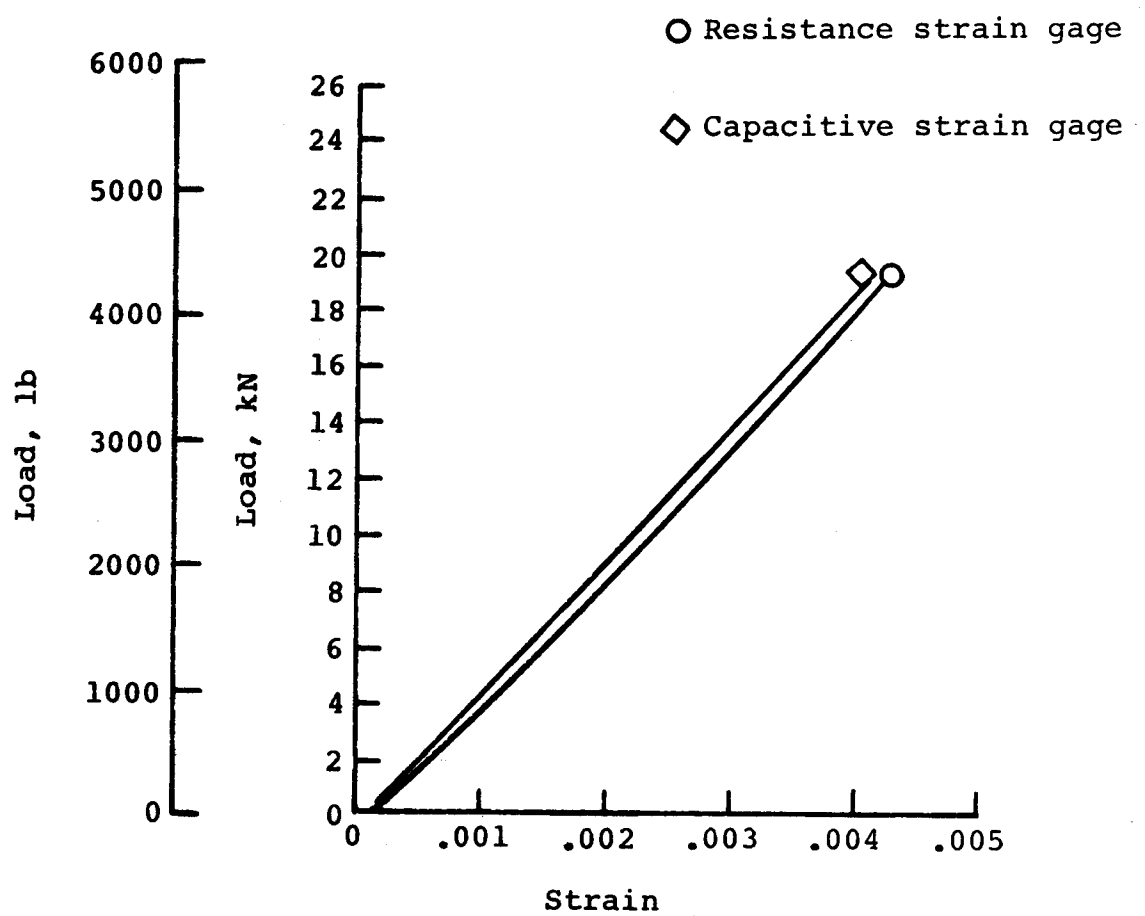
(f) 589 K (600 °F) .

Figure 6.1-9 - Concluded.
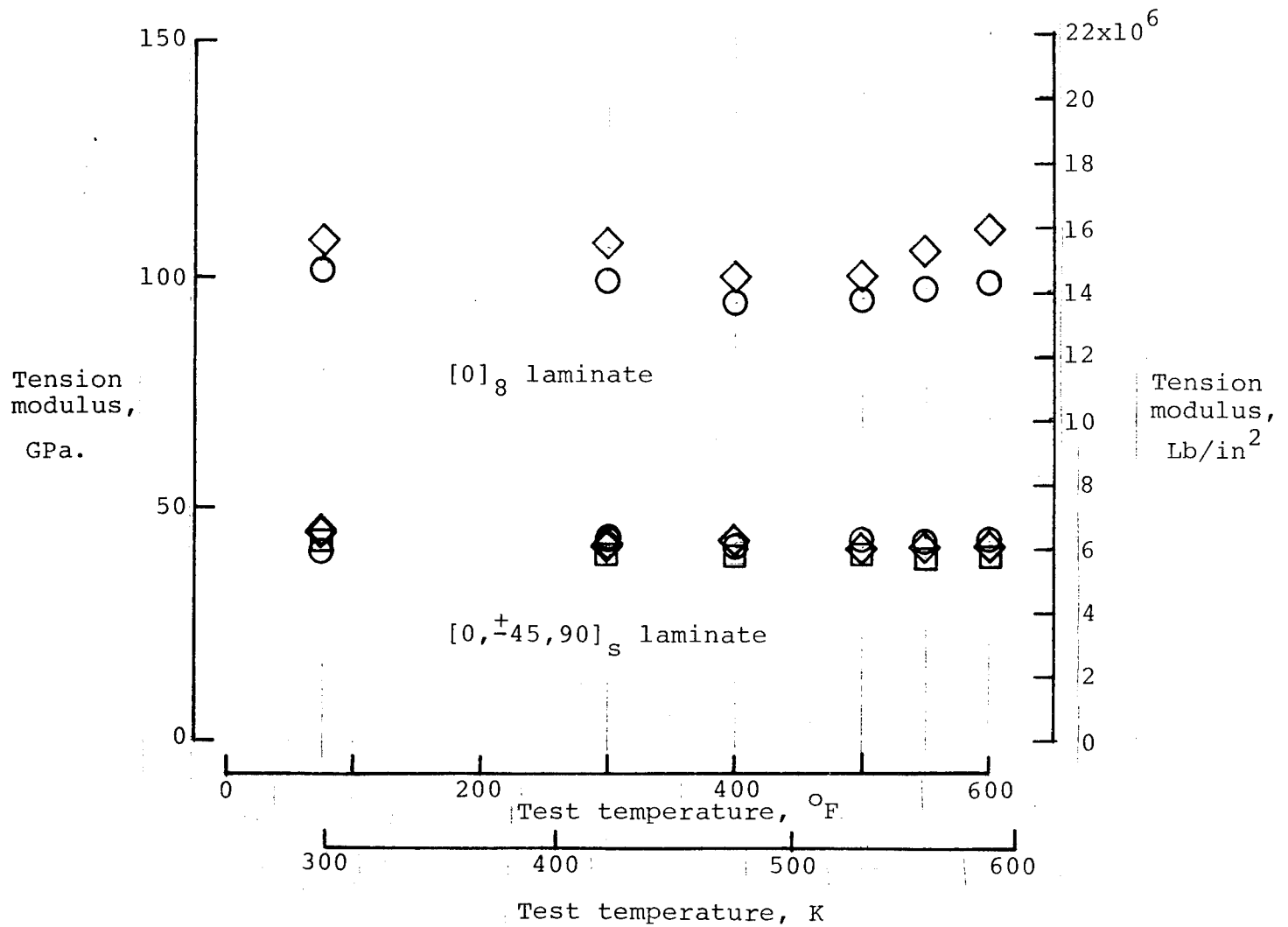
Figure 6.1-10 – Tension modulus variation with temperature for
HTS/PMR-15; resistance and capacitive strain gage
indications.
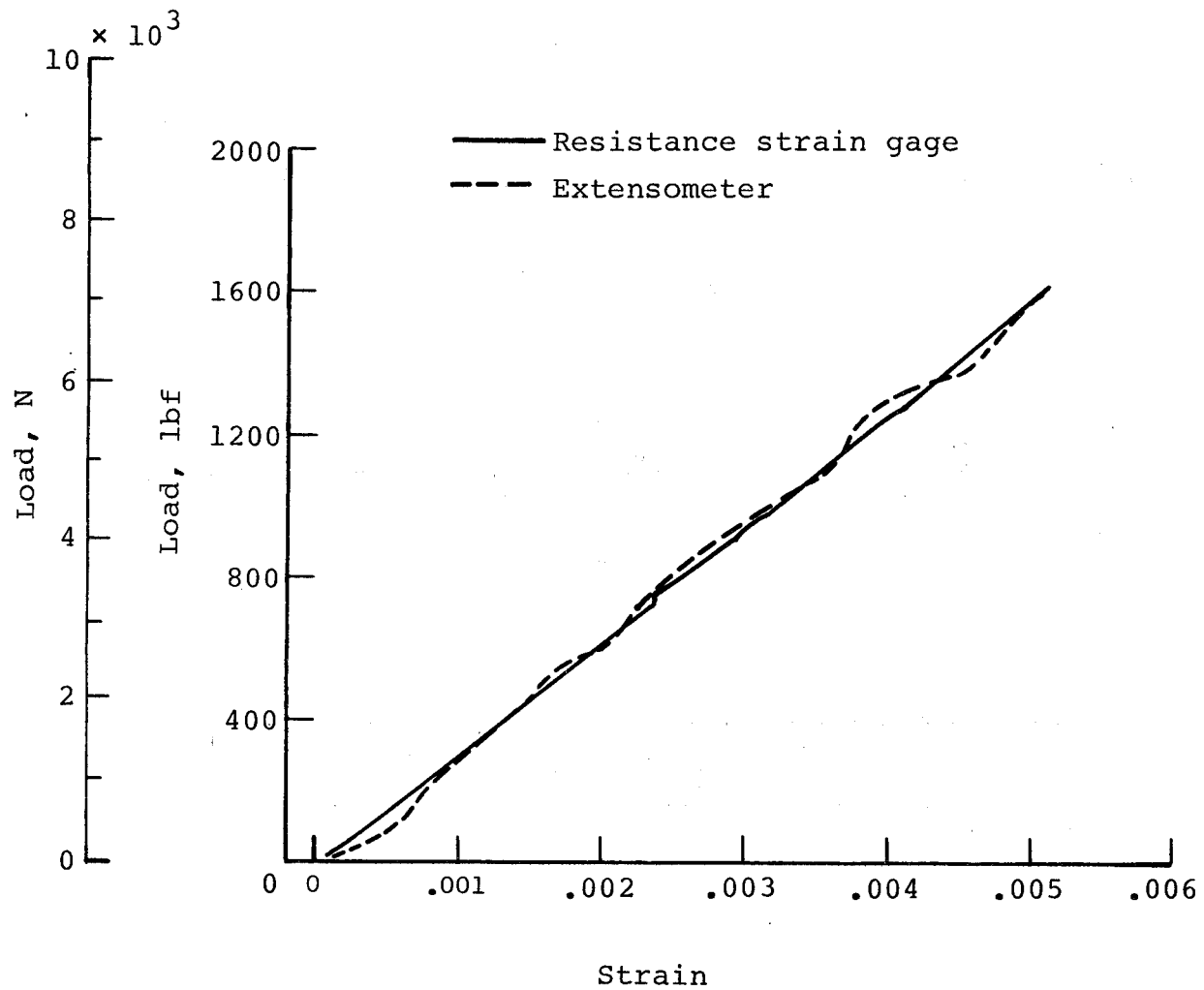
(a) Test at room temperature.

Figure 6.1-11 – Tension test comparison of resistance strain gages and an extensometer; HTS/NR-150B2 graphite/polymide $[0, \pm45, 90]_s$ laminate.
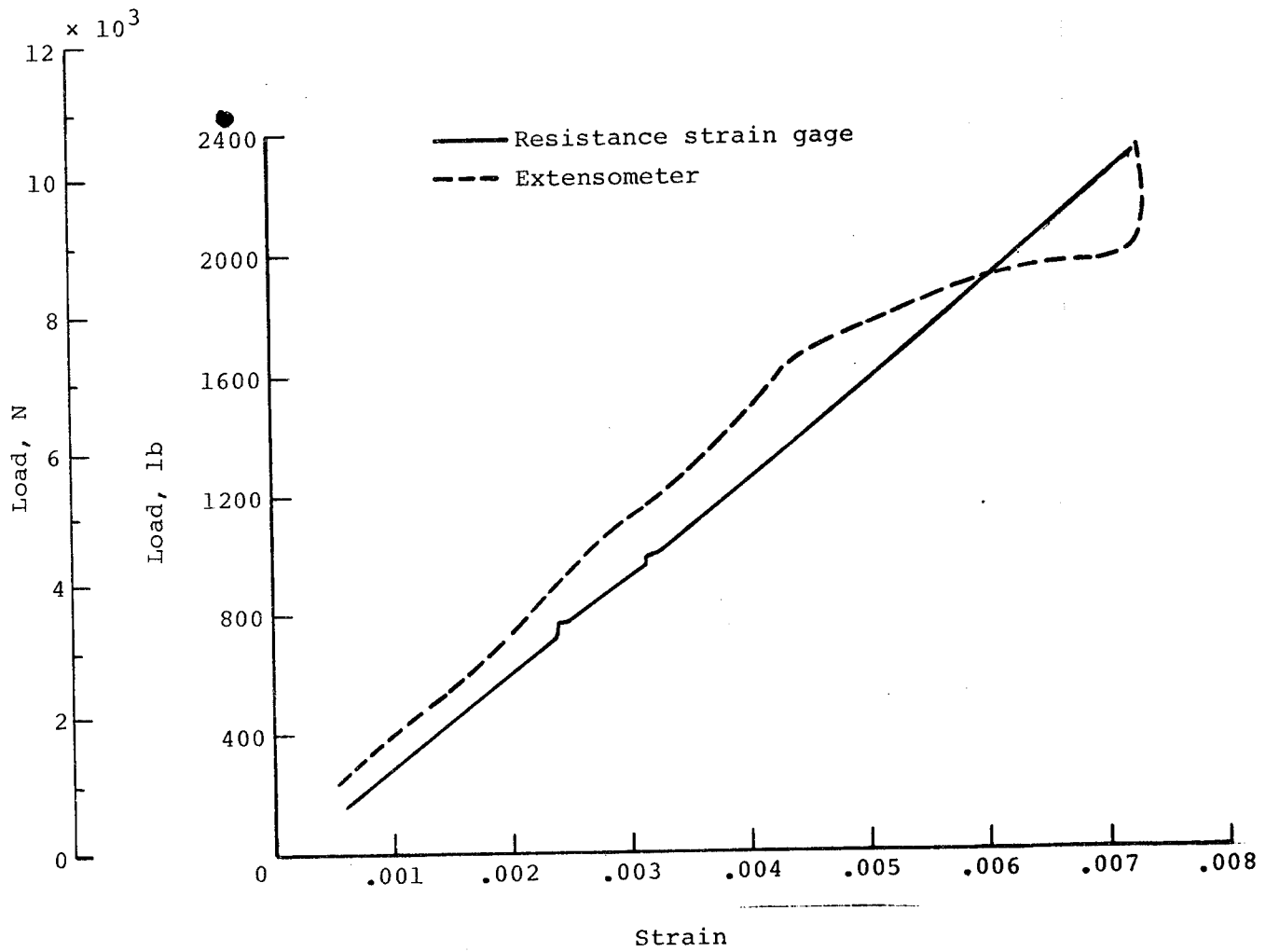
(b) Test temperature 590 K (600 ^{O}F).

Figure 6.1-11 - Concluded.
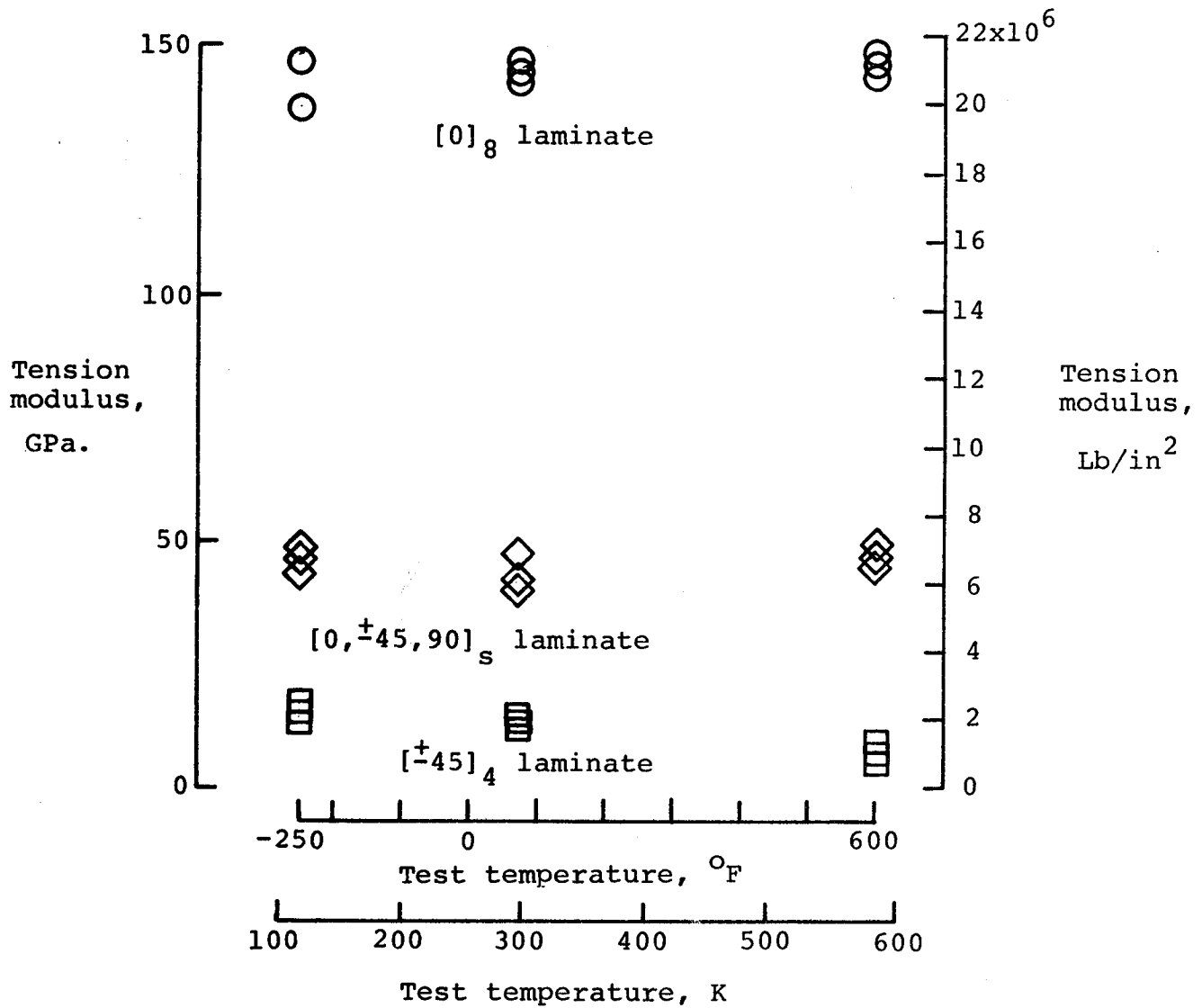
Figure 6.1-12 - Tension modulus variation with temperature for HTS/NR-150B2.

6.2 IITRI Compression Test Method
B. Basava Raju and Charles J. Camarda

Difficulties in the development of compressive test techniques for
specimens prepared from thin sheets of advanced composite material have
included end splitting, buckling, and load alinement problems. While the
sandwich beam flexure specimen has been the most successful and widely
accepted technique for obtaining compression data, its high cost per
test severely limits its use where data on quantitative environmental effects
are of interest. The purpose of the current study is to evaluate a new,
inexpensive test method using the IITRI compression test fixture (fig.
6.2-1) which promises to alleviate previous problems (ref. 6.2-1). Experi-
mental results for the standard IITRI specimen (0.6 cm (1/4 in) wide) and
data from selected variations of that specimen will be compared with a 3-D
finite-element analysis in an effort to evaluate and possibly improve the
test technique for room and elevated temperature testing.

Graphite-polyimide (HTS/PMR-15) composite specimens were fabricated
in widths of 0.6 cm (1/4 in.), 1.3 cm (1/2 in.), 1.9 cm (3/4 in.), and
2.5 cm (1 in.) and laminations of $[0]_{15}$, $[90]_{20}$ $[\pm45]_{5s}$, and $[0,\pm45,90]_{2s}$
for testing at room temperature, and 589K (600°F). Back-to-back strain
gages were used to confirm proper load alinement and to determine longi-
tudinal and transverse strains. Typical stress-strain curves of the $[0]_{15}$
ply laminate are shown in figure 6.2-2 for RT and 589K (600°F) respectively
for a displacement rate of 0.1 cm/min (0.05 in./min). A difference between
back-to-back longitudinal strain readings of less than 10 percent confirmed
nearly perfect load alinement and the absence of bending or buckling during
loading to failure. Average compressive modulus and strength data of several
tests are given in Figures 6.2-3 and 6.2-4. Scatter in the results was
limited, with a maximum variation of 7.5 percent in compressive modulus for
the 589K (600°F) tests and a maximum variation of 2.5 percent for the room
temperature tests. The remaining specimens will be tested to study the
effects of specimen width and temperature on compressive material properties
and failure.

The average compression modulus of the 589°K (600°F) specimen increased
by 17 and 29 percent over the room temperature specimen for stress levels of
352 MPa (51 ksi) and 614 MPa (89 ksi) respectively. The results were consistent
and warrant further investigation by a different compression test method such as
the sandwich beam flexure test. Also, the ultimate compression strength at
elevated temperature decreased by 37 percent of the room temperature value.

The object of most material property tests is to produce a uniform state
of stress in the test section of a specimen so that material properties can
be determined from constitutive relationships. End constraints, tab effects,
extraneous additional end loads, free edge effects, and thermal effects add to
the three-dimensional nature of stresses in the specimen. To fully understand
results of a particular test technique, such as ultimate strength and modulus

values, it is necessary to know the exact state of stress of the specimen. Thus, a fully three-dimensional finite-element analysis of the IITRI specimen was performed. Due to symmetry about its three midplanes, only one-eighth of the 0.6 cm (1/4 in.) IITRI test specimen including the graphite-polyimide laminate, glass-polyimide tabs, and FM-34 adhesive layer was idealized by three-dimensional finite elements (fig. 6.2-5) using ATLAS (ref. 6.2-2). The primary means of mechanical load introduction is by tab shear (fig. 6.2-6), however, the effect of extraneous loads such as a uniform end load and a clamp load could be important.

The axial stress distribution in the top lamina of a $[\underline{+45}]_{4s}$ laminate subject to only a tab shear load across the face of the tab in the X-direction is shown in figure 6.2-7. Results indicate a nonuniform stress distribution with peak values occurring near the tab region as expected. Similar stress-distributions for each of the remaining five stress components were obtained and are being analyzed to determine areas of stress concentrations and possible failure initiation. Analysis of the effects of other mechanical end loads (fig. 6.2-6) and thermal loads on stress distributions will also be made.

References

6.2-1. Hofer, K. E.; and Rao, P. N.: A New Static Compression Fixture for Advanced Composite Materials. Journal of Testing and Evaluation, JTEVA, Vol. 5, No. 4, July 1977, pp. 278-283.

6.2-2. Miller, Ralph E. Jr.: Structures Technology and Impact of Computers. Proceedings of ASME Winter Annual Meeting, Integrated Design and Analysis of Aerospace Structures, Houston, Texas, Nov. 30 thru December 5, 1977, pp. 57-70.
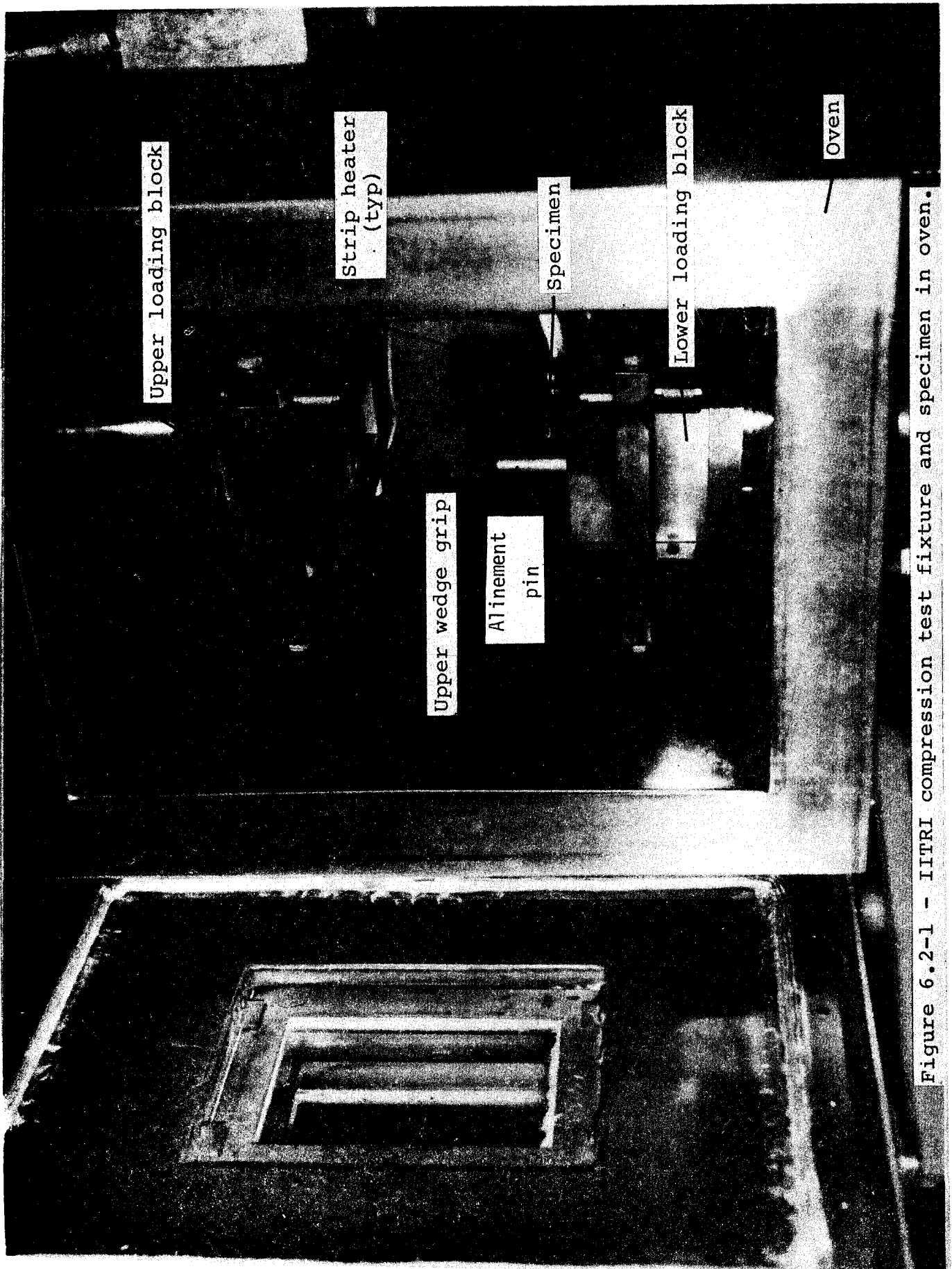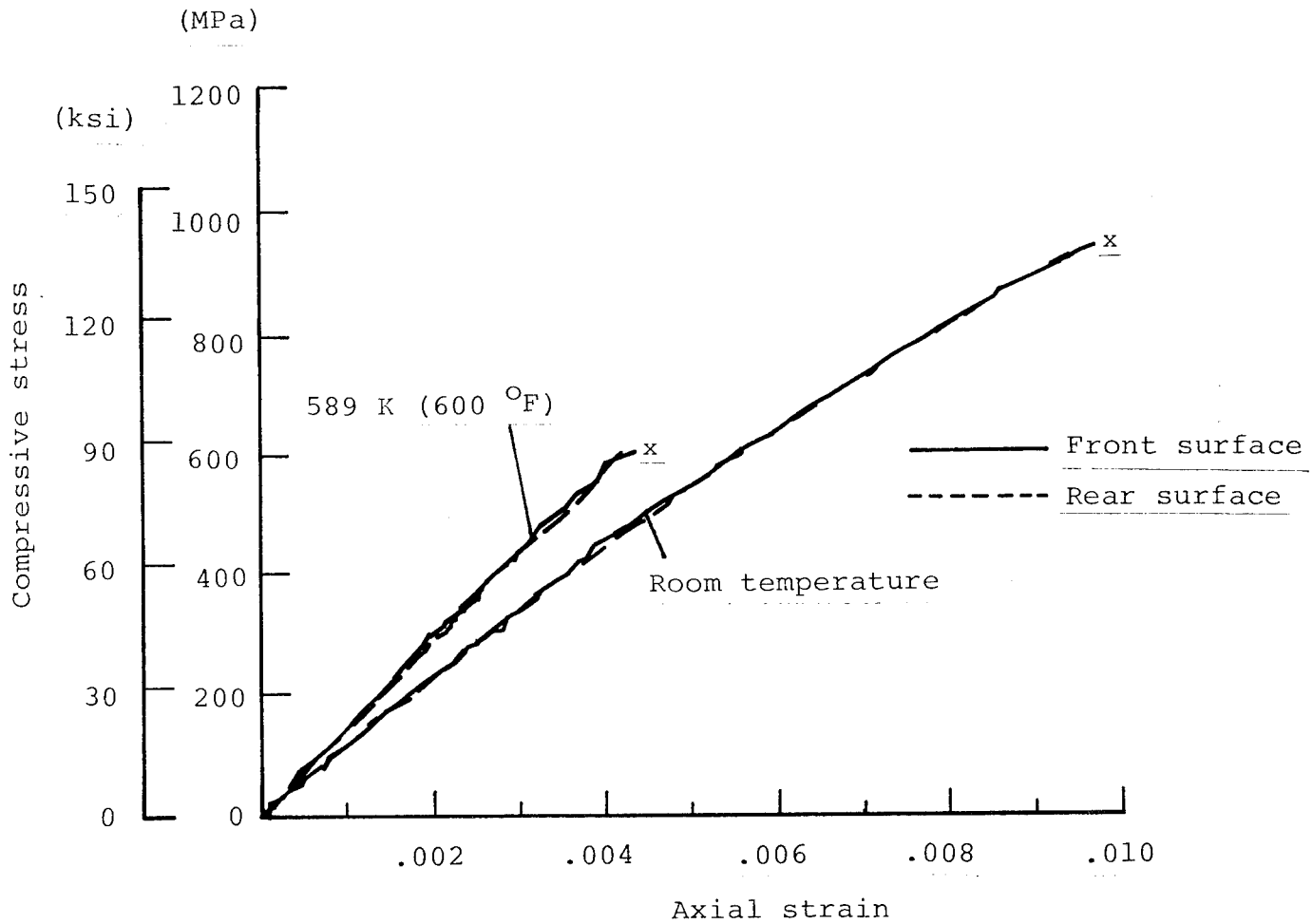
Figure 6.2-1 - IITRI compression test fixture and specimen in oven.

Figure 6.2-2.- Stress-strain curve for $[0]_{15}$ ply HTS/PMR-15 composite IITRI specimen at room and elevated temperatures.

Stress limits MPa (ksi)		Strain limits		E Compressive modulus MPa $\times 10^{-3}$ (ksi $\times 10^{-3}$)	Temperature, K (°F)
FROM	TO	FROM	TO		
0	353 (51.2)	0	0.0031	114 (16.6)	291 (64)
353 (51.2)	696 (101)	0.0031	0.0065	101 (14.6)	291 (64)
696 (101)	972 (141)	0.0065	0.0099	76.5 (11.1)	291 (64)

Values shown represent average results of four tests.

Lamination: [0]$_{15}$

Width: 1.3 cm (0.5 in)

Stress at failure: 972 MPa (141 ksi)

Strain at failure: 0.0099

Figure 6.2-3 - Average room temperature strength and modulus of HTS/PMR-15 compression specimen.

Stress limits MPa (ksi)		Strain limits		E Compression modulus MPa × 10^{-3} (ksi × 10^{-3})	% increase in modulus from room temperature value	Temperature, K (°F)
FROM	TO	FROM	TO			
0	350 (50.7)	0	0.0025	139 (20.2)	17	589 (600)
350 (50.7)	611 (88.6)	0.0025	0.00455	129 (18.7)	29	589 (600)

Values shown represent average results of three tests

Lamination: [0]$_{15}$

Width: 1.3 cm (0.5 in)

Stress at failure: 611 MPa (88.6 ksi)

Strain at failure: 0.00455

Decrease in strength from room temperature value: 37%

Figure 6.2-4 – Average elevated temperature strength and modulus of HTS/PMR-15 compression specimen.
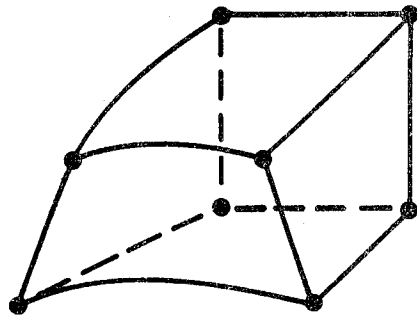
(a) 8-node isoparametric solid element.
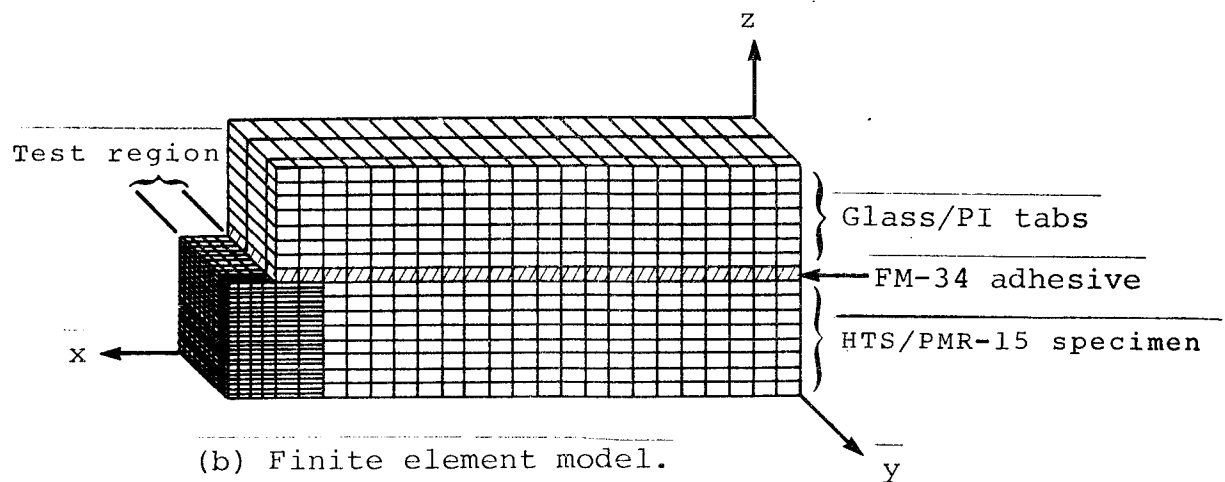
(b) Finite element model.

Figure 6.2-5 - Finite element idealization of IITRI compression
test specimen.
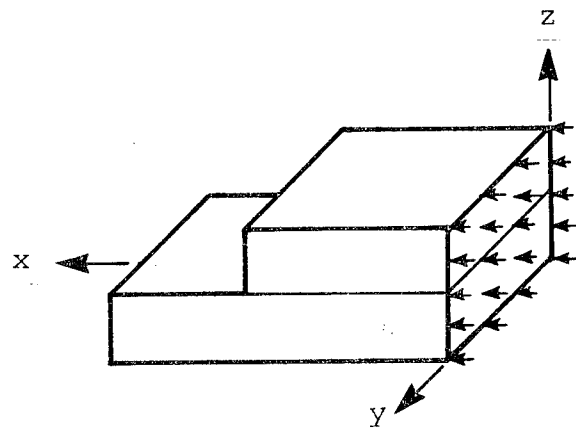
(a) Uniform end load.
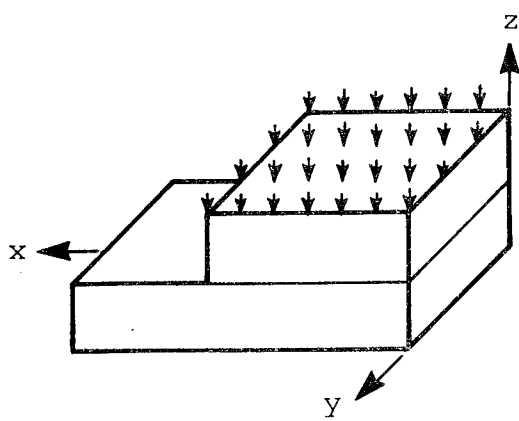
(b) Clamp load.
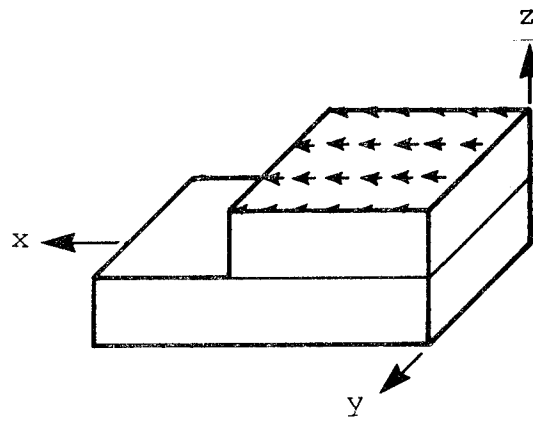
(c) Shear load.

Figure 6.2-6 – End loading conditions of IITRI compression specimen.

Contour #	Stress	
	MPa	ksi
2	-414	- 60
3	-552	- 80
4	-690	-100
5	-827	-120
6	-965	-140

Tab shear load = 22.15 MPa (3.21 ksi)

Top layer +45°

6.32 cm (2.49 in.) 0.64 cm (0.25 in.)

+45°
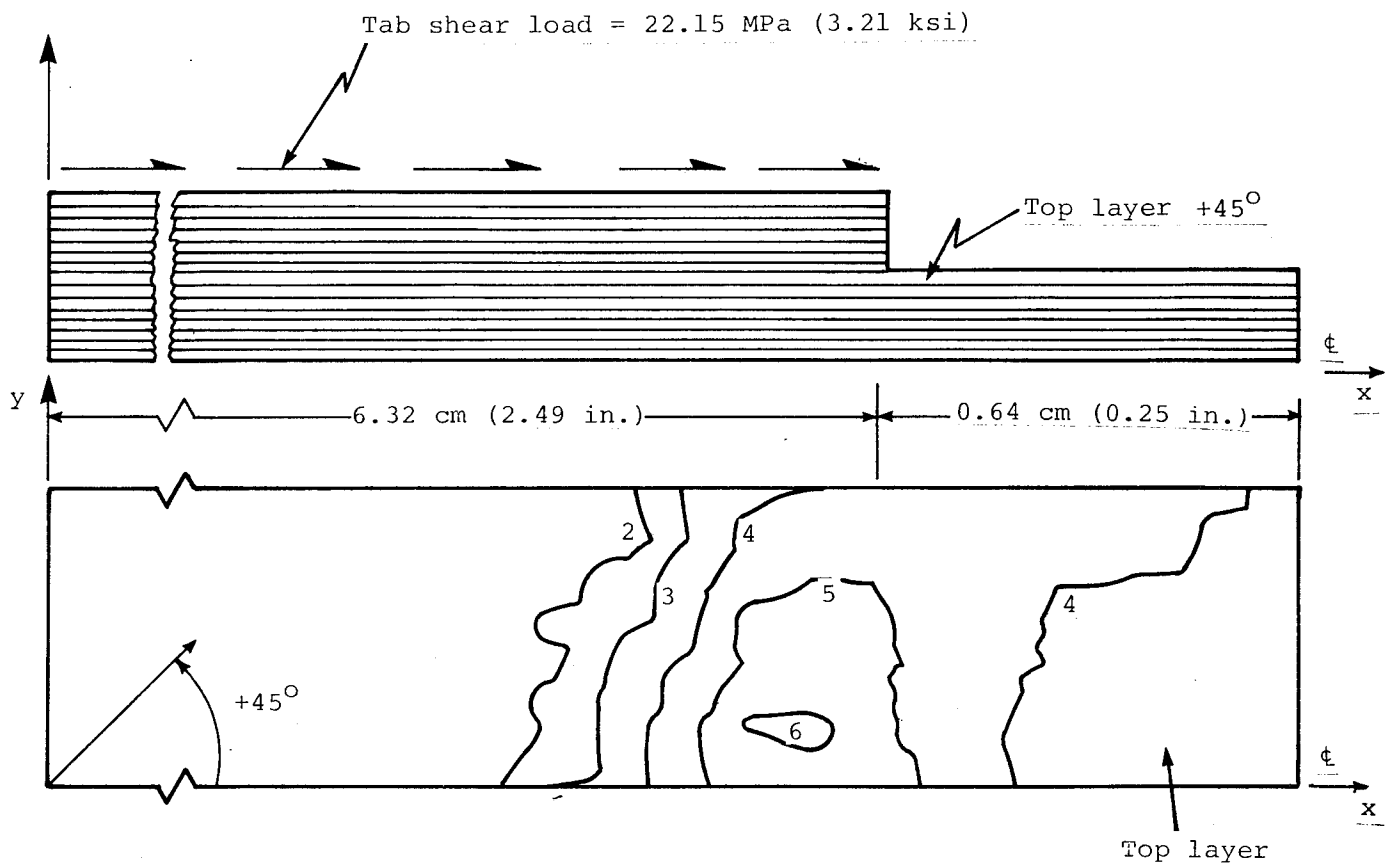
Top layer

Figure 6.2-7 - Axial stress contours in top layer of 0.64 cm (0.25 in.) wide HTS/PMR-15 $[\pm45]_{4s}$ IITRI specimen.

6.3 Sandwich Beam Compressive Test Method
Mark J. Shuart

The purpose of this study was to develop a test method to obtain design data for compressive loading of graphite/polyimide composite materials for a temperature range from 117K (-250°F) to 589K (600°F). Compressive tests were performed using the honeycomb sandwich beam in four-point bending (ref. 6.3-1 through 6.3-4). A finite element computer program was used to analyze the stress distribution in the test section of the sandwich beam. Constituents of the beam were tested to obtain input for the analysis.

The HTS/PMR-15 composite material was used to fabricate $[0_8]$, $[90_8]$, $[(\pm45_2]_s$, and $[0/\pm45/90]_s$ laminates. The range of fiber volume fractions for all laminates was calculated to be 53 to 55 percent. Composite tensile specimens and honeycomb core compressive specimens measuring 25 x 3 x 0.2 cm (10 x 1 x 0.06 in) and 10 x 10 x 3.8 cm (4 x 4 x 1.5 in) respectively, were used to obtain beam constituent data (figure 6.3-1). The sandwich beam specimens were used to obtain compressive data for the HTS/PMR-15 system and for 2024-T3 aluminum alloy. The data from the 2024-T3 beam specimens were compared with documented 2024-T3 compressive data (ref. 6.3-5) to identify any effects of specimen geometry on mechanical properties. The composite sandwich beam specimens measured nominally 56 x 3 x 4 cm (22 x 1 x 1.7 in). As shown in figure 6.3-2, these specimens were assembled using a composite top cover, a metal bottom cover, and a honeycomb core. The honeycomb core combines different densities, depending on the composite laminate configuration, as discussed in reference 6.3-3 and specified in figure 6.3-3. The 2024-T3 sandwich beam specimens measured nominally 55 x 2 x 4 cm (22 x 1 x 1.8 in). The specimens were assembled using 2024-T3 top and bottom covers and lightweight aluminum honeycomb core. The honeycomb was 5052 aluminum alloy, 0.3 cm (1/8 in) hexagonal cell size, 0.004 cm (0.0015 in) wall thickness, and 98 kg/m^3 (6.1 lb/ft^3) core density.

Two types of composite beam specimens were used for compressive testing: beams with aluminum honeycomb core and beams with titanium honeycomb core. Composite beams with aluminum honeycomb core had been used previously at room temperature to obtain compressive data (ref. 6.3-4) but could not withstand a 589K (600°F) test environment. Instead, beams for tests in the range 117K to 589K were designed using titanium honeycomb core. Hence, four sets of composite beam specimens were fabricated. One set of specimens used aluminum honeycomb core for tests at room temperature and three sets of specimens used titanium honeycomb core for tests at 117K, room temperature, and 589K.

Approximately sixty percent of the experimental program has been completed. The coordinate systems used in this investigation are shown in figure 6.3-4. Compression data were obtained from the honeycomb core located beneath the composite test section (fig. 6.3-3). The honeycomb cores tested were 5052 aluminum alloy [with 0.3 cm (1/8 in) hexagonal cell size, 0.004 cm (0.0015 in) wall thickness, and 98 kg/m^3 (6.1 lb/ft^3)] and Ti-3Al-2.5V

titanium alloy [with 0.6 cm (1/4 in) diamond cell size, 0.008 cm (0.003 in)
wall thickness, and 112 kg/m^3 (7 lb/ft^3) core density]. The tests were
performed at room temperature, and data are presented in figure
6.3-5.

All laminate configurations were tested in tension in 117K
(-250°F), room temperature, and 589K (600°F) test environments. The
available data are presented in figures 6.3-6 - 6.3-8. Failed room
temperature tensile specimens are shown in figure 6.3-9. The [0$_8$] and
[0/$\pm$45/90]$_s$ specimens are shown without the glass/epoxy end tabs; the end
tabs unbonded during testing. Figure 6.3-10 shows failed tensile specimens
which were tested at 589K (600°F). A [0$_8$] specimen is not shown in the
figure since these specimens splintered into several pieces upon failure.
All tensile specimens tested at 589K and 117K used glass/polyimide
end tabs. These tabs were chosen to minimize any thermal stresses due to
tab-specimen differences in thermal expansion.

The results of room temperature sandwich beam tests from composite
beams with aluminum honeycomb core, composite beams with titanium honeycomb
core, and 2024-T3 beams are tabulated in Figures 6.3-11 - 6.3-13, respectively.
Figure 6.3-14 shows a typical sandwich beam specimen in the test fixture
being loaded in four-point bending. Figures 6.3-15 - 6.3-19 show failed
composite/aluminum honeycomb beam specimens. The [0$_8$] specimen (fig. 6.3-16)
failed in bearing under the point of load application. As illustrated in
figure 6.3-17, the [90$_8$] specimen buckled in the test section. The [($\pm$45)$_2$]$_s$
specimen shown in Figure 6.3-18 failed along a 45° axis with respect to the
length of the beam. Ply delamination accompanied failure. Figure 6.3-19
portrays a failed [0/$\pm$45/90]$_s$ specimen. This failed beam had the most
curvature of the laminates investigated. A failed 2024-T3 beam specimen is
shown in Figure 6.3-20. The metal covers did not cause failure of the beam
specimen. Failure was caused by the buckling of the honeycomb core as seen
in the figure. The buckling occurred due to the transverse (through the beam
depth) shear loading.

A finite-element model was used for the analytical program of this
study. This program is based on the assumption of linear elastic material
behavior. The assumption is also made that the composite cover and the
honeycomb core are homogeneous orthotropic materials. The composite-
honeycomb interface will be of particular importance in this analysis. Any
effects the specimen geometry may have on mechanical properties will occur
in this region.

The model used in the finite-element analysis is shown in figure
6.3-21. A total of 750 elements and 1248 nodes are used. Each node has
three translational degrees of freedom. This model approximates a 0.5 x
1.3 x 4.29 cm   (0.20 x 0.50 x 1.69 in), . region of the beam test section
as shown in figure 6.3-21. The model is symmetric about the x-z plane.
The metal cover is represented by plate elements having isotropic
material behavior. Both the composite cover and the honeycomb core
are modeled by brick elements with orthotropic material behavior.

Material property input for the composite cover and honeycomb core were
obtained from the previous constituent tests. It is assumed that each of
these materials has identical elastic properties in tension and compression.
The moment acting in the beam test section is applied by a prescribed
linear displacement across the y-z plane of the model. The neutral axis
of the cross-section is calculated from elementary theory (ref. 6.3-6).

During the next reporting period, sandwich beams will be tested in 117K
and 589K environments and all remaining test data will be reduced. Also,
the finite-element model will be made operational, and test cases will be
run of composite sandwich beam specimens in 117K, room temperature, and 589K
environments. 2024-T3 sandwich beam specimens will also be modeled in room
temperature test environments. The comparison of these test cases with the
experimental results is expected to lead to conclusions regarding effects
of specimen geometry on mechanical properties and to a definition of the
limiting parameters within which the sandwich beam provides a reliable
compressive test method for design data.

References

6.3-1. Advanced Composite Airframe Structures. First Monthly Progress
        Report for AF Contract F 33615-68-C-1301, Grumman Aircraft
        Engineering Corporation, March 1967.

6.3-2. Waddoups, M. E.: Characterization and Design of Composite
        Materials. Composite Materials Workshop, S. W. Tsai, J. C.
        Halpin, Nicholas J. Pagano, eds., Technomic Publishing Co.,
        Inc., 1968, pp. 254-308.

6.3-3. Development of Engineering Data on the Mechanical and Physical
        Properties of Advanced Composites Materials. AFML-TR-72-205
        Part I, IIT Research Institute, Sept. 1972, pp. 121-135.

6.3-4. Viswanathan, Chittur N.; Davis, John G., Jr.; and Herakovich,
        Carl T.: Tensile and Compressive Behavior of Borsic/Aluminum
        Composite Laminates. VPI-E-75-12, Virginia Polytechnic
        Institute and State University, College of Engineering, June
        1975.

6.3-5. Metals Handbook. Taylor Lyman, ed., 8th edition, vol. 1, American
        Society for Metals, 1961, pp. 938-940.

6.3-6. Popov, E. P.: Mechanics of Materials. Prentice-Hall Inc., 1952.

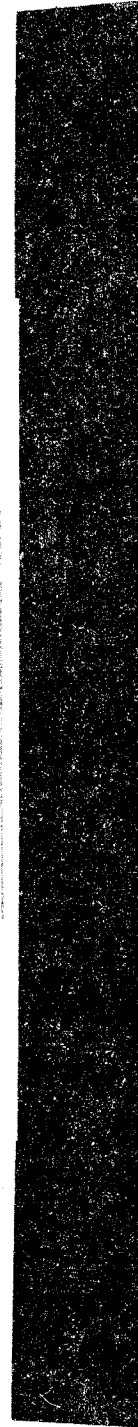Honeycomb core compressive specimens
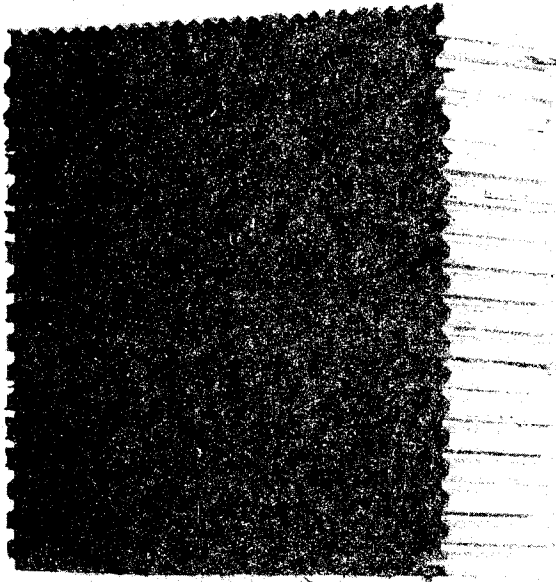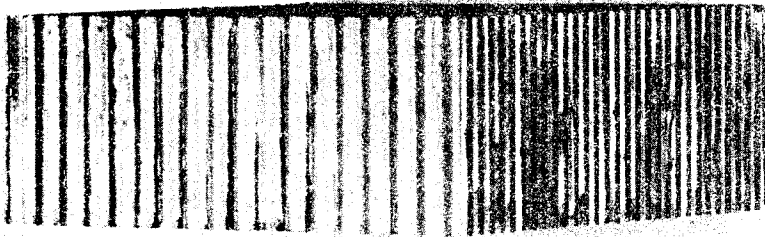
Gr/PI tensile specimen

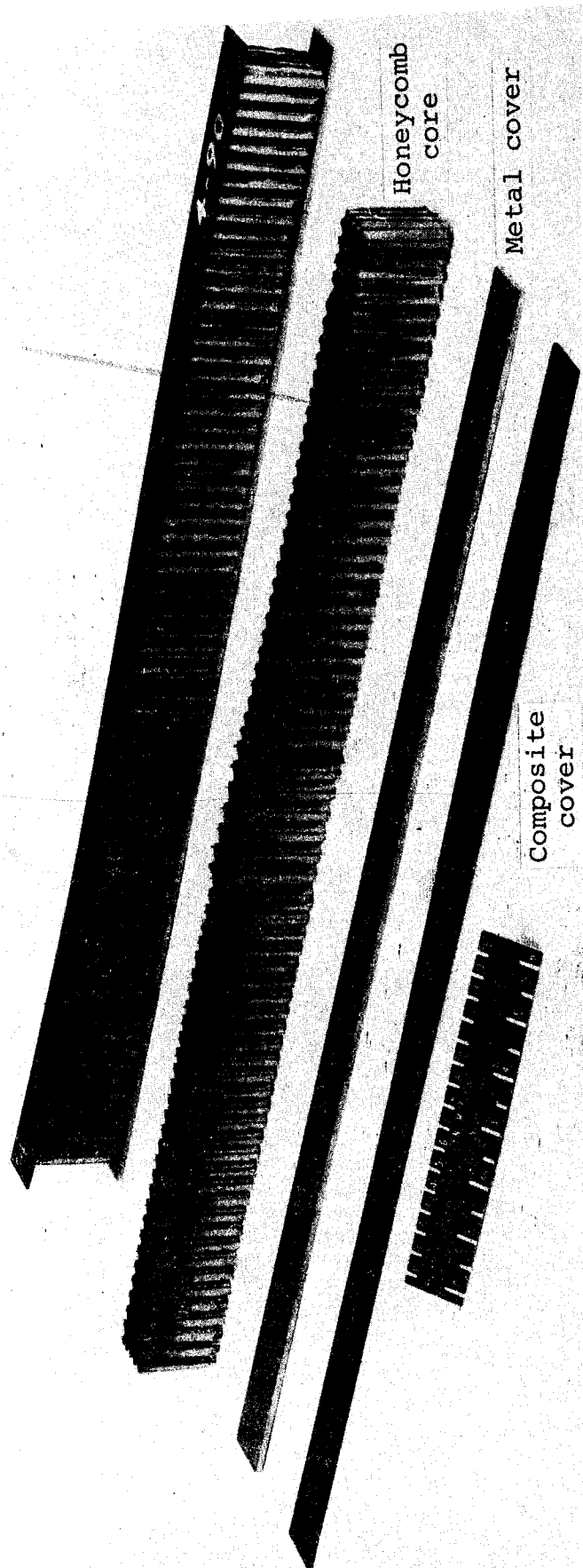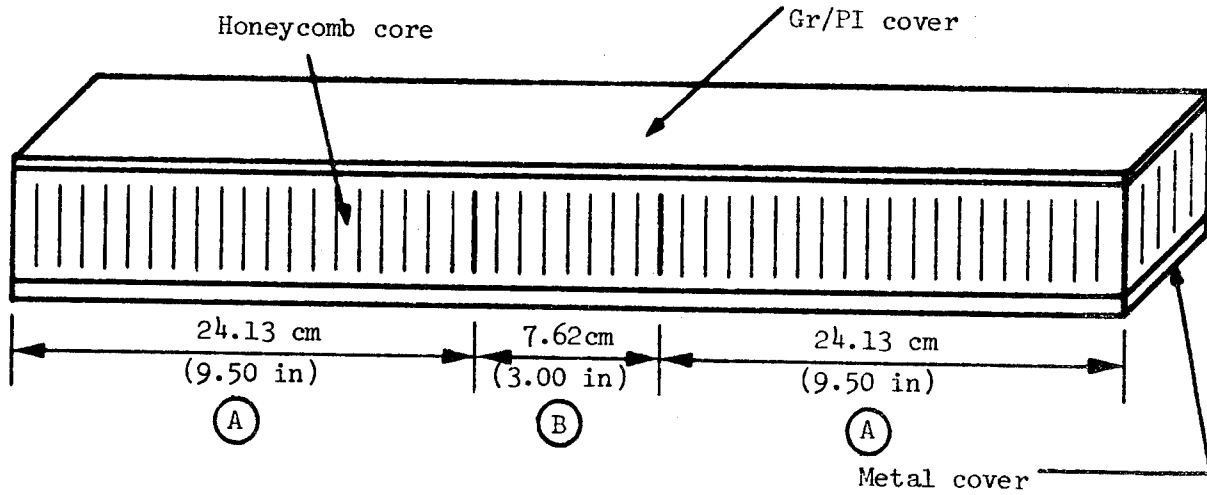Figure 6.3-1 - Constituent test specimens.

Figure 6.3-2 - Assembly of beam specimens.

(a) Aluminum honeycomb beams

Laminate Configuration	Density, kg/m^3		Metal cover
	(A)	(B)	
$[0_8]$	254.0	97.71	0.32 cm Ti-6Al-4V
$[90_8]$	97.71*	97.71*	0.32 cm 2024-T3
$[(\pm 45)_2]_s$	254.0	97.71	0.32 cm 2024-T3
$[0/\pm 45/90]_s$	254.0	97.71	0.32 cm 2024-T3

(b) Titanium honeycomb beams

Laminate Configuration	Density, kg/m^3	
	(A)	(B)
$[0_8]$	208.2	112.1
$[90_8]$	112.1*	112.1*
$[(\pm 45)_2]_s$	208.2	112.1
$[0/\pm 45/90]_s$	208.2	112.1

* continuous piece of honeycomb

Figure 6.3-3 - Graphite/polyimide sandwich beam specimens.

(b) Laminate

(a) Honeycomb core
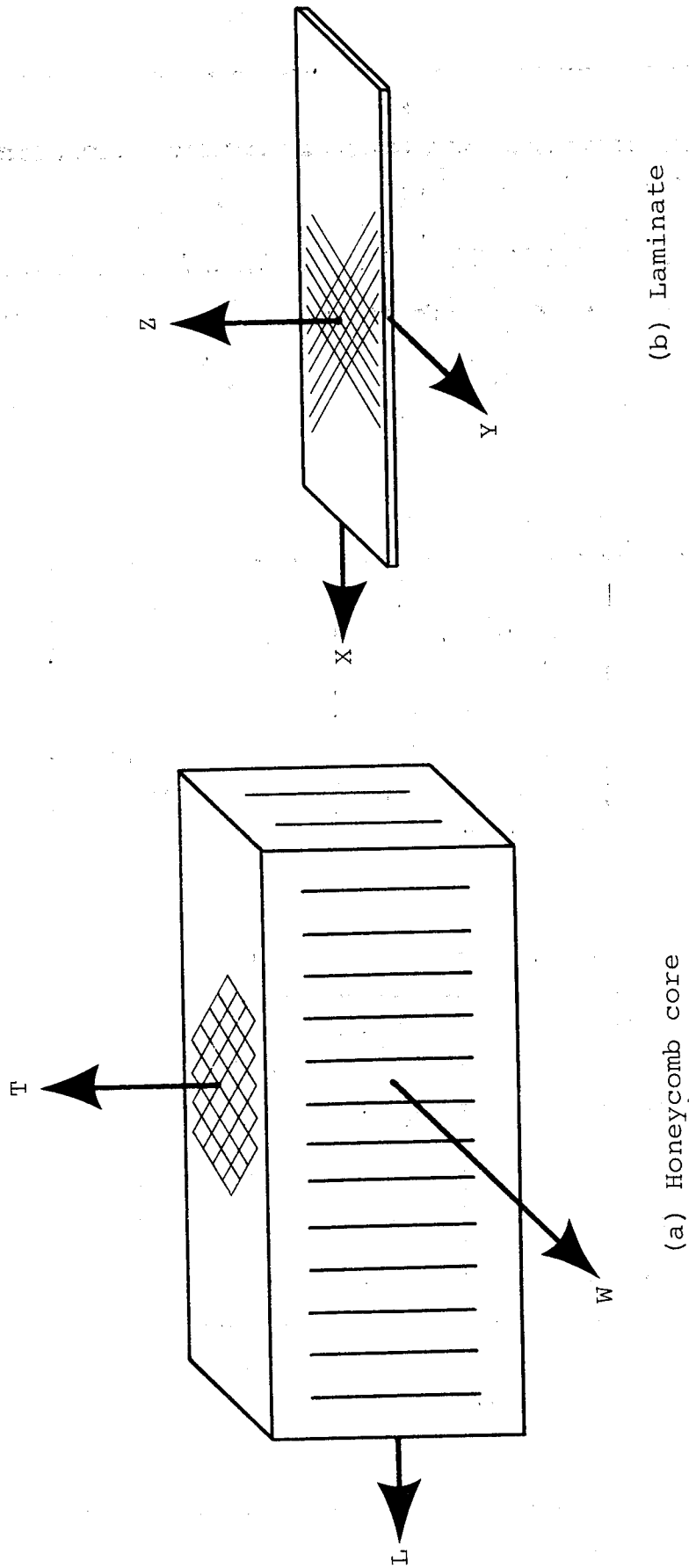
Figure 6.3-4 - Coordinate systems for test materials.

Honeycomb material	Specimen number	Young's modulus E_L, kPa (psi)	Poisson's ratio ν_{LW}	Young's modulus E_W, kPa (psi)	Poisson's ratio ν_{WL}
5052 Aluminum Alloy	Al-1	1751.3 (254.0)	1.08	–	–
	Al-2	1779.5 (258.1)	1.12	–	–
	Al-3	–	–	1068.0 (154.9)	0.71
	Al-4	–	–	1011.5 (146.7)	0.72
Ti-3Al-2.5V Titanium Alloy	Ti-1	588.1 (85.3)	0.90	–	–
	Ti-2	510.9 (74.1)	0.95	–	–
	Ti-3	–	–	166.8 (24.2)	0.45
	Ti-4	–	–	169.6 (24.6)	0.38

Figure 6.3-5 – Honeycomb core compressive data.

Laminate configuration	Ultimate stress, σ_x^u, MPa (ksi)	Ultimate strain, ε_x^u, %	Young's modulus E_x, GPa ($\times 10^6$ psi)	Poisson's ratio ν_{xy}
$[0_8]$	1274.8 (184.9)	0.99	129.0 (18.71)	0.330
$[0_8]$	1434.1 (208.0)	1.08	132.9 (19.28)	0.332
$[90_8]$	24.34 (3.53)	0.30	8.20 (1.19)	0.010
$[90_8]$	42.75 (6.20)	0.54	8.27 (1.20)	0.013
$[(\pm45)_2]_s$	118.6 (17.21)	1.36	15.37 (2.23)	0.775
$[(\pm45)_2]_s$	100.1 (14.52)	1.09	13.72 (1.99)	0.738
$[0/\pm45/90]_s$	459.5 (66.64)	1.01	47.92 (6.95)	0.336
$[0/\pm45/90]_s$	441.7 (64.07)	0.95	47.64 (6.91)	0.325

Figure 6.3-6 – Room temperature graphite/polyimide tensile test data.

Laminate configuration	Ultimate stress, σ_x^u MPa (ksi)	Ultimate strain, ε_x^u, %	Young's modulus E_x, GPa ($\times 10^6$ psi)	Poisson's ratio, ν_{xy}
$[0_8]$	1285.2 (186.4)	0.97	132.1 (19.16)	0.355
$[0_8]$	1296.2 (188.0)	0.99	131.8 (19.11)	0.345
$[90_8]$	22.89 (3.32)	0.55	5.03 (0.73)	0.007
$[90_8]$	22.61 (3.28)	0.45	5.79 (0.84)	0.010
$[(\pm45)_2]_s$	82.39 (11.95)	1.06*	9.10 (1.32)	0.766
$[(\pm45)_2]_s$	65.64 (9.52)	0.95*	8.27 (1.20)	0.671
$[0/\pm45/90]_s$	438.0 (63.52)	0.96	46.06 (6.68)	0.358
$[0/\pm45/90]_s$	451.2 (65.44)	1.04	44.26 (6.42)	0.321

* maximum readable strain

Figure 6.3-7 – 587K (600°F) graphite/polyimide tensile test data.

Laminate configuration	Ultimate stress, σ_x^u, MPa (ksi)	Ultimate strain, ε_x^u, %	Young's modulus, E_x, GPa (× 10^6 psi)	Poisson's ratio ν_{xy}
$[0_8]$	1077.8 (156.33)	-*	123.7 (17.94)	-*
$[0_8]$	1146.6+ (166.3)	0.83+	127.4 (18.48)	0.349
$[90_8]$	33.30 (4.83)	0.34	10.07 (1.46)	0.062
$[90_8]$	28.54 (4.14)	0.32	9.31 (1.35)	0.054
$[(\pm45)_2]_s$	95.08 (13.79)	0.52	18.89 (2.74)	0.688
$[(\pm45)_2]_s$	110.8 (16.07)	0.85	16.75 (2.43)	0.676
$[0/\pm45/90]_s$	238.8 (34.64)	0.54	44.95 (6.52)	0.366
$[0/\pm45/90]_s$	464.6 (67.38)	0.23	43.23 (6.27)	0.263

* strain gage malfunction
+ machine capacity

Figure 6.3-8 – 117K (–250°F) graphite/polyimide tensile test data.

[0/±45/90]$_s$ specimen

[(±45)$_2$]$_s$ specimen

[90$_8$] specimen
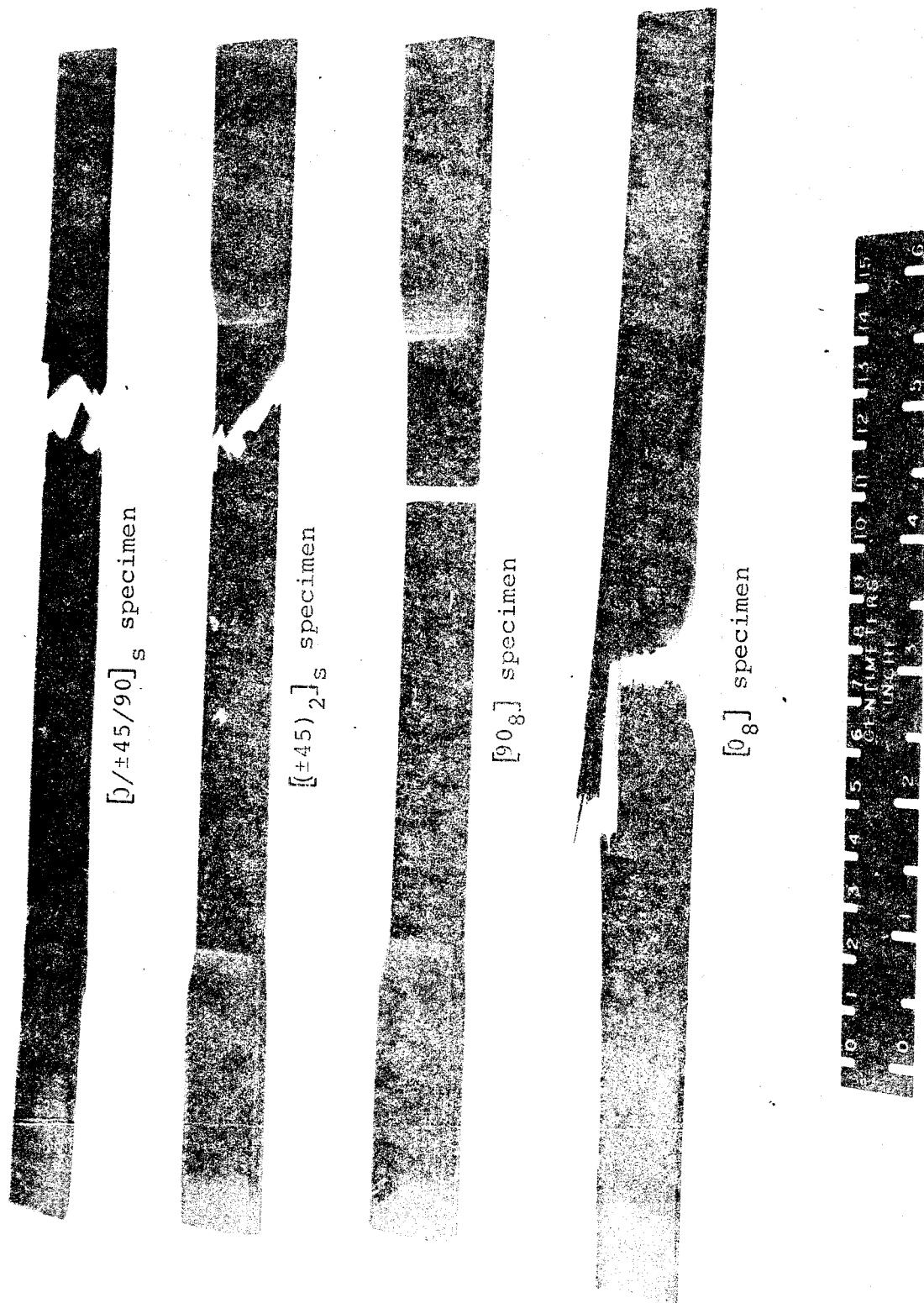
[0$_8$] specimen

Figure 6.3-9 - Gr,PI tensile specimens tested at room temperature.

[90$_8$] specimen

[(±45)$_2$]$_s$ specimen

[0/±45/90]$_s$ specimen
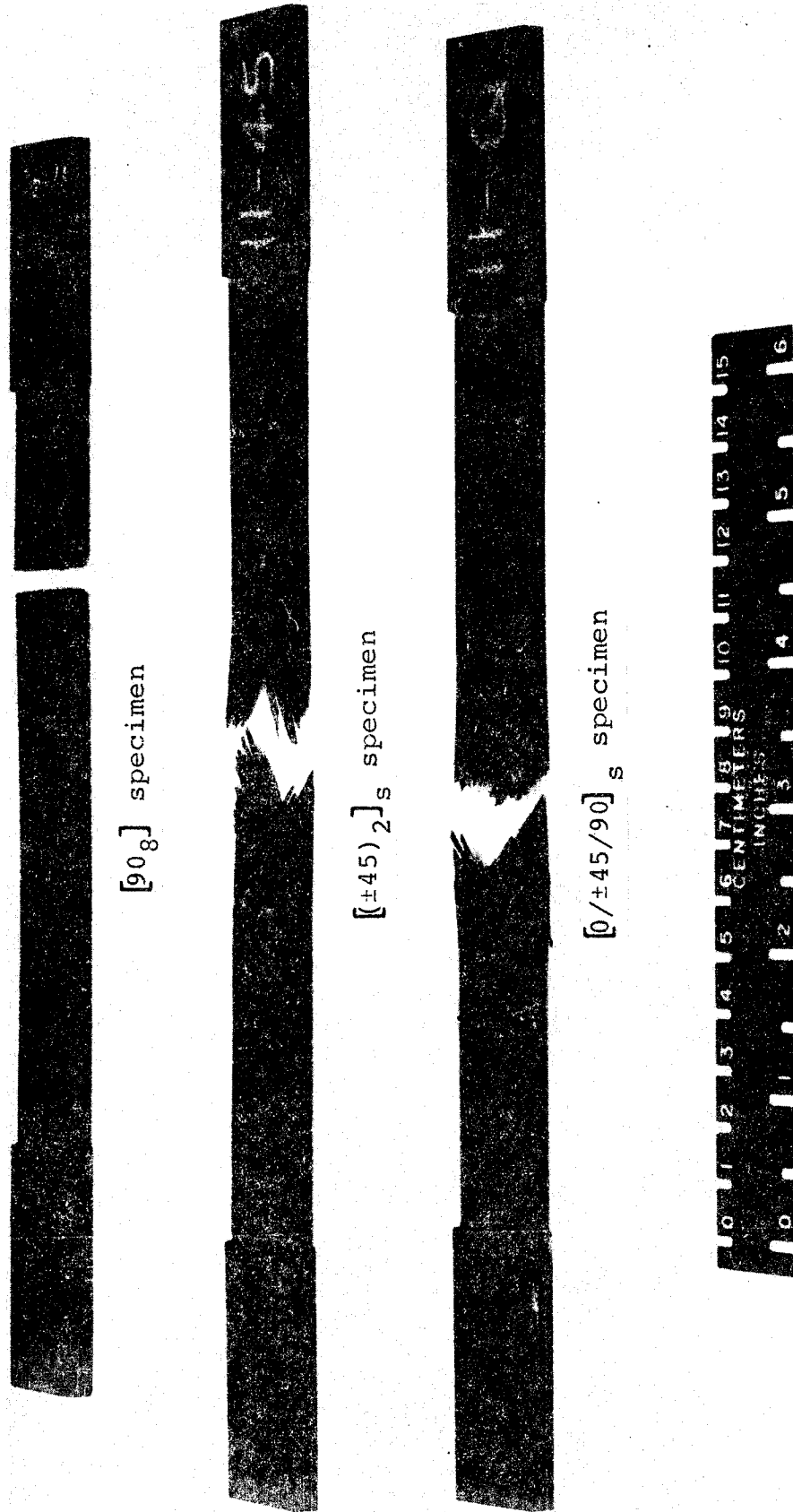
Figure 6.3-10 - Gr/PI tensile specimens tested at 589K (600°F).

Laminate configuration	Ultimate stress, σ_x^u, MPa (ksi)	Ultimate strain, ε_x^u, %	Young's modulus, E_x, GPa ($\times 10^6$ psi)	Poisson's ratio ν_{xy}
$[0_8]$	1281.7 (185.9)	1.16	122.2 (17.73)	0.374
$[0_8]$	1270.0 (184.2)	1.19	119.0 (17.26)	0.353
$[0_8]$	1344.5 (195.0)	1.33	120.1 (17.42)	0.398
$[90_8]$	220.6 (32.00)	2.63	10.20 (1.48)	0.016
$[90_8]$	211.7 (30.70)	2.60	9.52 (1.38)	0.027
$[90_8]$	208.4 (30.22)	1.48	11.79 (1.71)	0.014
$[(\pm45)_2]_s$	187.7 (27.22)	2.76	16.55 (2.40)	0.507
$[(\pm45)_2]_s$	136.5 (19.80)	1.78	16.06 (2.33)	0.793
$[(\pm45)_2]_s$	136.5 (19.80)	2.07	16.75 (2.43)	0.743
$[0/\pm45/90]_s$	552.6 (80.15)	1.65	46.75 (6.78)	0.278
$[0/\pm45/90]_s$	529.8 (76.84)	1.33	47.02 (6.82)	0.296
$[0/\pm45/90]_s$	535.1 (77.61)	1.29	48.54 (7.04)	0.277

Figure 6.3-11 – Graphite/polyimide room temperature compressive data (Aluminum honeycomb core).

Laminate configuration	Ultimate stress, σ_x^u, MPa (ksi)	Ultimate strain, ε_x^u, %	Young's modulus, E_x, GPa ($\times 10^6$ psi)	Poisson's ratio ν_{xy}
$[0_8]$	287.0* (41.63)	0.34*	120.2 (17.44)	0.336
$[0_8]$	520.5* (75.49)	0.44*	125.2 (18.16)	0.350
$[0_8]$	416.2* (60.36)	0.72*	58.54 (8.49)	0.418
$[90_8]$	197.5 (28.65)	2.39	10.34 (1.50)	0.012
$[90_8]$	189.5 (27.48)	2.22	10.34 (1.50)	0.009
$[90_8]$	188.4 (27.32)	2.11	10.69 (1.55)	0.011
$[(\pm 45)_2]_s$	138.4 (20.07)	1.01	18.00 (2.61)	0.778
$[(\pm 45)_2]_s$	152.5 (22.12)	1.27	17.24 (2.50)	0.761
$[(\pm 45)_2]_s$	173.0 (25.09)	1.31	16.48 (2.39)	0.733
$[0/\pm 45/90]_s$	191.9* (27.83)	0.40*	49.85 (7.23)	0.292
$[0/\pm 45/90]_s$	75.57* (10.96)	0.17*	47.78 (6.93)	0.283
$[0/\pm 45/90]_s$	193.4* (28.05)	0.95*	23.03 (3.34)	0.296

* fabrication failure

Figure 6.3-12 – Graphite/polyimide room temperature compressive data (Titanium honeycomb core).

Specimen number	Ultimate stress, σ_x^u, MPa (ksi)	Ultimate strain, ε_x^u, %	Young's modulus, E_x, GPa ($\times 10^6$ psi)	Poisson's ratio, ν_{xy}
2024-1	230.3 (33.40)	0.32	72.53 (10.52)	0.282
2024-2	235.9 (34.21)	0.33	73.43 (10.65)	0.324
2024-3	229.7 (33.32)	0.32	72.81 (10.56)	0.328

Figure 6.3-13 – 2024-T3 Aluminum alloy room temperature compressive data.
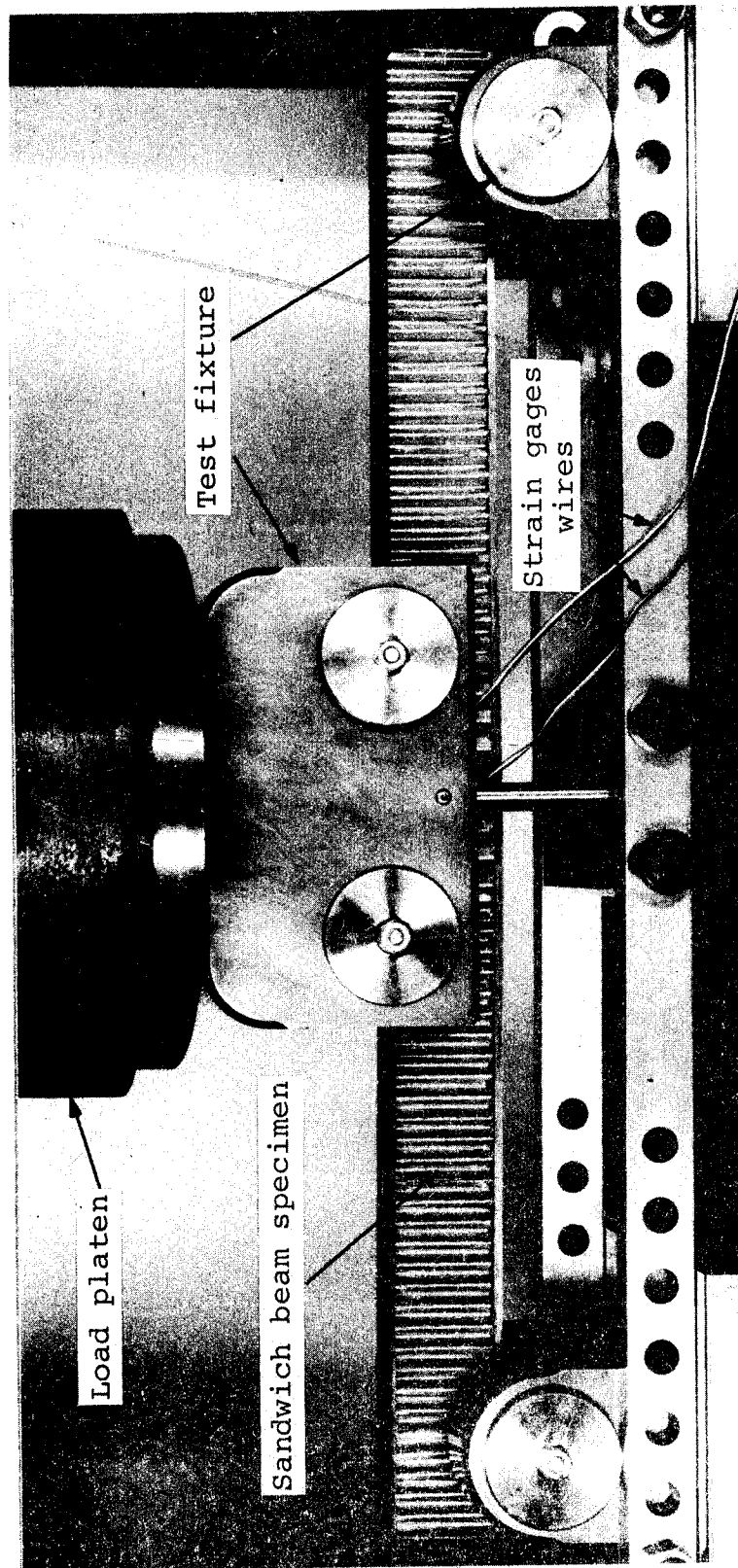
Figure 6.3-14 - Typical sandwich beam specimen loaded in four-point bending.

$[0/\pm45/90]_s$ $[(\pm45)_2]_s$ $[90_3]$ $[0_8]$
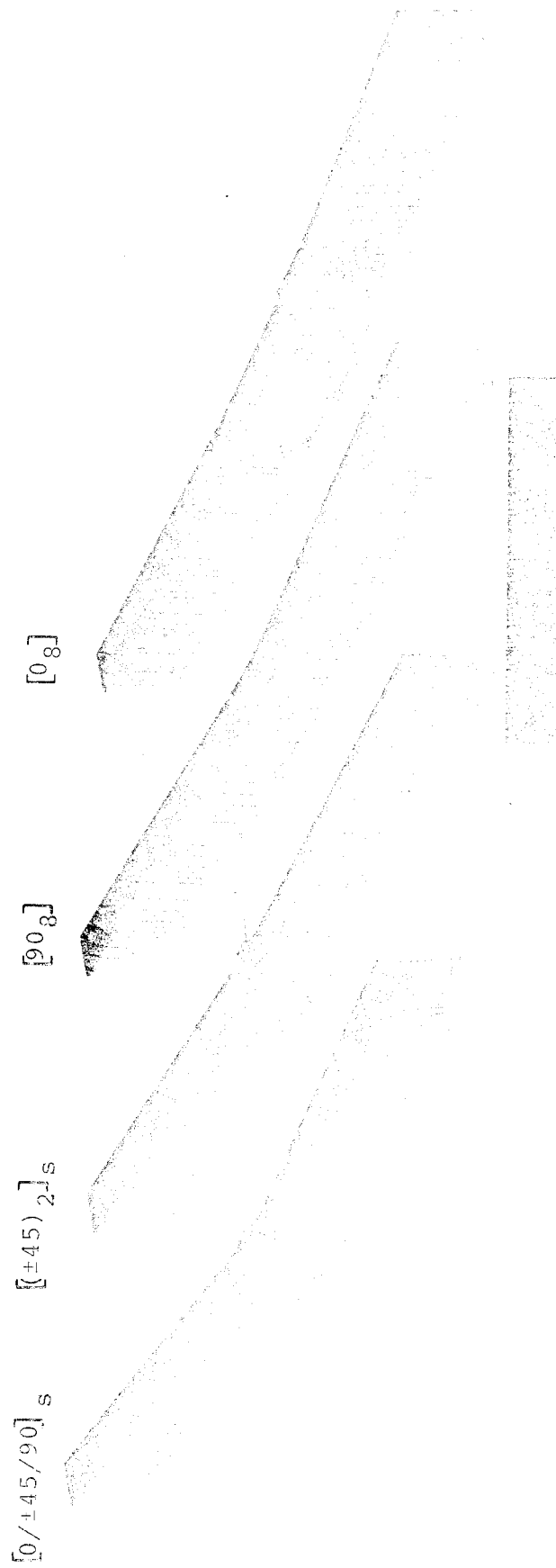
Figure 6.3-15 - Composite/aluminum honeycomb sandwich beam specimens tested at room temperature.

163
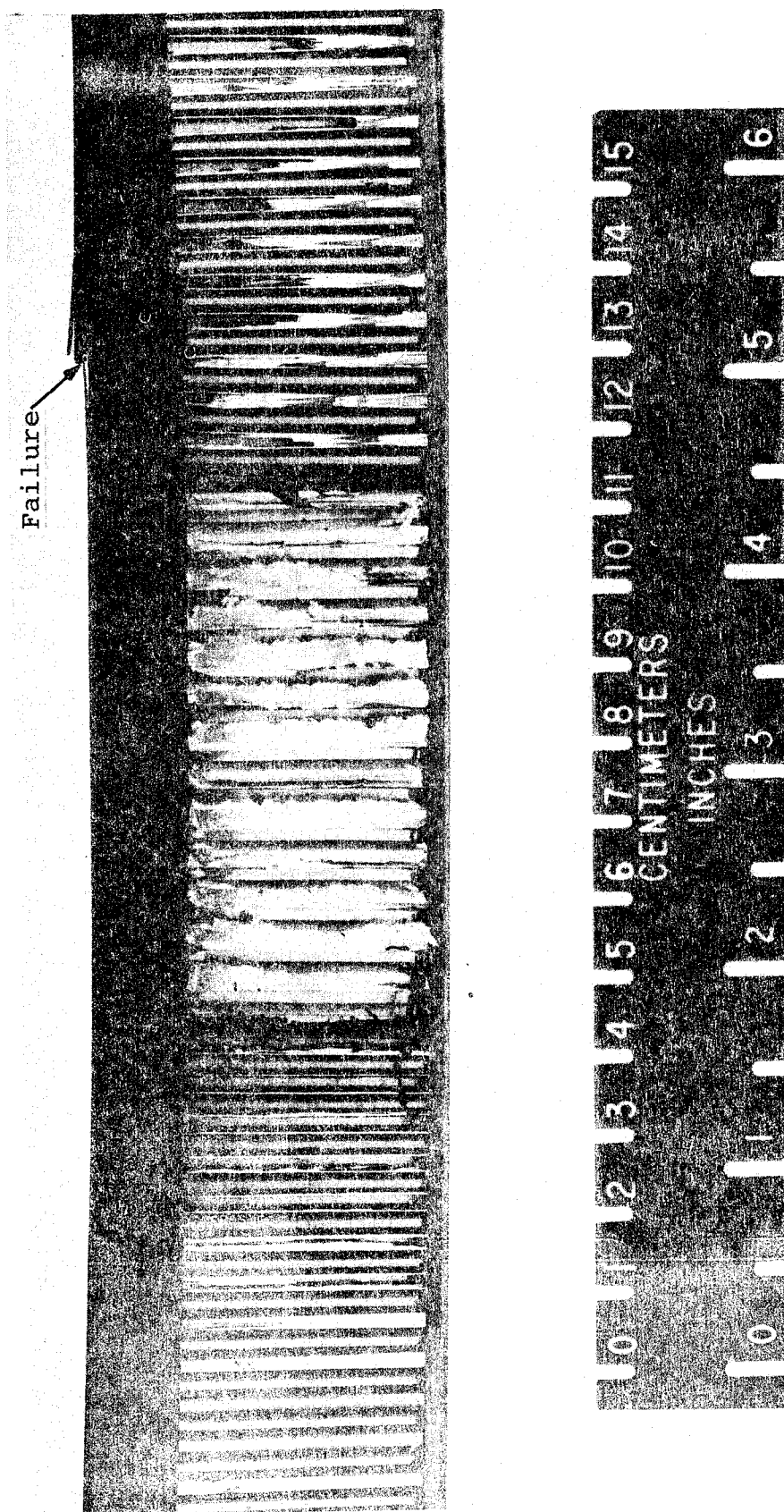
Figure 6.3-16 – $[0_8]$ sandwich beam specimen tested at room temperature.

Failure
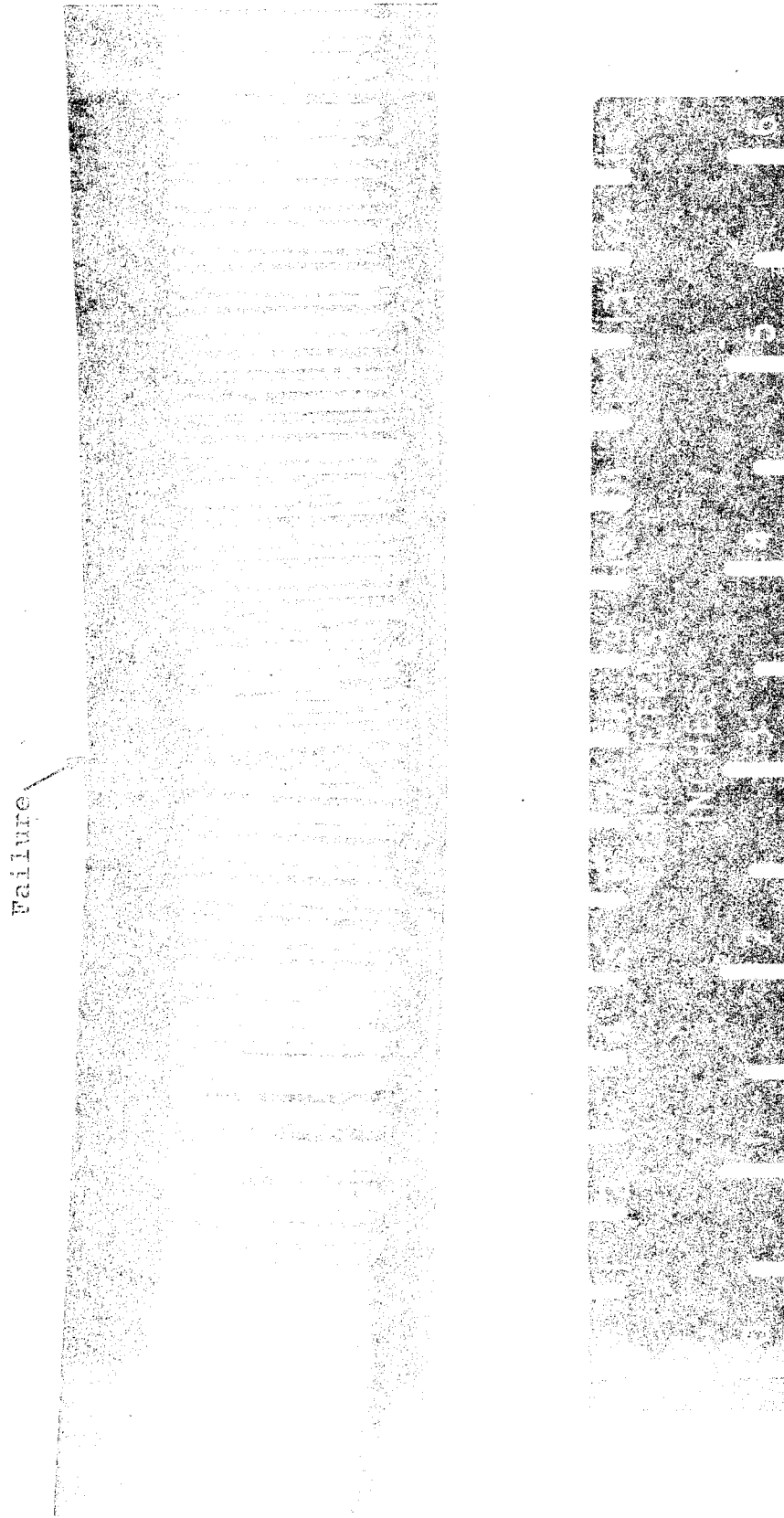
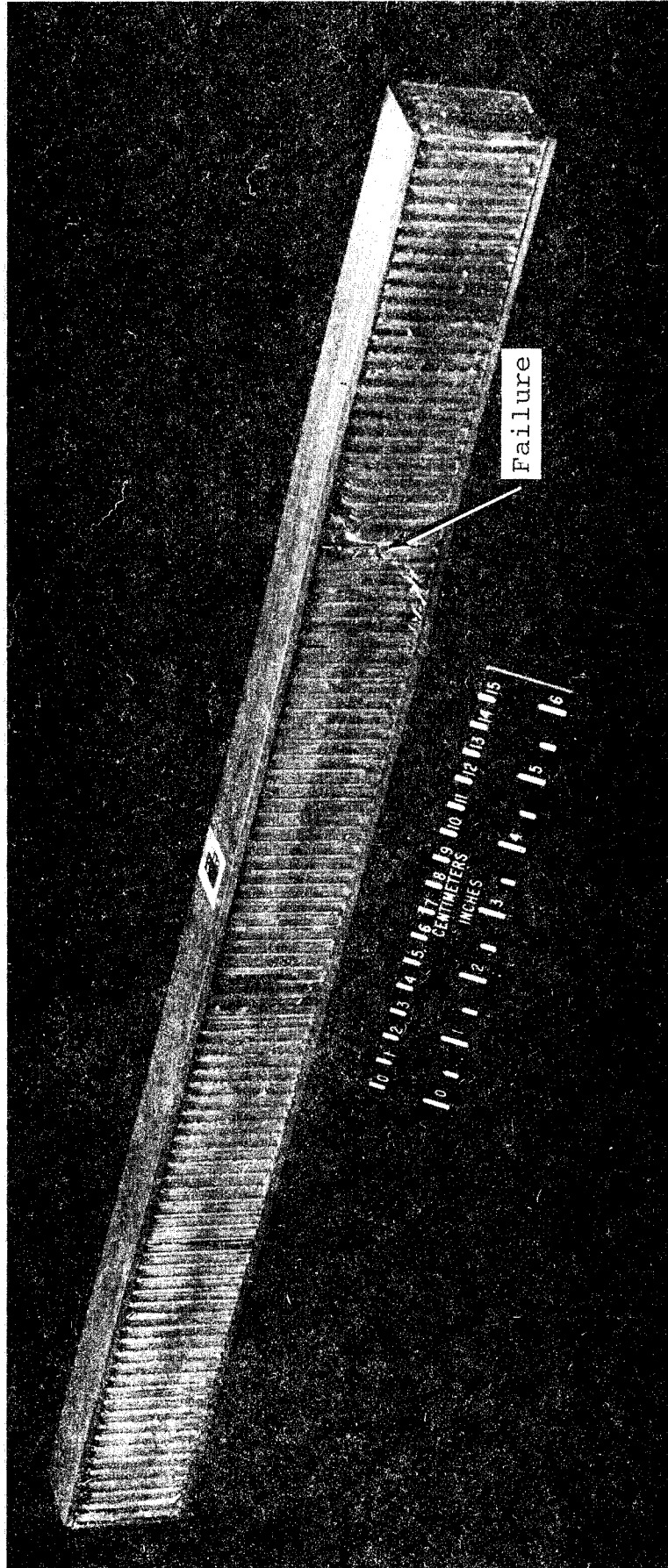Figure 6.3-17 – $[90_8]$ sandwich beam specimen tested at room temperature.
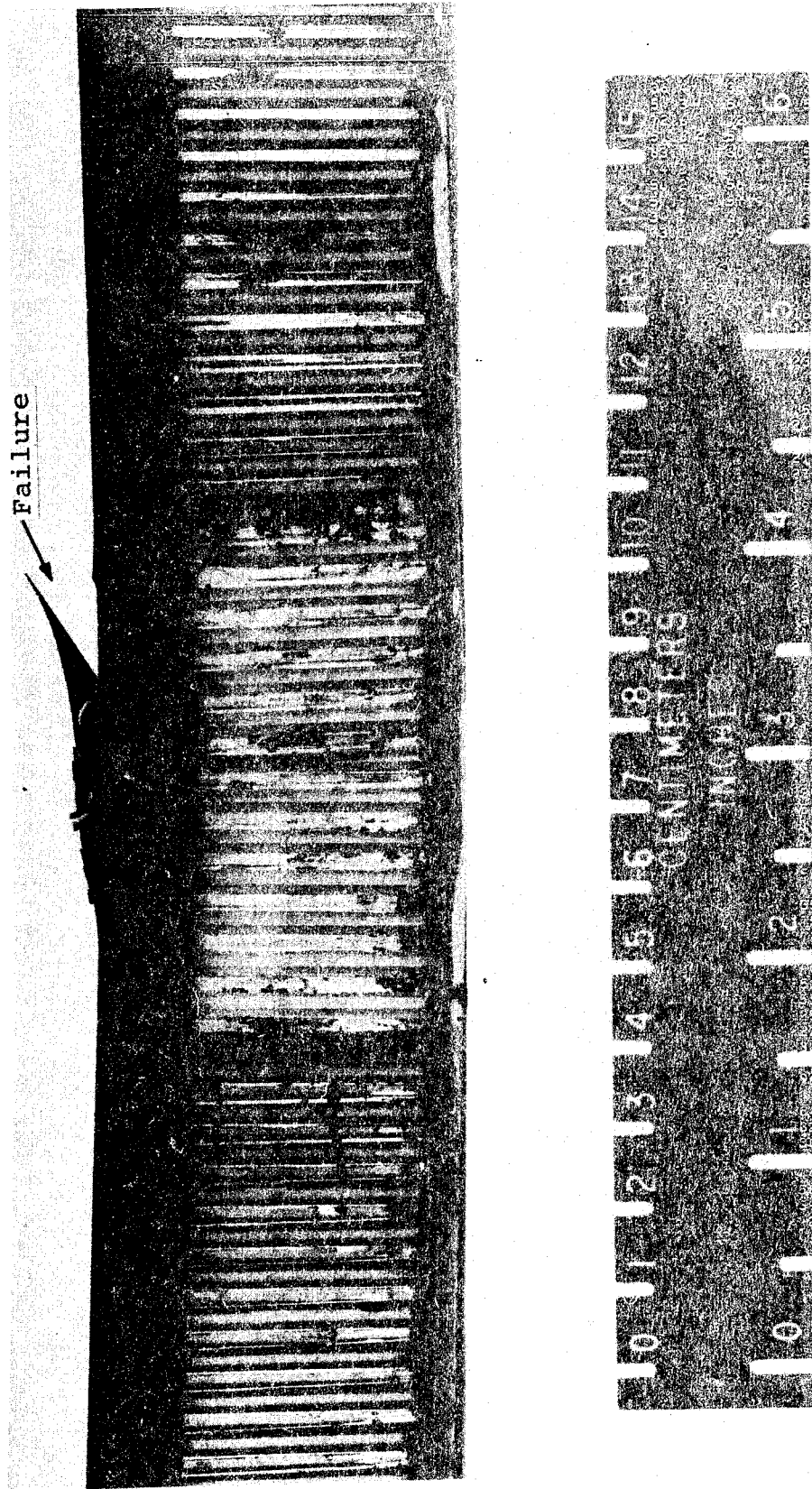
Figure 6.3-18 - $[(\pm 45)_2]$ sandwich beam specimen tested at room temperature.
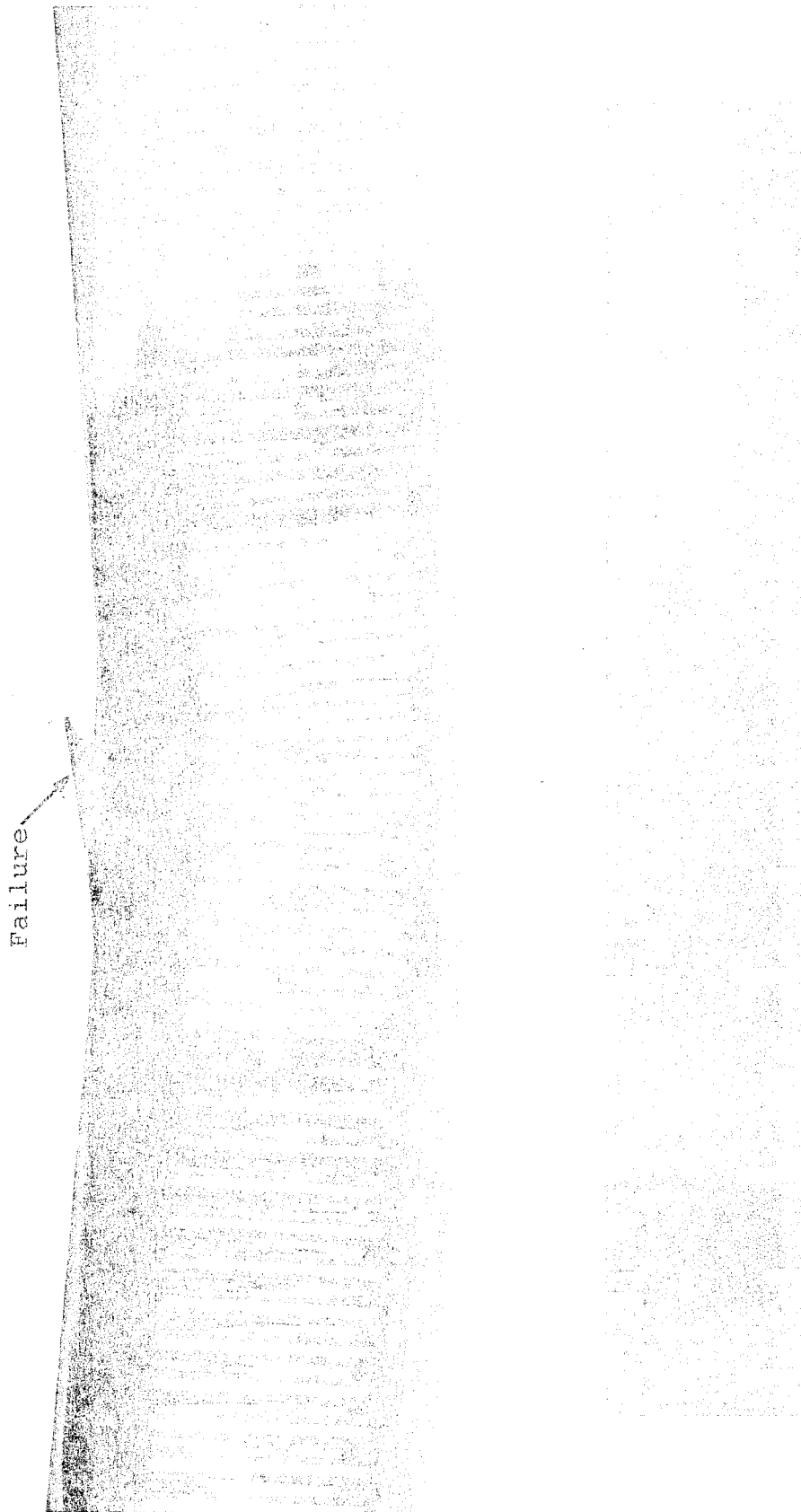
Figure 6.3-19 - $[0/\pm45/90]$ sandwich beam specimen tested at room temperature.

Figure 6.3-20 – 2024-T3 sandwich beam specimen.
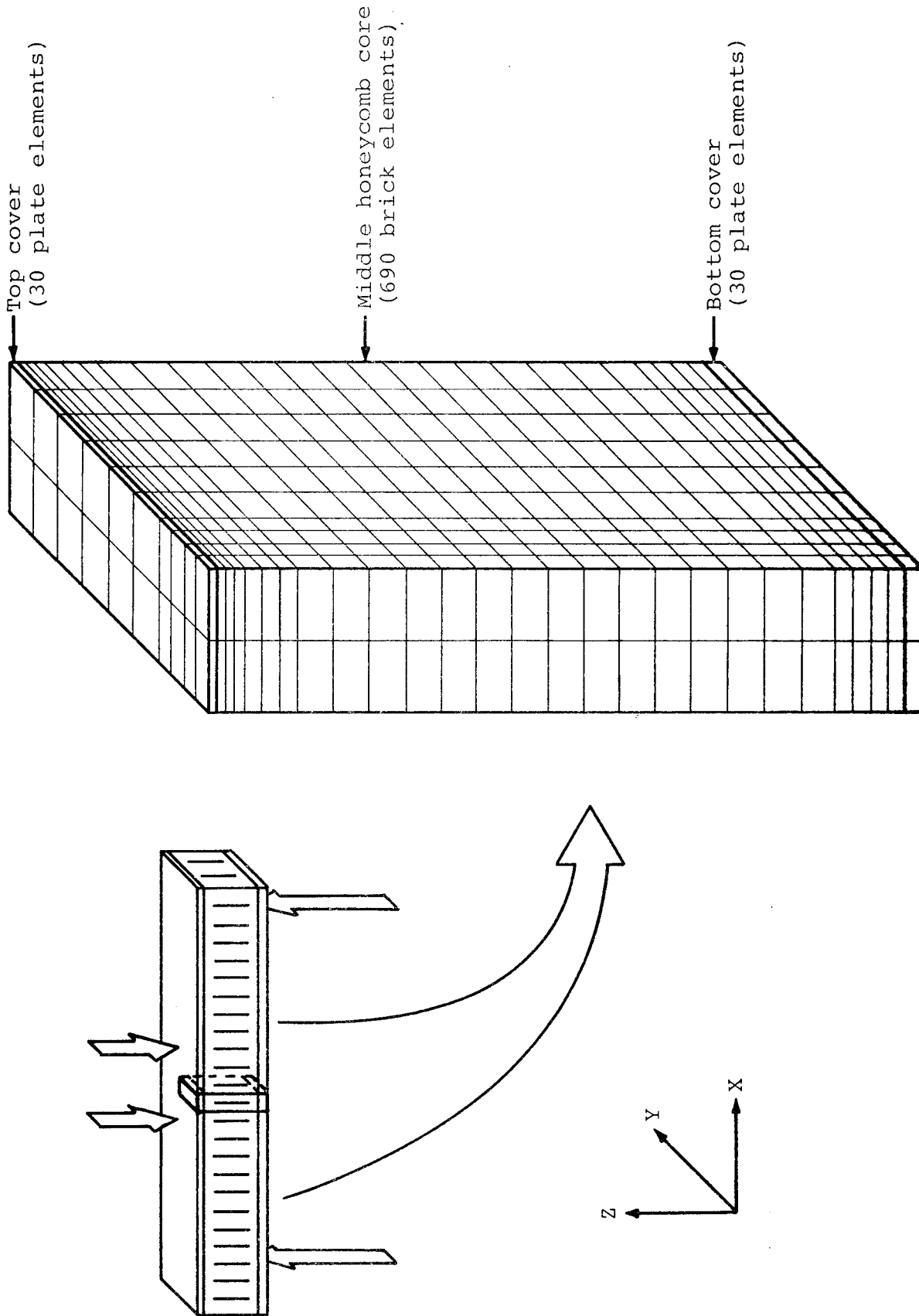
Figure 6.3-21 - Finite element model of sandwich beam.

6.4   Rail Shear Test Method
Robert R. McWithey, Ramon Garcia, Terry A. Weisshaar

Research is being conducted to investigate the rail shear test method for obtaining Gr/PI shear properties at elevated temperatures up to 589K (600°F) and to determine Gr/PI laminate shear properties at room temperature and at 589K (600°F). The scope of the work includes analytical and experimental investigations that include the following Gr/PI laminates: $[0_{12}]$, $[90_{12}]$, $[\pm 45_2]_s$, and $[0, \pm 45, 90]_s$.

Two types of rails were used in this task: tapered rails that are bonded to the Gr/PI laminate and untapered rails that are clamped to the Gr/PI laminate. Both types of rails are shown in figure 6.4-1 in assembled rail-shear specimen configurations. The clamped configuration offers two advantages over the bonded configuration when testing at elevated temperatures. First, a test technique under development that uses a bolted fastener allows clamping of the specimen between the rails at the test temperature just prior to loading. This technique eliminates undesirable thermally induced stresses that would result from differences between thermal expansion coefficients of the specimen and rails. (A similar method utilizing the bonded configuration is not presently possible because of adhesive cure-cycle requirements.) Secondly, the bolted configuration is easily fabricated and eliminates the complexities in obtaining high-strength adhesive bonds at elevated temperature.

The specimens are tested in an oven positioned between the heads of a screw driven tensile testing machine. Load is applied to the specimen using a machine head velocity of 2 μm/sec. (.005 inches/minute). Strain data are obtained using resistance strain gage rosettes. Three rosettes were positioned along the centerline as shown in figure 6.4-1. A fourth rosette was positioned back to back with the rosette at the center of the specimen. Examples of the types of information obtained from these tests are shown in figure 6.4-2 for a $[0, \pm 45, 90]_s$ laminate at room temperature and at 589K (600°F). The preliminary test results from the back to back strain gage rosettes indicate a state of nearly pure shear exists at the center of the specimen for all laminates.
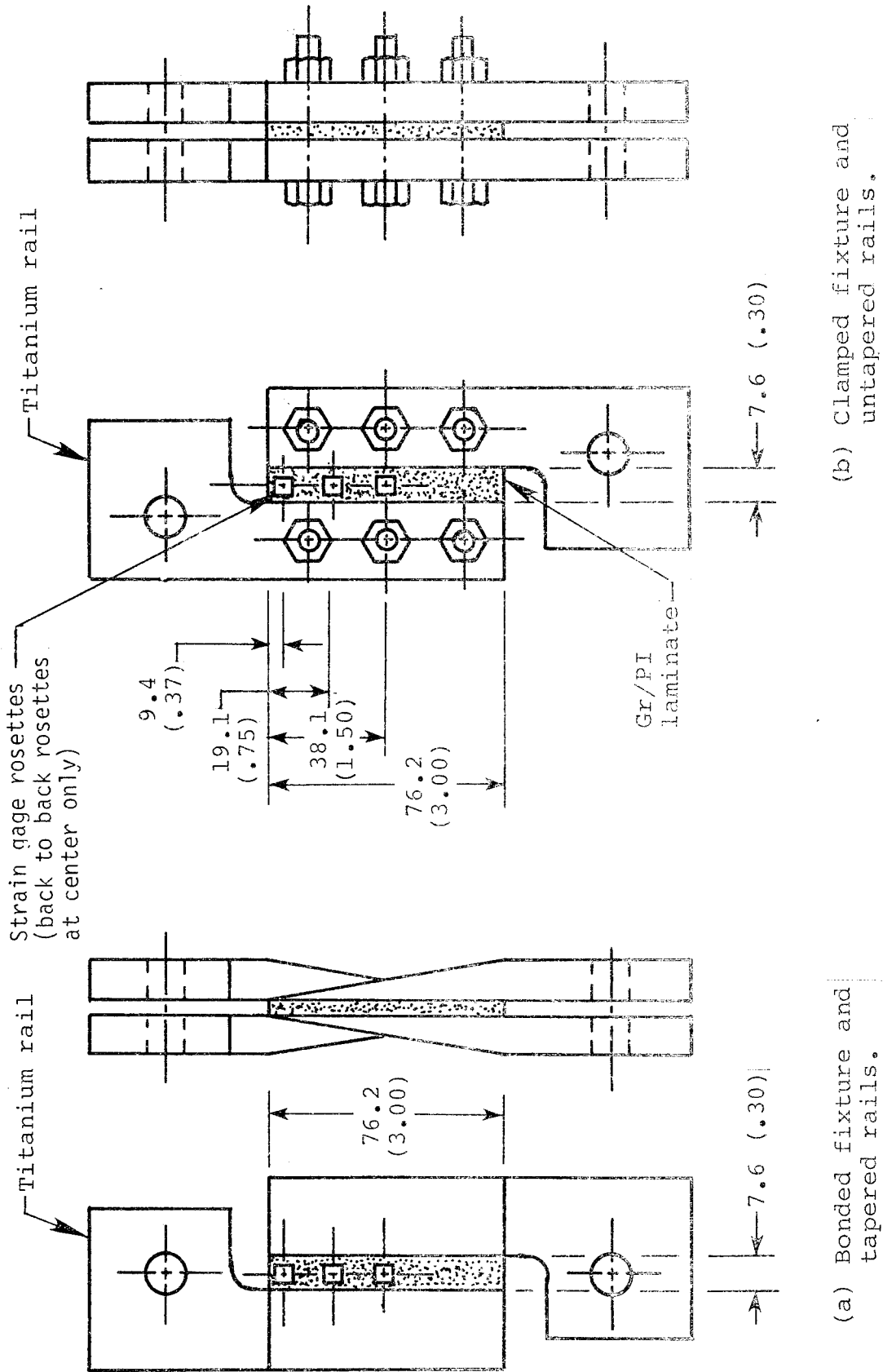
Analytical investigations of both configurations shown in figure 6.4-1 were made using the finite element program SPAR (see ref. 6.4-1). The configurations were modeled using plate elements to represent the specimen between the rails and beam elements to represent the rails. Analysis of the configurations determined the effect of aspect ratio (ratio of length to width of Gr/PI between rails) and thermally induced strains on the apparent material properties of the Gr/PI laminates. Analytical results that indicate the effect of aspect ratio on the shear stress distribution along the specimen centerline are given in figure 6.4-3. The results for this laminate indicate the actual shear stress along the centerline of the specimen is within a few percent of the value anticipated from measurement of the applied load when the aspect ratio is greater than 8. An aspect ratio of 10 was used

in the experimental investigation. The analytical results indicate a state of nearly pure shear exists in the specimen except for small regions near the free edges.

During the next few months the analytical and experimental investigations will be completed and formal reports prepared for publication. The status and scope of the test program is indicated in figure 6.4-4. Although tests are complete on the $[0, \pm 45, 90]_s$ and $[\pm 45_2]_s$ laminates, the data have not yet been analyzed.

References

6.4-1. Whetstone, W. D.: SPAR Structural Analysis System Reference Manual
        System Level II – Volume 1 – Program Execution. NASA CR 145098-1,
        February 1977.

Figure 6.4-1 - Rail shear fixtures and instrumentation.

Dimensions in millimeters (inches)
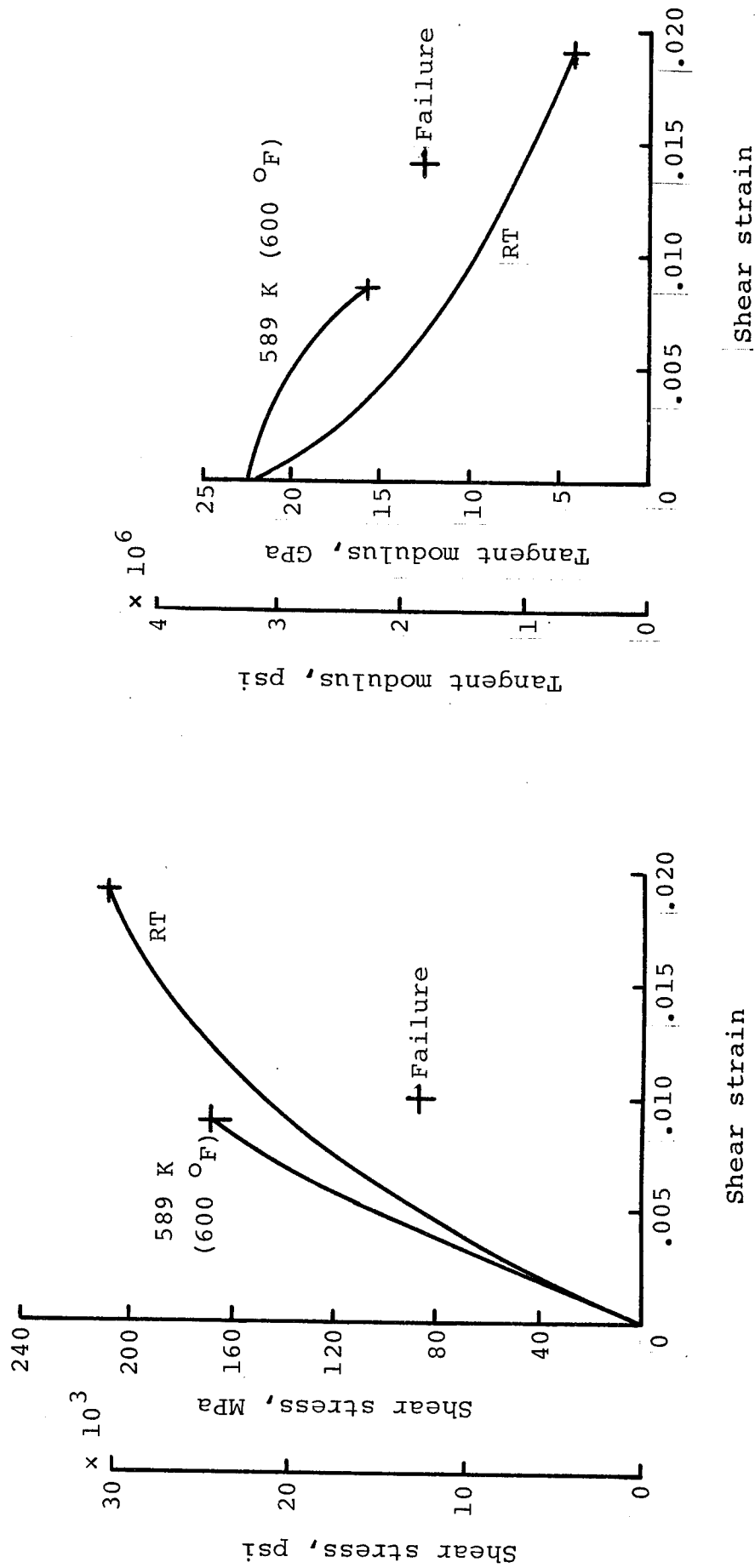
(a) Bonded fixture and tapered rails.

(b) Clamped fixture and untapered rails.

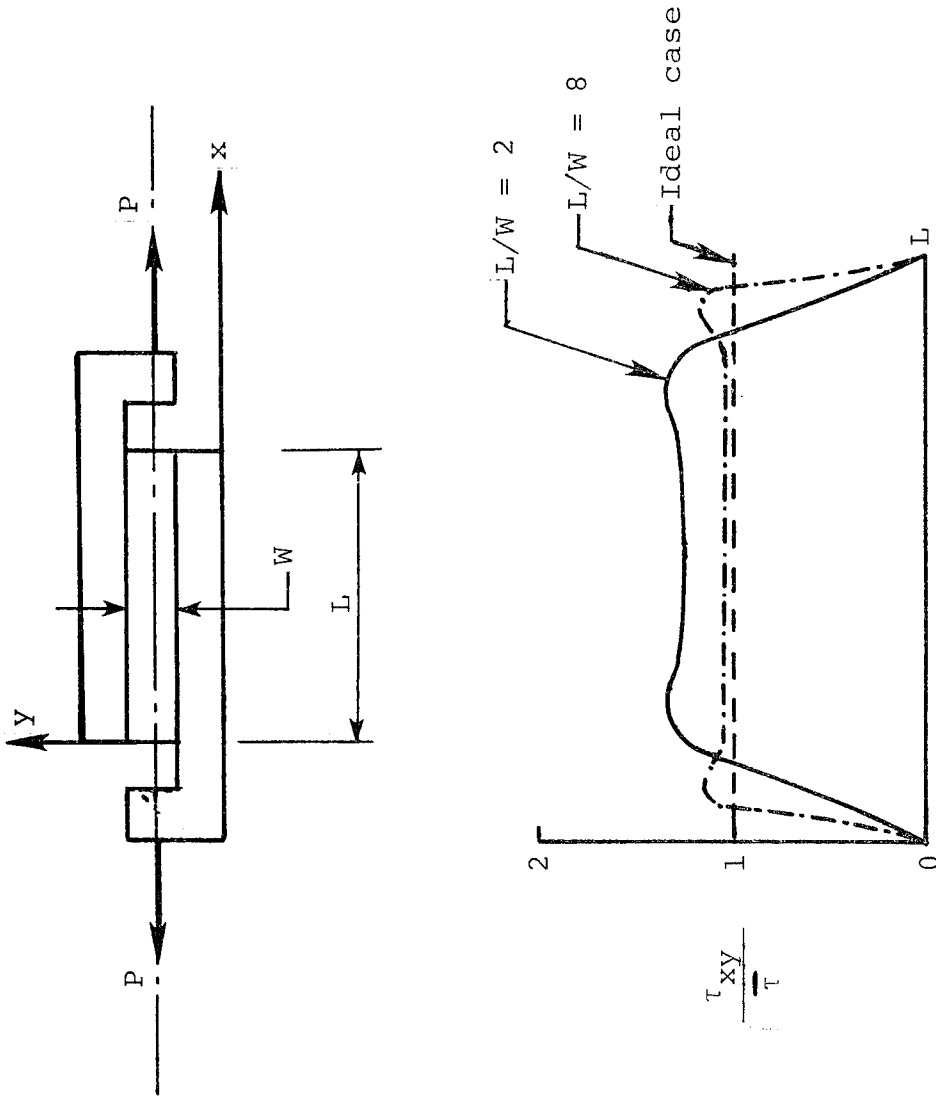Figure 6.4-2 – Preliminary experimental results from a clamped specimen for a $[0, \pm 45, 90]_s$ Gr/PI laminate.

Figure 6.4-3 – Effect of aspect ratio on shear stress distribution in a $[0,\pm45,90]_s$ Gr/PI laminate at room temperature.

Completed tests			
Laminate	Test temperature K (°F)	Fixture	No. of tests
$[0,\pm45,90]_s$	RT	Bonded	5
	RT	Bolted	7
	589(600)	Bolted	5
	589(600)	Bolted*	4
$[\pm45_2]_s$	RT	Bonded	5
	RT	Bolted	5
	589(600)	Bolted	3
Tests to be completed			
$[0_{12}]_T$	RT	Bolted	3
	589(600)	Bolted*	4
$[90_{12}]_T$	RT	Bolted	4
	589(600)	Bolted*	5

*Specimens bolted in test fixture after reaching test temperature.

Figure 6.4-4 – Summary of tests on Gr/PI laminates.

6.5 Bolt Bearing Strengths
Gregory R. Wichorek

The purpose of this task is to experimentally determine bolt bearing
strengths of graphite/polyimide composite laminates for preliminary CASTS
bolted joint designs. An attempt will be made to modify statistical models
developed for graphite/epoxy joints.

Specimen and test variables were selected based on the near term
objective of the CASTS project to design and fabricate a Space Shuttle Orbiter
aft-body flap for ground test. The first graphite/polyimide composite
material selected for fabrication and test was HTS/PMR-15. A quasi-isotropic
laminate composed of 16 plies was selected with a ply orientation of [0, 45,
90, -45, 0, 45, 90, -45]$_s$. Joint strengths and failure modes will be deter-
mined for a variety of width-to-diameter and edge-to-diameter ratios (figs.
6.5-1a and 6.5-1b). Double-lap shear specimens (fig. 6.5-1c) with a 4.8 mm
(.19 in) diameter bolt are to be tested at 117K (-250°F), room temperature,
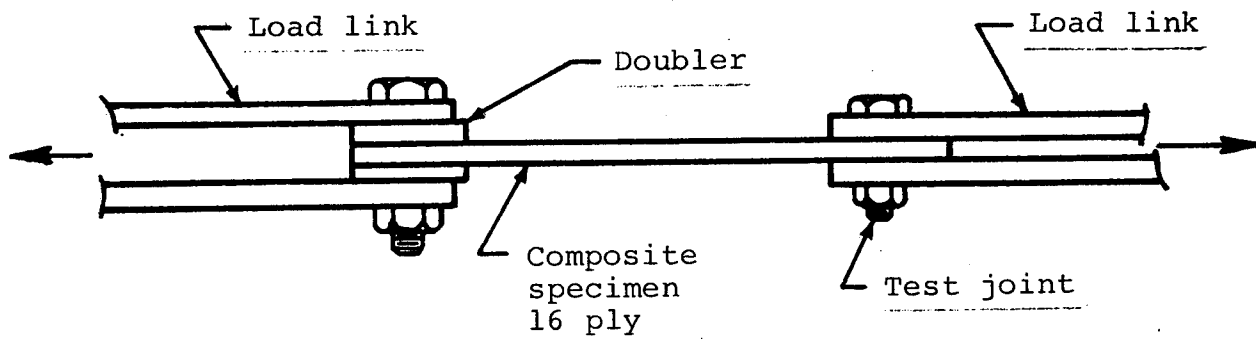and 589K (600°F).

For the next reporting period experimental test equipment and methods
will be checked and qualified. Fabrication and testing of double-lap shear
specimens at the planned test temperatures will begin.
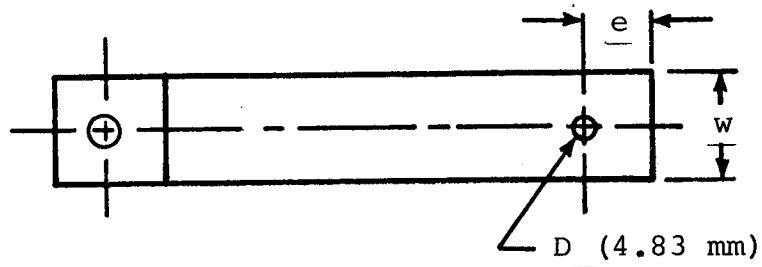
(a) Specimen configuration.

(b) Specimen variables.

(c) Test set-up.

Figure 6.5-1 - Bolted joint specimen variables and test set-up.

6.6 Adhesively Bonded Scarf Joints
William E. Howell

The purpose of this task is to evaluate the static and fatigue properties of graphite/polyimide bonded scarf joints. Two scarf lengths, 20 and 40 times the laminate thickness, will be evaluated. All material will be 8-ply of HTS/PMR-15 with a $[0/+45/90/-45]_s$ orientation and a nominal thickness of 0.13 cm (0.050 in.). To evaluate the influence of temperature and aging on bond strength, static tensile and constant amplitude fatigue tests will be conducted at 117K, RT, 533K, and 589K (-250°F, RT, 500°F, and 600°F) in the "as received" condition and after 125 hours of aging at 589K. To evaluate resistance to thermal cycling, specimens will be cycled 100 times from 117 to 589K and then tested in static tension and in constant amplitude fatigue at room temperature. Four replicates of each test will be conducted.

Large panels are being machined into small panels with appropriate scarfs. These panels will be bonded into scarf joint panels from which test specimens will be machined.

During the next reporting period fabrication of 160 test specimens of the configuration shown in figure 6.6-1 should be completed. FM-34 polyimide adhesive will be used to bond the scarf joints. LARC 13 adhesive will also be evaluated. A finite element analysis of the bonded joint design and a joint strength analysis will be conducted. Tensile testing will be initiated.
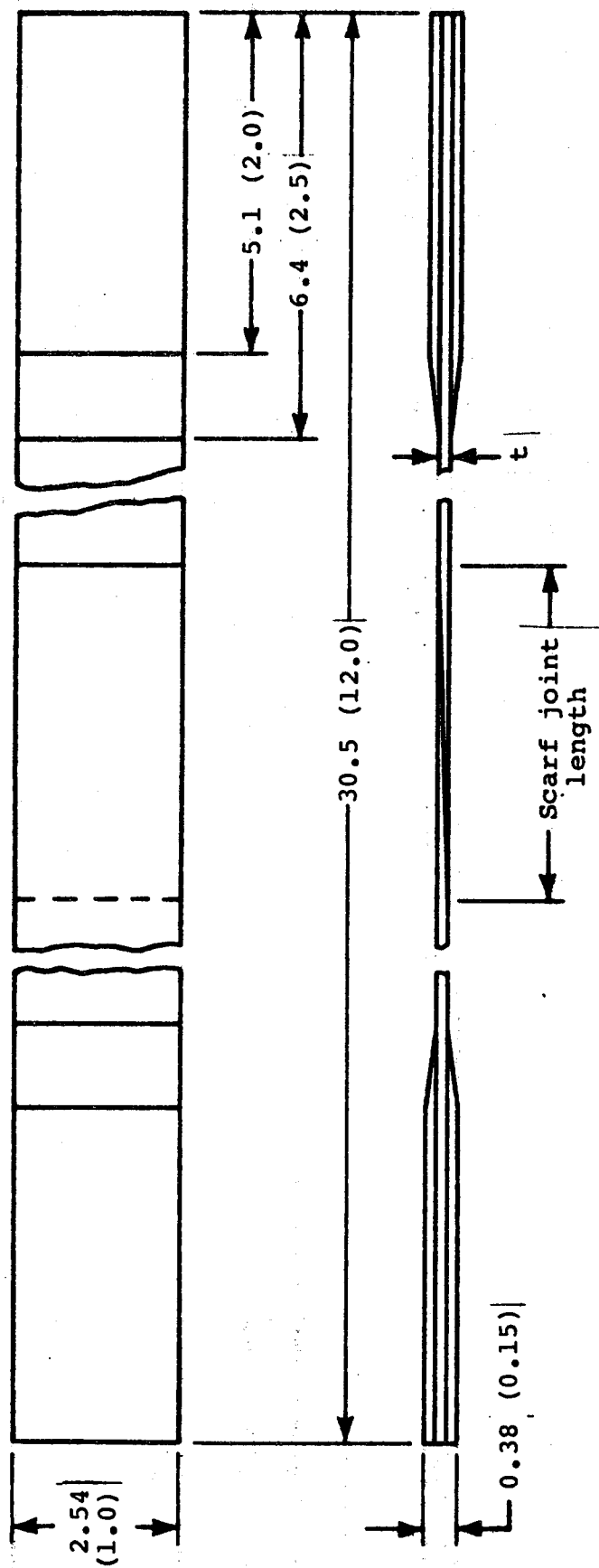
NOTES:

1. t = 8 ply laminate thickness

2. Scarf joint length: (1) 20t
                        (2) 40t

3. All dimensions are in centimeters and (in.)

Figure 6.6-1 - Graphite/polyimide adhesively bonded joint test specimen configuration.

7.0 THERMAL, PHYSICAL, AND MOISTURE PROPERTIES

The objectives of this program are to define environmental spectra for space shuttle and assess the sensitivity and durability of graphite/polyimide composites to various environmental parameters. The effects of moisture, temperature, thermal cycling, and shuttle fluids on the thermal, physical, and mechanical properties of Gr/PI composites will be determined under simulated environmental conditions for Space Shuttle. The program is divided into five major tasks: environmental definition, test procedures and baseline data definition, environmental sensitivity, thermal physical properties and Space Shuttle fluids exposure. The status of each of these tasks are discussed in the following sections.

7.1 Environmental Definition

Darrel Tenney, Jalaiah Unnam, and Edward Long

Ground Storage Model

Moisture absorption by polymer matrix composites can take place by capillary action along the fiber/matrix interface, through cracks or voids in the resin, and by diffusion through the matrix. In large, well-bonded composite hardware, the primary mechanism is by surface absorption and diffusion through the matrix. Diffusion into the material in the direction normal to the surface can be mathematically described by Fick's Second Law with an effective diffusion coefficient. The surface moisture content (boundary condition) is usually a function of the relative humidity of the environment adjacent to the composite panel. A computer program was written to solve the appropriate diffusion equations by a finite-difference technique allowing for time-dependent changes in the humidity and temperature of the environment. This program is being documented and will be made available through COSMIC. Because the diffusion coefficients and the equilibrium moisture contents for the graphite/polyimide systems are not available at this time, the above analysis was tested by simulating the moisture pickup in T300/5208 system for which the data are known. National Weather Bureau data tapes are used to update the boundary conditions. The findings of these simulations are reported in reference 7.1-1. The techniques and the methodology utilized in these simulations should be directly applicable to the moisture content prediction in graphite/polyimide systems.

Moisture Absorption Kinetics

An important input to the diffusion analysis is the relationship between equilibrium moisture content for the composite and the humidity of the environment. Whereas the equilibrium moisture content is determined by the relative humidity of the environment, the rates of absorption and desorption of moisture are controlled by the rates of diffusion in the composite. The effective diffusion coefficient depends on the diffusivity of the matrix, the diffusivity of the fibers, the volume fraction of the fibers, and the orientation of the fibers with respect to the exposed surface. Although analytical relationships among these parameters have been developed, the simplest and perhaps most reliable method of obtaining the effective diffusion coefficient is to experimentally measure it for the composite laminates of interest.

Specimens were fabricated from the (0) and $(0, \pm45, 90)_s$ lay-up of HTS graphite fibers in PMR-15 polyimide matrix. These specimens are being exposed to different combinations of relative humidity and temperature. Weight gain data will be obtained by weighing the specimens at predetermined intervals. The equilibrium moisture content will be noted as a function of relative humidity. The rates of absorption and desorption will be obtained by solving the diffusion equation to find the diffusion coefficients

which give solutions that match the experimental weight gain curves. These diffusion coefficients will be noted as a function of the filament lay-up and the temperature of the environment.

HTS/NR150B2 specimens, 8 cm x 1.3 cm x 10 ply (3 in x 1/2 in x 10 ply), with uni-directional lay-up were vacuum dried in an oven at 339K (150 F). These specimens had been previously exposed to the ambient lab environment. After 38 days, the average weight loss was 0.45%. All of this weight loss has been attributed to loss of absorbed water. Under this assumption and using the weight loss histories, a moisture desorption coefficient of 7.2×10^{-13} m^2/s was determined with the method described by (ref. 7.1-2). Assuming that the initial absorption and desorption coefficients of the material at low temperature (311-339 K) (100-150 F) are the same, the desorption coefficient of 7.2×10^{-13} m^2/s is approximately equal to the absorption coefficient of 6.7×10^{-13} m^2/s for T300/5208 used in reference 7.1-1. These results indicate that the absorption and desorption behavior of graphite/polyimides may be similiar to that of graphite/epoxies.

References

7.1-1. Tompkins, Stephen S.; Tenney, Darrel R.; and Unnam, Jalaiah:
        Prediction of Moisture and Temperature Changes in Composites
        During Atmospheric Exposure. NASA TM 78711, April 1978.

7.1-2. Shen, C. H. and Springer, G. S.: Effects of Moisture and
        Temperature on the Tensile Strength of Composite Materials,
        J. Composite Materials, vol. 11, Jan. 1977, p. 2.

7.2 Test Procedures and Baseline Data Definition

W. Barry Lisagor and Jalaiah Unnam

Work is underway to determine the effects of moisture on the mechanical properties of graphite/polyimide composite. This will be accomplished by subjecting specimens to controlled moisture conditioning and subsequent heat treatment at temperatures from 117 K (-250 F) to 589 K (600 F). Mechanical tests will include tension, compression, flexure, interlaminar shear, and rail shear.

An environmental chamber and platens with provision for heating and cooling will be used to obtain the desired test conditions. Mechanical extensometers will be used rather than strain gages for the moisture conditioned specimens so that the effects of moisture conditioning will not be compromised during the time required to apply strain gages. The extensometers can be encapsulated to provide protection.

The test techniques for both tension and compression specimens at all test temperatures have been formulated and verified using 2024-T4 aluminum specimens. For the verification tests at room temperature and 117 K (-250 F), strain was monitored using both strain gages and a mechanical extensometer. Agreement between gages and extensometer was within 1% for all tests. The extensometer was modified to allow use with the heating/cooling support platens.

Temperature profiles were obtained on a graphite/polyimide specimen 0.0445 m wide for a gage length of 0.0603 m at temperatures from 117 K (-250 F) to 589 K (600 F). Temperature distributions were considered satisfactory.

Rail shear test fixtures have been fabricated and preliminary test specimens have been instrumented with strain gages for formulation and verification of satisfactory test technique. Rail shear, short beam shear, and flexure specimens will be tested using a controlled environmental chamber currently being procured.

Testing of specimens in the moisture effects test matrix is expected to begin in the next reporting period.

7.3 Environmental Sensitivity

W. Barry Lisagor, Darrel R. Tenney, Jalaiah Unnam, and Stephen S. Tompkins

Moisture Effects

The objective of this task is to quantitatively determine the effect of moisture on the mechanical properties of Gr/PI composites. Two material systems will be investigated. The laminates to be studied are: (0), (90), (± 45), and $(0, \pm 45, 90)_s$. Tension, compression, flexure, interlaminar shear, and in-plane shear tests will be conducted on specimens in a dry and saturated condition. Two complex conditioning treatments consisting of combined moisture exposure and thermal cycling will also be investigated. Tests will be conducted at 117 K (-250 F), RT, and 589 K (600 F). This activity will commence when the test procedures and baseline data have been established.

Thermal Cycling

The objective of this activity is to determine the effects of thermal cycling on the residual mechanical properties of candidate materials for CASTS. Temperatures and pressure ranges for these tests will be 117 K (-250 F) to 589 K (600 F) and 1×10^{-4} Pa to 101 kPa (10^{-6} to 760 mm Hg), respectively. A thermal/pressure cycle simulating a Space Shuttle mission will be used. The residual strengths of the material in tension, compression, short beam shear, flexure and rail shear will be measured. Specimens will be thermal cycled after long time storage at ambient laboratory temperature and relative humidity. Wet and dry specimens will also be thermally cycled in an attempt to evaluate combined coupled effects of moisture and thermal cycling on residual strength.

Thermal cycling equipment to conduct tests for this study is being designed and built under contract. This equipment is scheduled for delivery in August 1978. Test specimens are being cut from panels of one of the test materials as these panels become available.

7.4 Thermal Properties

Ronald K. Clark

The work in this area is being performed under contract. The objectives are to determine the thermal conductivity, thermal expansions, specific heat, and emittance of HTS/PMR15 and HTS/NR150B2 graphite/polyimide composite materials in quasi-isotropic and unidirectional layups over the temperature range of 117 (-250F) to 589 K (600F). Thermal conductivity data and thermal expansion data will be obtained for the directions of the three major axes. The contractor has completed all thermal-physical properties tests of HTS/PMR15 graphite/polyimide. The HTS/NR150B2 tests will be completed during the next report period. The contract is expected to be completed in August 1978.
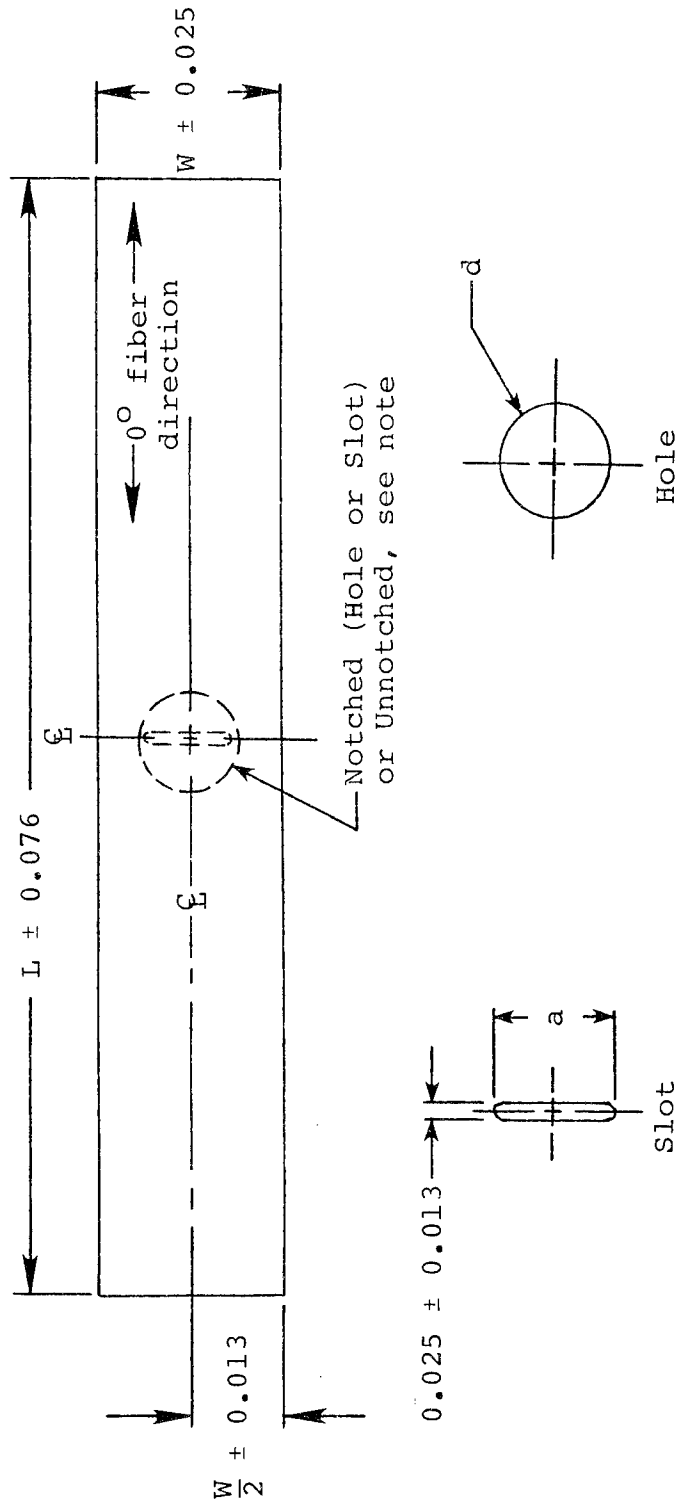
8.0 STRUCTURAL INTEGRITY

8.1 Fracture Behavior

Richard A. Everett, Jr.

The purpose of this task is to apply existing analyses or develop new analyses that will predict the fracture strength of graphite/polyimide. This will be accomplished by testing a series of specimens with different hole sizes and widths and using the test data to determine the validity of the fracture model. The specimen geometry and test matrix is shown in figures 8.1-1, 8.1-2, and 8.1-3. The test program consists of 369 specimens, of which 252 will contain a notch and 117 specimens will be unnotched. Residual strength tests after constant amplitude fatigue cycling will also be conducted on notched specimens. Fracture data will be obtained at room temperature, 117 K (-250° F), and 589 K (600° F). Moisture will not be controlled during these tests. The composites being studied are HTS/PMR-15 and HTS/NR150-B2.

Fracture tests will be initiated during the next report period. The tests at cryogenic and elevated temperatures will be conducted in a commercial environmental chamber which uses liquid nitrogen for the cryogenic tests and radiant heating for the elevated temperature tests.

Figure 8.1-1 - Unnotched and notched specimen geometry.

Matrix Material	Laminate Layup	W, cm	L, cm	No. of Specimens	
PMR-15	$[(\underline{+}45)_2]_s$	2.54	33.0	9	
	$[0]_8$	2.54	33.0		
	$[+45/0/-45/0]_s$	2.54	33.0		
	$[0/+45/90/-45]_s$	2.54	33.0		
	$[(\underline{+}45)_2]_s$	1.91	33.0		
	$[(\underline{+}45)_2]_s$	5.08	35.6		
	$[+45/90/-45/90]_s$	2.54	33.0		
	$[90]_8$	2.54	33.0		
	$[(0/+45/90/-45)_2]_s$	2.54	35.6		
	$[(\underline{+}45)_4]_s$	2.54	35.6		
	$[(\underline{+}45)_2]_s$	10.2	38.1		
NR150-B2	$[0/+45/90/-45]_s$	2.54	33.0		
NR150-B2	$[(\underline{+}45)_2]_s$	2.54	33.0		

Figure 8.1-2 – Unnotched specimens.

Matrix Material	Laminate Layup			W, cm	L, cm	a, cm	d, cm	Total Specimens
	a[1]	b[1]	c[1]					
PMR-15	9	9	9	10.0	41.9	–	0.159	27
	18	18	18			–	0.476	54
	9	9	9			–	0.953	27
	9	9	9			–	2.54	27
	3	3	3			0.159	‑‑	9
						0.476	–	9
						0.953	–	9
				↓	↓	2.54	–	9
				1.91	30.5	–	0.476	9
				2.54	30.5	–	0.476	9
	↓	↓	↓	5.08	30.5	–	0.476	9
↓	$[(0/+45/90/-45)_2]_s$			10.0	41.9	–	0.476	9
NR150-B2	$[0/+45/90/-45]_s$			10.0	41.9	–	0.159	9
						–	0.476	18
						–	0.953	9
↓	↓			↓	↓	–	2.54	9

NOTE: 1.) Laminate Layups

(a) $[(\pm45)_2]_s$

(b) $[+45/0/-45/0]_s$

(c) $[0/+45/90-45]_s$

Figure 8.1-3 – Notched fracture specimens.

8.2 Cyclic Debonding

Richard A. Everett, Jr.

The purpose of this task is to develop the relationship between strain energy release rate and cyclic debond rate in a titanium and graphite/ polyimide bonded joint. Cyclic debond rates can be used to establish inspection intervals for fail-safe design criteria and to indicate the minimum load at which cyclic debonding will occur. The geometry of the specimen used in this study is shown in figure 8.2-1. The test program consists of 100 tests which are separated into four groups of specimens with each group being a different matrix and adhesive combination. The composites being used are HTS/PMR-15 and HTS/NR150-B2. The two adhesives are FM-34 and modified LARC-13. Each group of specimens will be tested at room temperatures, 117 K (-250° F) and 589 K (600° F).

Acoustic emission has undergone preliminary evaluation as a debond monitoring technique. The results as of this date show good correlation between an established photoelastic technique (Ref. 8.2-1) and the acoustic emission technique if both sides of the joint debond simultaneously. Several debond specimens have been fabricated to explore the parameters which govern the settings on the acoustic emission equipment. This will insure that the data that define the debond front are accurate.

Debond tests will begin during the next report period and about 50 tests will be completed in time for the next CASTS report. The remaining 50 tests will be completed in early 1979.

References

8.2-1. Roderick, George L.; and Everett, Richard A., Jr.; and Crews, John H., Jr.: Cyclic Debonding of Unidirectional Composite Bonded to Aluminum Sheet for Constant-Amplitude Loading. NASA TN D-8126, 1976.
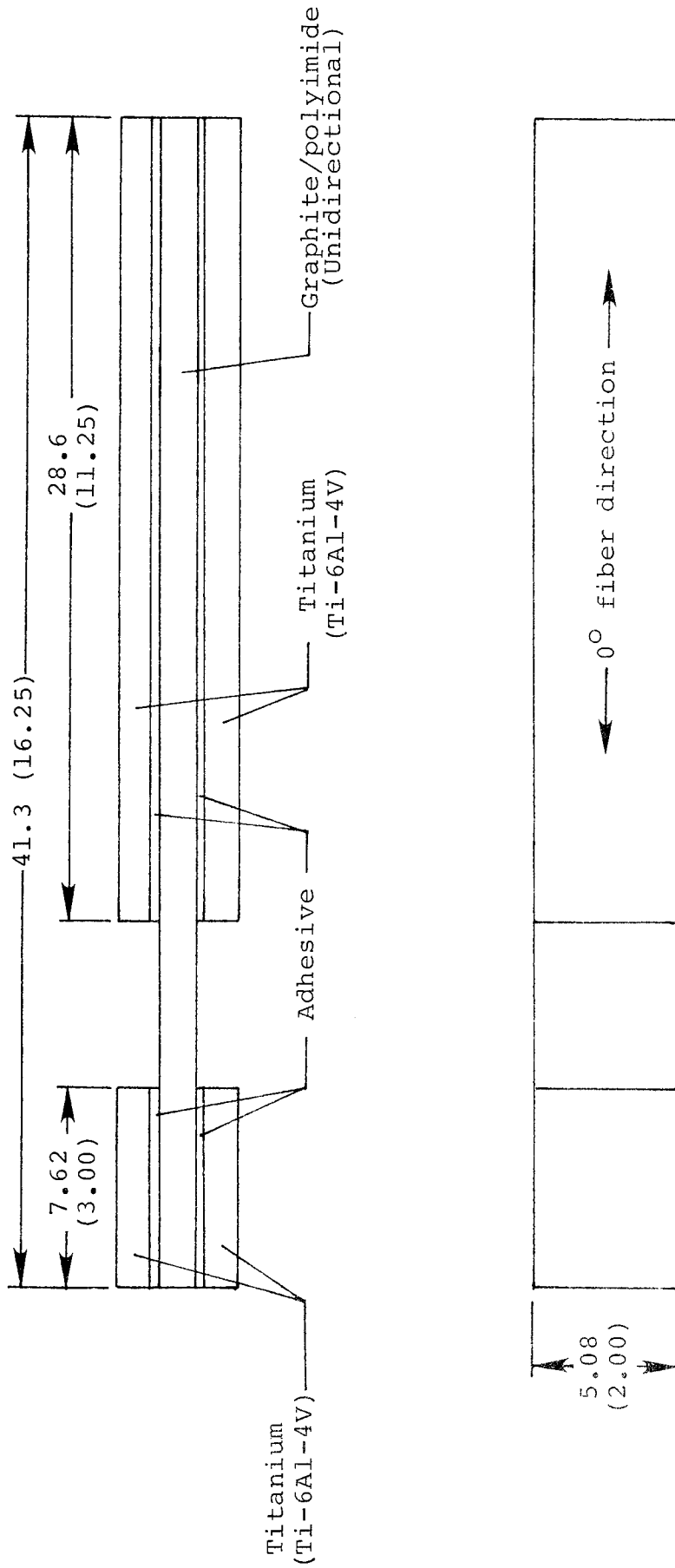
Figure 8.2-1 - Debond specimen.

8.3 Fatigue Behavior

L. A. Imig

The objectives of this task are: (1) To develop procedures and equipment required to conduct fatigue tests of graphite/polyimide under constant-amplitude loads at 117K, RT and 589K (-250°F, RT, and 600°F); (2) to develop procedures and equipment required to conduct real-time and accelerated fatigue tests of graphite/polyimide under variable-amplitude loads with cyclic temperatures between 117K and 589K; and to perform a limited number of fatigue tests of graphite/polyimide material to determine preliminary fatigue properties of selected composite layups.

Procedures were developed and verified for both constant and variable-amplitude fatigue tests. Specimens with a central hole (figs. 8.3-1 and 8.3-2) were used in all tests. Preliminary constant-amplitude fatigue data for graphite/polyimide [0, 45, 90, -45]$_s$ are shown in figure 8.3.3. The data were obtained from test specimens of HTS/PMR-15 laminates prepared in-house. These preliminary data indicate a significant effect of temperature on the fatigue strength of the material. Additional test specimens have been ordered.

CASTS project requirements to conduct fatigue tests at 117K, room temperature, 589K, and with cyclic temperature from 117K to 589K called for the development of a compact device with which to heat or cool the small test specimens. Existing equipment was too large or was not compatible with cyclic temperature extending to the cryogenic range. The system developed is shown in figures 8.3-4 through 8.3-7 and is currently in use. Figure 8.3-4 identifies the components required to maintain a constant cryogenic temperature. Figure 8.3-5 shows the assembled components, and figure 8.3-6 shows the assembly installed in a testing machine. The appearance of the system during operation at 117K (-250°F) is shown in figure 8.3-7. The cryogenic-control system requires a source of liquid nitrogen and a thermocouple feedback from the specimen to the solenoid controlller.

To conduct elevated temperature tests, the thermocouple feedback operates a standard temperature controller which controls electrical power to the heating cartridges.

Cyclic temperatures are facilitated by installing a separate thermo-couple to two controllers, and activating the two controllers alternately. The two controllers can be activated either by suitable timers or from a programming device which synchronizes the temperature changes with other events (loading, hold time, etc.) in the test.

During the next reporting period, the control equipment for the variable-amplitude fatigue tests will be received and installed. About 50 of the constant-amplitude and variable-amplitude tests will be completed. Additional coupon specimens will be ordered for tests to fill gaps in the results. A total of about 100 tests will be conducted in this activity.
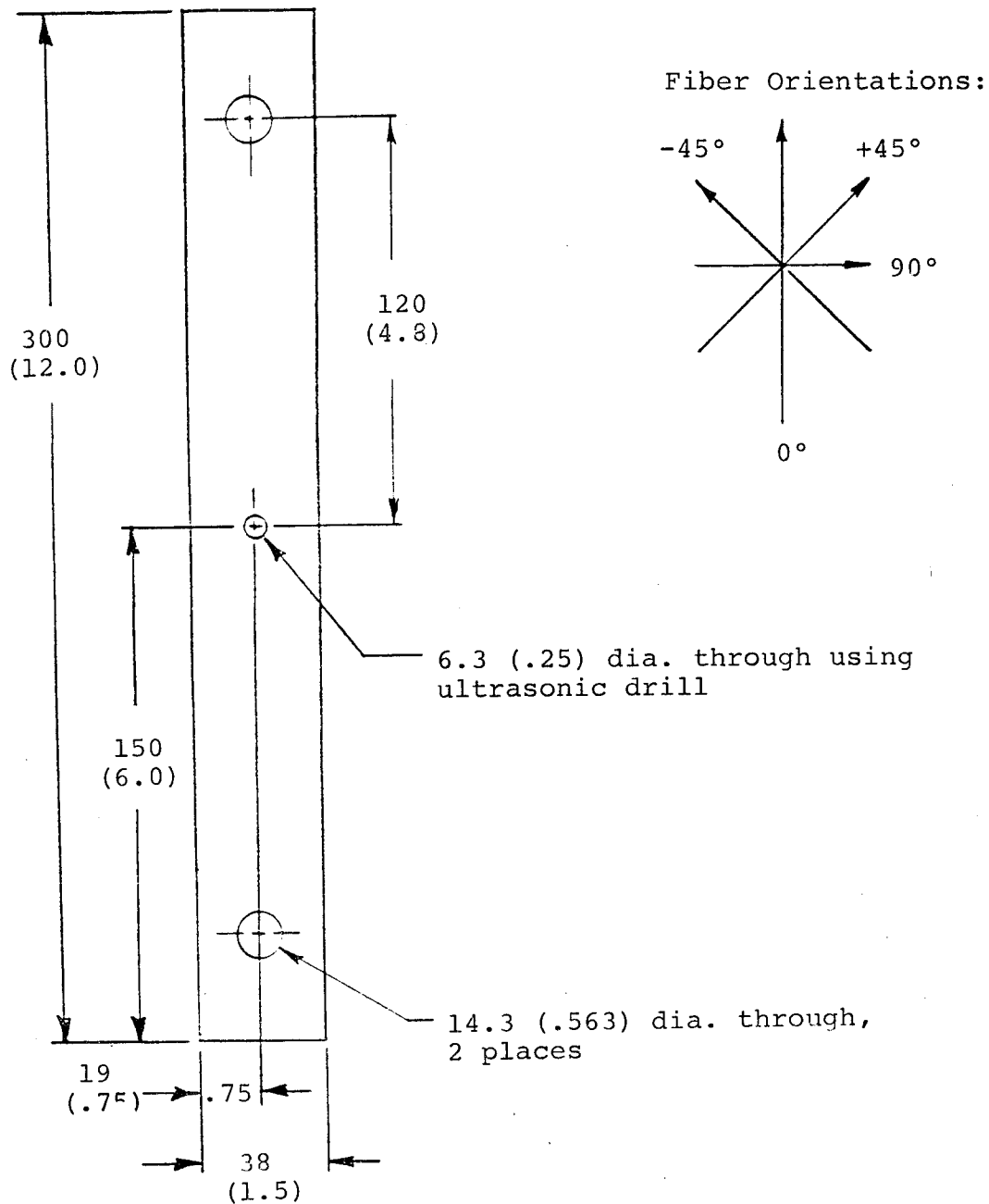
Figure 8.3-1 - Graphite/polyimide fatigue specimen.
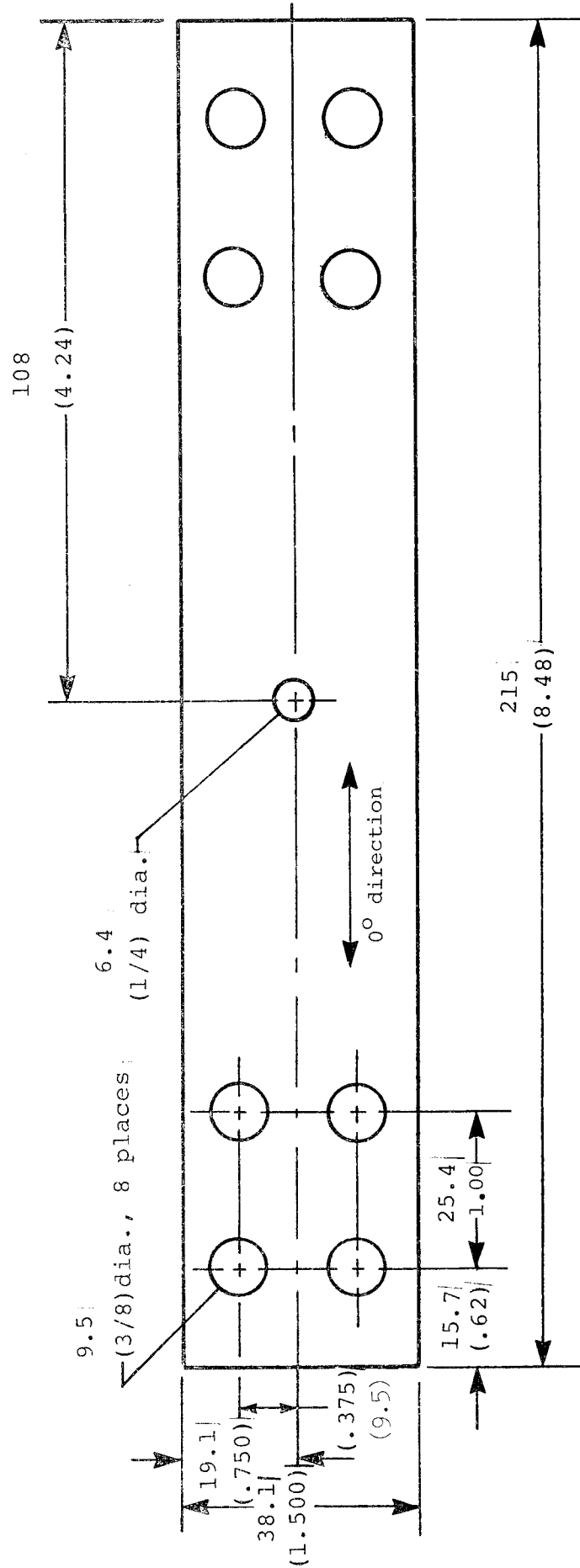(Dimensions in millimeters (inches).)

Figure 8.3-2 — Composite fatigue specimen for real-time tests. (Dimensions in millimeters (inches).)
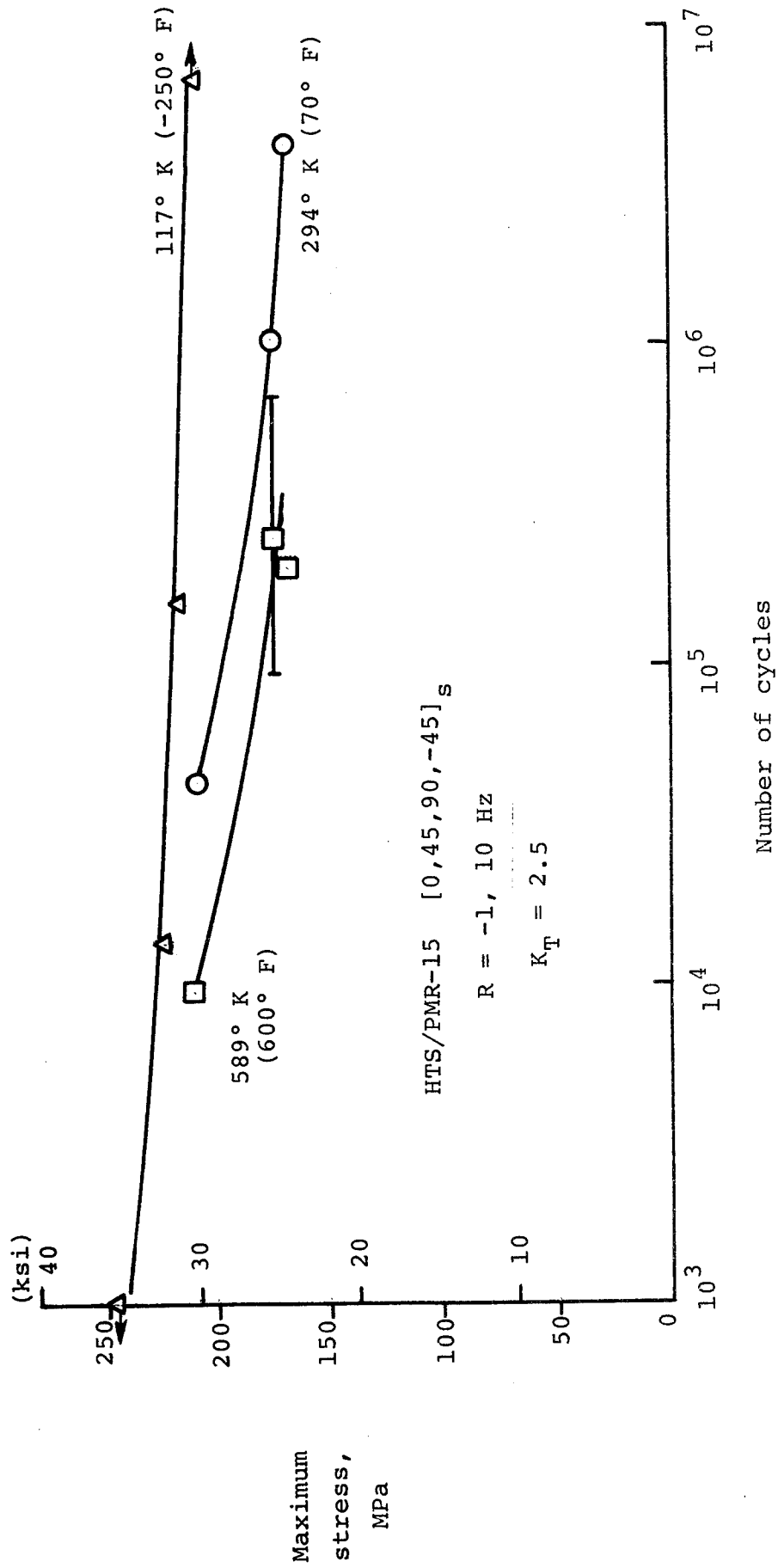
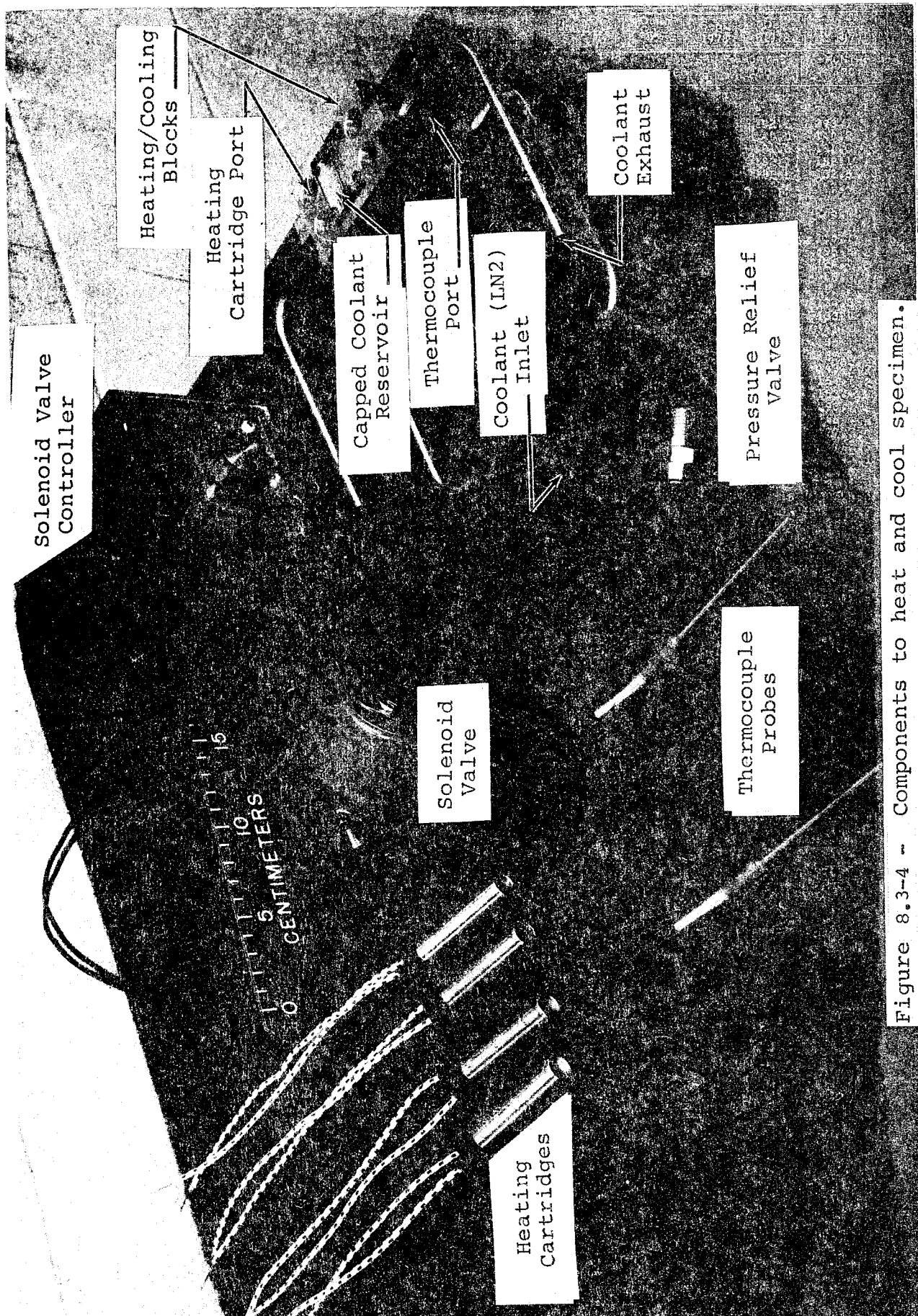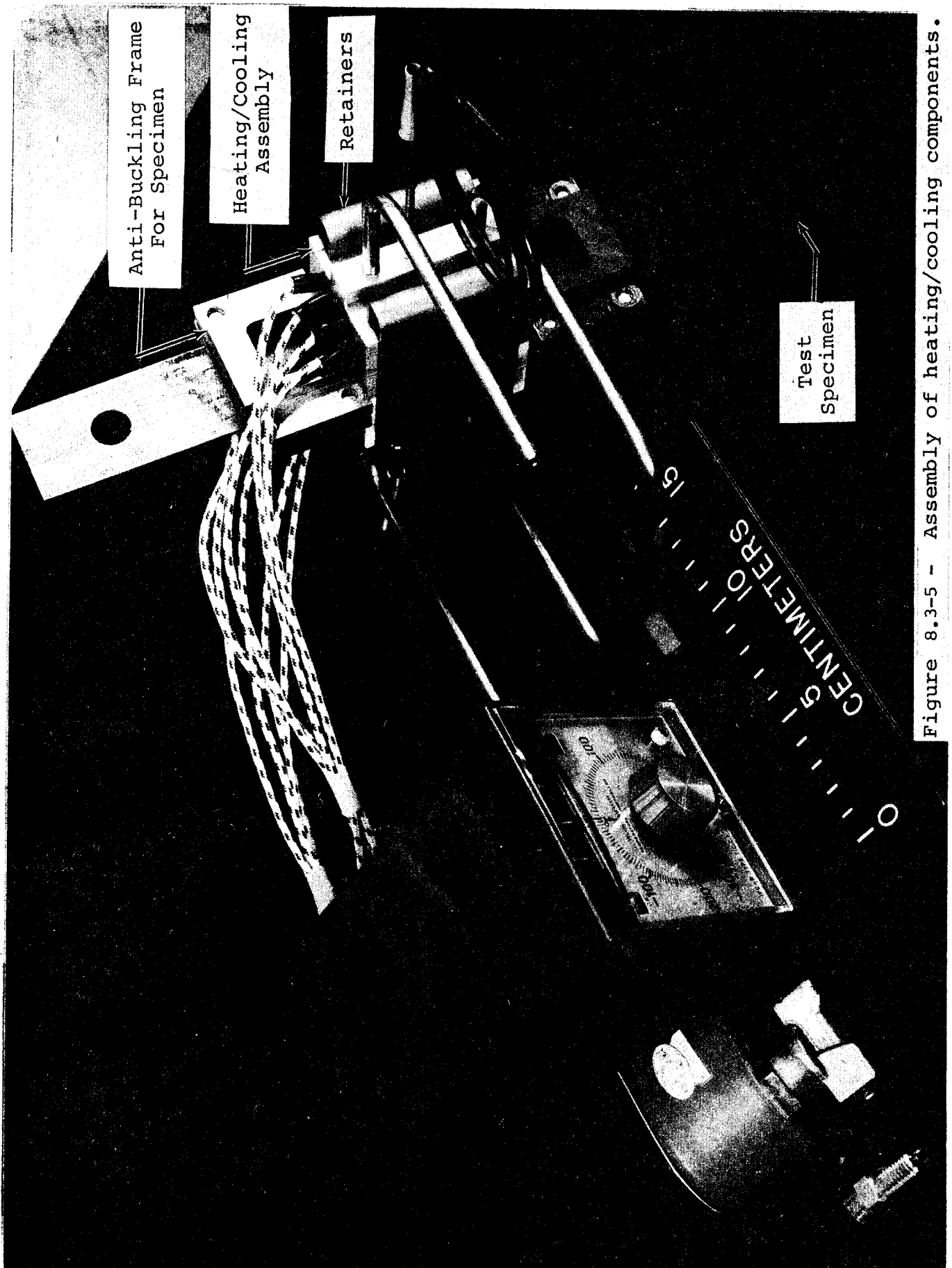Figure 8.3-3 - Preliminary fatigue strength of graphite/polyimide.

Figure 8.3-4 — Components to heat and cool specimen.

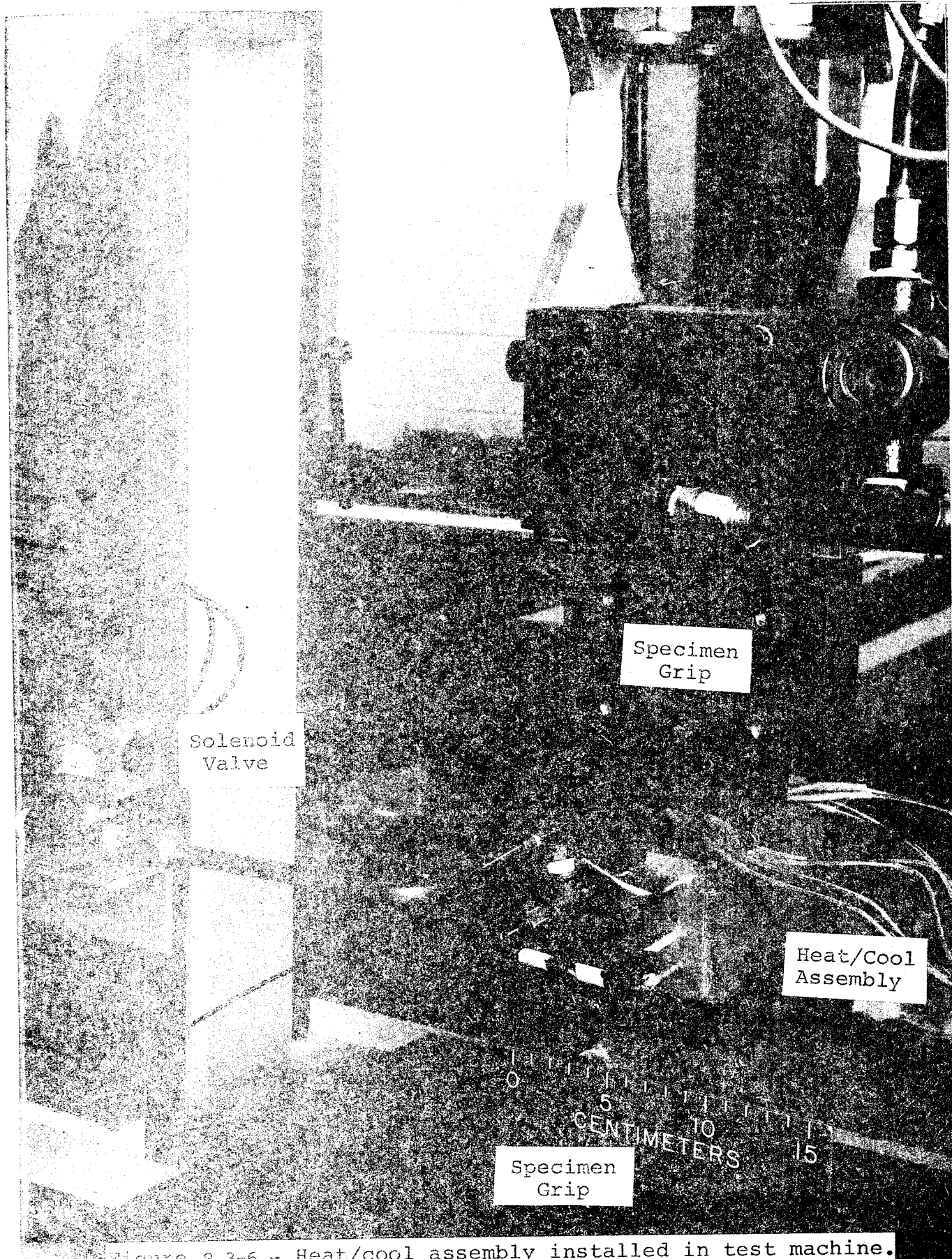Figure 8.3-5 – Assembly of heating/cooling components.

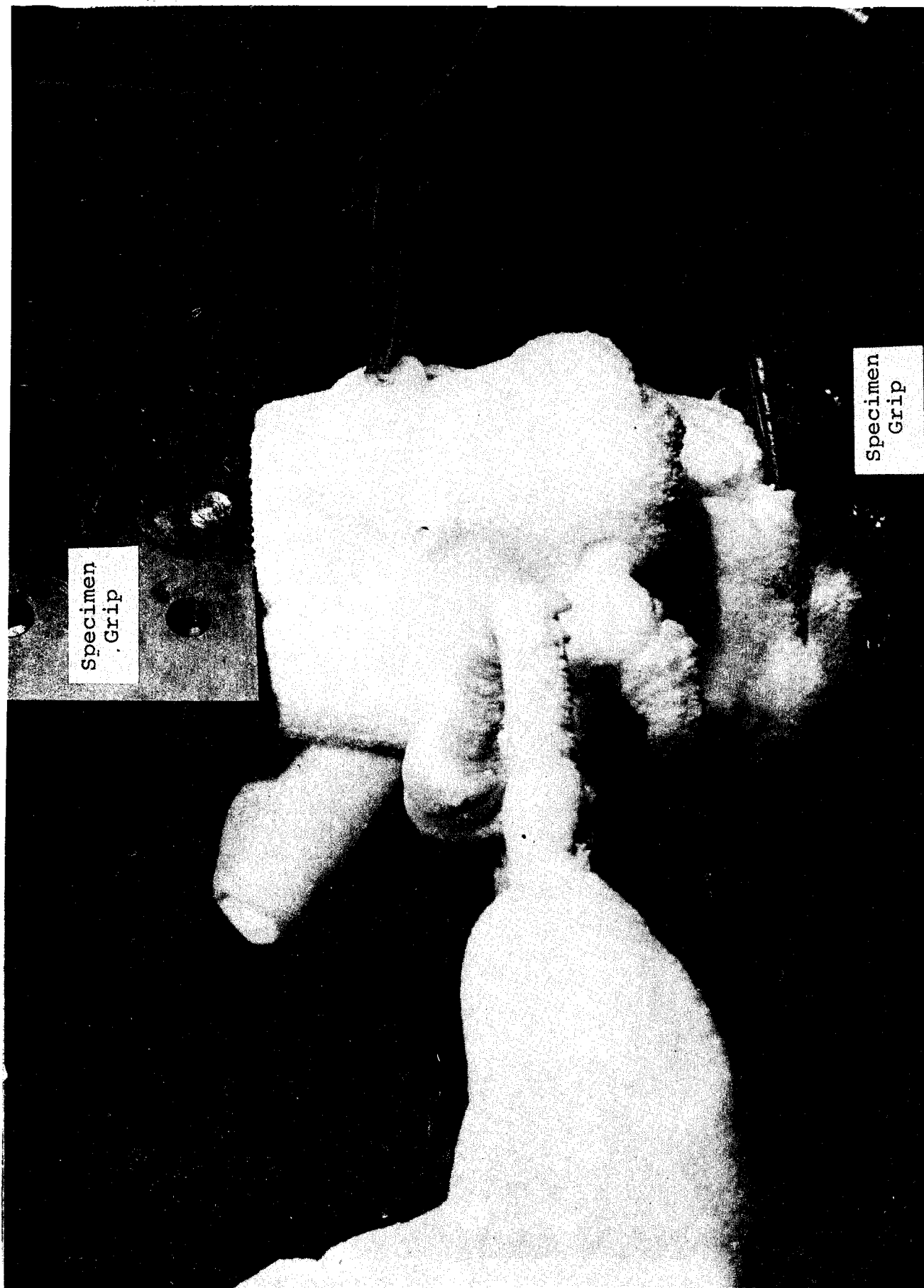Figure 8.3-6 — Heat/cool assembly installed in test machine.

Figure 8.3-7 – Heat/cool assembly in operation at −250° F.

9.0 STRUCTURAL ANALYSIS AND DESIGN STUDIES

9.1 Computer Code Development and Modification

James C. Robinson and Charles L. Blackburn*

Finite element analysis of structures composed of fiber-reinforced advanced-composite materials, such as those being considered in the CASTS project, involves complications not encountered in the analysis of structures of isotropic materials. The highly orthotropic stiffness, strength, and thermal properties of the individual layers require that either the orientation and properties of each layer be defined or the equivalent anisotropic properties of the laminate be specified.

The low stiffness and strength, normal to the fiber direction, of a single layer requires that several layer orientations be used in practical structures. In some cases, it may not be possible or practical to use laminates that are symmetric about their mid-plane. For such laminates, bending-extensional coupling exists and must be considered in the analysis if an accurate estimate of laminar behavior is to be obtained (refs. 9.1-1 and 9.1-2).

When simple two-dimensional structural finite elements (i.e., having three or four nodes) are used, quadrilateral elements are preferable to triangular elements because they yield more accurate results for a given number of degrees of freedom (refs. 9.1-3 and 9.1-4). Generally, for curved structures it is impossible to guarantee that all four nodes of a quadrilateral are in a plane. Therefore, the availability of a simple quadrilateral finite element capable of accommodating small amounts of "warping" - (i.e. not all four nodes in a plane), is desirable for general purpose applications. Previously used approximate methods which allow for small amounts of warping of simple quadrilateral elements have been described in references 9.1-3 - 9.1-7.

The development of a hybrid, anisotropic quadrilateral element which accounts for bending-extensional coupling and recovery of layer stresses is described in reference 9.1-8 and briefly summarized herein. This element was incorporated, under NASA contract, in the SPAR structural analysis system (available through COSMIC) (ref. 9.1-9 and 9.1-10). As a part of the validation of this new element, the following studies have been conducted:

(1) Buckling of general laminated plates.

(2) Thermal stresses of laminated plates cured at elevated temperatures.

(3) Displacements of a bi-metallic beam.

(4) Displacements and stresses of warped isotropic and anisotropic panels.

*Assistant Professor, University of Tennessee at Nashville,
(NASA Grant NSG-1455)

In addition, flat and spherical orthotropic and anisotropic segments were analyzed and the results are compared with results from higher-order plate and shell finite element analyses.

Partial results from some of these studies are presented herein. A detailed and complete discussion of the results from all studies is given in reference 9.1-11.

The ability to predict buckling loads of flat, multi-layered, aniso-tropic panels with this element is demonstrated by comparison with results from an extended Galerkin analysis (ref. 9.1-12). Non-dimensional shear and axial buckling loads from reference 9.1-12 and for several finite-element mesh sizes are shown in figure 9.1-1 for a square panel. The positive sign conventions are defined by the sketch shown on the table. As indicated by these results, convergence of the finite element solution has been attained for all practical purposes. Further, these results correlate well with the Galerkin solution except for a single case of a two layer panel with a 45° orientation. A 25 percent difference occurred for the shear buckling load. This difference may be attributed to non-convergence of the Galerkin solution which gave higher buckling loads than the monotonically decreasing converged finite element solutions.

Thermal stresses due to the high-temperature curing of a multi-layered, graphite/epoxy panel have been calculated to demonstrate the capability of the new element to recover layer stresses. A 3-layered laminate; namely, $0/90_{10}/0$ (i.e., a middle layer 10 times thicker than either outer layer) is analyzed. The stresses within each layer are compared with the results from a closed form solution in reference 9.1-13 for an identical panel. As indicated in figure 9.1-2 nearly identical results are obtained. Similar results are obtained for square, "quasi-isotropic" ($[90/0/\pm45]_s$ and $[0/\pm60]_s$), graphite/polyimide, laminated panels that were typical of those considered in the CASTS project. These panels were subjected to a temperature differential of 550K (530°F) which approximates the difference between the curing temperatures and the low operating temperature of space. A compressive longitudinal stress and a tensile transverse stress of approximately 69 MPa (10 ksi) was determined. The linear tensile transverse stress and its associated strain are greater than the ultimate stresses and strains given in reference 9.1-14 for graphite/polyimide materials.

Results obtained with the new element are compared with results obtained using several higher order quadrilateral elements for a plate problem analyzed in reference 9.1-15. The higher order elements are based on linear shallow-shell theory, including effects of shear deformation, material anisotropy and bending-extensional coupling. Two elements designated SQ12 and SQH, are based on assumed displacement fields. The element SQ12 has 12 nodes and 60 (shell) or 36 (plate) degrees of freedom and the SQH element has four nodes and 80 (shell) or 48 (plate) degrees of freedom. Displacement and moment distributions were calculated for a uniformly loaded, simply supported, anisotropic (45/-45/45/-45/45/-45/45/-45/45) square plate, having thickness-to-side ratios (t/a) of 0.01

and 0.001. Since the new element does not include the effects of transverse shear deformations, an example problem in which the effect of shear deformation is very small was selected. Results were obtained using a 4 x 4 and 8 x 8 finite element mesh and are compared with results from reference 9.1-15 in figure 9.1-3. Results for the 8 x 8 mesh are nearly coincident with results for the higher order elements. Results for the 4 x 4 finite element mesh are also in good agreement with reference 9.1-15.

The following observations resulted from the evaluation:

(1) Accurate results can be obtained for the buckling characteristics of flat laminated plates.

(2) Thermal curing stresses are accurately determined by the new element.

(3) The new element displays generally good agreement with results from several higher-order elements for orthotropic and anisotropic plate and shell configurations.

The above considerations indicate that this element has broad application to the analysis of structures being considered in the CASTS program.

References

9.1-1. Ashton, J. E.; Halpin, J. C.; and Petit, P. H.: Primer on Composite Materials: Analysis. Technomic Pub. Co., Inc., 1969.

9.1-2. Jones, R. M.: Mechanics of Composite Materials. McGraw-Hill Book Co., c. 1975.

9.1-3. Turner, M. J.; Clough, R. W.; Martin, H. C. and Top, L. J.: Stiffness and Deflection Analyses of Complex Structures. Journal of the Aeronautical Sciences, Vol. 23, No. 9, Sept. 1956, p. 805.

9.1-4. Robinson, John: A Warped Quadrilateral Strain Membrane Element Computer Methods in Applied Mechanics and Engineering 7, 1976, p. 359.

9.1-5. Argyris, J. H. and Kelsey, S.: Modern Fuselage Analysis and the Elastic Aircraft. Butterworth, London, 1963.

9.1-6. Taig, I. C. and Kerr, R. I.: Some Problems in the Discrete Element Representation of Aircraft Structures. Matrix Methods of Structural Analysis, AGARDograph 72 (1964) 267-314, B.M. Fraeijs de Veubeke (ed.).

9.1-7. MacNeal, R. H., ed.: The NASTRAN Theoretical Manual. NASA SP 221, 1970.

9.1-8. Whetstone, W. D.; Yen, C. L.; and Jones, C. E.: SPAR Structural Analysis System Reference Manual-System Level II - Volume 2 - Theory. NASA CR 145098-2, February 1977.

9.1-9. Whetstone, W. D.: SPAR Structural Analysis System Reference Manual System Level 11 - Volume 1 - Program Execution. NASA CR 145098-1. February 1977.

9.1-10. Giles, G. L. and Hafka, R. T.: SPAR Data Complex: Description and Programmer Instructions. NASA TM-78701, 1978.

9.1-11. Robinson, J. C. and Blackburn, C. L.: Evaluation of a Hybrid, Anisotropic, Multi-Layered, Quadrilateral Finite Element. NASA TP-1236, 1978.

9.1-12. Sawyer, J. W.: Flutter and Buckling of General Laminated Plates. Journal of Aircraft, Vol. 14, No. 4, April 1977, pp. 387-393.

9.1-13. Tsai, S. W.: Strength Characteristics of Composite Materials. NASA CR-224, April 1965.

9.1-14. Boeing Commercial Airplane Co., Preliminary Design Dept.: Study of
         Advanced Composite Structural Design Concepts for an Arrow Wing
         Supersonic Cruise Configuration. NASA CR-145192, January 1978.

9.1-15. Noor, A. K. and Mathers, M. D.: Shear-Flexible Finite-Element
         Models of Laminated Composite Plates and Shells. NASA TN D-8044,
         December 1975.

| Stacking sequence	Ref. 9.1-12	Mesh size		
		4 × 4	6 × 6	8 × 8
	Axial buckling load = $(N_x b^2)/(\bar{D}_{11}\pi^2)$			
[0]	1.306	1.307	1.304	1.303
[90]	0.890	0.931	0.902	0.896
[−45]$_s$	1.576	1.583	1.507	1.478
[45/−45]$_s$	1.900	1.913	1.865	1.849
[−45/45−45]$_s$	2.080	2.112	2.087	2.080
	Shear buckling load = $(N_{xy} b^2)/(\bar{D}_{11}\pi^2)$			
[0]	2.880	3.069	2.984	2.927
[90]	2.880	3.069	2.984	2.894
[−45]$_s$	7.850 −2.120	7.929 −1.851	7.744 −1.637	7.698 −1.584
[45/−45]$_s$	7.180 −2.670	7.355 −2.818	7.170 −2.601	7.135 −2.550
[−45/45/−45]$_s$	6.440 −3.530	6.660 −3.752	6.470 −3.539	6.437 −3.493
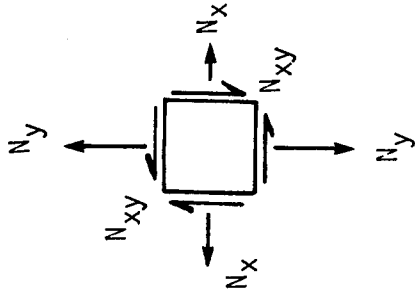
Figure 9.1-1 – Comparison of axial and shear buckling load from the extended Galerkin solution (ref. 9.1-12) and solutions for various finite element mesh sizes for a square panel.

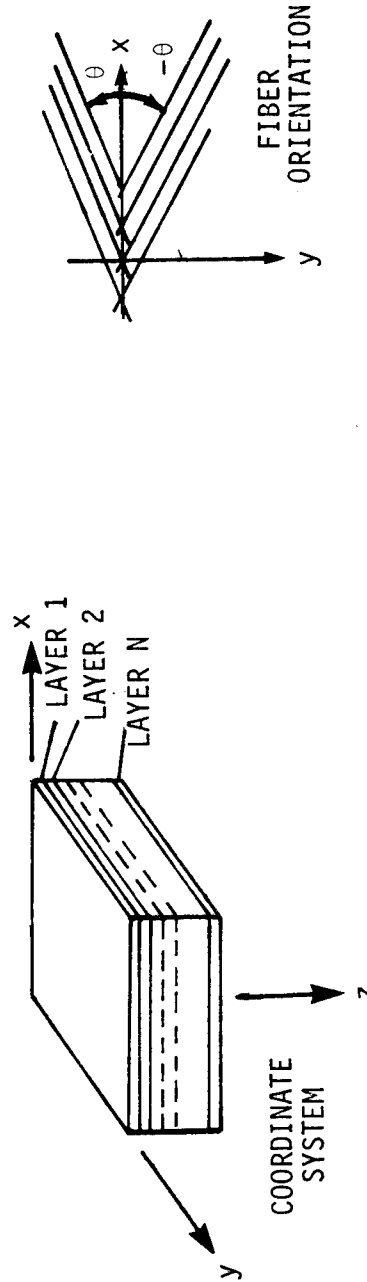|	New element				Reference 2		
Layer	σ_x psi (Pa)	σ_y psi (Pa)	τ_{xy} psi (Pa)		σ_x psi (Pa)	σ_y psi (Pa)	τ_{xy} psi (Pa)
	$[0/90_{10}/0]$ laminate						
1	-7105.0 (-48.987×10⁶)	3185.0 (21.960×10⁶)	0.0 (0.0)		-7100.0 (48.953×10⁶)	3200.0 (22.063×10⁶)	0.0 (0.0)
2	1421.0 (9.797×10⁶)	-637.0 (-4.392×10⁶)	0.0 (0.0)		1420.0 (9.791×10⁶)	-640.0 (-4.413×10⁶)	0.0 (0.0)
3	-7105.0 (-48.987×10⁶)	3185.0 (21.960×10⁶)	0.0 (0.0)		-7100.0 (-48.953×10⁶)	3200.0 (22.063×10⁶)	0.0 (0.0)

Figure 9.1-2 – Comparison of induced thermal curing stresses in a square, G/EP panel cured at 405.4 K (270°F).
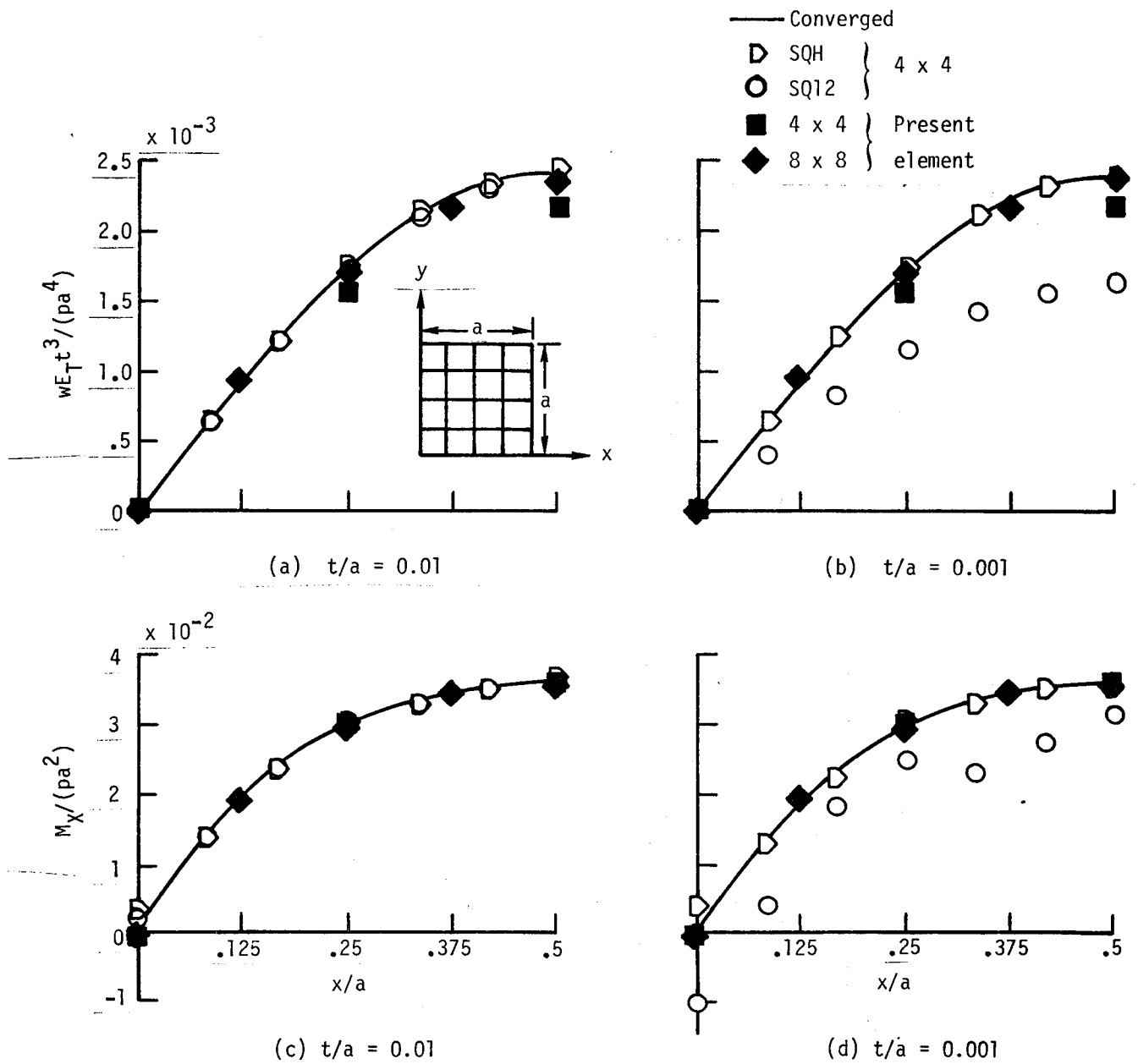
Figure 9.1-3 — Distribution of transverse displacement w and bending-moment resultant M_X along Y = a/2. Simply supported, nine-layered (45/-45/45/-45/45/-45/45/-45/45), anisotropic square plate (ref. 9.1-15).

9.2 Aft Body Flap Design Studies

James C. Robinson and Charles L. Blackburn*

Work is underway in-house on a preliminary design of an advanced composite body flap for the space shuttle. A relatively coarse finite element model (fig. 9.2-1), which had approximately 500 D.O.F. for a half model and stiffness properties based on the aluminum body flap, was used for determination of in-plane loads. For pressure bending of the cover panels, two more-detailed models (about 600 D.O.F.) of a quarter of a panel were used with assumed boundary conditions (fixed on long sides, simply-supported on short sides). Stiffness properties of the panel models were for graphite polyimide. The SPAR structural analysis system (ref. 9.2-1) was used for analysis.

The external loads considered on these models were aerodynamic pressure, inertial loads, and forced support deflections due to orbiter structural deformation. Thermal loading was not imposed because appropriate temperature distributions for the composite structure were not available. Also, thermal stresses due to temperature gradients in an all composite structure are much less than in a similar aluminum structure due to the lower coefficient of thermal expansion. Assessment of local thermal stresses due to attachment of titanium fittings to a composite body flap at elevated or cryogenic temperatures will require detailed models for analysis.

Panel loads (or stresses) are defined in figure 9.2-2 and shown in figure 9.2-3. Due to the preliminary nature of the calculations and the low values of the calculated load, maximum values of a given load component are presented even though they may not occur at the same location.

Based on these loads, structural concepts for a preliminary design of an advanced composite body flap were selected and are shown in figure 9.2-4. The relatively low loads in the body flap sandwich cover panels require that the face sheets be minimum gage. A pseudo-isotropic lay-up, (0, $\pm$45, 90) was selected. Therefore, a minimum gage face sheet would be 4 layers thick or 0.30 mm (0.012 in) if 0.076 mm (0.003 in) tape were used. The intracell buckling capability of this thin sheet cannot be readily determined from the literature due to the lack of symmetry in the ply stacking. The SPAR program was used to determine the approximate intra-cell buckling stress of several laminates as shown in figure 9.2-5. A comparison of intra-cell buckling coefficients for isotropic materials as determined by SPAR and those used in industry (specifically the Boeing Company stress manual) is also shown. From the figure, it appears that the core cell size should not exceed 6.3 mm (0.25 in).

A refined finite element model (fig. 9.2-6) of the body flap has been developed. This model has approximately 6000 degrees of freedom and 1600

*Assistant Professor, University of Tennessee at Nashville,(NASA Grant NSG-1455)

elements. Both models have been analyzed using metallic properties for comparison with existing results collected under contract NAS1-14170 with Rockwell International.

During the next few months, efforts will be focused on the determination of internal loads in the aluminum body flap from the refined model results, and development of a composite body flap model using these loads. Also, several small thermal models will be developed to determine local temperature distributions.

References

9.2-1. Whetstone, W. D.: SPAR Structural Analysis System Reference Manual
        System Level 11 – Volume 1 – Program Execution. NASA CR 145098-1.
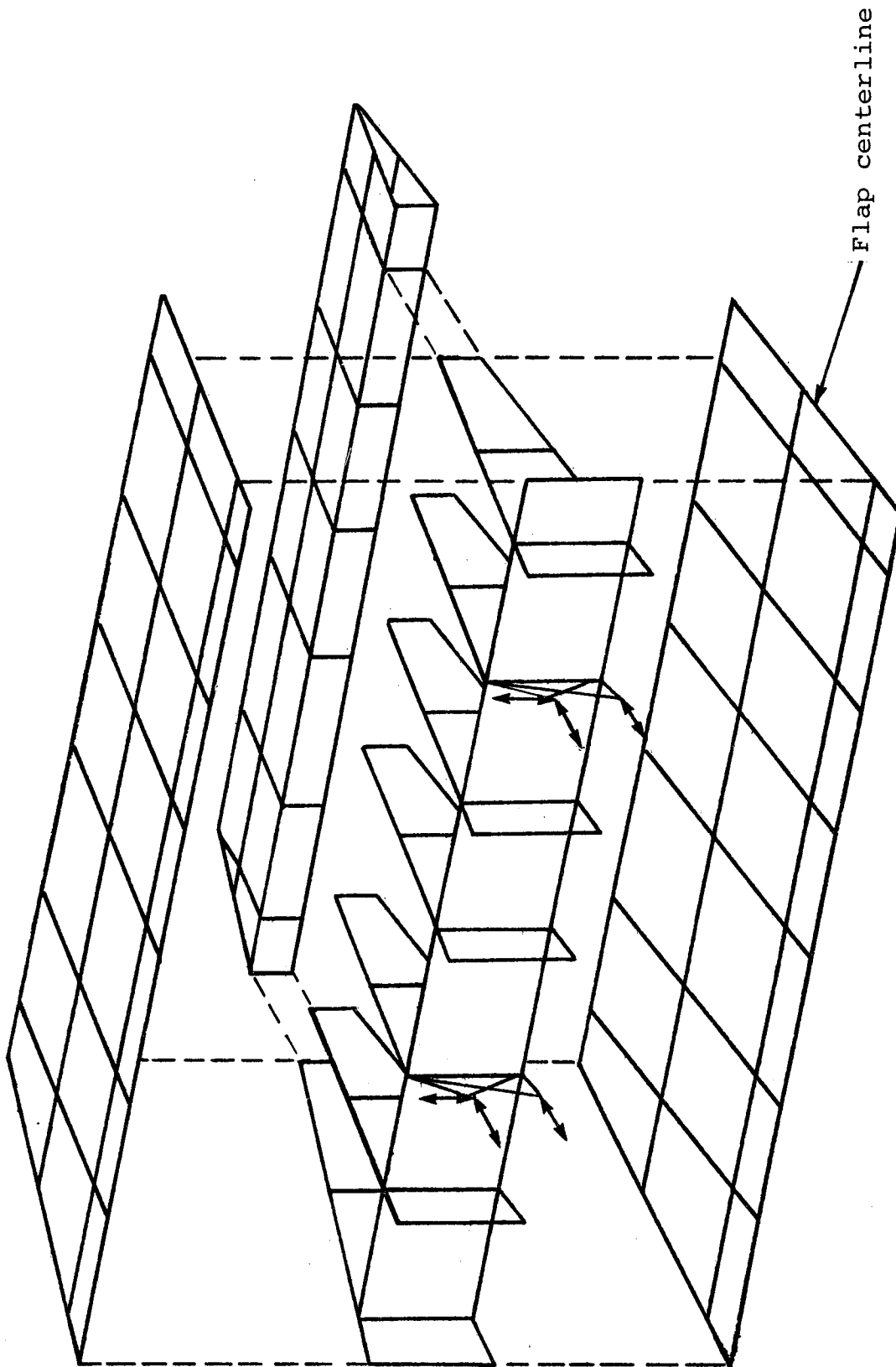   February 1977.

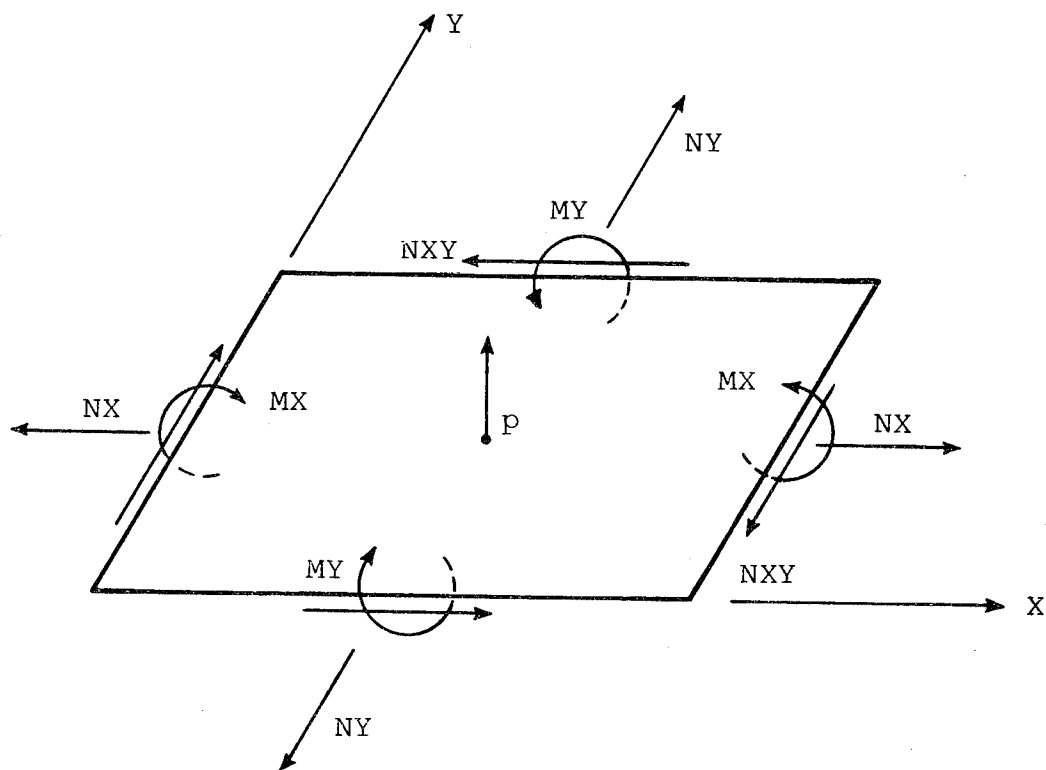Figure 9.2-1 - Coarse finite element model of half of body flap.

Figure 9.2-2 - Panel loads.

Component	N_x		N_x		N_{xy}		M_y		P	
	N/m*10³	lb/in	N/m*10³	lb/in	N/m*10³	lb/in	Nm/m	in-lb/in	kPa³	psi
Cover panel	74	420	74	420	32	180	448	100	21	3.0
Support rib	89	500	114	650						
Stability rib	44	250	32	180						
Front spar	58	330	284	1620	30	170				

Figure 9.2.3 – Body flap preliminary design load levels.

Figure 9.2-4 — Preliminary composite design for body flap.
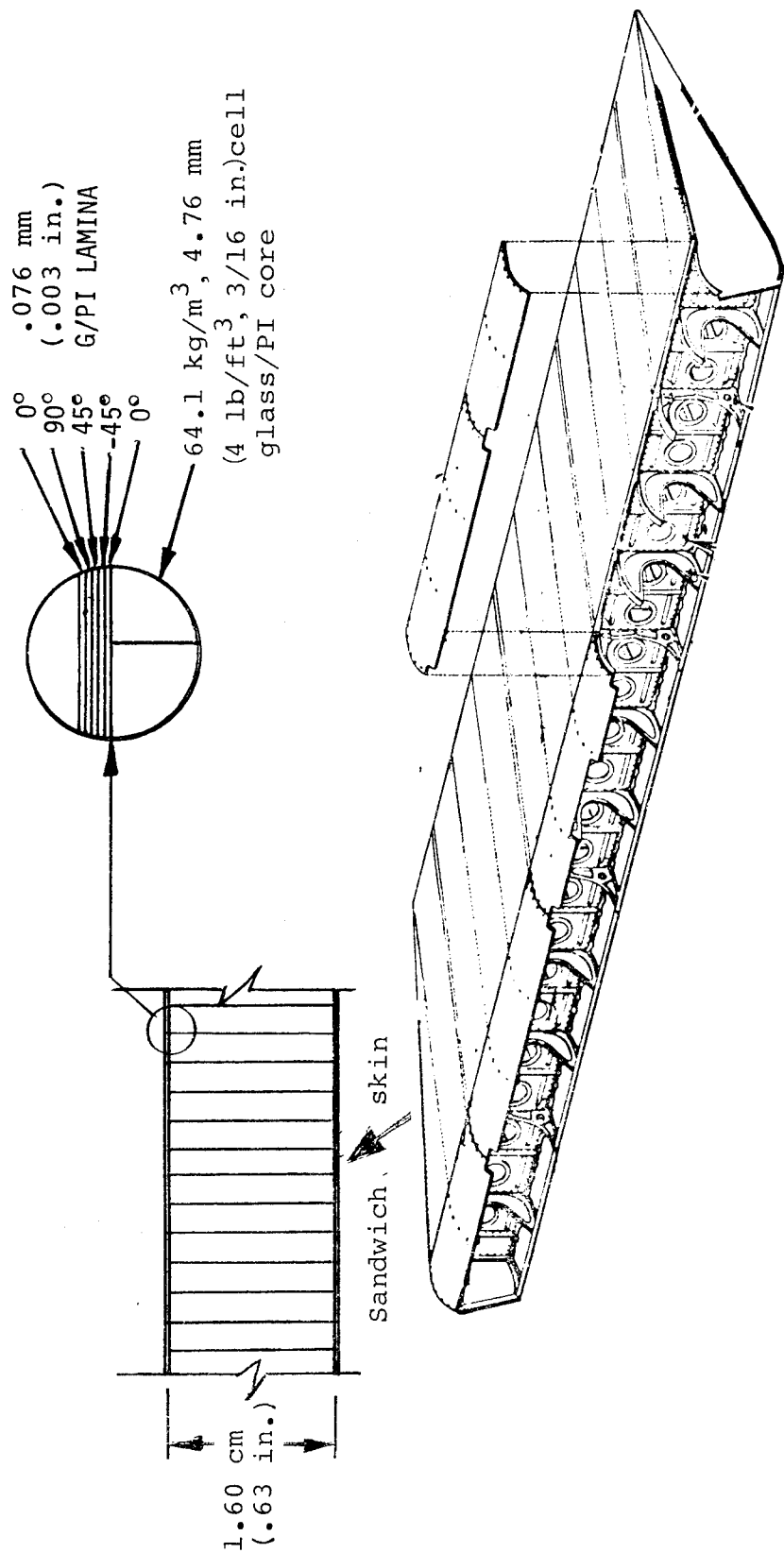
Material	Structure weight kg (lbs)		TPS weight kg (lbs)	
Aluminum	195	(430)	390	(860)
Gr/PI	154	(340)	275	(607)

0°   .076 mm
90°   (.003 in.)
45°   G/PI LAMINA
-45°
0°

64.1 kg/m³, 4.76 mm
(4 lb/ft³, 3/16 in.)cell
glass/PI core

Sandwich skin

1.60 cm
(.63 in.)

Isotropic

$$\text{Source} \qquad P_{cr}\Big/ \frac{E}{(1-\nu^2)}\left(\frac{t}{s}\right)^2$$

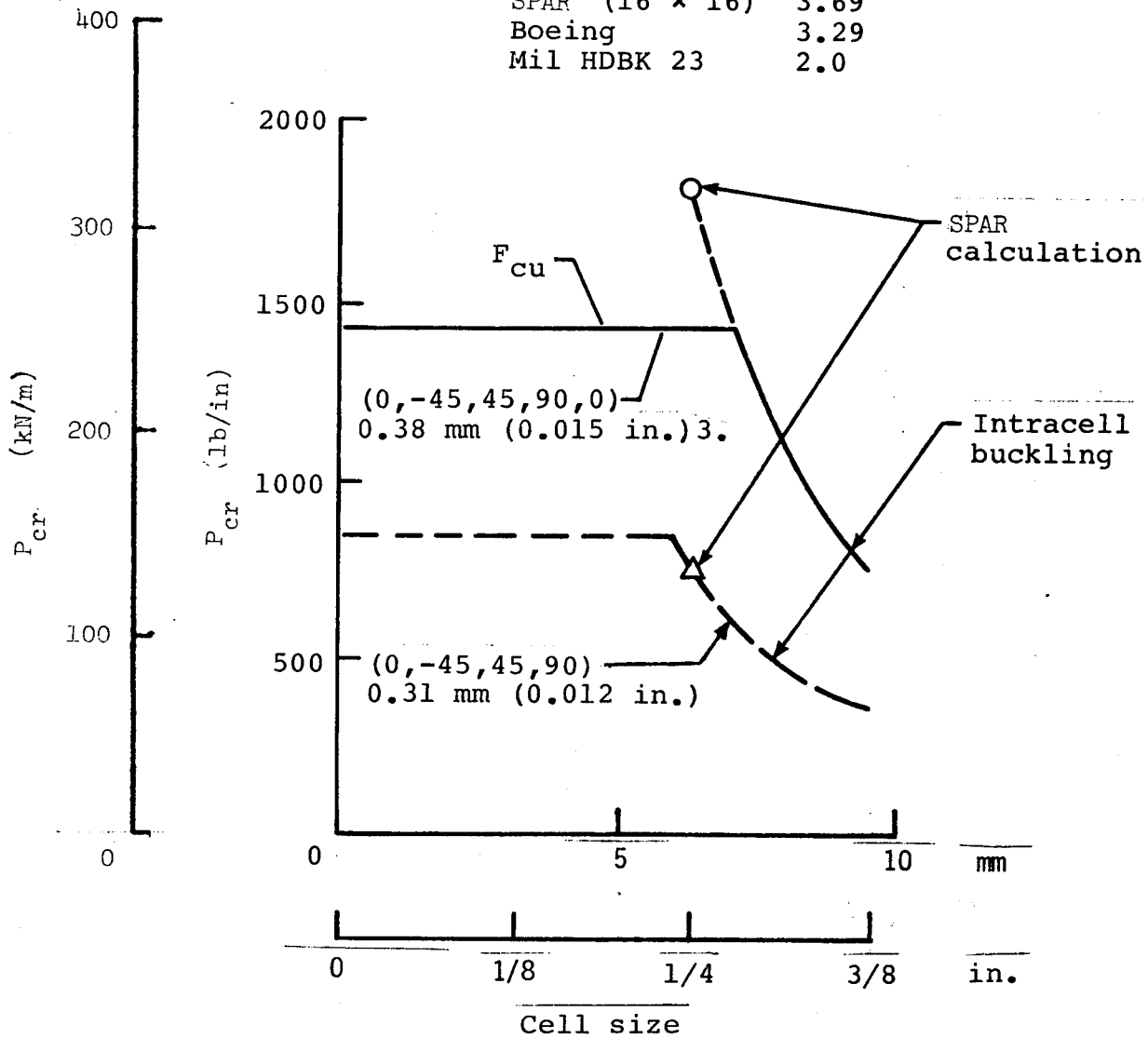| Source	
SPAR (8 × 8)	3.85
SPAR (16 × 16)	3.69
Boeing	3.29
Mil HDBK 23	2.0

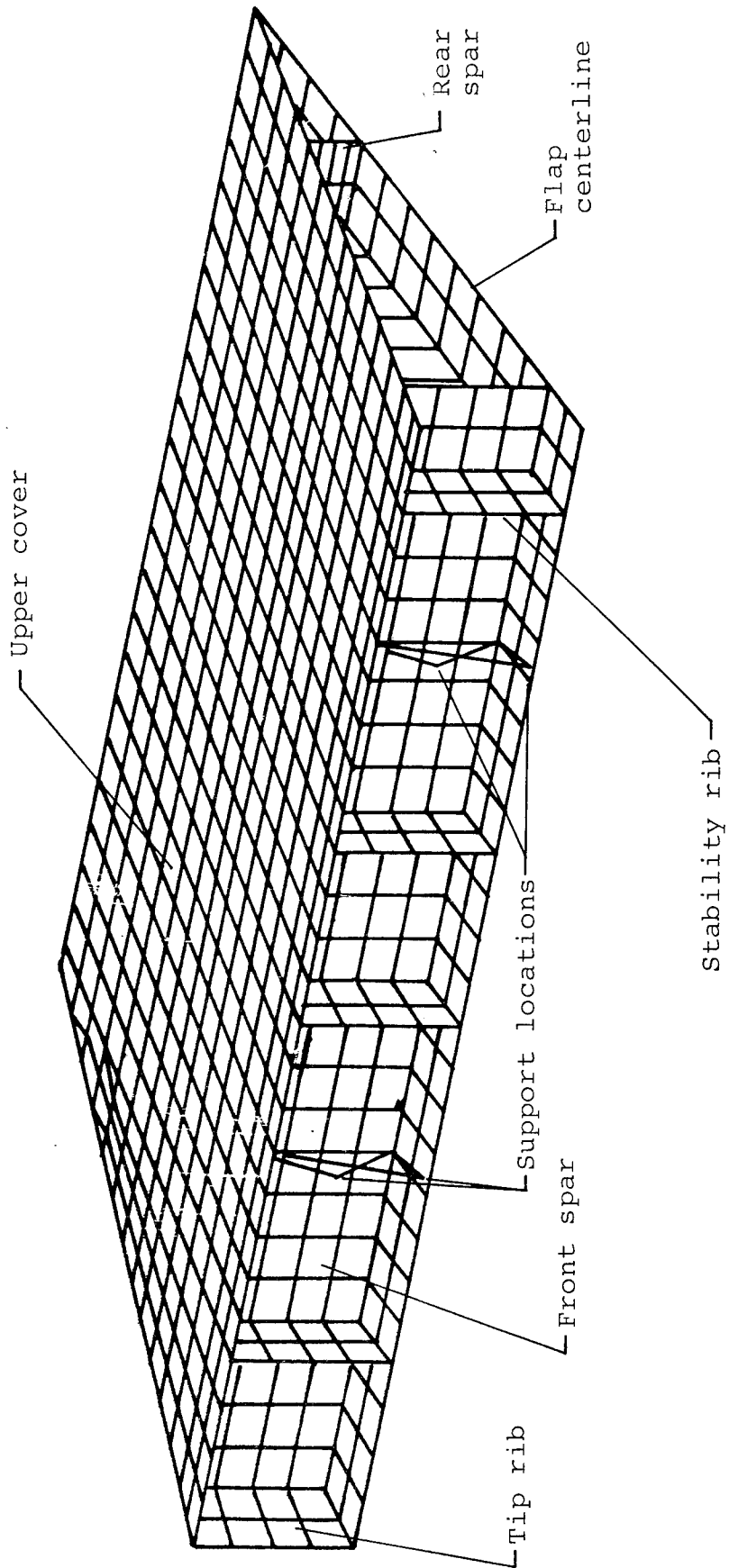Figure 9.2-5 Intracell buckling of thin face sheets.

Figure 9.2-6 – Refined finite element model of half body flap.

10.0 IN-HOUSE DESIGN AND TEST OF STRUCTURAL ELEMENTS

10.1 Stiffened and Sandwich Compression Panels
Robert R. McWithey and Charles J. Camarda

Development of full-scale, lightweight, advanced composite compression panels depends heavily on data generated by sub-element design, analysis, and test. The purpose of this research is to develop full scale Gr/PI stiffened and sandwich panels that are structurally efficient and satisfy temperature design requirements and local and general stability requirements for static compressive load conditions.

The stiffened panel program began in January 1978 and is scheduled to continue through 1980. The program is divided into three basic phases. The first phase, which is presently underway, will be an analytical investigation to optimize the four stiffened panel concepts shown in figure 10.1-1. The second phase of the program will include the fabrication and test of crippling specimens representative of the more structurally efficient designs. This phase of the program will determine the local buckling behavior of the full scale panel-designs. The third and final phase of the program will be the fabrication and test of full scale Gr/PI compression panels (approximately) 1 m by 1.5 m (3 ft by 5 ft).

During the next few months, optimum panel designs will be established for the stiffened panel concepts for a wide range of loads and temperatures up to 589K (600°F). In addition, Gr/PI crippling specimens will be fabricated under contract.

The compression sandwich panel program, which began in July 1977, will continue through 1979 and will parallel the stiffened panel program. Methods for bonding facesheets to honeycomb core using FM-34 and LaRC 13 tape and Br-34 and LaRC 13 cell edge adhesives are being investigated by a series of face-to-face tension tests in an effort to develop strong, lightweight, reliable, adhesive bonds. Material property data at cryogenic and elevated temperature will be obtained by sandwich beam flexure tests and compared with direct tension test and IITRI compression test results. A total of 80 face-to-face tension specimens and 40 flexure beam specimens, all fabricated with HTS/PMR-15 facesheets and HRH-327 glass/PI honeycomb core, will be tested at 117K, RT, and 589K (-250, RT, and 600°F).

To support the development of a design procedure for lightweight, advanced composite, honeycomb sandwich compression panels, an experimental program has been initiated to study local and general instability modes of failure. Local buckling specimens will be designed to fail in different modes (dimpling, wrinkling and crimping) and minimum weight full scale panels will be designed to fail in general buckling modes at various loads and temperatures. Both local and general buckling specimens will be fabricated under contract.
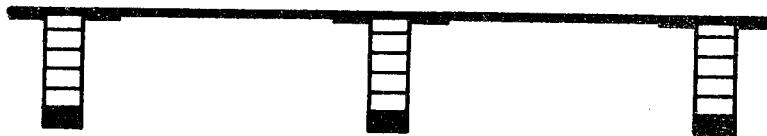
Hat stiffened skin

Hat stiffened honeycomb sandwich panel
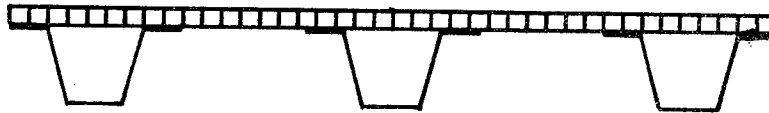
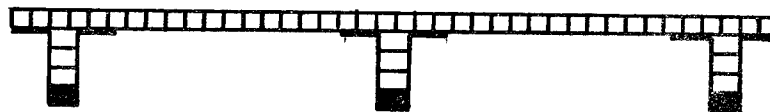Blade stiffened skin

Blade stiffened honeycomb sandwich panel

Figure 10.1-1 - Stiffened panel concepts.
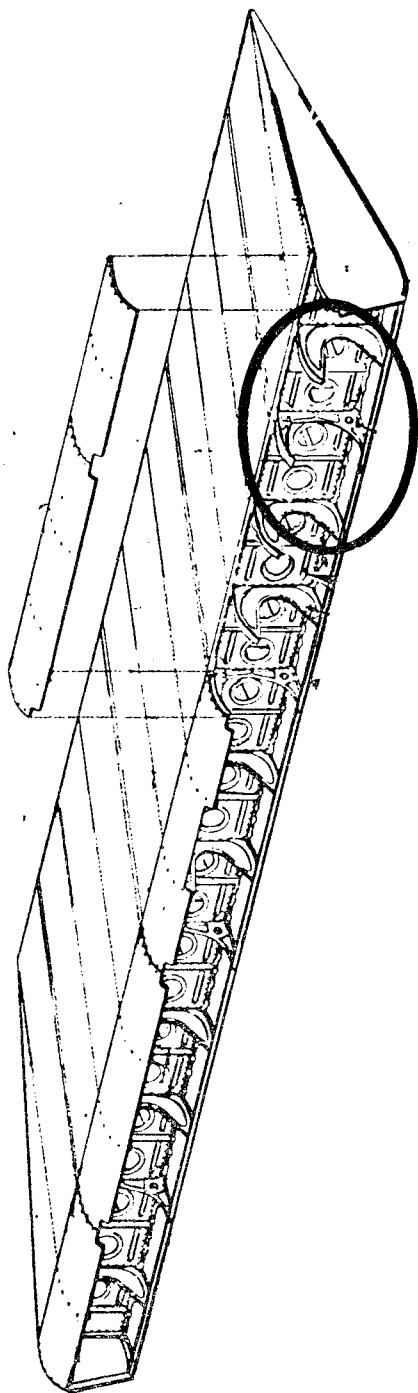
10.2 Shear Panels

Ramon Garcia

The use of composite materials to achieve efficient airframe structure requires the study of composite shear panels because they are a basic element in many airframe components. The objective of this program is to demonstrate design methods for graphite/polyimide shear panels for lightly loaded applications.

Several graphite/polyimide shear panels will be designed, fabricated and tested. Two basic types of panels will be considered, sandwich and skin-stringer. Both of these types will include solid panels as well as panels with access holes. Some panels will be designed for the low loads determined from a preliminary composite design for the space shuttle body flap and are expected to be minimum gage panels. Other panels will be designed for heavier loads to obtain experience with shear panels of other than minimum gage design.

One preliminary finite-element model of a test panel is shown in figure 10.2-1. The shear panel model comes from the previously mentioned design study of the space shuttle body flap. The panel is 1 m (40 inches) long with a rib spacing of 0.5 m (20 inches) and has four 13 cm (5-inch) diameter access holes. The spar caps and access holes will be reinforced. Other panel concepts will be examined.

The test method will be the "short beam" type of test. Tests will be conducted at both room and elevated temperatures. Test results will be compared with analytical predictions.

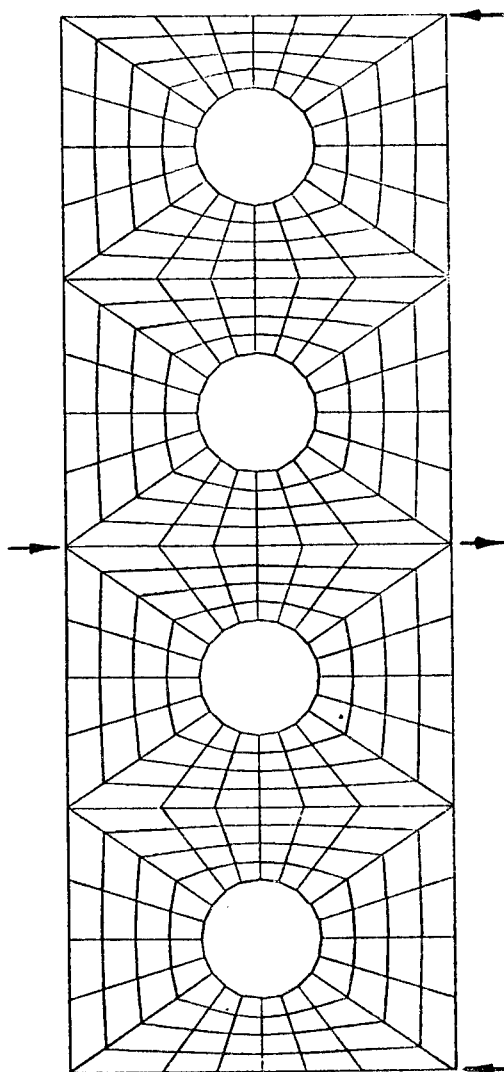SPACE SHUTTLE BODY FLAP

PRELIMINARY SHEAR PANEL MODEL

Figure 10.2-1 - Composite shear panel design.

10.3 Static Analysis and Tests of Bonded Joints

James Wayne Sawyer and Paul A. Cooper

Bonded composite lap joints are being investigated both analytically and experimentally to obtain a better understanding of joint behavior and to develop improved designs. The major thrust of the investigation is for 589K (600°F) temperature applications but initial work involves only ambient temperatures. The analytical work includes both approximate closed form analysis similar to that reported in reference 10.3-1 and linear, two dimensional, finite element analysis using the SPAR code (ref. 10.3-2). Experimental work is being conducted to verify the analysis results and to check the practicality of various concepts. The investigation presently includes single lap joints with both Gr/PI composite and titanium metallic adherends with a FM-34 adhesive.

Single lap joints have been shown by several investigators (see ref. 10.3-1, 10.3-3 and 10.3-4) to have high stress concentrations near the edges of the joint even for ambient temperatures. Concentrations of both the peel stress and the shear stress occur and may be considerably higher than the average stress in the joint. Since most composite materials have low interlaminar strength characteristics, high peel and shear adhesive stresses which are introduced into the first few plies of the composite adherends are especially detrimental to composite joints. Also the stress concentrations make it extremely difficult to obtain average mechanical material properties for the adhesive under realistic use conditions that are independent of the stress concentrations. Thus, any modifications to the joint design which would more evenly distribute the stresses would significantly increase the load carrying capability of the joint and aid in obtaining more realistic mechanical material properties for the adhesive. Two such concept modifications are presently being investigated.

The first concept consists of applying a clamping force along the edge of the joint perpendicular to the adhesive layer as shown in figure 10.3-1. The clamping force is concentrated near the edge of the joint so as to counteract the high peel stresses. In practical applications, the clamping force could be applied by small, light weight fasteners located near the edges of the joint. The clamped joint shown in figure 10.3-1 has been analyzed using the SPAR finite element computer code and the element mesh shown in figure 10.3-2. Note that the mesh size is reduced considerably near the joint edges and that the adherends and the adhesive layer are each divided into 5 element layers.

Some preliminary results obtained from the finite element analysis are given in figure 10.3-3 for 0.13 cm (0.05 in.) thick titanium adherends bonded with FM-34 adhesive. The peel stress nondimensionalized by the average applied normal stress in the adherend is shown along the length of the joint through the center of the first finite element mesh layer of the adherends. The solid line is for a basic single lap joint and the dashed line is for a single lap joint with an applied clamping force equal

to 1/4 of the applied joint load. For the basic lap joint, the maximum peel stress occurs at the edge of the joint and is slightly higher than the applied normal stress in the adherend. The clamping force reduces the maximum peel stress by over 35 percent without any significant increases in the other stresses in the joint. In fact the clamping force also slightly reduces (by 10 percent) the maximum shear stress in the joint. Thus for a joint where the peel stress is critical, significant improvements in the load carrying capability of the joint may be obtained by some clamping of the joint edges.

Preliminary experimental results have been obtained on four standard ASTM 1.3 cm (1/2 in.) overlap specimens with 0.3 cm (1/8 in) thick Gr/PI adherends and FM-34 adhesive (ref. 10.3-5). A clamping force approximately 1/8 of the maximum load capability of an identical unclamped specimen was applied at the edges of the joint using a c-clamp. The results are shown in figure 10.3-4 compared with results from identical unclamped specimens. The clamping force results in approximately a 70 percent increase in the total load carrying capability of the joint. However, the adherend material had relatively low interlaminar strength characteristics which resulted in failure in the first few layers of the adherend in each case. For adherend materials with higher interlaminar strength characteristics, clamping the joint edges may result in less improvement in the load carrying capability of the joint. Note that the experimental and analytical results were obtained using different adherend materials and thicknesses and clamping forces but show similar trends.

The second concept being investigated consists of pre-forming the adherends (ref. 10.3-6) outside the overlap area so as to minimize the bending caused by the asymmetric joint. A typical joint with pre-formed adherends is shown in figure 10.3-5. Photoelastic analyses and the SPAR finite element computer program are both being used to study joints with pre-formed adherends. A finite element mesh similar to that used for the basic lap joint (fig. 10.3-2) was used in the analysis.

Comparisons between the photoelastic fringe patterns for geometric simulations of standard and pre-formed lap joints can be made in the photographs of figure 10.3-6. The fringe patterns indicate that pre-forming the adherends results in a considerably more uniform stress distribution and a substantial reduction in the stress concentrations in the joint. Similar results are shown by the preliminary analysis results given in figure 10.3-7 where nondimensional peel and shear stress distributions are shown along the length of the joint. The peel stress distributions (fig. 10.3-7 (a)) are for the center of the first layer of the adherend and are nondimensionalized with respect to the average applied normal stress in the adherend. The shear stress distributions (fig. 10.3-7 (b)) are for the center of the adhesive layer and are nondimensionalized with respect to the average shear stress. The solid lines are for a standard single lap joint with a straight adherend and the dashed lines are for pre-formed adherends with bend angles θ of 3, 5, 8 and 10°. Both the maximum peel stress and shear stress are reduced by

increasing the bend angle. For the particular joint investigated, a bend angle of 8° virtually eliminates the peel and shear stress concentrations.

Both the clamped joint and the pre-formed adherend concepts will be investigated further. Additional work will include an analytical parametric study using a closed form approximate solution for the pre-formed adherend concept, an experimental program to investigate each concept more thoroughly, and an extension of the theoretical and experimental program to include temperatures up to 589K (600°F).

References

10.3-1.   Reissner, E.; and Goland, M.:   The Stresses in Cemented Joints,
          Journal of Applied Mechanics, March 1944, pp. A17-A27.

10.3-2.   Whetstone, W. D.; SPAR Structural Analysis System Reference Manual,
          NASA CR 145098, Vol. I, February, 1977.

10.3-3.   Volkersen, O.:   Die Nietrattverteilung in zugbeanspruchten Nieverbindungen
          mit konstanten Laschenquerschnitten, Luffart-forschung, Vol. 15,
          1938, pp. 41-47.

10.3-4.   Hart-Smith, L. J.:   Adhesive-Bonded Single-Lap Joints.   NASA-CR
          112236, January, 1973.

10.3-5.   ASTM Standard D 1002-72, Strength Properties of Adhesives in Shear
          by Tension Loading.

10.3-6.   DasGupta, S.; and Sharma, S. P.:   Stresses in an Adhesive Lap Joint,
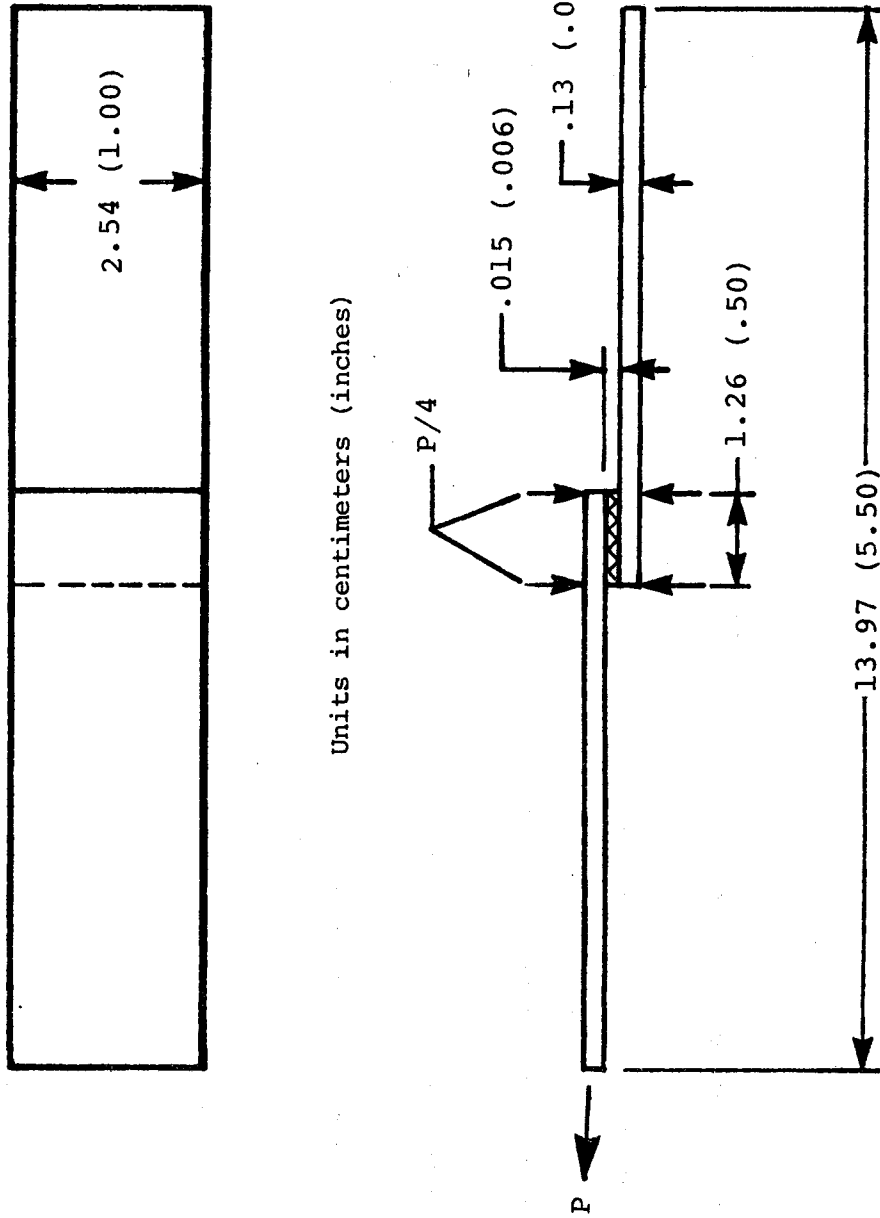   ASTM Publication August, 1976.

Units in centimeters (inches)

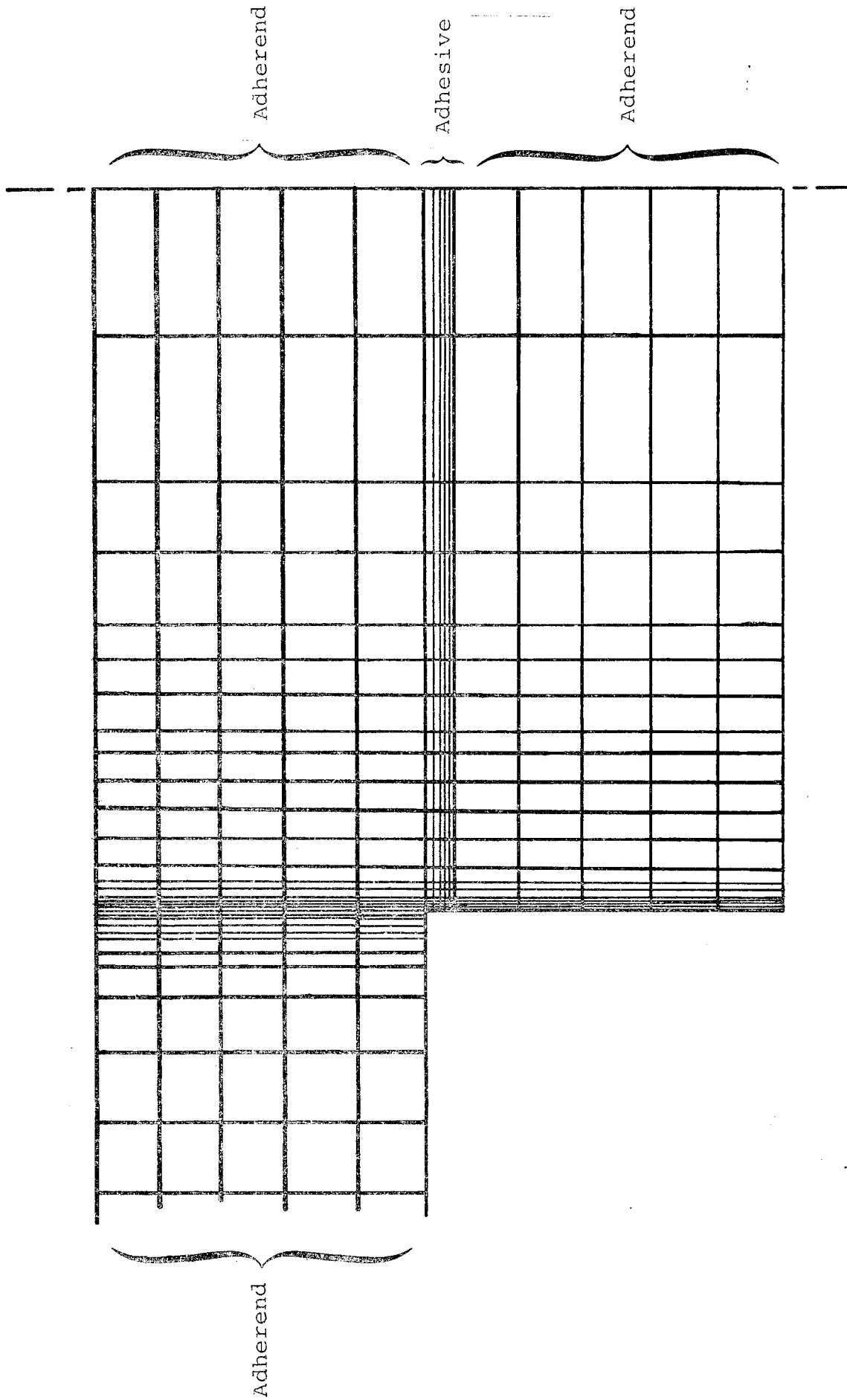Figure 10.3-1 – Typical lap joint with edge clamping.
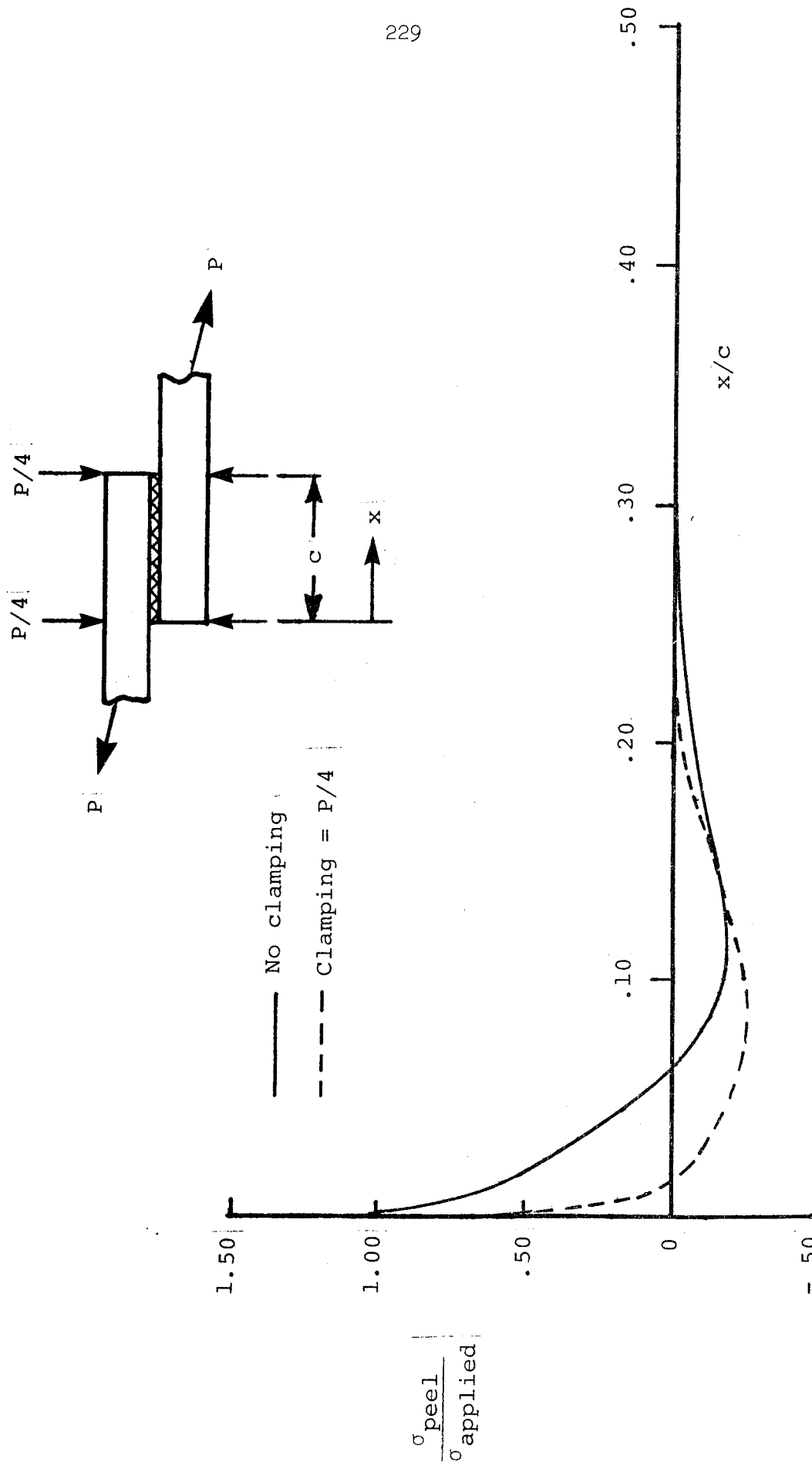
Figure 10.3-2 – SPAR finite element mesh used for clamped joints.

Figure 10.3-3 - Effect of edge clamping on peel stress distribution in simple lap joint.

Specimen no.	Failure load - N (lbf)	
	No clamping	Clamping = P/8
1	4400 (990)	5960 (1340)
2	4250 (955)	7960 (1790)
3	3960 (890)	7470 (1680)
4	3960 (890)	6760 (1520)

Figure 10.3-4 - Effects of clamping on failure loads for G/PI-FM 34 bonded single lap joints.

2.54 (1.00)
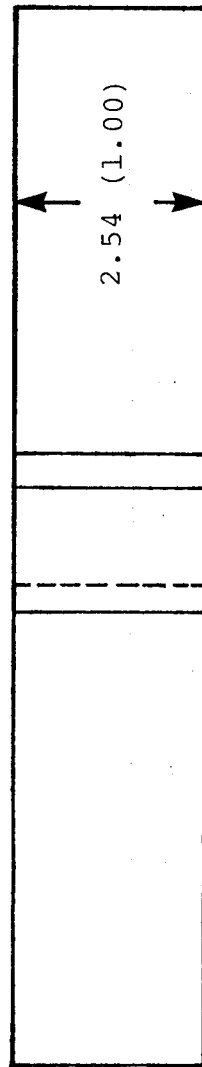
Dimensions in centimeters (inches)

θ

.32 (.12)

1.26 (.50)

.13 (.05)

13.97 (5.50)

.015 (.006)

P

P
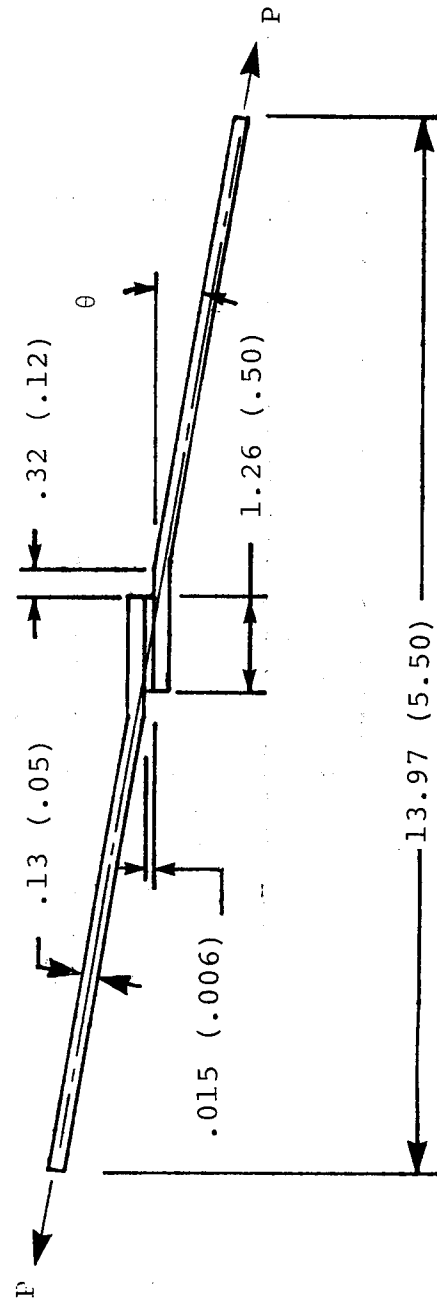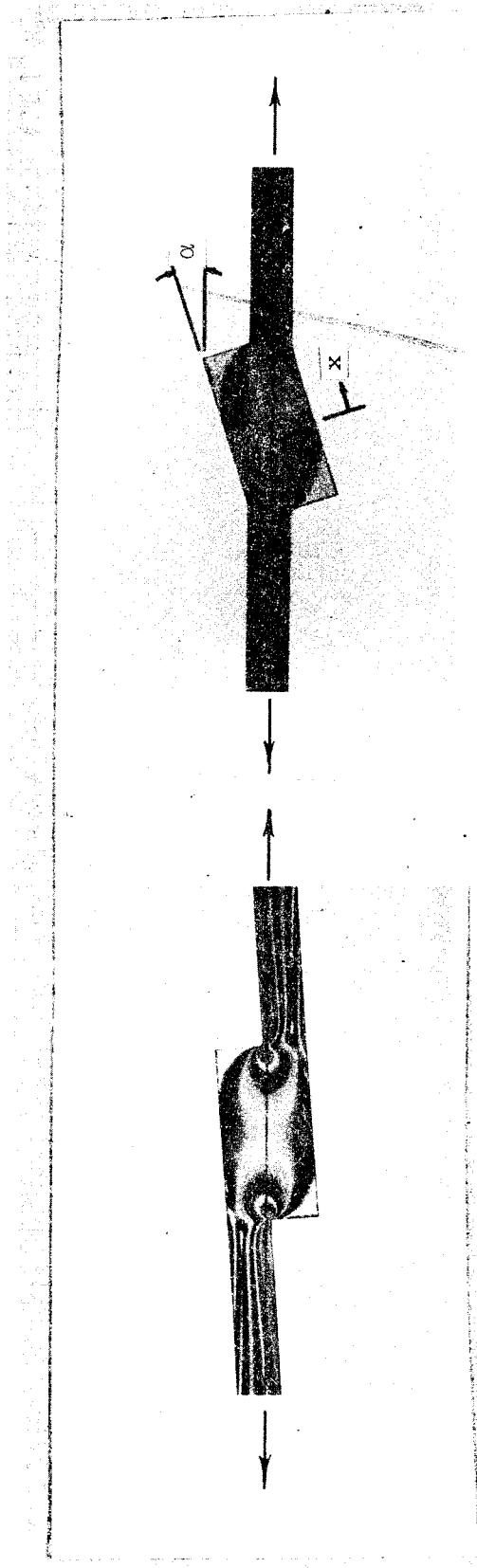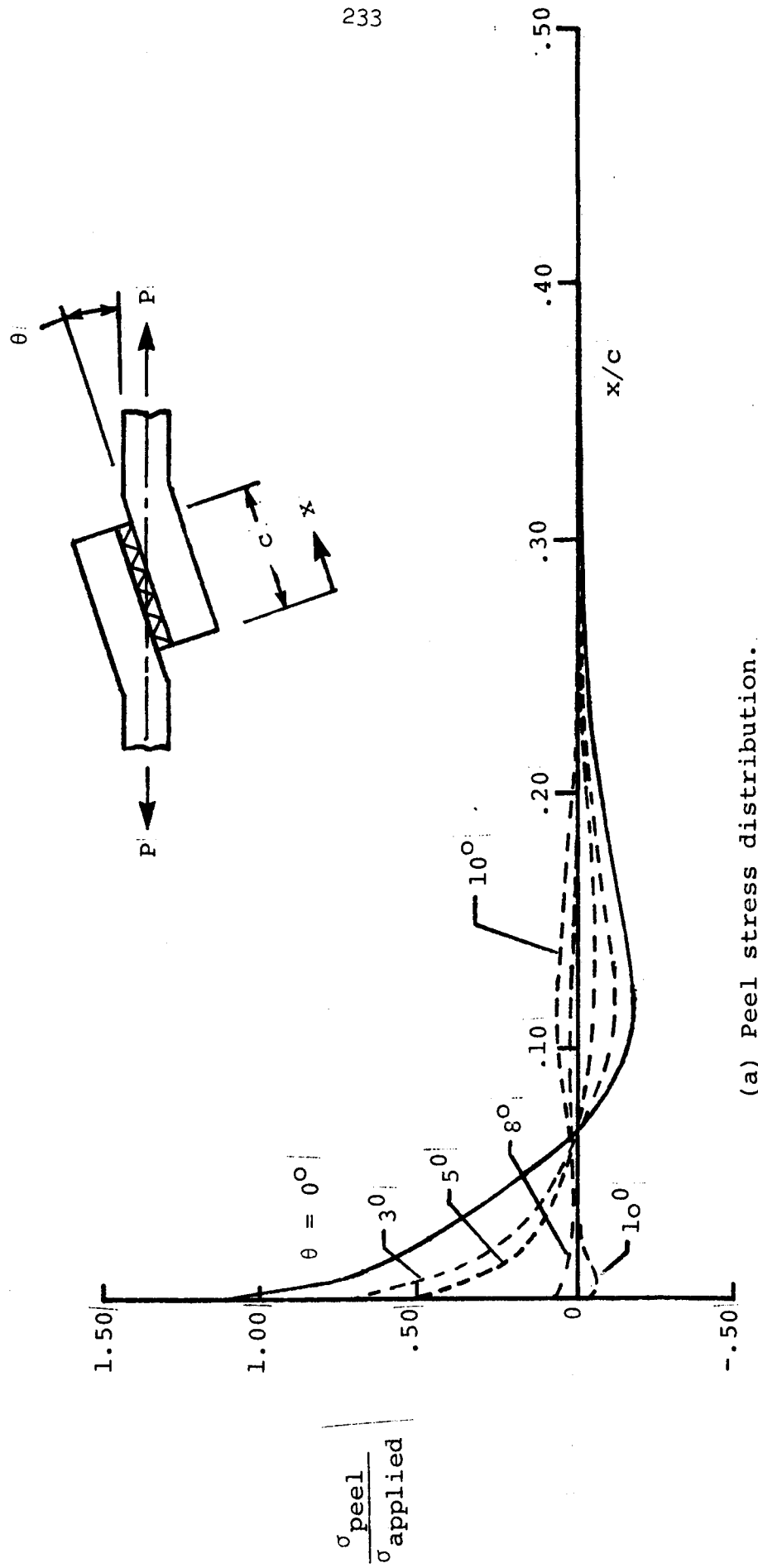
Figure 10.3-5 - Typical lap joint with pre-formed adherends.

Standard lap joint

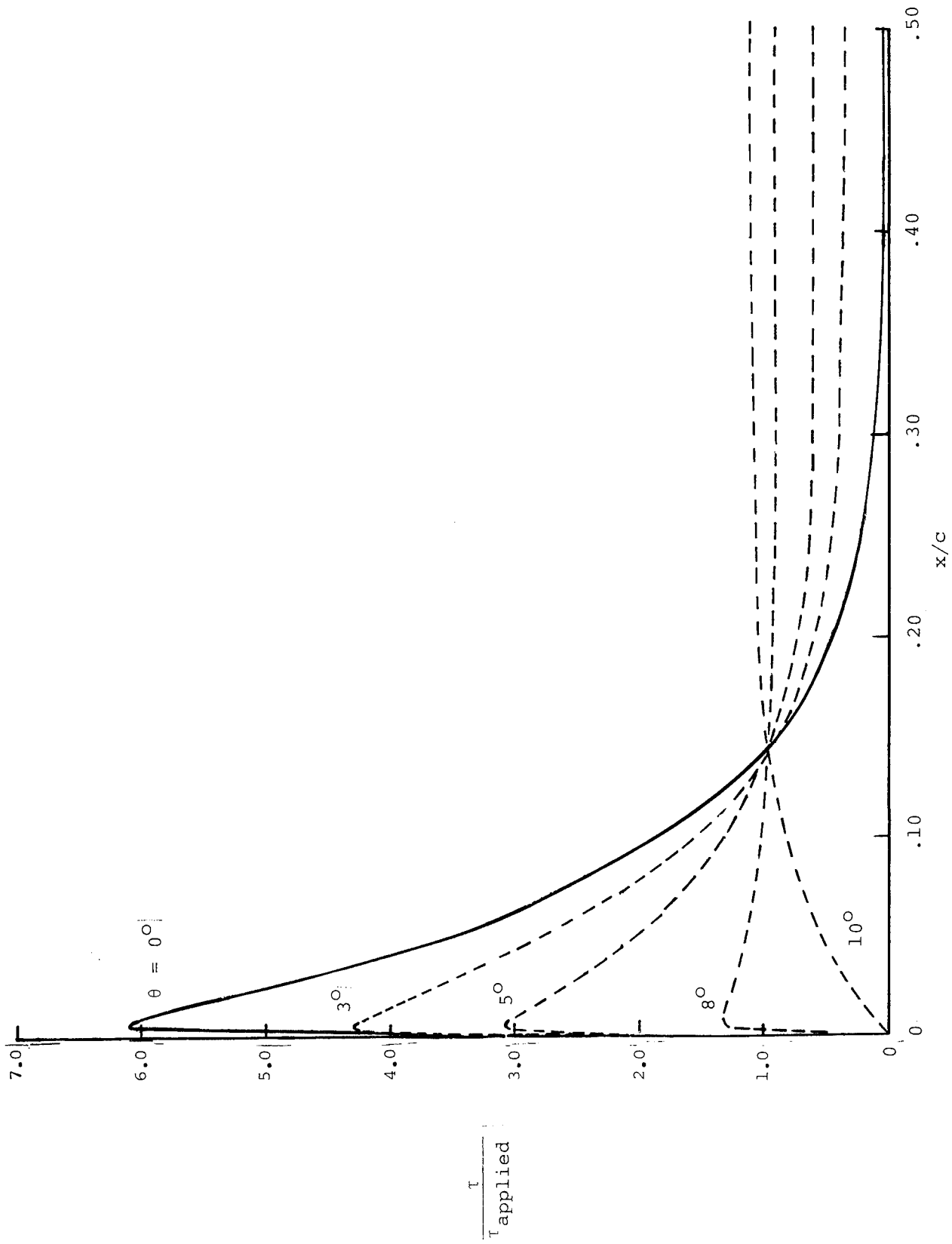Pre-formed lap joint

Figure 10.3-6 - Photoelastic fringe patterns for standard and pre-formed lap joints.

(a) Peel stress distribution.

Figure 10.3-7 - Effects of pre-formed adherends on stress distributions in lap joint.

(b) Shear stress distribution.

Figure 10.3-7 – Concluded.

11.0 CONTRACTUAL STUDY OF ATTACHMENTS AND JOINTS

P. A. Cooper, J. W. Sawyer, and J. H. Crews, Jr.

Because of the limited strain levels supported by organic matrix composite structures, load transfer in such structures joined by mechanical fastening or adhesive bonding presents a more difficult design problem than the joining of isotropic metallic structures, especially when large temperature differences occur during cure of the composite material and during its service life. Large stress concentrations, which theoretically occur in joined metallic structures, but are in reality reduced due to local plastic deformation, do in fact exist in composite structures because of the low ductility of the composite material system. Thus, failure modes of mechanically fastened and adhesively bonded composite structures are more complex than those of metallic structures.

Contractual activity will be carried out to extend the technology in joint and attachment design which currently exists for epoxy-matrix composites to include polyimide matrix composites so that proper data are available to build graphite/polyimide (Gr/PI) lightly loaded flight components. The objectives of this contract are twofold: first, to identify and evaluate design concepts for specific joining applications of built-up attachments which can be used at rib-skin and spar-skin interfaces; secondly, to explore advanced concepts for joining simple composite-to-composite and composite-to-metal structural elements, identify the fundamental parameters controlling the static strength characteristics of such joints, and compile data for design, manufacture and test of efficient structural joints using the Gr/PI material system.

The major technical activities will consist of : (1) design and static and fatigue tests of specific built-up attachments and (2) evaluation of standard and advanced bonded joint concepts.

Attachments

The purpose of this activity is the identification and evaluation through analysis and test of specific types of bonded and bolted Gr/PI composite attachments suitable for use in lightly loaded sandwich structure. The primary objective of the research is the development of efficient composite attachment design concepts which operate reliably at temperatures in the 117 to 589°K (-250 to 600°F) temperature range. The specific attachment types of interest are shown in figures 11.0-1 - 11.0-4.

At the conclusion of this activity, the contractor will have established the design and checked its acceptability through a series of static and fatigue tests of both a primarily bonded and a primarily bolted attachment concept for each of four types of attachments, a total of eight concepts in all. A bonded attachment is defined as one which transfers its major loads across an adhesively bonded surface. A co-cured connection is classified as a bonded connection. A bolted attachment, while it might have some

secondarily bonded or co-cured components, transfers its major loads by means of mechanical fasteners.

The contractor will initially design and analyze several concepts for each bonded and each bolted attachment type. He will select two of the most promising bonded and two of the most promising bolted concepts for each attachment type. Concurrently with this analytical study, the contractor will design and perform a series of laboratory tests to determine the adequacy of the material processing and fabrication procedures, determine the material allowables, and evaluate bonding and fastener strengths at elevated temperatures.

Upon selection and approval of the two bonded and two bolted concepts for each type of attachment, the contractor will fabricate, inspect, and test under static load to failure attachments based on each of the sixteen concepts. The static test will be configured to give sufficient information for a logical comparison of the two bonded and two bolted concepts for each type of attachment. On the basis of test results and other engineering considerations such as ease and practicality of fabrication and projected fatigue behavior, the contractor will select the eight most promising bonded and bolted concepts.

The eight concepts selected will be fabricated on a scaled-up manufacturing basis to assure that reliable attachments can be fabricated for full-scale components. A series of static tests to failure will be performed on specimens cut from the scaled-up attachment to verify the validity of the manufacturing process. The remaining specimens will be thermally conditioned and tested in a series of static and fatigue tests to evaluate the structural integrity of the eight concepts. Test results will be compared with analytical results used to establish the designs and an evaluation of design procedures will be made. At the conclusion of the task, sufficient information will be available for the contractor to judge the relative efficiency of bonded and bolted concepts for each attachment type.

Standard Bonded Joints

The purpose of this activity is the establishment of a limited data base describing the influence of variations in basic design parameters on the static strength and failure modes of G/PI bonded composite joints at elevated temperatures. The primary objectives of this research are to provide data useful for evaluation of standard bonded joint concepts and design procedures, to provide the designer with increased confidence in the use of bonded high-performance composite structures, and to evaluate possible modifications to the standard joint concepts for improved efficiency.

     To accomplish these objectives, the contractor will design, fabricate,
and statically test several classes of composite-to-composite and composite-
to-metallic bonded joints including single-and-double-lap joints, scarf
joints, and step-lap joints. Test parameters will include lap length,
adhesive thickness, and adherend stiffness and ply stacking sequence at
room and elevated temperatures. The contractor and NASA will select advanced
lap joint concepts which show promise of improving joint efficiency.
Possible concepts are performed adherends, mixed adhesive systems, and lap
edge clamping. These concepts will be added to the static strength test
program and their performance compared with the performance of the standard joints.
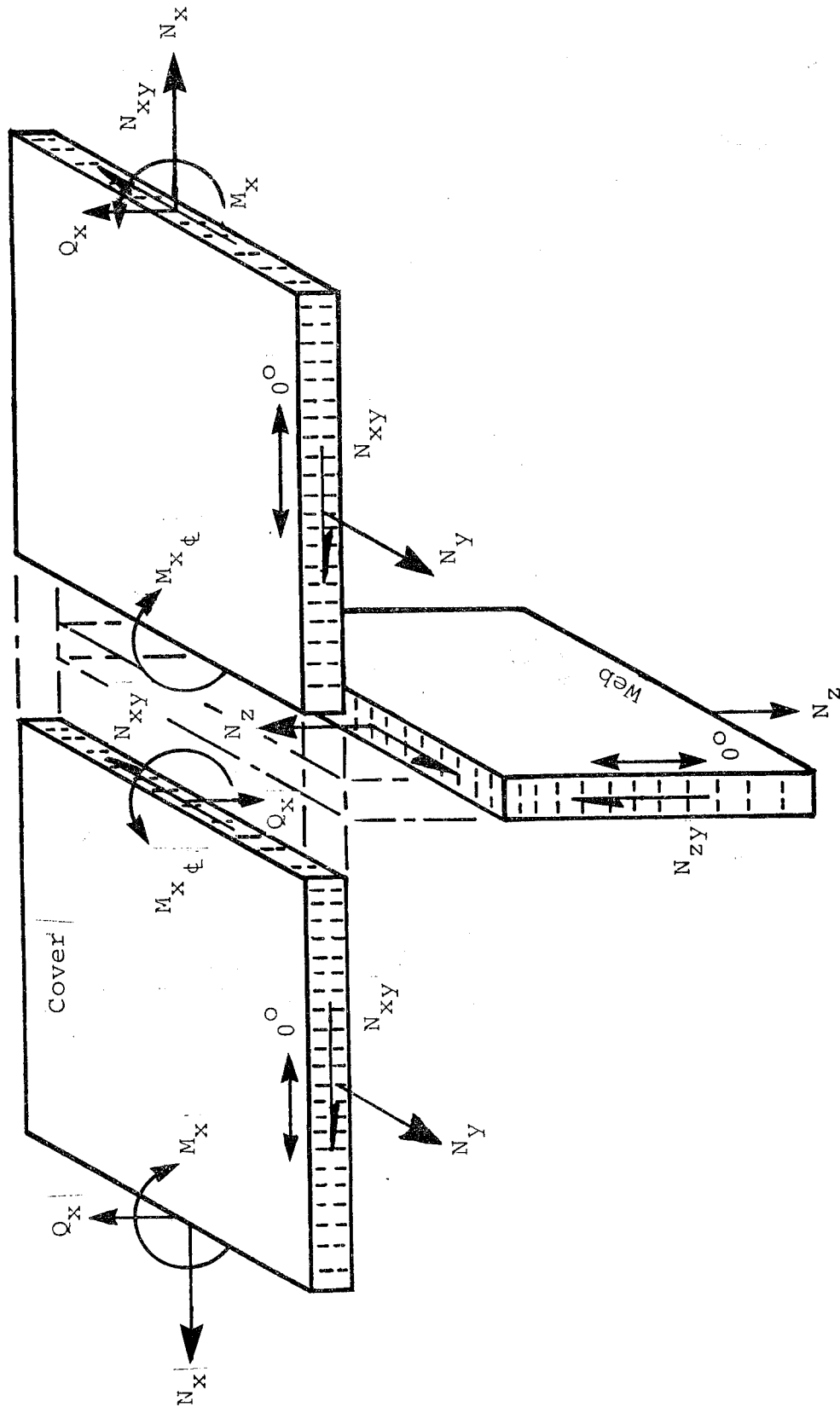
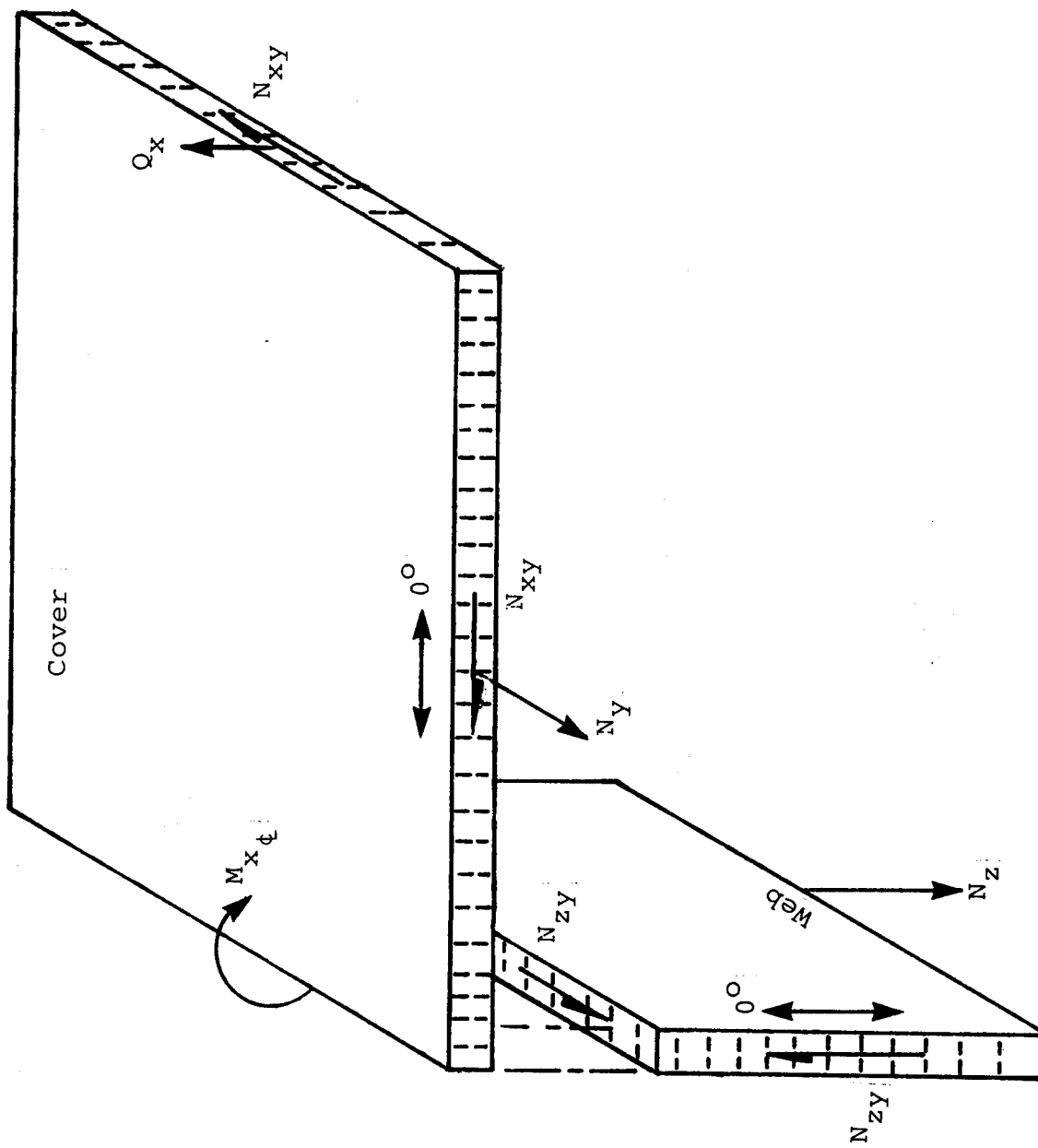Figure 11.0-1 - Attachment type no. 1.
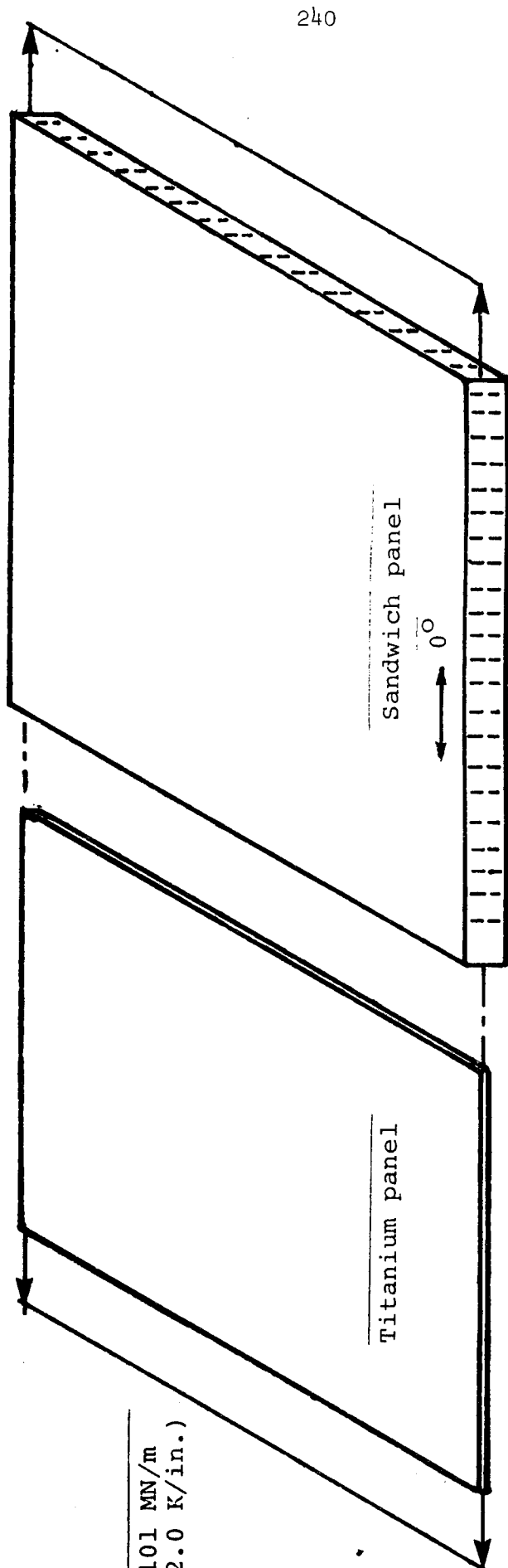
Figure 11.0-2 - Attachment type no. 2.

2.101 MN/m
(12.0 K/in.)

Titanium panel

Sandwich panel

0°

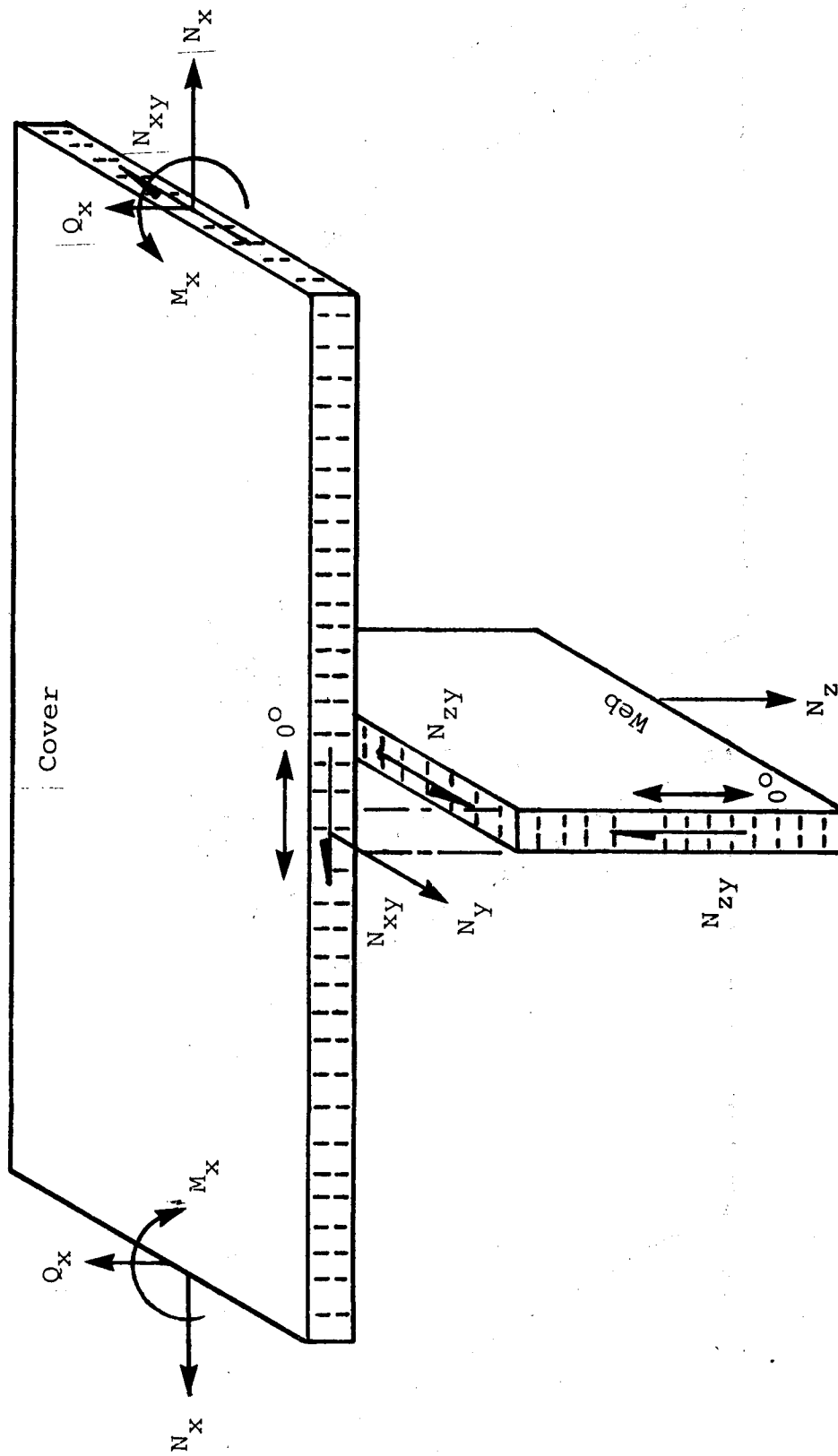Figure 11.0-3 - Attachment type no. 3.

Figure 11.0-4 - Attachment type no. 4.

12.0   ADVANCED TECHNOLOGY DEVELOPMENT

12.1   NR-150 Adhesive Development

T. L. St. Clair

The objective of this contractual program (ref. 12.1-1) was to develop NR-150B2 polyimide resin into an adhesive for bonding high temperature graphite/polymer matrix composites. The adhesive was to be designed to have acceptable durability for 125-500 hours at 589K (600°F) in air and a significant improvement in processibility compared to standard high temperature aromatic condensation polyimide adhesives. Lap shear strengths of 20 MPa (3000 psi) at room temperature and 14 MPa (2000 psi) at 589K (600°F) were also goals.

The investigation included three tasks: (1) evaluating variations in the monomer solution stoichiometry as it affects the flow and glass transition temperature (T_g) of the polyimide resin derived from the solution, (2) optimizing the bonding conditions within the limits obtainable in commercial production autoclaves, and (3) demonstrating the capability of the newly defined adhesive composition and process using titanium adherends. The utility of the adhesive was then demonstrated by: (1) exposing lap shear samples prepared from graphite fiber/NR-150B2 adherends to four different environments, (2) preparing and evaluating wide area bonds [greater than 25 cm^2 (10 $in.^2$)] and face sheet/honeycomb core flatwise tensile specimens, and (3) evaluating adhesive crack propagation at 589K (600°F).

During task 1, it was found that improved resin flow at significantly lower adhesive prepreg volatile levels, which would lead to low void bond lines, could only be obtained using an adhesive resin which had a T_g well below 589K and, therefore, was unsuitable for use at that temperature.

In task 2, no combination of autoclave bonding and free-standing postcure conditions could be found which produced acceptable lap shear bonds at both R.T. and 589K using NR-150 polyimide adhesive systems based on N-methylpyrrolidone (NMP) as the solvent. However, replacement of the NMP with diglyme (the dimethyl ether of diethylene glycol) in the adhesive system resulted in a dramatic improvement in processibility of the adhesive and the attainment of acceptable bond strengths at both R.T. and 589K using the following bonding cycle and prepreg:

Bonding cycle: R.T. to 589K at 2.8° K/min (5°F/min) under full vacuum, 1.4 MPa (200 psi), then 1/2 hour bonding, full vacuum, 1.4 MPa at 589K and 1 hour postcure, full vacuum, zero pressure at 589K.

Prepreg: 0.3 mm (13 mils) thick, 8-9% volatiles, 112-38 Style E glass scrim with a I-621 finish.

This newly developed NR-150 adhesive system was used in task 3. Lap shear samples, prepared from composite adherends, were exposed to the following environments: 500 hours in 589K air (figure 12.1-1); 35 days

in 322 K (120°F), 95% RH (figure 12.1-2); 34 days immersed in JP-4 jet fuel at R.T. (figure 12.1-3); and 34 days immersed in methyl ethyl ketone (MEK) at R.T. These studies indicated that this new adhesive bond had excellent resistance to these environments.

Evaluation of bonding wide areas using this adhesive (fig. 12.1-4) indicated that acceptable bond strengths could only be obtained using abnormally long cure cycles in order to allow diffusion of the volatiles out of the bond line.

Flatwise tensile specimens prepared using composite face sheets and titanium honeycomb core (fig. 12.1-5) had low strengths because of poor techniques in curing the primer coating on the honeycomb cell edge. More effort will be required to produce honeycomb sandwich panels with the flatwise tensile strength levels expected from this new adhesive.

A wedge-type crack propagation test at 589 K using 3 mm (1/8") thick unidirectional graphite fiber/NR-150B2 adherends confirmed the excellent toughness and stability of the new NR-150 adhesive (fig. 12.1-6).

The results of these these tests indicate that the newly developed experimental adhesive has potential as a high temperature adhesive for use in the harsh environments to which jet engine parts, high performance military aircraft, and space vehicles are exposed.

The problem area yet to be overcome is that of large-area bonding. Low strengths in the center of these bonds is a definite drawback to this adhesive as well as other commercially available condensation-type adhesives.

Reference

12.1-1. Blatz, Philip S.: NR150B2 Adhesive Development. NASA CR 3017, April 1978.

Lap Shear Strength*

Exposure Hours	Test Temp. K(°F)	Lap Shear Strength MPa (psi)					Standard Deviation	Decrease in Strength %	Sample Weight Loss Average %
		Sample 1	Sample 2	Sample 3	Sample 4	Average			
None (Control)	R.T.	11.82 (1714)	16.67 (2418)	16.36 (2373)	17.74 (2573)	15.62 (2270)	2.62 (380)		
125	R.T.	20.18 (2926)	10.74 (1557)	17.67 (2563)	16.28 (2361)	16.22 (2352)	4.00 (580)	NIL	0.26
250	R.T.	12.19 (1768)	16.55 (2401)	21.08 (3058)	13.91 (2017)	15.93 (2311)	3.87 (561)	NIL	0.42
None (Control)	589(600)	12.60 (1828)	17.67 (2563)	14.50 (2103)	14.94 (2167)	14.93 (2166)	2.09 (303)		
125	589(600)	14.55 (2110)	10.70 (1552)	18.35 (2661)	15.99 (2319)	14.90 (2160)	5.27 (265)	NIL	0.30
250	589(600)	9.00 (1306)	13.25 (1921)	16.47 (2389)	14.45 (2095)	13.29 (1928)	3.28 (475)	11.0	0.54
None (Control)	R.T.	19.79 (2870)	9.54 (1383)	16.22 (2353)		15.21 (2206)	5.21 (755)		
500	R.T.	15.99 (2319)	14.34 (2080)	17.02 (2469)	8.14 (1180)	13.87 (2012)	3.98 (577)	9.0	0.97
500	561(550)	13.22 (1918)	15.81 (2293)	16.75 (2430)	7.30 (1059)	13.27 (1925)	4.25 (617)		0.71
None (Control)	589(600)	16.24 (2356)	16.84 (2443)	17.24 (2500)	16.73 (2426)	16.76 (2431)	0.41 (59)		
500	589(600)	14.27 (2070)	14.04 (2036)	17.24 (2501)	10.07 (1461)	13.91 (2017)	2.74 (427)	17.0	0.98

* All samples failed within the composite adherend.

Composite used: 3.175 mm (1/8") thick "Modmor" II/NR-150-150B2 unidirectional laminates.

Adhesive prepreg used: 0.38 mm (15 mils) thick containing 11.5% volatiles, 28.5% cured resin solids, 50% aluminum powder, 11% glass scrim cloth.

Samples exposed at least 15 minutes before testing at 589K.

Figure 12.1-1 – Lap shear strength of composite samples bonded with NR-150 adhesive and exposed to 589K (600°F) in air.

| | | Lap Shear Strength MPa (psi) | | | | | | | Sample Weight Increase | Sample Thickness Increase |
Exposure Conditions	Test Temp.	Sample 1	Sample 2	Sample 3	Sample 4	Average	Standard Deviation	Decrease in Strength %	Ave. %	Ave. %
R.T. Air Control	R.T.	17.83 (2586)	18.14 (2631)	17.70 (2567)	16.98 (2462)	17.66 (2562)	0.49 (71)			
35 days at 22 K (120°F) 95% R.H.	R.T.	12.20 (1770)	16.40 (2379)	12.19 (1768)	13.25 (1921)	13.51 (1959)	1.99 (289)	24.0	2.09	NIL
R.T. Air Control	589(600)	17.58 (2551)	16.79 (2435)	16.80 (2437)	17.72 (2570)	17.22 (2498)	.43 (91)			
35 days at 22 K (120°F) 95% R.H.	589(600)	8.15* (1182)	9.09* (1319)	11.55 (1675)	11.75* (1704)	10.14 (1470)	1.55 (225)	40.0	2.00	NIL

*Samples failed cohesively within adhesive bond line.

All other samples failed within the composite adherend.

Samples tested at 589 K (600°F) were conditioned for 7 mins. before test was started.

Figure 12.1-2 – Lap shear strength of composite samples bonded with NR-150 adhesive and exposed to 95% RH for 35 days at 120°F.

Exposure Conditions	Test Temp.	Lap Shear Strength* MPa (psi)						Decrease in Strength %	Sample Weight Increase Ave. %	Sample Thickness Increase Ave. %
		Sample 1	Sample 2	Sample 3	Sample 4	Average	Standard Deviation			
R.T. Air Control	R.T.	12.19 (1768)	19.37 (2810)	24.44 (3545)	20.04 (2907)	18.98 (2752)	5.07 (736)			
34 days in 24 jet fuel at R.T.	R.T.	16.31 (2365)	20.17 (2926)	20.25 (2937)	17.22 (2497)	18.49 (2681)	2.03 (294)	NIL	5.11	0.6
R.T. Air Control	589(600)	13.71 (1988)	15.26 (2213)	14.65 (2125)	16.80 (2437)	15.10 (2191)	1.30 (188)			
34 days in 24 jet fuel at R.T.	589(600)	NOT		TESTED						

* All failures occurred within composite adherends.

Figure 12.1-3 - Lap shear strength of composite samples bonded with NR-150 adhesive and exposed to JP-4 jet fuel.

Autoclave Bonding Temperature	Position of Lap Shear Sample in Wide Area Bond*	Test Temperature K (°F)	Lap Shear Strength MPa (psi)	Failure Mode	Bond Line Tg K (°F)
589 K (600°F)	Outside (50.8 mm from edge)	R.T.	11.10(1610)	Within Adhesive	
	Next to Center	R.T.	13.10(1901)	Within Composite	
	Center	R.T.	4.34(630)	Within Adhesive	581 (586)
	Next to Outside	589 (600)	1.68 (244)	Within Adhesive	
	Outside (50.8 mm from edge)	589 (600)	7.18(1042)	Within Adhesive	
616 K (650°F)	Outside (50.8 mm from edge)	R.T.	9.93(1440)	Within Composite	
	Next to Center	R.T.	10.66(1546)	Within Composite	
	Center	R.T.	13.19(1913)	Within Composite	558 (545)
	Next to Outside	589 (600)	12.17(1765)	Within Adhesive	
	Next to Outside (76.2 mm from edge)	589 (600)	13.75(1994)	Within Adhesive	

* Wide area bonds, 0.254 m x 0.254 m (10" x 10"), were made from composite adherends and experimental NR-150 diglyme adhesive solution and bonded in an autoclave.

Figure 12.1-4 - Lap shear strength of samples cut from wide area bonds.

Sample History	Test Temperature K (°F)	Flatwise Tensile Strength MPa (psi)	Failure Mode
As Prepared	R.T.	.74 (108)	Adhesive between face sheet and honeycomb cell edge
After 1800 KS (500 hours) exposure to 589 K (600°F) air	R.T.	.93 (135)	Cohesive within composite face sheet
As Prepared	589 (600)	.19 (27)	Cohesive within composite face sheet
After 1800 KS (500 hours) exposure to 589 K (600°F) air	589 (600)	.35 (51)	Adhesive between face sheet and honeycomb cell edge

Figure 12.1-5 – Flatwise tensile strength of composite face sheet/titanium honeycomb sandwich panels.
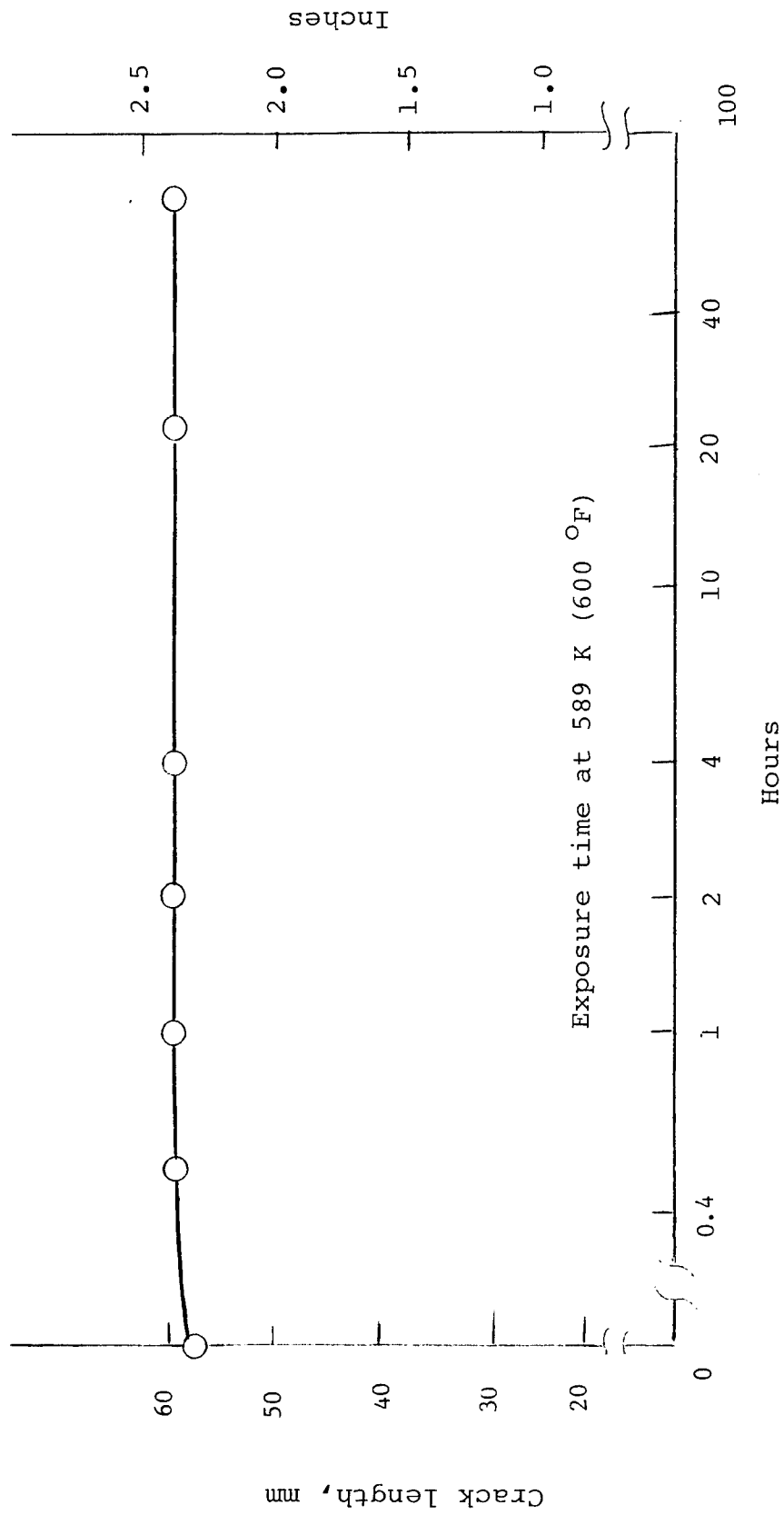
Figure 12.1-6 — Evaluation of adhesive crack propagation at 589 K (600 °F) using the wedge crack propagation test.

12.2 LARC-13 Adhesive Development

T. L. St. Clair

The CASTS project needs an adhesive which can withstand 125-500 hours at 589K (600°F) in air with lap shear strength goals of 20 MPa (3000 psi) at room temperature and 14 MPa (2000 psi) at 589K both before and after aging at 589K. Commercially available high-temperature adhesives come close to meeting this goal, but volatile evolution during cure precludes their use in large-area bonding. LARC-13 is very low in volatiles, and therefore shows promise for large-area bonding. Physical and chemical changes to the existing resin as well as processing studies could lead to an improved version of the resin.

The present version of the Langley-developed LARC-13 has been successfully used to bond high temperature [533-589K (500-600°F)] graphite/polyimide composites and some metals in various NASA in-house programs. This adhesive is an addition-type polyimide with nadic end caps which contains 30 percent by weight aluminum powder.

LARC-13 is an oligomeric amic-acid after coating on a glass scrim to 450K (350°F). The resulting adhesive cures without the evolution of volatiles through the nadic end groups. Lap shear strengths for titanium-titanium bonds are 21-28 MPa (3000-4000 psi) at room temperature and 8-10 MPa (1100-1500 psi) at 589K. The 589K strengths increase with aging at the test temperature due to an increase in glass transition temperature of the system. A maximum strength is attained after approximately fifty hours with a gradual loss in strength occurring with subsequent aging at 589K.

A one year contract will be awarded to alter the LARC-13 formulation physically and/or chemically in order to optimize for lap shear strength at both room temperature and 589K before and after aging. Physical modifications may involve changes in type and quantity of fillers and in solvents. Chemical modifications may include partial monomer substitution for 3,3'-methylenedianiline with another aromatic diamine in order to increase the glass transition temperature (T_g), the use of the esters of benzophenone tetracarboxylic dianhydride (BTDA) and nadic anhydride (NA) in a monomeric mixture approach, or variations in stoichiometry. Thermo-mechanical analyses will be determined on both cured neat resin and bonded adherends. Other resin characterization techniques such as infra-red, thermogravimetric analysis and differential scanning calorimetry will be employed.

A processing study will be undertaken to optimize the LARC-13 system for use in titanium-titanium and composite-composite bonding. The study will include optimization of adhesive prepreg preparation (volatile content, carrier, percent resin, "B"-stage) as well as optimization of bonding conditions.

A surface treatment compatible with LARC-13 will be chosen for both titanium and composite. This treatment may be one in common usage (Pasa-Jell, phosphate-fluoride) or a proprietary anodizing procedure.

Standard lap shear samples (composite-composite and titanium-titanium) will be fabricated (4 specimens for each test condition) and tested according to ASTM D-1002. Tests will be performed both before and after 589K aging in air. The same aging and testing will also be conducted for 6.4 x 6.4 x 2.5 cm (2 1/2 in x 2 1/2 x 1 in) flatwise tensile samples which will consist of composite facesheet and glass/ polyimide core. The composite will be graphite/NR150B2, PMR-15, or LARC-160. The composite will be tested for quality by C-scan and physical property tests.

12.3 Development of NR150B2/LARC-160 Polyimide Graphite Hybrid Composites

Robert A. Jewell

In the CASTS project, development of high temperature graphite reinforced composite structures has centered upon several polyimide matrix materials, two of which are Dupont's NR150B2 and NASA-Langley's LARC-160 resin systems. The primary objective of this contractual task is to develop and optimize a method for co-curing these two dissimilar polyimide prepregs into hybrid composites which exhibit the best properties of both resin systems.

Preliminary work conducted at NASA-Langley has shown that by combining NR150B2 and LARC-160 graphite prepreg to produce a hybrid laminate beneficial effects in terms of fabrication and thermooxidative stability may be achieved without sacrificing desirable mechanical properties. Dupont's NR150B2 system cures to a linear, high molecular weight material and has demonstrated excellent thermooxidative stability; however, NR150B2 graphite prepreg is difficult to process, particularly in fabricating thick sections. The NASA/LARC-160 system cures by an addition reaction to a highly crosslinked material and is amenable to autoclave processing; however, LARC-160 composites are brittle and exhibit marginal thermooxidative stability at 589K (600°F). In developing methods for cocuring these systems, the activities are defined in three subtasks.

In subtask A, each graphite/polyimide system will be characterized for prepreg quality assurance, prepreg processability, and laminate physical and mechanical properties. The success of the task will largely depend on establishing a rigorous quality assurance effort and a solid data base for subsequent evaluations of cocuring efforts. In subtask B, emphasis will be on process development – defining heating rates, dwell temperatures and times, pressures, bleeder arrangements, and postcure requirements. Work in subtask C will be devoted to final optimization and testing of both clad and interdispersed types of hybrid composites. The utility of the hybrid composites will be assessed by comparative measurements of the pertinent properties of graphite/LARC-160 and graphite/NR150B2 laminates which were processed in subtask A.

The contractual effort is expected to last 12 months.

12.4 Porous Vented Tooling

Robert Baucom

The removal of solvents and reaction by-products during the cure cycle of reinforced high temperature polymers is critical to the manufacture of structurally sound laminates. Porous tooling has the potential of providing an endless path for effluent removal during the cure cycle for graphite/polyimides which could reduce or eliminate the possibility of entrapment of solvents or reaction by-products. A contractual study is planned for the determination of the feasibility of castable porous ceramic tooling for curing HTS graphite reinforced PMR-15 polyimide resin. Contract award for this study is anticipated in July, 1978. The duration of the contract will be 9 months, inclusive of the final report.

12.5   Fabrication and Test of Glass/Polyimide Honeycomb Cores for

Advanced Space Transportation Systems

Mark J. Shuart

The primary objective of this task is to fabricate and test specific
types of lightweight, high temperature resistant glass/polyimide honeycomb
cores. The material systems will be evaluated for application to advanced
space transportation systems. Accomplishment of this objective will require
demonstration of the ability to fabricate glass/polyimide honeycomb and
to characterize the material at both room and elevated temperatures.

The contractor will fabricate glass/polyimide honeycomb cores using
108 glass fabric with LARC-160, PMR-15, and NR150B2 polyimide resins. The
honeycomb cores will also be tested in compression and shear. Tests will
be performed on as-fabricated and 589K (600°F) aged specimens at both room
temperature and 589K. All work will be performed over an eight and one-half
month period.

12.6 Elevated Temperature Bolted Joint Test

Paul A. Cooper

The primary objective of this grant program with the University of Delaware is the development of test techniques to evaluate the elevated temperature behavior of mechanically fastened joints of composite materials. In addition the creep/relaxation behavior of these systems will be studied. During the first year of this grant the influence on joint strength of temperature, laminate geometry, loading condition (i.e. pin versus bolt), and joint geometry were investigated for a contemporary graphite-epoxy composite system. In order to develop the required information, a test program was implemented. The parameters studied included laminate configuration, specimen geometry (fig. 12.10-1) and temperatures of 297K, 394K, 450K (75, 250, 350°F). The laminates investigated ranged from the fiber dominated system $[\pm45/0_3/\pm45/0_3/90]_s$ to the quasi-isotropic laminate, $[0/\pm45/90]_{2s}$. In addition, specimen widths of 1.9, 2.5, and 3.8 cm (0 3/4, 1, and 1 1/2 in) were examined. Finally, pin end distance was set at 1.9 cm (3/4 in).

The University is now examining the behavior of graphite-polyimide composite joints over a greater temperature range in order to establish a correspondence between the behavior of the polyimide and epoxy matrix composite joints. Since the parameter which governs the elevated temperature response of polymeric composites is the glass transition temperature of the polymer, elevated temperature response for the polyimide will be examined as a function of temperature, nondimensionalized with respect to glass transition temperature. Hence, the first phase will focus upon development of polyimide bolted joint data which duplicates that generated for the epoxy matrix composite during the first year of the grant.

The test program will allow evaluation of the ultimate strength and failure mode of single element bolted joints as a function of test specimen geometry. In addition the laminates examined will range from the fiber dominated laminate $[\pm45/0_3/\pm45/0_3/90]_s$ to the matrix dominated laminate $[\pm45/90_3/\pm45/90_3/0]_s$ and thereby reflect all potential failure modes.

Experimental studies underway with graphite/epoxy specimens will examine the influence of out-of-plane restraint due to fastener interference upon joint strength and failure mode. This will be accomplished by restraining the laminate thickness expansion by a Teflon surfaced annular disk of given contact area. No torque will be applied through the bolt. The results of this study will determine the specimen configuration for the specimen configuration for the proposed graphite/polyimide test program.

The object of the second phase of the program will be the determination of the time dependent behavior and loading rate sensitivity of polyimide bolted joint elements. This phase of the program should be complete by February 1979.
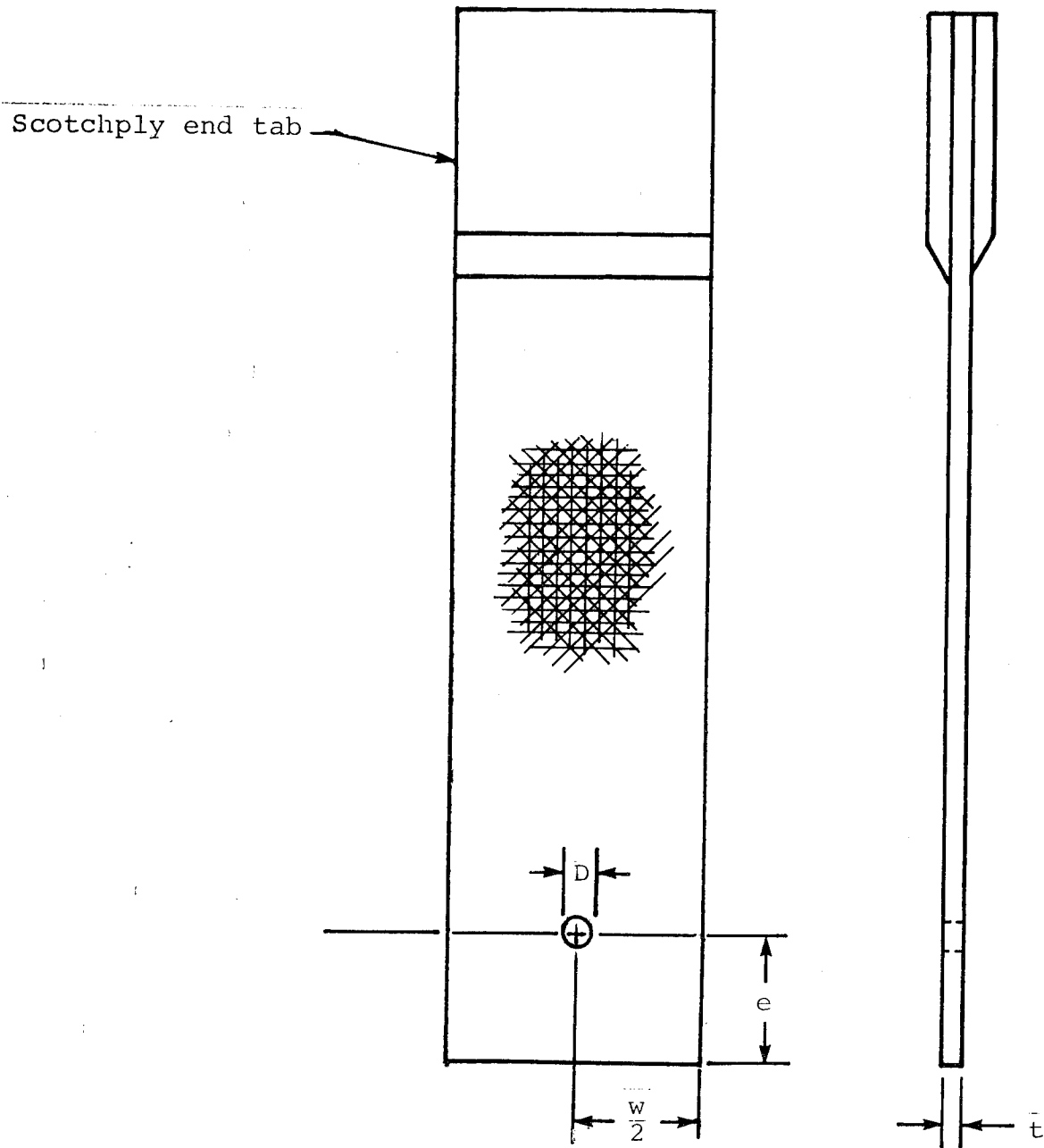
Scotchply end tab

D

e

$\frac{w}{2}$

t

Figure 12.6-1 - Test coupon geometry.

12.7 Orthotropic Photoelasticity

Paul A. Cooper

Filamentary composite structures have high in-plane stiffness and strength but quite low structural properties normal to the plane of the fibers. Thus, composite structures are usually designed most efficiently as two-dimensional structures. Transmission photoelastic experimental techniques are particularly well suited for use in the study of such structures. If orthotropic transparent birefringent material were available, studies could be made using photoelasticity to verify closed-form analytical or finite-element solutions of the stress distributions in plane orthotropic structures with complex boundary geometry, complex in-plane loading, and areas of high stress concentrations.

During the last several years attempts have been made to develop orthotropic transparent material with sufficient birefringence for use in transmission photoelastic studies of two-dimensional structural models (ref. 12.7-1 - 12.7-6). With the successful development of these materials and the formulation of appropriate stress (or strain)-optic laws, full-field photoelastic studies can be made of stress distributions in plane composite structures of complex configurations. However, there is no ready availability of such material nor is there agreement as to the constituent makeup of the matrix for highest optical sensitivities. A contract is therefore planned to support the development, manufacture, and delivery of optically sensitive orthotropic photoelastic materials. The contractor will formulate an appropriate fiber/matrix mixture so that the component constituents of the mixture have similar optical characteristics, develop a procedure for manufacture of unidirectional filamentary composite prepreg and subsequently fabricate and deliver a number of multilayer laminated sheets of various ply orientations.

A small photoelastic stress analysis laboratory with a transmission type polariscope has been installed at the Langley Research Center to aid in the evaluation of stress distributions for various joining concepts. A stress or strain-optic law will be formulated and verified by comparing experimental stress results with an analytical solution of a well defined composite structural problem. Techniques for oblique incidence methods to separate principal stresses will likewise be developed and these procedures will be applied to the experimental evaluation of composite bonded joints.

References

12.7-1. Sampson, R. C.: A Stress-Optic Law for Photoelastic Analysis of Orthotropic Composites. Experimental Mechanics, Vol. 10, No. 5, May 1970.

12.7-2. Dally, J. W.; and Prabhakaran, R.: Photo-orthotropic-elasticity. Experimental Mechanics, Vol. 11, No. 8, August 1971.

12.7-3. Prabhakaran, R.; and Dally, J. W.: The Application of Photo-orthotropic Elasticity. Journal of Strain Analysis, Vol. 7, No. 4, 1972.

12.7-4. Pipes, R. B.; and Rose, J. L.: Strain-Optic Law for a Certain Class of Birefringent Composites. Experimental Mechanics, Vol. 14, No. 9, September 1974.

12.7-5. Pih, H.; and Knight, C. E.: Photoelastic Analysis of Anisotropic Fibre Reinforced Composites. Journal of Composite Materials, Vol. 3, No. 1, January 1969.

12.7-6. Knight, C. E.; and Pih, H.: Orthotropic Stress-Optic Law for Plane Stress Photoelasticity of Composite Materials. Fibre Science and Technology, Vol. 9, 1976.

12.8 Fracture Under Biaxial Loading

G. L. Roderick

The George Washington University will investigate the room temperature biaxial fracture behavior of graphite/polyimide composites. Initially, some graphite/epoxy specimens will be tested for reference data.

Over the previous twelve months, the University has tested its biaxial loading frame (fig. 12.8-1), developed a suitable cruciform specimen (fig. 12.8-2), set up displacement gages, and checked performance on specimens of aluminum.

During the next report period, the University plans to test twenty graphite/epoxy specimens, and twenty graphite/polyimide specimens.
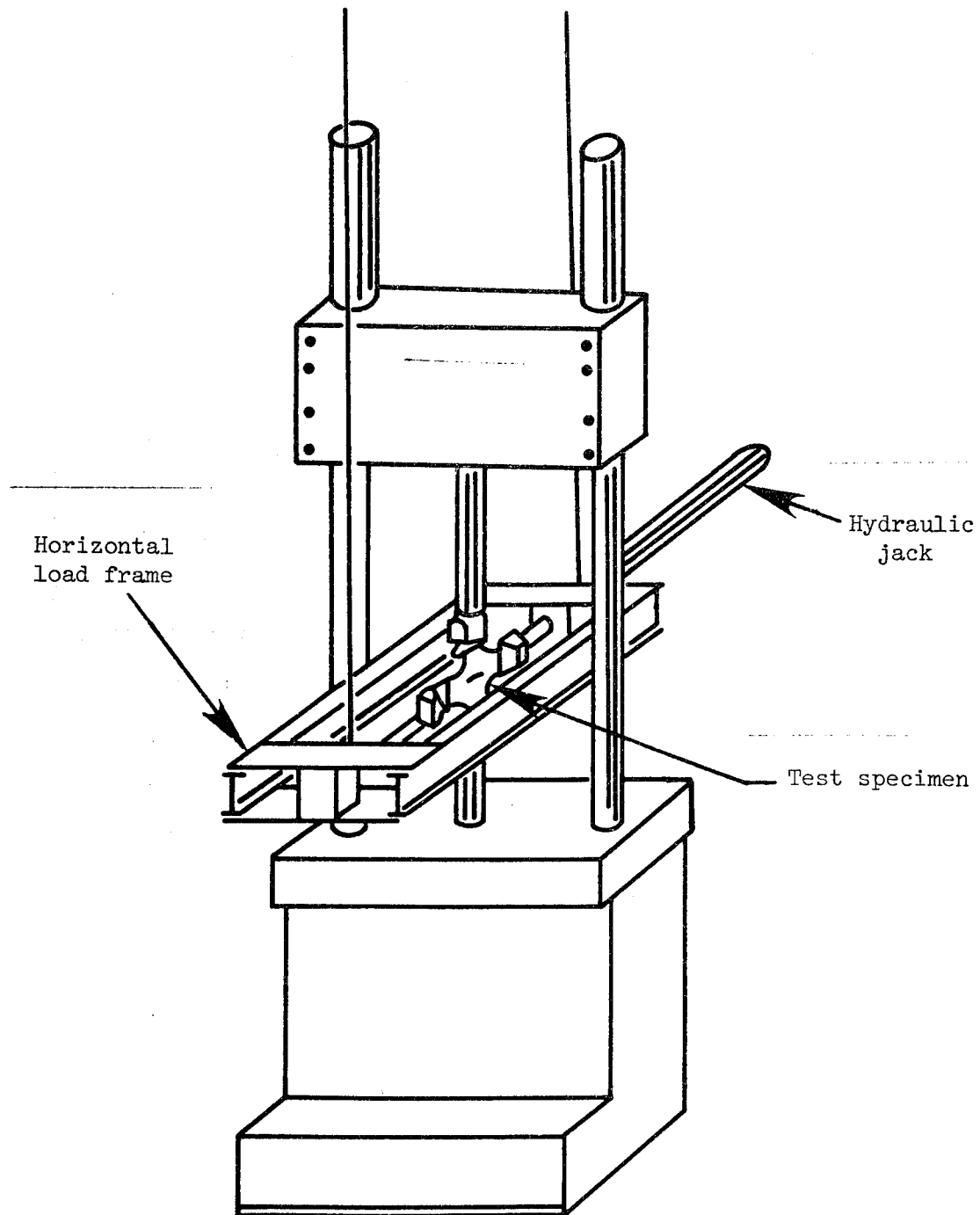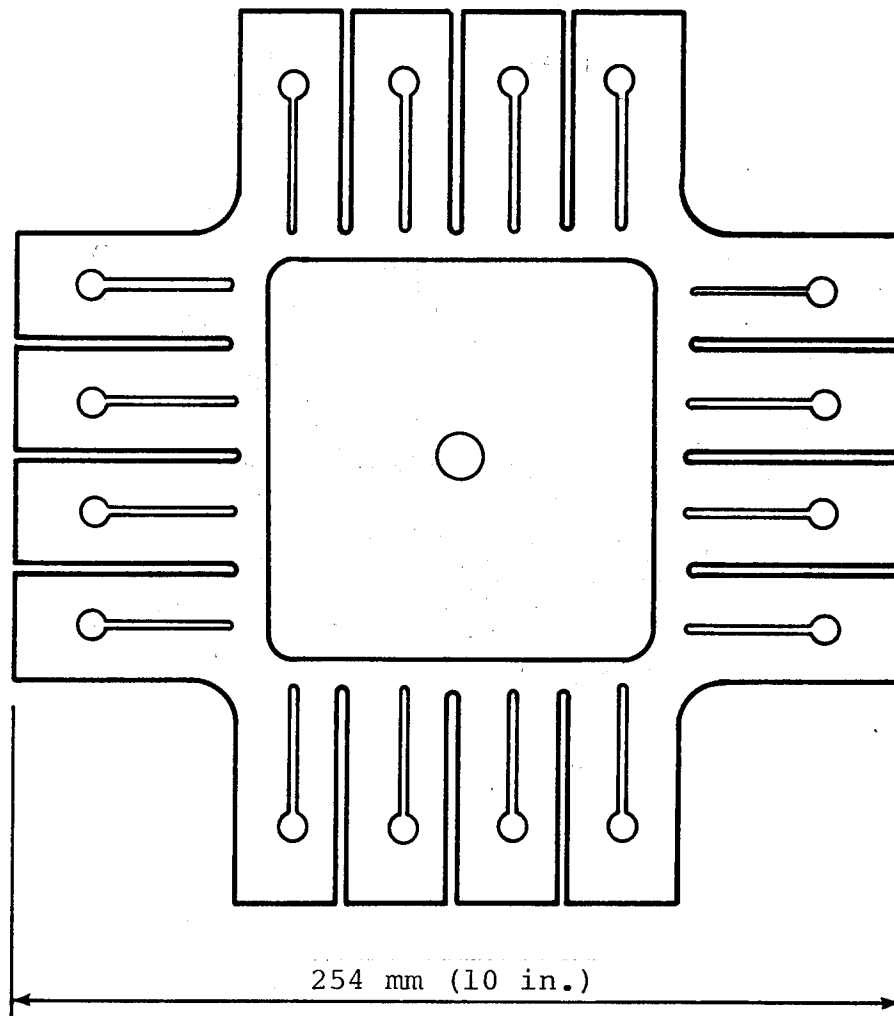
Figure 12.8-1 - Biaxial test system.

254 mm (10 in.)

Figure 12.8-2 - Biaxial test specimen with reinforced tabs.

12.9 Failure Analysis of Fiber Reinforced Composites

Gary L. Farley

The objective of this research is to develop a rigorous mathematical procedure for modeling the failure of a composite specimen subject to certain mechanical and environmental loading conditions. The failure process is characterized by a succession of local failures modeled as a crack propagation procedure. Initiation and stable crack growth is defined by application of an existing local failure criterion, such as Tsai-Wu or maximum strain.

In this study, the tensile coupon was chosen as the composite specimen for both analytical and experimental investigations. These specimens were fabricated with Celion fiber and PMR-15 polyimide resin. This specimen selection was based upon economic considerations, reliability of results, and the number of different phenomena exhibited by the specimen through failure.

A general purpose linear elastic finite element code (SPAR) will be employed as the analysis tool. Processors, compatible with SPAR, have been developed to include the modeling of material and geometric nonlinearities as well as residual stresses induced through manufacturing.

An experimental program has been undertaken to verify the aforementioned analytical procedure. This includes material property characterization for ambient and 589°K (600°F) temperature conditions and characterization of the basic extensional and shearing failure modes.

To date, all major computer code development has been completed. Individual specimens are being machined from large panels; the machining and strain gaging of specimens will soon be completed. The material property characterization, the experimental and analytical phases of the extensional and shearing failure mode investigation, and the ultimate strength tests will soon be completed. The remainder of the data reduction and reporting of results is expected to be completed during the coming three months.

1. Report No. NASA TM-80038	2. Government Accession No.	3. Recipient's Catalog No.
4. Title and Subtitle Composites for Advanced Space Transportation Systems - CASTS		5. Report Date March 1979
		6. Performing Organization Code
7. Author(s) John G. Davis, Jr. (Compiler)		8. Performing Organization Report No.
9. Performing Organization Name and Address NASA Langley Research Center Hampton, VA 23665		10. Work Unit No. 524-71-03-01
		11. Contract or Grant No.
12. Sponsoring Agency Name and Address National Aeronautics and Space Administration Washington, D.C. 20546		13. Type of Report and Period Covered Technical Memorandum
		14. Sponsoring Agency Code

15. Supplementary Notes

16. Abstract

This document summarizes the in-house and contract work accomplished under the CASTS Project. In July 1975 the CASTS Project was initiated to develop graphite fiber/polyimide matrix (Gr/PI) composite structures with 589K (600°F) operational capability for application to aerospace vehicles. Major tasks include: screening composites and adhesives, developing fabrication procedures and specifications, developing design allowables test methods and data, design and test of structural elements and construction of an aft body flap for the Space Shuttle Orbiter Vehicle which will be ground tested. Portions of the information are from ongoing research and must be considered preliminary. The CASTS Project is scheduled to be completed in September 1983.

17. Key Words (Suggested by Author(s)) Composites Composite Structures	18. Distribution Statement Unclassified - Unlimited Subject Category 24
19. Security Classif. (of this report) Unclassified	20. Security Classif. (of this page) Unclassified	21. No. of Pages 267	22. Price* $10.75